

Dental and Medical Problems

QUARTERLY ISSN 1644-387X (PRINT) ISSN 2300-9020 (ONLINE)

www.dmp.umed.wroc.pl

2020, Vol. 57, No. 4 (October–December)

Ministry of Science and Higher Education – 20 pts.
Index Copernicus (ICV) – 113.05 pts.



WROCLAW
MEDICAL UNIVERSITY

Dental and Medical Problems

ISSN 1644-387X (PRINT)

ISSN 2300-9020 (ONLINE)

www.dmp.umed.wroc.pl

QUARTERLY
2020, Vol. 57, No. 4
(October–December)

“Dental and Medical Problems” is a peer-reviewed open access journal published by Wrocław Medical University. Journal publishes articles from different fields of dentistry and other medical, biological, deontological and historical articles, which were deemed important to dentistry by the Editorial Board – original papers (clinical and experimental), reviews, clinical cases, and letters to the Editorial Board.

Address of Editorial Office

Marcinkowskiego 2–6
50-368 Wrocław, Poland
Tel.: +48 71 784 11 33
E-mail: dental@umed.wroc.pl

Publisher

Wrocław Medical University
Wybrzeże L. Pasteura 1
50-367 Wrocław, Poland

© Copyright by Wrocław Medical University
Wrocław 2020

Online edition is the original version of the journal.

Editor-in-Chief

Tomasz Konopka

Vice-Editor-in-Chief

Marcin Mikulewicz

Thematic Editors

Anna Zalewska (Cariology)
Mariusz Lipski (Endodontics)
Urszula Kaczmarek (Pedodontics
and Dental Prevention)
Renata Górka (Oral Pathology)
Korkud Demirel (Periodontology)
Piotr Majewski (Implant Dentistry)

Andrzej Wojtowicz (Oral Surgery)
Marcin Kozakiewicz (Maxillofacial Surgery)
Teresa Sierpińska (Prosthodontics)
Jolanta Kostrzewa-Janicka (Disorders
of Masticatory System)
Marcin Mikulewicz (Orthodontics)
Ingrid Różyło-Kalinowska (Dental Radiology)

International Advisory Board

Akira Aoki (Japan)
Einar Berg (Norway)
Ewa Czochrowska (Poland)
Patrizia Defabianis (Italy)
Korkud Demirel (Turkey)
Marzena Dominiak (Poland)
Barbara Dorocka-Bobkowska (Poland)
Omar El-Mowafy (Canada)
Katarzyna Emerich (Poland)
Piotr Fudalej (Czech Republic, Switzerland)
Thomas Gedrange (Germany)
Hanna Gerber (Poland)
Renata Górka (Poland)
David Herrera (Spain)
Michał Jeleń (Poland)
Urszula Kaczmarek (Poland)
Milan Kamínek (Czech Republic)
Kazimierz Kobus (Poland)
Krystyna Konopka (USA)
Marcin Kos (Germany)
Marcin Kozakiewicz (Poland)
Tadeusz F. Krzemiński (Poland)
Monika Łukomska-Szymańska (Poland)

Piotr Majewski (Poland)
Agnieszka Mielczarek (Poland)
Marcin Mikulewicz (Poland)
Joseph Nissan (Israel)
Raphaël Olszewski (Belgium)
Hyo-Sang Park (South Korea)
Alina Pūrienė (Lithuania)
Małgorzata Radwan-Oczko (Poland)
Monique-Marie Rousset-Caron (France)
Ingrid Różyło-Kalinowska (Poland)
Teresa Sierpińska (Poland)
Franciszek Szatko (Poland)
Jacek C. Szepietowski (Poland)
Selena Toma (Belgium)
János Vág (Hungary)
Andreas Wielgosz (Canada)
Mieszko Więckiewicz (Poland)
Andrzej Wojtowicz (Poland)
Dariusz Wołowicz (Poland)
Grażyna Wyszyńska-Pawelec (Poland)
Anna Zalewska (Poland)
Marek Ziętek (Poland)

Statistical Editor

Krzysztof Topolski

Technical Editorship

Adam Barg

Joanna Gudarowska

Marek Misiak

Paulina Piątkowska

English Language Copy Editors

Eric Hilton

Sherill Howard-Pociecha

Jason Schock

Marcin Tereszewski

Editorial Policy

During the reviewing process, the Editorial Board conforms to the "Uniform Requirements for Manuscripts Submitted to Biomedical Journals: Writing and Editing for Biomedical Publication" approved by the International Committee of Medical Journal Editors (<http://www.icmje.org/>). Experimental studies must include a statement that the experimental protocol and informed consent procedure were in compliance with the Helsinki Convention and were approved by the ethics committee.

Indexed in: MEDLINE, Web of Science, Scopus, DOAJ, GFMER, Index Copernicus, Ministry of Science and Higher Education, CiteFactor, WorldCat, Directory of Research Journal Indexing.

This publication has been co-financed by the Ministry of Science and Higher Education.

Typographic design: Monika Kołęda, Piotr Gil

Cover: Monika Kołęda

DTP: Wrocław Medical University Press

Printing and binding: EXDRUK

Contents

Original papers

- 351 Hojjat Ghahramanzadeh Asl, Akgün Alsaran
In vitro comparison of commercial and ultrafine-grained titanium osteosynthesis miniplates used on mandibular fractures
- 359 Enas Abdalla Etajuri, Eshamsul Suliman, Wan Adida Azina Mahmood, Norliza Ibrahim, Muaiyed Buzayan, Noorhayati Raja Mohd
Deviation of dental implants placed using a novel 3D-printed surgical guide: An in vitro study
- 363 Feni Istikharoh, Hidayat Sujuti, Edi Mustamsir, Astika Swastirani
Preparation and biodegradable properties of hydroxyapatite nanoparticle composite coated with poly lactic-co-glycolic acid/polyvinyl alcohol for bone regeneration
- 369 Mohammd Ayoub Rigi Ladiz, Alireza Mirzaei, Seyedeh Sareh Hendi, Roya Najafi-Vosough, Amirarsalan Hooshyarfard, Leila Gholami
Effect of photobiomodulation with 810 and 940 nm diode lasers on human gingival fibroblasts
- 377 Ali Raef Abboud, Ali Mohammad Ali, Tihama Youssef
Preparation and characterization of insulin-loaded injectable hydrogels as potential adjunctive periodontal treatment
- 385 Zakaria Vahabzadeh, Zahra Moaven Hashemi, Bijan Nouri, Fatemeh Zamani, Faranak Shafiee
Salivary enzymatic antioxidant activity and dental caries: A cross-sectional study
- 393 Hakan Aydın, Kürşat Er, Alper Kuştarıcı, Murat Akarsu, Gül Merve Gençer, Hakan Er, Rasih Felek
Antibacterial activity of silver nanoparticles activated by photodynamic therapy in infected root canals
- 401 Arghavan Kamali Sabeti, Zahra Karimizadeh, Rezvan Rafatjou
Maximum equivalent stress induced and the displacement of the developing permanent first molars after the premature loss of primary second molars: A finite element analysis
- 411 Sylwia Rogużińska, Anna Pelc, Marcin Mikulewicz
Orthodontic-care burden for patients with unilateral and bilateral cleft lip and palate
- 417 Elham Ahmadi, Masoumeh Hasani Tabatabaei, Sina Mohammadi Sadr, Faezeh Atri
Comparison of the marginal discrepancy of PFM crowns in the CAD/CAM and lost-wax fabrication techniques by triple scanning
- 423 Barbara Paśnik-Chwałik, Tomasz Konopka
Impact of periodontitis on the Oral Health Impact Profile: A systematic review and meta-analysis
- 433 Kazem Dalaie, Vahid Reza Yassaee, Mohammad Behnaz, Mohsen Yazdani, Farbod Jafari, Reza Morvaridi Farimani
Relationship of the rs10850110 and rs11611277 polymorphisms of the MYO1H gene with non-syndromic mandibular prognathism in the Iranian population

Reviews

- 441 Farheen Fatima, Waqar Jeelani, Maheen Ahmed
Current trends in craniofacial distraction: A literature review
- 449 Zbigniew Raszewski
Acrylic resins in the CAD/CAM technology: A systematic literature review

Clinical cases

- 455 Zuzanna Ślebioda, Agnieszka Mania-Końsko, Barbara Dorocka-Bobkowska
Scarlet fever – a diagnostic challenge for dentists and physicians: A report of 2 cases with diverse symptoms

Acknowledgements

We would like to express our gratitude to all reviewers who devoted their time and expertise to evaluate manuscripts in “Dental and Medical Problems”. We sincerely appreciate all your hard work and dedication. It is due to your contribution that we can achieve the standard of excellence.

Editors

Reviewers in 2020:

Akira Aoki, Julia Bar, Einar Berg, Marek Bochnia, Renata Chałas, Maria Chomyszyn-Gajewska, Beata Dejak, Elżbieta Dembowska, Korkud Demirel, Tadeusz Dobosz, Barbara Dorocka-Bobkowska, Irena Duś-Ilńska, Omar El-Mowafy, Katarzyna Emerich, Tomasz Gedrange, Hanna Gerber, Ludmiła Halczy-Kowalik, Michał Jeleń, Kamil Jurczyszyn, Milan Kamínek, Bożena Karolewicz, Andrzej Kiejna, Edward Kijak, Kazimierz Kobus, Tomasz Konopka, Marcin Kos, Jolanta Kostrzewa-Janicka, Jan Kowalski, Marcin Kozakiewicz, Tomasz Kulczyk, Stanisław Kuć, Bogumił Lewandowski, Mariusz Lipski, Magdalena Łukaszewska-Kuska, Monika Łukomska-Szymańska, Irena Makulska, Agnieszka Mielczarek, Marcin Mikulewicz, Hyo-Sang Park, Elżbieta Pawłowska, Jan Pietruski, Lidia Postek-Stefańska, Małgorzata Radwan-Oczko, Ingrid Różyło-Kalinowska, Teresa Sierpińska, Małgorzata Skucha-Nowak, Tomasz Staniowski, Leszek Szalawski, Franciszek Szatko, János Vág, Danuta Waszkiel, Mieszko Więckiewicz, Andrzej Wojtowicz, Piotr Wójcicki, Grażyna Wyszyńska-Pawelec, Anna Zalewska, Piotr Ziółkowski

In vitro comparison of commercial and ultrafine-grained titanium osteosynthesis miniplates used on mandibular fractures

Hojjat Ghahramanzadeh Asl^{1,A-F}, Akgün Alsarar^{2,A,C}

¹ Department of Mechanical Engineering Department, Karadeniz Technical University, Trabzon, Turkey

² Independent researcher, Eskişehir, Turkey

A – research concept and design; B – collection and/or assembly of data; C – data analysis and interpretation;

D – writing the article; E – critical revision of the article; F – final approval of the article

Dental and Medical Problems, ISSN 1644-387X (print), ISSN 2300-9020 (online)

Dent Med Probl. 2020;57(4):351–358

Address for correspondence

Hojjat Ghahramanzadeh Asl

E-mail: h.kahramanzade@ktu.edu.tr

Funding sources

Scientific Research Projects of Atatürk University in Erzurum, Turkey (project No.2013/98).

Conflict of interest

None declared

Acknowledgements

This study was derived from a doctoral thesis, defended on January 28, 2016. The authors wish to thank the TST Medical Devices for miniplate geometries. We also would like to thank Dr. Genççağ Pürçek for permitting us to use the mechanical engineering laboratory facilities in Karadeniz Technical University in Trabzon, Turkey. Hojjat Ghahramanzadeh Asl would like to thank the Scientific and Technological Research Council of Turkey (TÜBİTAK) for the Directorate of Science Fellowships and Grant Programmes (BİDEB) 2215 Scholarship.

Received on April 17, 2020

Reviewed on May 20, 2020

Accepted on June 13, 2020

Published online on December 31, 2020

Cite as

Ghahramanzadeh Asl H, Alsarar A. In vitro comparison of commercial and ultrafine-grained titanium osteosynthesis miniplates used on mandibular fractures. *Dent Med Probl.* 2020;57(4):351–358. doi:10.17219/dmp/123932

DOI

10.17219/dmp/123932

Copyright

© 2020 by Wrocław Medical University

This is an article distributed under the terms of the

Creative Commons Attribution 3.0 Unported License (CC BY 3.0)

(<https://creativecommons.org/licenses/by/3.0/>).

Abstract

Background. Implants called miniplates, with different geometries, are used for the treatment of a fractured or diseased mandible. Generally, Ti-based miniplates in various quantities and with various geometries are fixed into the bone tissue according to the location and shape of the fracture by embedding.

Objectives. The aim of this study was to increase the strength of the material used in the production of miniplates by means of the equal-channel angular pressing (ECAP) treatment, and to provide a high-rigidity fixation system with fewer miniplates.

Material and methods. In this study, the ECAP method, which is one of the methods of severe plastic deformation, was applied at 4 passes at 300°C in route Bc to increase the strength of pure Ti. Then, miniplates were produced with 2 different geometries (regular and long) and 2 different properties of the Ti material (untreated and ECAP-treated). The produced miniplates were placed in the fracture line formed in the angular region of an artificial, synthetic-bone mandible. The 2-point and 3-point bending and torsion tests were conducted on these fixation systems.

Results. As a result, after the ECAP process, the yield and tensile strength of pure Ti increased by 65%, while elongation decreased by 13%. After the ECAP process, the grain size of the material was reduced from 110 µm to 200 nm.

Conclusions. This study showed that the fixation system became more rigid due to using ECAP-treated miniplates, and this ensured lesser displacement of the fixation system.

Key words: equal-channel angular pressing, bending, torsion, mandible fracture, miniplate

Introduction

Today, biomaterials are frequently used in healing the fractures of the mandible caused by diseases, accidents and war. Diseases and fractures in the mandible are found in the condyle, body, angle, symphysis, alveolar bone, and coronoid regions. Metal implants called miniplates, with different geometries, are used for treatment. In the angular region, which is one of the most frequently fractured regions in the mandible, fixations are applied using different geometries and various numbers of miniplates and screws according to the fracture type and size. It is also considered to be more advantageous to use a single miniplate in the fixation system. In the literature, the advantage of using a single miniplate has been noted by researchers as minimal dissection and a reduction in the volume of the implanted material.¹⁻⁴

The most important issue in the case of miniplates, which are usually made of Ti and its alloys, is the rigidity of the fixation formed.⁵⁻¹⁰ Esen et al. studied different types of plates and fixation systems under different loads by mounting miniplates on angle fractures in sheep mandibles.¹¹ As a result, the Ti plate/screw system proved to be the most reliable system for fixation in mandible angle fractures. In that study, it was also stated that if the rigidity of the fixation system is excessive, more load should be applied to break the fracture areas of the mandible.¹¹ The mechanical fixation system formed by plates on a mandible bone fracture has been investigated in the literature, mostly in terms of the plate geometry and the bone fixation method. In a majority of studies, miniplates are placed on a sheep mandible or an artificial mandible, and then compared with regard to the displacement values under a certain load. The main aim of such studies is to determine which type of plate is more durable in terms of both geometry and mandible placement.^{5,12-15} When displacement is low, the broken parts of the mandible are hardly separated from each other, and therefore the fixation system exhibits more rigid behavior. For example, when the number of screws or miniplates is increased, the fixation becomes more rigid.¹⁶

Due to the fact that miniplates are often mounted by embedding them into the bone tissue, an important consideration is the number of miniplates. When the number of miniplates is increased, the surgical area expands, and the duration of the treatment is also prolonged. For this reason, it is important to establish the most rigid fixation system with minimum miniplate usage. This can be achieved by making the fixation with a more durable material or by increasing the strength of the material used. Miniplates are generally manufactured from commercially pure (CP) Ti grade 2 or grade 4. These materials are suitable in terms of biocompatibility, but they are ineligible in terms of strength. In order to overcome this deficiency, the equal-channel angular pressing (ECAP) mechanical process is preferred.

Severe plastic deformation (SPD) techniques are used to increase the strength of different types of materials. A commonly used SPD method is ECAP.¹⁷ This method is based on the principles of increasing grain density and dislocation density in massive forms. It was first proposed by Segel et al. in 1977.^{acc.18} The ECAP method begins with passing the material through 2 channels of an identical cross-section. During this transition, plastic deformation occurs in the inner structure of the material due to a simple sliding mechanism; then, the grain size decreases.^{19,20} One of the characteristics that stands out in this method is that the material becomes ultrafine-grained (UFG), which increases its strength and does not cause severe decreases in its ductility.^{17,19,21} Valiev et al. proved the cell compatibility of pure UFG Ti and its usage as an implant material.^{22,23} There are also studies indicating that the biocompatibility properties of the material may improve after the ECAP treatment.^{24,25}

The manufacturing of UFG-structured Ti miniplates and the fixations made from these structures have not been biomechanically evaluated by researchers. The use of the ECAP method in miniplate-like implant applications will contribute to similar work being done. For this reason, the main purpose of this study was to examine the biomechanical performance of UFG-structured Ti miniplate fixations under static conditions. The aim of this study was to create a more rigid fixation system by increasing the strength of the material used in the production of miniplates by means of the ECAP treatment. At the same time, providing high rigidity with the use of fewer miniplates is the other main purpose of this study. To this end, first, the strength of pure Ti was increased using the ECAP method, and then miniplates with 2 different geometries were produced. The structural and mechanical analyses of the coarse-grained (CG) and UFG structures were performed. To achieve this, the 2-point and 3-point bending and torsion tests were conducted on the fixative models which were formed on the mandible. The particle size and surface topography were investigated using scanning electron microscopy (SEM), the focused ion beam (FIB) technique, transmission electron microscopy (TEM), and optical microscopy (OM).

Material and methods

The material selected for this study was CP Ti grade 2 with a composition of wt%, 0.030% N, 0.100% C, 0.015% H, 0.300% Fe, and 0.250% O. The material was received in a hot-rolled and annealed condition, with the initial average grain size of ~110 μm . The ECAP billets of a length of 130 mm and a cross section of 30 mm \times 30 mm were cut using wire electrical discharge machining (wire-EDM).

The billets were processed with 4 passes of ECAP at 300°C, using a die angle of 90° with a sharp corner,

at the rate of 1 mm/s. Route Bc was selected as the ECAP processing route. Route Bc consists in the alternating rotation of the billets by 90° counterclockwise for each successive pass. During this process, the ECAP billets were coated with a graphite-based lubricant before each step.

Samples for the tensile tests were machined with a wire-EDM cut from a billet, where their tensile axis was oriented parallel to the extrusion direction. The tensile test sample geometry is shown in Fig. 1. The tensile tests of the untreated and ECAP-treated samples were performed at a strain rate of $5 \times 10^{-4}/s$,¹³ each on 3 samples. The tensile tests were conducted using the Instron 8872 universal testing machine (Instron, Norwood, USA) with an optical extensometer, at room temperature.

Transmission electron microscopy and OM were used to investigate the microstructures of the ECAP-treated and untreated samples. The sample for OM was prepared using standard polishing techniques, and then etched with Kroll's reagent (3 mL HF + 6 mL HNO₃ in 100 mL of distilled water).¹⁹ The TEM sample was produced using FIB (Nova NanoLab 600i; Thermo Fisher Scientific, Waltham USA) with the dimensions $10 \mu\text{m} \times 3 \mu\text{m} \times 1 \mu\text{m}$. The TEM (IEF30; Shinei Tecno Co., Ltd., Tokyo, Japan) observations were conducted at a nominal voltage of 300 kV.

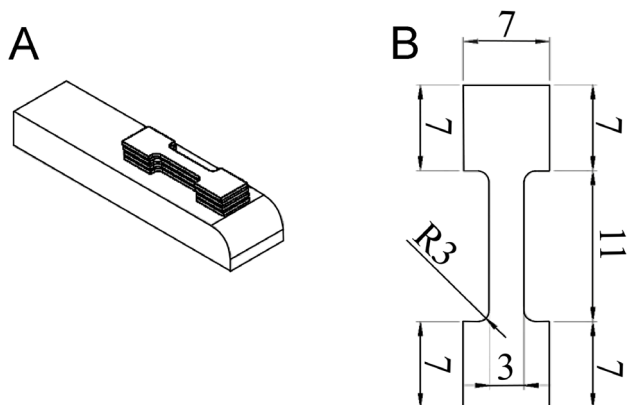


Fig. 1. Schematic representation of the extruded billets and the orientation of the tensile test samples (A), and the tensile test sample dimensions [mm] (B)

In this study, 2 geometries of miniplate implants (TST Medical Devices, Istanbul, Turkey) were investigated. The miniplate implants were manufactured from the untreated and ECAP-treated materials. The dimensions and orientation of the miniplate implants are shown in Fig. 2.

Sixty synthetic polyurethane hemimandible replicas (model No. 8596; Synbone AG, Malans, Switzerland), having medullar and cortical portions, were used as 4 groups ($n = 15$). To simulate a hemimandible fracture, an acrylic-resin template was used in the mandibular angle region.

The fixation groups used in the study are presented in Table 1.

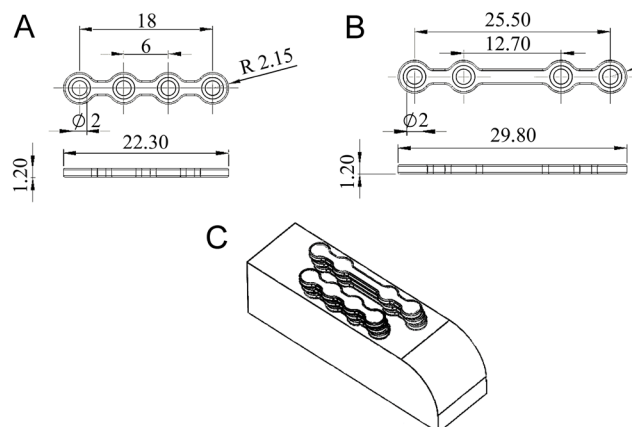


Fig. 2. Dimensions [mm] of the miniplates – regular (A) and long (B) – and their orientation (C)

Table 1. Fixation groups

Group	Miniplate used in the fixation system
Group 1	regular miniplate produced from the untreated CP Ti
Group 2	regular miniplate produced from the ECAP-treated CP Ti
Group 3	long miniplate produced from the untreated CP Ti
Group 4	long miniplate produced from the ECAP-treated CP Ti

CP – commercially pure; ECAP – equal-channel angular pressing.

The hemimandibles were fixed with 4 different miniplates, which were then stabilized with a support apparatus. The 2-point and 3-point bending and torsion tests were performed within the scope of this study to simulate the forces which the muscles transmit to the bone during chewing or the movement of the mandible.²⁶

The AG-IS universal testing machine (Shimadzu, Kyoto, Japan) was used for the 2-point and 3-point bending tests (Fig. 3). A vertical compression force was applied at a rate of 2 mm/min.²⁷ The tests were recorded with a camera recording system (5 images per second).

The torsion tests were performed using the NDW-200 machine (Jinan Liangong Testing Technology Co., Ltd., Jinan, China). The torsional force was applied to the rotating side at a rate of 5°/min (Fig. 4).²⁸ The torsion test continued until the rotation angle reached 30°.

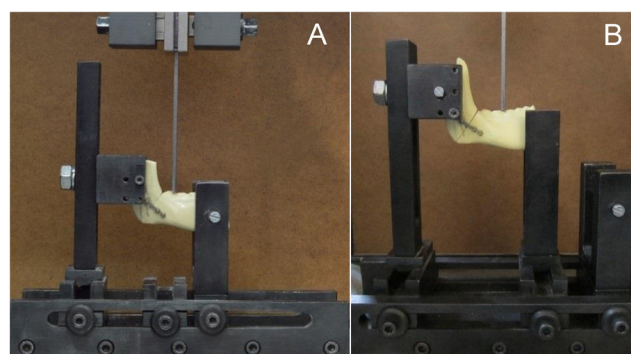


Fig. 3. Hemimandible models fixed to the supporting base for the 3-point (A) and 2-point (B) tests

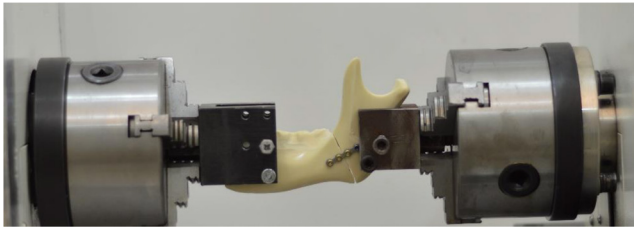


Fig. 4. Arrangement for the torsion test

Results

Figure 5A shows an optical micrograph of the untreated CP Ti grade 2. The grain size distribution was not homogeneous and the average grain size was determined as 110 μm . A TEM micrograph of the ECAP-treated billet is shown in Fig. 5B. The preparation of the TEM sample using FIB is shown in Fig. 5C and 5D. The grain size of the ECAP-treated CP Ti grade 2 was ~ 200 nm.

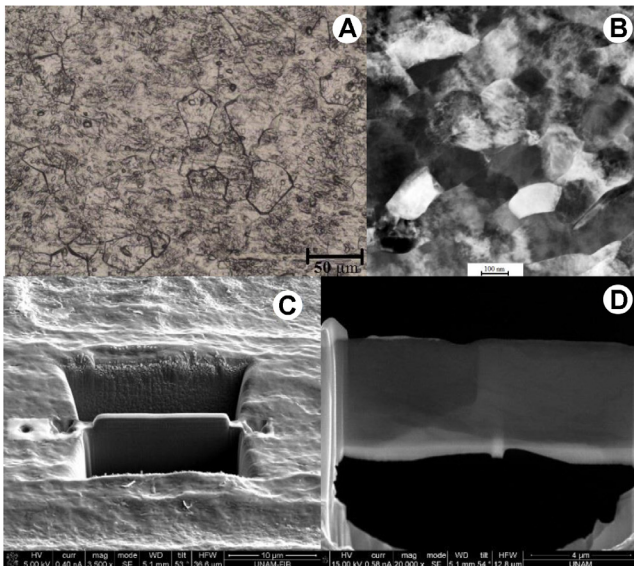


Fig. 5. Optical micrograph of the untreated CP Ti grade 2 (A), the transmission electron microscopy (TEM) micrograph of the ECAP-treated CP Ti grade 2 (B) and the TEM sample (C, D)

The engineering stress–strain curves and the tested samples of CG and UFG Ti are shown in Fig. 6. These curves indicate that, while ECAP processing increased the strength, it also caused a reduction in the overall elongation. The yield strength of CP Ti grade 2, which corresponds to 0.02% plastic deformation, considerably improved after 4 passes of ECAP. The yield stress increased from ~ 310 MPa to ~ 650 MPa after the ECAP process. On the other hand, the tensile stress increased from ~ 535 MPa to ~ 795 MPa. After the ECAP process, the failure strain of the CP Ti grade 2 decreased from 32% to 19%.

A ductile fracture was observed after the tensile test of the untreated and ECAP-treated samples. Also, SEM images of the fractured surfaces were investigated. They are presented in Fig. 7.

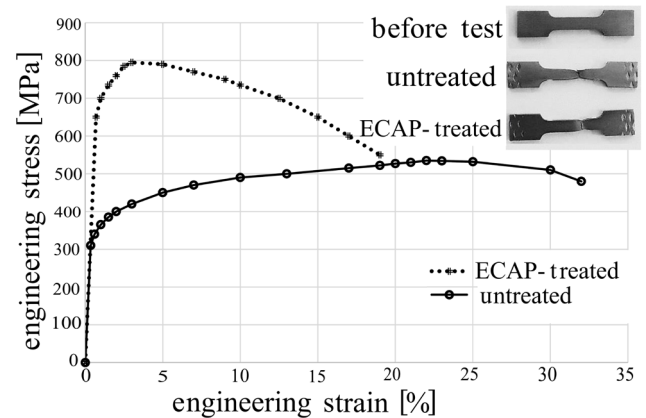


Fig. 6. Engineering stress–strain curves of the untreated and ECAP-treated CP Ti grade 2

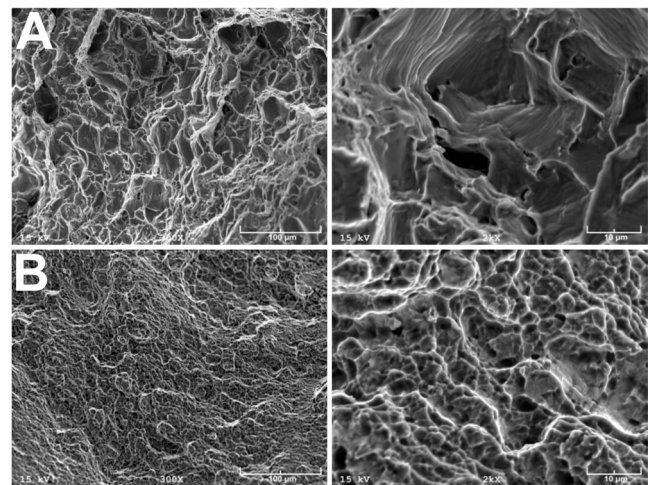


Fig. 7. Scanning electron microscopy (SEM) images of the untreated (A) and ECAP-treated (B) CP Ti grade 2

The force–displacement curves of the 2-point and 3-point bending tests after the application of a compressive load on the hemimandible models with different plate systems are shown in Fig. 8 and Fig. 10, respectively.

Figure 8 presents the strength in the 2-point bending tests. When this graph is examined, the regular and long miniplates produced from the untreated CP Ti show lower strength than the regular and long miniplates produced from the ECAP-treated CP Ti. The fixation model with the long miniplates produced from the untreated CP Ti material displaced 10 mm under a load of ~ 50 N. Under the same load, the long miniplate fixation system produced from the ECAP-treated CP Ti moved 4 mm. In addition, the fixations established with the long miniplates produced from the ECAP-treated material endured to 125 N. It can be seen that the fixation system established with the regular miniplates produced from the untreated CP Ti material displaced 10 mm under a load of 85 N. This value was 7 mm in the fixation system with the regular miniplates produced from ECAP-treated CP Ti. Also, the fixation systems which had the regular miniplates produced from the ECAP-treated material exhibited a strength of up to ~ 139 N. The images taken during the tests are presented as Fig. 9.

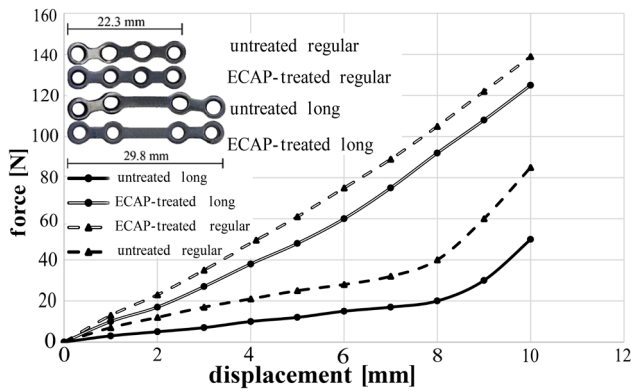


Fig. 8. Force–displacement curves of the 2-point bending tests

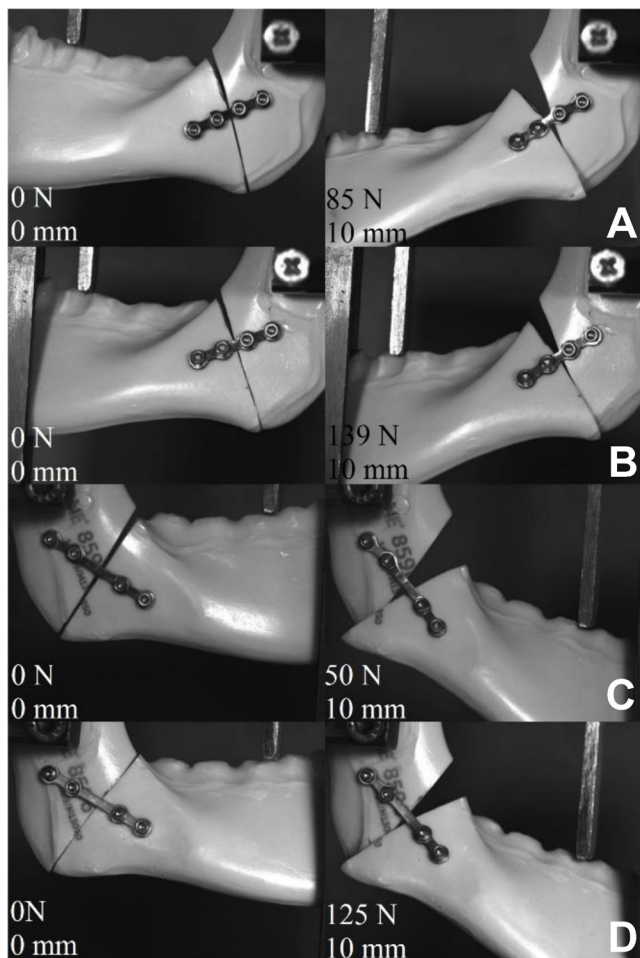


Fig. 9. Fixation systems after and before the 2-point bending tests
A – untreated-regular; B – ECAP-treated-regular; C – untreated-long;
D – ECAP-treated-long.

Figure 10 shows the 3-point bending test results of the miniplates produced from the untreated and ECAP-treated materials. From this graph, it can be seen that the ECAP-treated miniplates are more durable than the miniplates produced from the untreated material, as in the 2-point bending test. The fixation system established with the long miniplates produced from the untreated material displaced 10 mm under a load of ~330 N. The fixation system established with the long miniplates produced from the ECAP-treated material displaced 5 mm under the same load. In addition,

the fixation system with the long miniplates produced from the ECAP-treated material endured to 590 N. When the fixation systems established with regular miniplates were examined, those with the regular miniplates produced from the untreated material displaced 7 mm at ~395 N. This value was ~4.5 mm for the fixation system with the regular miniplates produced from the ECAP-treated material. Also, the fixation system established with the regular miniplates produced from the ECAP-treated material endured to ~515 N. The images taken during the tests are given in Fig. 11.

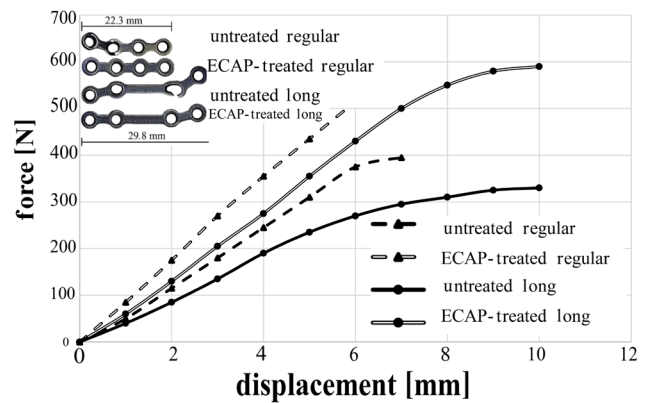


Fig. 10. Force–displacement curves of the 3-point bending tests

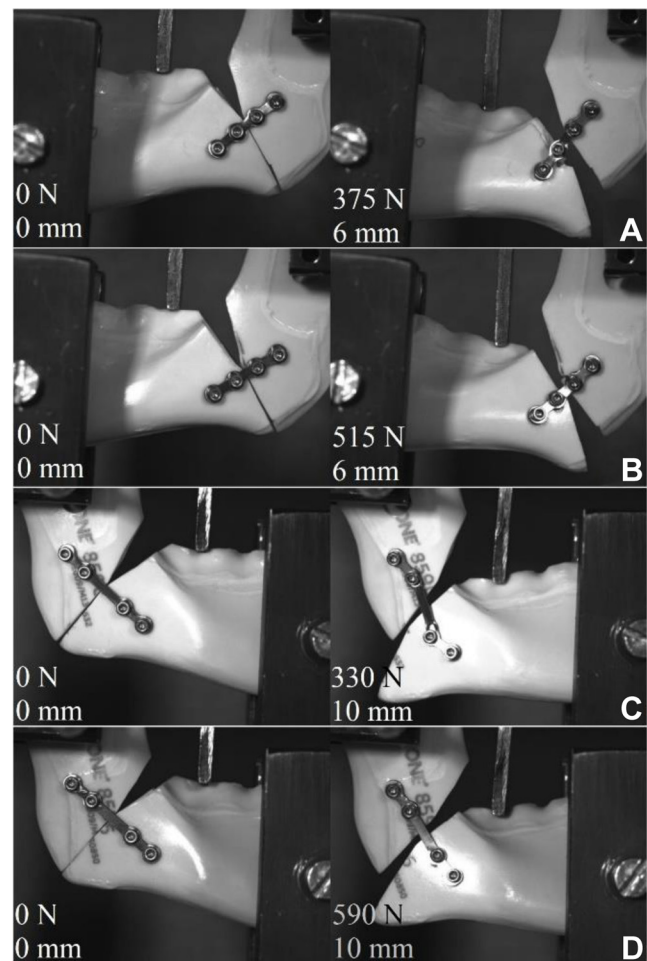


Fig. 11. Fixation systems after and before the 3-point bending tests
A – untreated-regular; B – ECAP-treated-regular; C – untreated-long;
D – ECAP-treated-long.

Figure 12 shows the loads corresponding to a 6-millimeter displacement during the 2-point and 3-point bending tests. According to these results, the ECAP-treated miniplates carried more load for both geometries. These results were especially related to a decrease in the grain size and an increase in the strength of the structure after the ECAP process. Also, the fixations established with regular miniplates were more durable within the same displacements than those with long miniplates. This behavior could be explained by greater movements on the long miniplate due to the area of the longer bar.

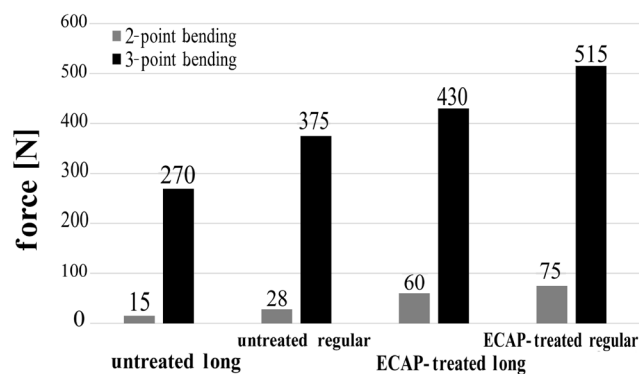


Fig. 12. Loads corresponding to a 6-millimeter displacement during the 2-point and 3-point bending tests

As explained above, using 2 miniplates increased the rigidity approx. two-fold. In this study, the stability was increased up to 400% in the 2-point bending test and 60% in the 3-point bending test after the ECAP process. For this reason, using the ECAP-treated miniplates ensures that higher rigidity can be achieved with fewer plates. Thus, for a surgical operation, it is possible to reduce the area of incision and shorten the healing time due to fewer screw holes in the mandible.

Figure 13 shows the torsion test results for different fixation models. The fixation systems established with the untreated long miniplates experienced 30° rotational deformations under the 0.22 N.m torque, while the fixation systems established with the ECAP-treated long

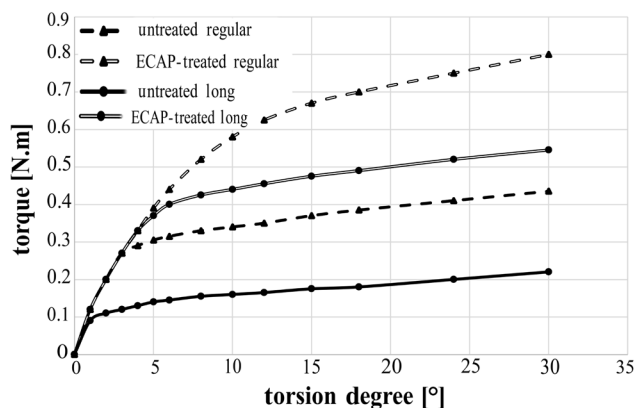


Fig. 13. Torque–rotation curves for the 4 fixation models

miniplates exhibited 3° deformations under the same torque value. In addition, the fixation systems with the ECAP-treated long miniplates endured to ~0.545 N.m. When the fixation systems established with regular miniplates were examined, the untreated regular miniplates showed ~30° contortion at ~0.435 N.m. This value was ~6° for the ECAP-treated regular miniplates. Moreover, the fixation systems established with the ECAP-treated regular miniplates endured to 0.8 N.m (Fig. 14). These results indicate that the miniplates produced from the ECAP-treated material are more durable in the torsion test than the untreated miniplates, and thus more rigid.

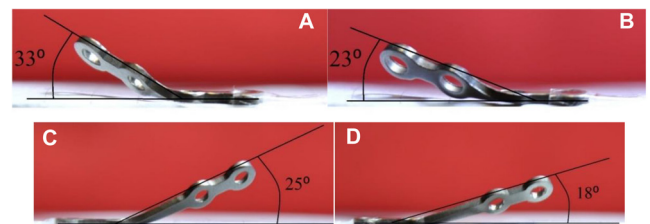


Fig. 14. Miniplates after the torsion tests

A – untreated-regular; B – ECAP-treated-regular; C – untreated-long; D – ECAP-treated-long.

Discussion

The micrographs of the samples showed that 4 passes of the ECAP treatment led to a significant refinement in the microstructure of CP Ti grade 2 and transformed the untreated structure to the UFG structure. The grain size is influenced by the process temperature, deformation rate and die channel angle after the ECAP process. In the literature, it has been determined that the grain size after the ECAP treatment is in the range of 100–250 nm. Meredith and Khan obtained similar results after a 4-pass ECAP process on the Ti material.²⁹

In the process of SPD, grain refinement begins with the transmutation of wide-angled grain boundaries into sub-grains through the sliding mechanism. In addition, due to SPD, grains are broken to smaller ones. As seen in the TEM picture, no elongation occurred in the grains. Also, in CP Ti after 4 passes, the ECAP-treated grains are more homogeneously distributed as compared to the internal structure of the untreated grains. The reason of the homogeneous dispersion of the grains is that a 4-pass ECAP process is a complete turn of the deformation cycle.

The reasons for the improvement of the mechanical properties are excessive grain refining and increasing dislocations. Titanium, which has wide-angled ultrafine grains, blocks dislocation movements, and this increases strength. After stress reaches the maximum level, the untreated pure Ti exhibits a large strain neck area. Also, the heterogeneous deformation area is larger than the

homogeneous area. After the ECAP treatment, while the yield and tensile strength of pure Ti increase, the homogeneous deformation area is reduced, but the heterogeneous deformation area is still in the range of processibility. Hence, the deformability of the material is helpful for the surgeon during an operation.³⁰

Coaxial grooves and traces of plastic deformations are highly visible at the fracture sections. The examination of the grain size after the ECAP process showed that the coaxial cavity dimensions in the fracture images of these samples were smaller than in the untreated Ti.

Experimental studies with the 2-point bending tests have been carried out to achieve lesser displacement of the fracture region under load for different miniplate geometries and mounting positions.^{5,13} The fixations established with a double miniplate at the 5 mm displacement showed 140% higher load than the fixations established with a single miniplate.¹³ According to the results of this study, the fixation with the miniplate made from the ECAP-treated material at a displacement value of 5 mm endured 300% more than the fixation with the untreated miniplate.¹³

The studies which used the 3-point bending tests were conducted to obtain a more rigid fixation by changing the miniplate geometry, position and number. Ribeiro-Junior et al. used sagittal miniplates with different geometries and found that a sagittal-locked miniplate exhibited a more stable fixation than 4-hole and 6-hole locked and unlocked normal miniplates.³¹ In another study, Ribeiro-Junior et al. used locked and unlocked miniplates with 4 and 8 holes for fixations in the angular region.³² The 3-point bending tests were applied to the fixation systems. As a result of the study, they found that the locked fixation system with 8 holes was more rigid than the others.³² Nieblerová et al. used miniplates having the same geometry in single and double miniplate applications at 2 different positions; then, the 3-point bending tests were performed on the samples.³³ The authors reported that they achieved a more stable fixation when using a double miniplate. When these results were examined, it was seen that there was 55% less displacement in the fixation established using a double-bar miniplate under the 100 N load.³³ In our study, the fixation with the ECAP-treated miniplate was found to be 40% more rigid than the fixation which used the untreated miniplate.

The number of studies on the examination of the torsional force on the mandible is limited. However, when considering the geometry of the mandibular bone and the muscle forces acting on it, the torsional load has a significant role in curing mandibular fractures. When a load is applied on the opposite side of a fractured mandible, the torsional moment will occur. Feller et al. established different fixation systems, using microplates and miniplates, and then performed the torsion tests.²⁸ As a result of the study, they found that using a miniplate and a microplate in the same fixation made it more rigid as compared to

single-miniplate or single-microplate fixations.²⁸ In addition, due to the torsional moments which occur in the mini-screw because of torsion, screw loosening affects the patient's healing time. According to Champy, due to the moments which occur in the anterior region of the mandible, fixations should endure up to 1,000 N.m.^{acc.28} When the results of Feller et al. were examined, it was seen that the fixation established with a double miniplate was 4.25 times less displaced at 700 N.mm than the fixation established with a single miniplate.²⁸ In our study, it was observed that the fixations established with the miniplate produced from the ECAP-processed material were displaced 4.8 times less as compared to the fixations established with the untreated miniplate.

Conclusions

This study showed that fixation systems become more rigid when ECAP-treated miniplates are used, and this ensures lesser displacement of the fixation system. These results rely on the ECAP process, which causes the grain size to decrease and strength to increase. Due to these benefits, ECAP-treated miniplates exhibit more rigid behavior than their untreated equivalents. Along with this, ECAP-treated miniplates proved to be a suitable substitution for multiple miniplate fixations.

ORCID iDs

Hojjat Ghahramanzadeh Asl  <https://orcid.org/0000-0002-9078-1933>
Akgün Alsarar  <https://orcid.org/0000-0002-3258-2469>

References

- Hayter JP, Cawood JI. The functional case for miniplates in maxillofacial surgery. *Int J Oral Maxillofac Surg.* 1993;22(2):91–96.
- Regev E, Shiff JS, Kiss A, Fialkov JA. Internal fixation of mandibular angle fractures: A meta-analysis. *Plast Reconstr Surg.* 2010;125(6):1753–1760.
- Dogru SC, Cansiz E, Arslan YZ. Biomechanical evaluation of resorbable and titanium miniplates and of single and double miniplates for the treatment of mandibular condyle fractures. *Biocybern Biomed Eng.* 2019;39(3):709–718.
- Sukegawa S, Kanno T, Masui M, et al. Which fixation methods are better between three-dimensional anatomical plate and two miniplates for the mandibular subcondylar fracture open treatment? *J Craniomaxillofac Surg.* 2019;47(5):771–777.
- Oh JS, Kim SG. In vitro biomechanical evaluation of fixation methods of sagittal split ramus osteotomy in mandibular setback. *J Craniomaxillofac Surg.* 2015;43(2):186–191.
- Esen A, Dolanmaz D, Tüz HH. Biomechanical evaluation of malleable noncompression miniplates in mandibular angle fractures: An experimental study. *Br J Oral Maxillofac Surg.* 2012;50(5):e65–e68.
- Yener O, Saglam H, Dolanmaz D, Uckan S. Comparison of stability of 2.0 mm standard and 2.0 mm locking miniplate/screws for the fixation of sagittal split ramus osteotomy on sheep mandibles. *Br J Oral Maxillofac Surg.* 2011;49(2):135–137.
- Bayram B, Araz K, Uckan S, Balçık C. Comparison of fixation stability of resorbable versus titanium plate and screws in mandibular angle fractures. *J Oral Maxillofac Surg.* 2009;67(8):1644–1648.
- Zimmermann C, Henningsen A, Henkel KO, et al. Biomechanical comparison of a multidirectional locking plate and conventional plates for the osteosynthesis of mandibular angle fractures – a preliminary study. *J Craniomaxillofac Surg.* 2017;45(12):1913–1920.

10. Darwich MA, Albogha MH, Abdelmajeed A, Darwich K. Assessment of the biomechanical performance of 5 plating techniques in fixation of mandibular subcondylar fracture using finite element analysis. *J Oral Maxillofac Surg.* 2016;74(4):794.e1–e8.
11. Esen A, Ataoğlu H, Gemi L. Comparison of stability of titanium and absorbable plate and screw fixation for mandibular angle fractures. *Oral Surg Oral Med Oral Pathol Oral Radiol Endod.* 2008;106(6):806–811.
12. Trivellato PFB, Pepato AO, Ribeiro MC, Sverzut CE, Trivellato AE. In vitro evaluation of the resistance of a 2.0-mm titanium fixation system in the sectioned angle without continuity of the inferior border of the mandible. *Int J Oral Maxillofac Surg.* 2014;43(5):559–563.
13. Oguz Y, Watanabe ER, Reis JM, Spin-Neto R, Gabrielli MA, Pereira-Filho VA. In vitro biomechanical comparison of six different fixation methods following 5-mm sagittal split advancement osteotomies. *Int J Oral Maxillofac Surg.* 2015;44(8):984–988.
14. Gonzales DMC, Spagnol G, Sverzut CE, Trivellato AE. In vitro evaluation of the resistance of three types of fixation to treat fractures of the mandibular angle. *Br J Oral Maxillofac Surg.* 2017;55(2):136–140.
15. Sittitavornwong S, Denson D, Ashley D, Walma DC, Potter S, Freind J. Integrity of a single superior border plate repair in mandibular angle fracture: A novel cadaveric human mandible model. *J Oral Maxillofac Surg.* 2018;76(12):2611.e1–2611.e8.
16. Arbag H, Korkmaz HH, Ozturk K, Uyar Y. Comparative evaluation of different miniplates for internal fixation of mandible fractures using finite element analysis. *J Oral Maxillofac Surg.* 2008;66(6):1225–1232.
17. Hajizadeh K, Eghbali B, Topolski K, Kurzydowski KJ. Ultra-fine grained bulk CP-Ti processed by multi-pass ECAP at warm deformation region. *Mater Chem Phys.* 2014;143(3):1032–1038.
18. Rosochowski A. Processing metals by severe plastic deformation. *Solid State Phenom.* 2005;101–102:13–22.
19. Purcek G, Yapici GG, Karaman I, Maier HJ. Effect of commercial purity levels on the mechanical properties of ultrafine-grained titanium. *Mater Sci Eng A.* 2011;528(6):2303–2308.
20. Iwahashi Y, Wang J, Horita Z, Nemoto M, Langdon TG. Principle of equal-channel angular pressing for the processing of ultra-fine grained materials. *Scr Mater.* 1996;35(2):143–146.
21. Figueiredo RB, de C. Barbosa ER, Zhao X, et al. Improving the fatigue behavior of dental implants through processing commercial purity titanium by equal-channel angular pressing. *Mater Sci Eng A.* 2014;619:312–318.
22. Valiev RZ, Islamgaliev RK, Alexandrov IV. Bulk nanostructured materials from severe plastic deformation. *Prog Mater Sci.* 2000;45(2):103–189.
23. Valiev RZ, Semenova IP, Latysh VV, et al. Nanostructured titanium for biomedical applications. *Adv Eng Mater.* 2008;10(8):B15–B17.
24. Estrin Y, Kim HE, Lapovok R, Ng HP, Jo JH. Mechanical strength and biocompatibility of ultrafine-grained commercial purity titanium. *Biomed Res Int.* 2013;2013:914764.
25. Polyakov AV, Semenova IP, Valiev RZ. High fatigue strength and enhanced biocompatibility of UFG CP Ti for medical innovative applications. *Mater Sci Eng.* 2013;63:012113.
26. Rudderman RH, Mullen RL, Phillips JH. The biophysics of mandibular fractures: An evolution toward understanding. *Plast Reconstr Surg.* 2008;121(2):596–607.
27. Hakim SG, Wolf M, Wendlandt R, Kimmerle H, Sieg P, Jacobsen HC. Comparative biomechanical study on three miniplates osteosynthesis systems for stabilisation of low condylar fractures of the mandible. *Br J Oral Maxillofac Surg.* 2014;52(4):317–322.
28. Feller KU, Richter G, Schneider M, Eckelt U. Combination of microplate and miniplate for osteosynthesis of mandibular fractures: An experimental study. *Int J Oral Maxillofac Surg.* 2002;31(1):78–83.
29. Meredith CS, Khan AS. The microstructural evolution and thermo-mechanical behavior of UFG Ti processed via equal channel angular pressing. *J Mater Process Technol.* 2015;219:257–270.
30. Shikinami Y, Okuno M. Bioresorbable devices made of forged composites of hydroxyapatite (HA) particles and poly l-lactide (PLLA). Part II: Practical properties of miniscrews and miniplates. *Biomaterials.* 2001;22(23):3197–3211.
31. Ribeiro-Junior PD, Magro-Filho O, Shastri KA, Papageorge MB. Which kind of miniplate to use in mandibular sagittal split osteotomy? An in vitro study. *Int J Oral Maxillofac Surg.* 2012;41(11):1369–1373.
32. Ribeiro-Junior PD, Magro-Filho O, Shastri KA, Papageorge MB. In vitro evaluation of conventional and locking miniplate/screw systems for the treatment of mandibular angle fractures. *Int J Oral Maxillofac Surg.* 2010;39(11):1109–1114.
33. Nieblerová J, Foltán R, Hanzelka T, et al. Stability of the miniplate osteosynthesis used for sagittal split osteotomy for closing an anterior open bite: An experimental study in mini-pigs. *Int J Oral Maxillofac Surg.* 2012;41(4):482–488.

Deviation of dental implants placed using a novel 3D-printed surgical guide: An in vitro study

Enas Abdalla Etajuri^{1,A–D,F}, Eshamsul Suliman^{1,A,F}, Wan Adida Azina Mahmood^{1,A,E}, Norliza Ibrahim^{2,B,E}, Muaiyed Buzayan^{1,D}, Noorhayati Raja Mohd^{1,B,E}

¹ Department of Restorative Dentistry, Faculty of Dentistry, University of Malaya, Kuala Lumpur, Malaysia

² Department of Oral and Maxillofacial Surgical Sciences, Faculty of Dentistry, University of Malaya, Kuala Lumpur, Malaysia

A – research concept and design; B – collection and/or assembly of data; C – data analysis and interpretation;

D – writing the article; E – critical revision of the article; F – final approval of the article

Dental and Medical Problems, ISSN 1644-387X (print), ISSN 2300-9020 (online)

Dent Med Probl. 2020;57(4):359–362

Address for correspondence

Enas Abdalla Etajuri
E-mail: enas@um.edu.my

Funding sources

Research grant No. PPPC/C1-2015/DGS/25,
University of Malaya, Kuala Lumpur, Malaysia.

Conflict of interest

None declared

Received on May 2, 2020
Reviewed on May 30, 2020
Accepted on June 15, 2020

Published online on December 31, 2020

Cite as

Etajuri EA, Suliman E, Mahmood WAA, Ibrahim N, Buzayan M, Mohd NR. Deviation of dental implants placed using a novel 3D-printed surgical guide: An in vitro study. *Dent Med Probl.* 2020;57(4):359–362. doi:10.17219/dmp/123976

DOI

10.17219/dmp/123976

Copyright

© 2020 by Wrocław Medical University
This is an article distributed under the terms of the
Creative Commons Attribution 3.0 Unported License (CC BY 3.0)
(<https://creativecommons.org/licenses/by/3.0/>).

Abstract

Background. There is very little literature available on the reliability of the rapid prototyping technology in the production of three-dimension (3D)-printed surgical guides for accurate implant placement.

Objectives. The aim of the study was to evaluate the deviation of implant placement performed with a surgical guide fabricated by means of the rapid prototyping technique (the PolyJet™ technology).

Material and methods. Twenty sheep mandibles were used in the study. Pre-surgical cone-beam computed tomography (CBCT) scans were acquired for the mandibles by using the Kodak 9000 3D cone-beam system. Two implants with dimensions of 4 mm in diameter and 10 mm in length were virtually planned on the 3D models of each mandible by using the Mimics software, v. 16.0. Twenty surgical guides were designed and printed using the PolyJet technology. A total of 40 implants were placed using the surgical guides, 1 on each side of the mandible (2 implants per mandible). The post-surgical CBCT scans of the mandibles were performed and superimposed on the pre-surgical CBCT scans. The amount of deviation between the virtually planned placement and the actual implant placement was measured, and a descriptive analysis was done.

Results. The results showed that the mean deviation at the implant coronal position was 1.82 ± 0.74 mm, the mean deviation at the implant apex was 1.54 ± 0.88 mm, the mean depth deviation was 0.44 ± 0.32 mm, and the mean angular deviation was $3.01 \pm 1.98^\circ$.

Conclusions. The deviation of dental implant placement performed with a 3D-printed surgical guide (the PolyJet technology) is within the acceptable 2-millimeter limit reported in the literature.

Key words: dental implant, 3D-printing, cone-beam computed tomography, computer-aided design/computer-aided manufacturing

Introduction

Osseointegration is well-known and established as the key factor for success in implant dentistry,^{1–3} but nowadays, the success of dental implants should also be determined by functional and esthetic restorative objectives.^{4,5} The use of three-dimensionally (3D) guided implant placement is currently recommended to achieve these objectives and avoid surgical complications, such as unfavorable anatomical structures.^{6,7}

In the 21st century, digitalization plays a role in all aspects of life. It also refers to the field of dentistry. In implantology particularly, precise implant placement has become more predictable with the development of technology and with the invention of cone-beam computed tomography (CBCT) imaging in conjunction with the 3D reconstruction of structures, the virtual planning of the implant and surgical guides constructed using stereolithography (SLA).^{8,9}

Compared with the conventional computed tomography (CT), CBCT generates 6 times less radiation, enabling the acquisition of the 3D images of the soft and hard tissues of the patient with lower doses of radiation.^{10–12} A CBCT scan is able to show objects in 3D as precisely as a CT scan and can help replicate the tissues accurately enough to plan surgical procedures.^{13,14}

There are several software programs that permit virtual implant planning by using the 3D images of CBCT scans. A virtually planned implant can later be transferred to the patient; however, the accurate transfer of a virtually planned implant to the patient is the main concern.^{8,15–17}

The positioning of a virtually planned implant in the patient's mouth can be performed using a surgical guide, which can be either constructed on a cast (the conventional manual method) or created virtually by means of computer software and a milling process with the SLA technology.¹⁸ The PolyJet™ technology is an additive manufacturing process in which inkjet technologies are used to create physical models. The head of the inkjet moves along the X and Y axes, depositing the layers of the photopolymer, which are exposed to ultraviolet lamps for curing. The layer thickness produced in this process is 16 µm, which is considered high-resolution production.¹⁹

The aim of the present study was to evaluate deviations in implant placement performed using a surgical guide produced by the rapid prototype technique (the PolyJet technology).

Material and methods

A total of 20 sheep mandibles were collected from typical butcher shops and scanned using the Kodak 9000 3D cone-beam system (Carestream Health Inc., Rochester, USA). The setting of the CBCT machine was standardized at 70 kV, 120 mAs. The data was saved as DICOM

files and sent to the Mimics software, v. 16 (Materialise NV, Leuven, Belgium). For each of the 20 scanned mandibles, 2 implants (Neobiotech Co., Ltd., Seoul, South Korea) – 4 mm in diameter and 10 mm in length – were virtually planned on the Mimics software 3D model of the mandible.

A total of 40 virtual implants were planned (Fig. 1). The data was transformed into STL files and sent to the Centre for Biomedical and Technology Integration (CBMTI) Sdn. Bhd, at the Institute of Postgraduate Studies (IPS) of the University of Malaya in Kuala Lumpur, Malaysia, to design and print surgical guides for each mandible by using the PolyJet technology (Solid Concepts Inc., Valencia, USA).

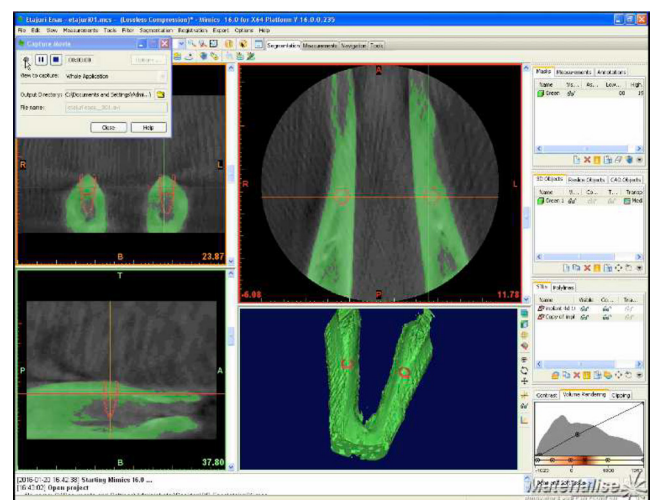


Fig. 1. Screenshot of virtual implant planning with the Mimics software

A total of 20 surgical guides were designed to accept a series of 5 stainless steel drill guides (sleeves) to accommodate 1.9-, 2.2-, 2.9-, 3.4-, and 4-millimeter twist drills. Each mandible sample was fixed on a plastic plate by using the ProBase® cold-cure acrylic resin (Ivoclar Vivadent Inc., Schaan, Liechtenstein) for drilling and scanning. Two implants were placed on the right and left sides of each mandible (Fig. 2).



Fig. 2. 3D-printed surgical guide and the drilling guides fitted on a mandible

Post-surgical CBCT scans were taken, adhering to the same position and settings of the machine as those used to perform pre-surgical CBCT scans. The data was sent to the Mimics software. The pre- and post-surgical 3D models were superimposed (Fig. 3), and the implant deviations in the coronal, apex, depth, and angular positions were measured using the Mimics software. The data was collected and a descriptive statistical analysis was done using IBM SPSS Statistics for Windows, v. 24.0 (IBM Corp., Armonk, USA).

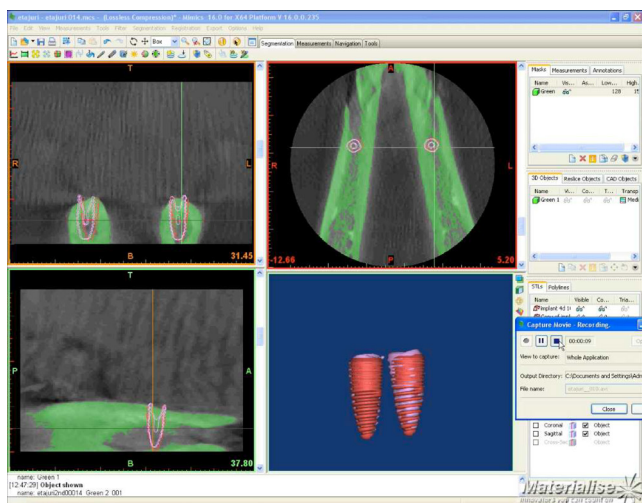


Fig. 3. Screenshot of the Mimics software showing the positions of the virtual and the placed implants after superimposing

Results

The implant deviation recorded at the coronal position ranged from 0.68 mm to 3.85 mm. The apex deviation ranged from 0.09 mm to 3.91 mm. The depth deviation ranged from 0.02 mm to 1.19 mm. The recorded angular deviation ranged from 0.38° to 6.72° (Table 1).

Table 1. Deviations of implant placement performed using a 3D-printed surgical guide

Deviation	Minimum	Maximum	<i>M</i>	<i>SD</i>
Coronal [mm]	0.68	3.85	1.82	0.74
Apex [mm]	0.09	3.91	1.54	0.88
Depth [mm]	0.02	1.19	0.44	0.32
Angular [°]	0.38	6.72	3.01	1.98

M – mean; *SD* – standard deviation.

Discussion

The average linear and angular deviations found in this study were within the clinically accepted limit, and are comparable to the previously published results.^{20–23} Accordingly, it can be suggested that the use of the rapid prototype technology to produce virtually planned and designed surgical guides following virtual implant placement is a potentially promising technique that can assist surgeons in placing implants in more precise positions.

Unlike previous studies, which used cast models^{24,25} or cadaver jaws,^{26,27} this study used sheep mandibular bones to simulate in vivo the drilling of a natural bone. In addition, the sheep mandibular bone has an adequate height and a sufficient edentulous area between the anterior and posterior teeth.

For each mandible, the distance between the planned and the actually placed implant axis was measured at 4 points – the linear distance between the central axis at the platform and the apex, the angular deviation and the depth deviation – with the use of the Mimics software.^{25,27}

The present study demonstrates the deviation of implant placement performed using a surgical guide (prototype) following 3D virtual planning. The results showed that the mean deviation at the implant platform was 1.82 ± 0.74 mm, the mean deviation at the implant apex was 1.54 ± 0.88 mm, the mean depth deviation was 0.44 ± 0.32 mm, and the mean angular deviation was $3.01 \pm 1.98^\circ$.

In a previous in vivo study, the distance between the virtually planned implants and the implants placed using an SLA surgical guide was evaluated.²⁸ The results showed a mean deviation between the planned and the positioned implants of 1.45 ± 1.42 mm at the implant platform, 2.99 ± 1.77 mm at the apex and an angular deviation of $7.25 \pm 2.67^\circ$.²⁸ In comparison, our results showed smaller deviations between the planned and the positioned implants, with smaller standard deviations (*SDs*).

It seems that the implant deviation is influenced by the surgeon's experience. Our findings show slightly higher deviations than those presented by Noharet et al.²⁷ This is because in their study, an experienced surgeon placed all dental implants,²⁷ while in our study, an inexperienced clinician performed implant placement. This factor has been discussed in other studies, where it was found that the accuracy of implant placement is affected by the surgeon's experience.^{29,30}

The implant deviations demonstrated in the present study were slightly higher than those in an in vitro study by Pettersson et al., in which 150 implants were placed in plastic models by using surgical guides designed according to virtual planning.²⁵ In their study, the implant deviation at the platform was 0.59 ± 0.60 mm, with 0.73 ± 0.73 mm at the apex, -0.51 to -0.52 mm in depth, where the actually placed implants did not reach the depth of the virtually planned implants, and the angular deviation of $0.61 \pm 1.27^\circ$. In that study, the surgical guide was designed with 3 anchor pins to stabilize it while drilling.²⁵ In contrast, the surgical guide in the current study was designed without any stabilizing pin, which might have had an effect on the stability of the guide during drilling, resulting in more implant deviations. Additionally, the diameters of the sleeves used in our study were bigger by about 0.2 mm than the drill diameters, which may have contributed to slightly higher deviations. Moreover, sheep mandibular bones are hard and stiff, requiring

more force during drilling than the plastic models used by Pettersson et al., which the authors said were easy to drill.²⁵ Thus, the model material could also have contributed to higher implant deviations in our study.

In a recent systematic review and meta-analysis of 2,238 implants placed using surgical guides, the mean linear coronal deviation was 1.04–1.44 mm and 1.28–1.58 mm at the apex, while the average angular deviation was 3.00–3.96°.³¹ Therefore, the results of the present study did not differ much from the clinical situation.

Conclusions

Within the limitations of this study, it can be concluded that surgical guides produced using the rapid prototype technique (the PolyJet technology) can be applied to minimize the implant placement deviation. However, further clinical trials are suggested.

ORCID iDs

Enas Abdalla Etajuri  <https://orcid.org/0000-0002-5389-2298>
 Eshamsul Suliman  <https://orcid.org/0000-0002-8438-8107>
 Wan Adida Azina Mahmood  <https://orcid.org/0000-0003-0463-3211>
 Norliza Ibrahim  <https://orcid.org/0000-0003-0591-1076>
 Muaiyed Buzayan  <https://orcid.org/0000-0002-6691-2008>
 Noorhayati Raja Mohd  <https://orcid.org/0000-0001-5106-3579>

References

- Adell R, Lekholm U, Rockler B, Brånemark PI. A 15-year study of osseointegrated implants in the treatment of the edentulous jaw. *Int J Oral Surg*. 1981;10(6):387–416.
- Albrektsson T, Zarb G, Worthington P, Eriksson AR. The long-term efficacy of currently used dental implants: A review and proposed criteria of success. *Int J Oral Maxillofac Implants*. 1986;1(1):11–25.
- Esposito M, Hirsch JM, Lekholm U, Thomsen P. Biological factors contributing to failures of osseointegrated oral implants. (II). Etiopathogenesis. *Eur J Oral Sci*. 1998;106(3):721–764.
- Palmer RM. Risk management in clinical practice. Part 9: Dental implants. *Br Dent J*. 2010;209(10):499–506.
- Checchi V, Gasparro R, Pistilli R, Canullo L, Felice P. Clinical classification of bone augmentation procedure failures in the atrophic anterior maxillae: Esthetic consequences and treatment options. *Biomed Res Int*. 2019;2019:4386709.
- Attard NJ, Zarb GA. Long-term treatment outcomes in edentulous patients with implant overdentures: The Toronto study. *Int J Prosthodont*. 2004;17(4):425–433.
- Sun Y, Luebbbers HT, Agbaje JO, et al. Accuracy of a dedicated bone-supported surgical template for dental implant placement with direct visual control. *J Healthc Eng*. 2015;6(4):779–789.
- Cushen SE, Turkyilmaz I. Impact of operator experience on the accuracy of implant placement with stereolithographic surgical templates: An in vitro study. *J Prosthet Dent*. 2013;109(4):248–254.
- Moin DA, Derksen W, Waars H, Hassan B, Wismeijer D. Computer-assisted template-guided custom-designed 3D-printed implant placement with custom-designed 3D-printed surgical tooling: An in vitro proof of a novel concept. *Clin Oral Implants Res*. 2017;28(5):582–585.
- Posadzy M, Desimpel J, Vanhoenacker F. Cone beam CT of the musculoskeletal system: Clinical applications. *Insights Imaging*. 2018;9(1):35–45.
- Bornstein MM, Scarfe WC, Vaughn VM, Jacobs R. Cone beam computed tomography in implant dentistry: A systematic review focusing on guidelines, indications, and radiation dose risks. *Int J Oral Maxillofac Implants*. 2014;29(Suppl):55–77.
- Pettersson A, Komiyama A, Hultin M, Näsström K, Klinge B. Accuracy of virtually planned and template guided implant surgery on edentate patients. *Clin Implant Dent Relat Res*. 2012;14(4):527–537.
- Kulczyk T, Rychlik M, Lorkiewicz-Muszyńska D, Abreu-Głowacka M, Czajka-Jakubowska A, Przystańska A. Computed tomography versus optical scanning: A comparison of different methods of 3D data acquisition for tooth replication. *Biomed Res Int*. 2019;2019:4985121.
- Arisan V, Karabuda ZC, Pişkin B, Özdemir T. Conventional multi-slice computed tomography (CT) and cone-beam CT (CBCT) for computer-aided implant placement. Part II: Reliability of mucosa-supported stereolithographic guides. *Clin Implant Dent Relat Res*. 2013;15(6):907–917.
- Bover-Ramos F, Viña-Almunia J, Cervera-Ballester J, Peñarocha-Diago M, García-Mira B. Accuracy of implant placement with computer-guided surgery: A systematic review and meta-analysis comparing cadaver, clinical, and in vitro studies. *Int J Oral Maxillofac Implants*. 2018;33(1):101–115.
- Bell CK, Sahl EF, Kim YJ, Rice DD. Accuracy of implant placed with surgical guides: Thermoplastic versus 3D printed. *Int J Periodontics Restorative Dent*. 2018;38(1):113–119.
- Turbush SK, Turkyilmaz I. Accuracy of three different types of stereolithographic surgical guide in implant placement: An in vitro study. *J Prosthet Dent*. 2012;108(3):181–188.
- Katsoulis J, Pazera P, Mericske-Stern R. Prosthetically driven, computer-guided implant planning for the edentulous maxilla: A model study. *Clin Implant Dent Relat Res*. 2009;11(3):238–245.
- Wong KV, Hernandez A. A review of additive manufacturing. *Int Sch Res Notices*. 2012;2012:208760.
- Vieira DM, Sotto-Maior BS, Villaça de Souza Barros CA, Reis ES, Francischone CE. Clinical accuracy of flapless computer-guided surgery for implant placement in edentulous arches. *Int J Oral Maxillofac Implants*. 2013;28(5):1347–1351.
- Cassetta M, Giansanti M, Di Mambro A, Stefanelli LV. Accuracy of positioning of implants inserted using a mucosa-supported stereolithographic surgical guide in the edentulous maxilla and mandible. *Int J Oral Maxillofac Implants*. 2014;29(5):1071–1078.
- Verhamme LM, Meijer GJ, Bergé SJ, et al. An accuracy study of computer-planned implant placement in the augmented maxilla using mucosa-supported surgical templates. *Clin Implant Dent Relat Res*. 2015;17(6):1154–1163.
- Verhamme LM, Meijer GJ, Soehardi A, Bergé SJ, Xi T, Maal TJJ. An accuracy study of computer-planned implant placement in the augmented maxilla using osteosynthesis screws. *Int J Oral Maxillofac Surg*. 2017;46(4):511–517.
- Kühl S, Zürcher S, Mahid T, Müller-Gerbl M, Filippi A, Cattin P. Accuracy of full guided vs half-guided implant surgery. *Clin Oral Implants Res*. 2013;24(7):763–769.
- Pettersson A, Kero T, Söderberg R, Näsström K. Accuracy of virtually planned and CAD/CAM-guided implant surgery on plastic models. *J Prosthet Dent*. 2014;112(6):1472–1478.
- Van Assche N, van Steenberghe D, Guerrero ME, et al. Accuracy of implant placement based on pre-surgical planning of three-dimensional cone-beam images: A pilot study. *J Clin Periodontol*. 2007;34(9):816–821.
- Noharet R, Pettersson A, Bourgeois D. Accuracy of implant placement in the posterior maxilla as related to 2 types of surgical guides: A pilot study in the human cadaver. *J Prosthet Dent*. 2014;112(3):526–532.
- Di Giacomo GAP, Cury PR, de Araujo NS, Sendyk WR, Sendyk CL. Clinical application of stereolithographic surgical guides for implant placement: Preliminary results. *J Periodontol*. 2005;76(4):503–507.
- Vasak C, Watzak G, Gahleitner A, Strbac G, Schemper M, Zechner W. Computed tomography-based evaluation of template (NobelGuide™)-guided implant positions: A prospective radiological study. *Clin Oral Implants Res*. 2011;22(10):1157–1163.
- Park SJ, Leesungbok R, Cui T, Lee SW, Ahn SJ. Reliability of a CAD/CAM surgical guide for implant placement: An in vitro comparison of surgeons' experience levels and implant sites. *Int J Prosthodont*. 2017;30(4):367–369.
- Tahmaseb A, Wu V, Wismeijer D, Coucke W, Evans C. The accuracy of static computer-aided implant surgery: A systematic review and meta-analysis. *Clin Oral Implants Res*. 2018;29(Suppl):416–435.

Preparation and biodegradable properties of hydroxyapatite nanoparticle composite coated with poly lactic-co-glycolic acid/polyvinyl alcohol for bone regeneration

Feni Istikharoh^{1,2,A-D}, Hidayat Sujuti^{3,E,F}, Edi Mustamsir^{4,E,F}, Astika Swastirani^{5,B,D}

¹ Master Program in Biomedical Science, Faculty of Medicine, Brawijaya University, Malang, Indonesia

² Department of Dental Materials, Faculty of Dentistry, Brawijaya University, Malang, Indonesia

³ Department of Biochemistry, Faculty of Medicine, Brawijaya University, Malang, Indonesia

⁴ Department of Orthopedics, Faculty of Medicine, Brawijaya University, Malang, Indonesia

⁵ Department of Oral Medicine, Faculty of Dentistry, Brawijaya University, Malang, Indonesia

A – research concept and design; B – collection and/or assembly of data; C – data analysis and interpretation;

D – writing the article; E – critical revision of the article; F – final approval of the article

Dental and Medical Problems, ISSN 1644-387X (print), ISSN 2300-9020 (online)

Dent Med Probl. 2020;57(4):363–367

Address for correspondence

Feni Istikharoh

E-mail: feni.istikharoh@ub.ac.id

Funding sources

LPPM PNBP 2019 from Brawijaya University, Malang, Indonesia (No. DIPA-042.01.2.400919/2019).

Conflict of interest

None declared

Received on August 28, 2019

Reviewed on June 15, 2020

Accepted on July 27, 2020

Published online on December 31, 2020

Cite as

Istikharoh F, Sujuti H, Mustamsir E, Swastirani A. Preparation and biodegradable properties of hydroxyapatite nanoparticle composite coated with poly lactic-co-glycolic acid/polyvinyl alcohol for bone regeneration. *Dent Med Probl.* 2020;57(4):363–367. doi:10.17219/dmp/125775

DOI

10.17219/dmp/125775

Copyright

© 2020 by Wrocław Medical University

This is an article distributed under the terms of the

Creative Commons Attribution 3.0 Unported License (CC BY 3.0)

(<https://creativecommons.org/licenses/by/3.0/>).

Abstract

Background. Bone loss rapidly increases 6 months post tooth extraction, which causes the atrophy of the alveolar bone. Two kinds of biomaterials which can stimulate bone regeneration are bioceramics and polymers. Making a composite of biomaterials results in better physical and biomolecular characteristics in comparison with a bioceramic or a polymer alone. Hydroxyapatite nanoparticles (HANPs) are one of the bioceramics commonly used for bone regeneration; they can degrade faster than hydroxyapatite (HA) microparticles, but have an insufficient pore size. Polyvinyl alcohol (PVA) and poly lactic-co-glycolic acid (PLGA) are polymers which have been used for biomedical applications. However, PLGA alone has insufficient cell attachment and PVA alone slowly degrades in the bone tissue.

Objectives. The aim of the present study was to analyze the biodegradation properties of the HANP/PLGA/PVA composites and investigate the pore size.

Material and methods. The HANP/PLGA/PVA composites were prepared using the freeze-drying method, with 20% (w/w) of HANP and 20% (w/w) of PLGA. Morphology and the pore size were determined by means of the field emission scanning electron microscopy (FE-SEM) analysis. Biodegradation properties were determined by calculating water uptake and water loss for 1, 3 and 6 weeks. Statistical analysis was performed based on the one-way analysis of variance (ANOVA) at $p < 0.05$.

Results. The HANP/PLGA/PVA composites had the greatest mean pore size and a rougher surface than others ($176.00 \pm 61.93 \mu\text{m}$; $p < 0.05$). Moreover, the HANP/PLGA/PVA composites had the greatest water uptake, significantly in the 3rd (730.46%; $p < 0.05$) and 6th weeks (731.07%; $p < 0.05$), and water loss in the 6th week (67.69%; $p < 0.05$).

Conclusions. The HANP/PLGA/PVA composites have optimal pore size, morphology and degradability, which shows their high potential as an effective bone scaffold to repair the alveolar defect post tooth extraction.

Key words: biodegradable, bone regeneration, hydroxyapatite nanoparticle, polyvinyl alcohol, poly lactic-co-glycolic acid

Introduction

Tooth extraction is one of the most common kinds of dental treatment in developing countries.^{1,2} A total of 944 tooth extraction procedures were performed in 450 patients throughout the year 2014 at Jember Dental Hospital, Indonesia, indicating that each patient was subjected to tooth extraction treatment at least twice a year, on average.³ Tooth extraction may negatively impact the alveolar bone, which can result in the atrophy of the alveolar bone, the collapse of the soft tissue, and a short and narrow alveolar ridge.^{4–7} The alveolar bone obviously will lose its function and rapidly disappear in the first 6 months post-extraction.⁴ Other consequences of bone loss include the reduction of esthetics, the inhibition of mastication processes, and the insufficient support of dental implants or prosthetic restorations.^{4–8} Accordingly, it is important to develop biomaterials which could stimulate bone regeneration and prevent bone loss, or for alveolar preservation.

Bone is an inorganic-organic composite material consisting of hydroxyapatite (HA) as the main component.^{9,10} In Indonesia, the most widely used bone grafting material to avoid bone loss following tooth extraction is HA.¹¹ However, HA slowly degrades, over approx. 24 months.^{10–13} It is a brittle material, and thus its application is limited to low-pressure areas. Hydroxyapatite nanoparticles (HANPs) are one of the bioceramics that have better osteoconductivity, biocompatibility and biodegradability, and also exhibit enhanced osteoblast adhesion as compared to those of conventional HA.^{10–12,14} This bioceramic may also be able to increase the tensile strength of the scaffold.¹⁰ However, HANPs have insufficient porosity and pore size.^{10,14} The ideal range of the pore size to promote bone regeneration is 50–300 μm .^{15–17} Accordingly, composites constituted by a combination of HANPs and other materials are needed to overcome the limitations of conventional HA.¹⁴

Polyvinyl alcohol (PVA) and poly lactic-co-glycolic acid (PLGA) are synthetic polymers which possess good stability for bone repair and regeneration.^{10,18} Polyvinyl alcohol exhibits highly favorable properties, such as biocompatibility, and physicochemical characteristics, and has been used for biomedical applications.^{19,20} It has shown better mechanical stability than other polymers, as demonstrated in previous studies. However, the degradation of PVA is very slow.^{10,19} Poly lactic-co-glycolic acid is one of the best biodegradable materials, which is also used as a drug carrier. It degrades into non-toxic products.^{21–23} Nevertheless, neither PVA nor PLGA support cell adhesion. They also have low mechanical support.^{10,19} One study showed that the addition of HA to a polymer scaffold resulted in enhanced osteoblast attachment, mineralization and metabolic activity.¹⁰

The present study focused on the development of the HANP/PLGA/PVA composites by using the freeze-drying method. This study aimed to analyze the biodegradation properties and pore size of the HANP/PLGA/PVA composites. The findings of the study are expected to provide

suggestions for synthetic bone grafts to avoid or recover bone loss following tooth extraction.

Material and methods

The following components were used: HANPs ± 60 nm (BATAN, Jakarta, Indonesia); PLGA 50:50 Mw 15,000–25,000 Da (PolySciTech, West Lafayette, USA); PVA fully hydrolyzed Mw 73,000 Da (Merck, Kenilworth, USA); phosphate-buffered saline (PBS) (Gibco™, Thermo Fisher Scientific, Waltham, USA); and ethyl acetate (Merck).

This study was conducted in May 2019. The study materials were divided into 4 groups: G1 (PVA alone); G2 (HANP/PVA); G3 (PLGA/PVA); and G4 (HANP/PLGA/PVA). The HANP/PLGA/PVA composites contained 20% (w/w) of HANP and 20% (w/w) of PLGA. All of these composite specimens were prepared by means of the freeze-drying method at -80°C for 24 h.

The pore size analysis was determined by field emission scanning electron microscopy (FE-SEM) (FEI Quanta™ FEG 650; Thermo Fisher Scientific, Waltham, USA).

The biodegradation test was performed in triplicate ($n = 3$) by immersing the composites in 10 mL of the PBS solution (pH 7.4). They were then incubated at 37°C for 1, 3 and 6 weeks. All the composite specimens were weighed before immersing to determine their initial weight (W_i). At the end of each degradation period, the swollen weight was measured immediately (W_s). The composite specimens were then dried to determine the final dried weight (W_f). Subsequently, the water uptake and water loss values were also determined. To calculate the water uptake value, equation 1 was used:

$$\text{Water uptake} = \left[\frac{W_s - W_f}{W_f} \right] \times 100 \quad [\%] \quad (1)$$

where:

W_s – swollen weight [mg];

W_f – final dried weight [mg].

Additionally, the water loss value was calculated with equation 2:

$$\text{Water loss} = \left[\frac{W_i - W_f}{W_i} \right] \times 100 \quad [\%] \quad (2)$$

where:

W_i – initial weight [mg];

W_f – final dried weight [mg].

Each measured sample contained 3 parallel test samples. Statistical analysis was performed using the one-way analysis of variance (ANOVA) (IBM SPSS Statistics for Windows, v. 25.0; IBM, Corp., Armonk, USA) and was considered statistically significant at $p < 0.05$.

Results

Figure 1 shows the FE-SEM images of the surface morphology and pore size of the composites. The representatives of the FE-SEM images show the natural distribution of the pore formation in the scaffold. Table 1 shows that the HANP/PLGA/PVA composites had the greatest pore size. Table 2 presents the initial weights, swollen weights and final dried weights of all composite specimens, which influenced the percentage of water uptake and water loss. Figure 2 shows the comparison of water uptake percentages for all composite specimens at different periods of time. The HANP/PLGA/PVA composites showed the highest water uptake percentage in the 3rd and 6th weeks (730.46% and 731.07%, respectively), indicating that water absorption was increased 7-fold as compared to the initial weight. Figure 3 shows that the HANP/PLGA/PVA composites exhibited a greater water loss value in the 6th week (67.69%) than other composites. With the absence of PLGA, the swelling ratio (water uptake percentage) of the HANP/PVA composites was half that of the HANP/PLGA/PVA composites, indicating that the incorporation of PLGA into the scaffold enhanced the biodegradation rate of the composites.

Table 1. Pore size of the composites (n = 3)

Composite	Pore size [μm]
PVA alone	51.34 ±31.85
HANP/PVA	54.53 ±35.74
PLGA/PVA	138.46 ±68.54*
HANP/PLGA/PVA	176.00 ±61.93*

Data presented as mean (M) ± standard deviation (SD).

* statistically significant differences in relation to all other groups (p < 0.05).

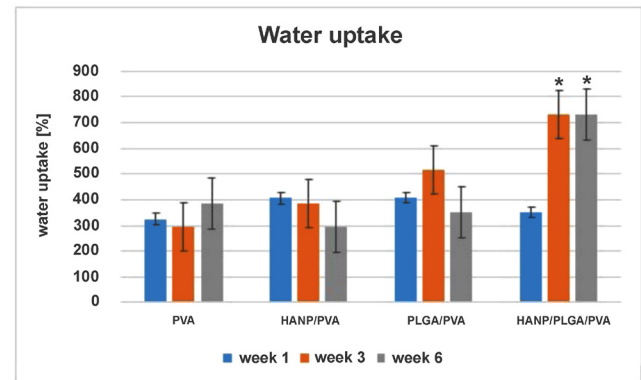


Fig. 2. Percentages of water uptake of the composites

* p < 0.05.

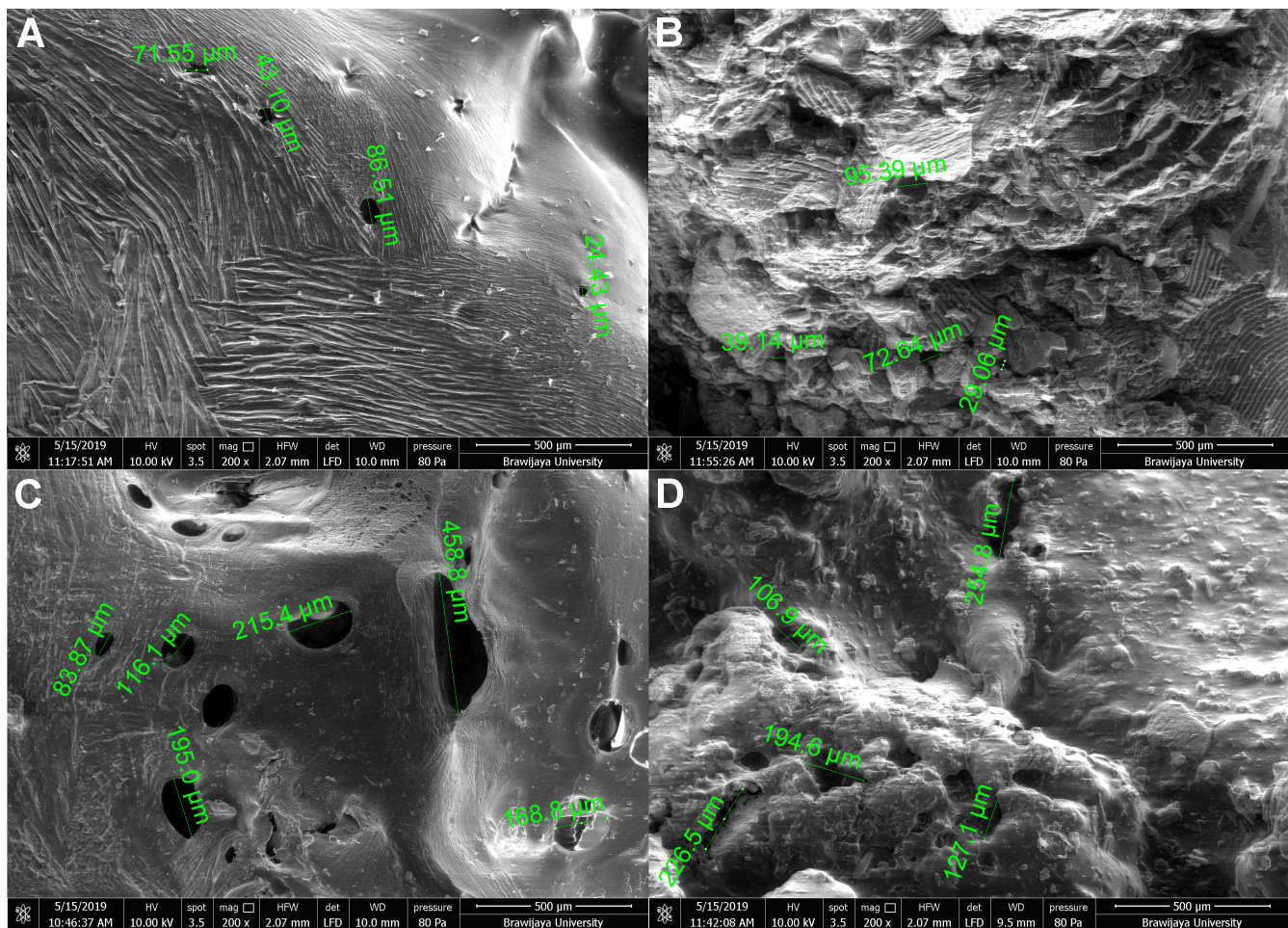


Fig. 1. Morphological analysis of the composites with field emission scanning electron microscopy (FE-SEM)

A – PVA alone; B – HANP/PVA; C – PLGA/PVA; D – HANP/PLGA/PVA.

PVA – polyvinyl alcohol; HANP – hydroxyapatite nanoparticle; PLGA – poly lactic-co-glycolic acid.

Table 2. Weights of the composites ($n = 3$)

Composite	W_i [mg]	Week 1		Week 3		Week 6	
		W_s [mg]	W_f [mg]	W_s [mg]	W_f [mg]	W_s [mg]	W_f [mg]
PVA alone	340.00 \pm 12.29	768.00 \pm 28.16	180.33 \pm 15.70	694.30 \pm 4.04	175.33 \pm 13.58	648.00 \pm 9.64	121.00 \pm 11.79
HANP/PVA	401.30 \pm 64.53	894.67 \pm 6.66	177.00 \pm 4.00	751.30 \pm 2.52	154.67 \pm 9.07	658.33 \pm 12.86	167.33 \pm 10.07
PLGA/PVA	352.67 \pm 75.70	913.00 \pm 7.55*	179.67 \pm 1.15	904.67 \pm 5.86	147.00 \pm 8.19	759.00 \pm 10.58	168.00 \pm 16.09
HANP/PLGA/PVA	348.67 \pm 49.89	902.33 \pm 16.26	200.33 \pm 18.77	1,027.00 \pm 29.51*	123.67 \pm 14.19*	936.30 \pm 8.50*	154.67 \pm 11.59

Data presented as $M \pm SD$.

W_i – initial weight; W_s – swollen weight; W_f – final dried weight; * statistically significant differences in relation to all other groups ($p < 0.05$).

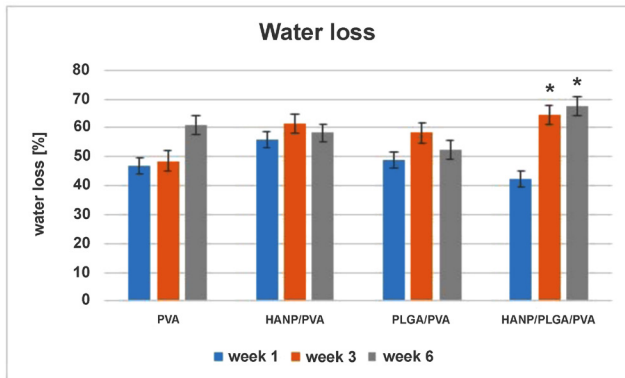


Fig. 3. Percentages of water loss of the composites

* $p < 0.05$.

Discussion

Over the last decade, polymer and bioceramic composites have attracted much attention as biomaterials to be developed for bone regeneration.^{12,14,24,25} Figure 1 shows that the surface area of the HANP/PLGA/PVA composites was rougher than that of other composites, indicating that the addition of HANPs to the scaffold increases the surface area and its roughness.¹⁵ The surface roughness of composites influences their interaction with the biological environment.^{26,27} It also enhances cell adhesion, differentiation and proliferation.^{26–29} The pore size is mainly responsible for cell proliferation, migration and nutrition.^{15,16} Specific cells require different pore sizes for optimal attachment and proliferation.²⁶ Research by Chang and Wang showed that osteoblast migration was faster through scaffolds with a pore size larger than 100 μm .²⁶ A study by Loh and Choong demonstrated that the optimal pore size of a scaffold to enhance cell migration and proliferation ranged from 100 μm to 350 μm .¹⁵ An interconnected network serves the improvement in the mechanical stability of the implant through the incorporation of PLGA.³⁰ Moreover, the selection of the technique to prepare the composite scaffold for bone regeneration has a great impact on the pore size and porosity of the scaffold.^{15,16,31,32} Freeze drying is a conventional technique that allows frozen water to sublimate directly and results in pore formation.^{15,31,32} The pore size of the composite depends on

the ratio of water to the polymer solution, the freezing temperature and the viscosity of the emulsion.¹⁵ The pore size also affects the expression of gene markers and the secretion of glycosaminoglycan (GAG).¹⁵ Biodegradable materials are ideal biomaterials in oral and maxillofacial surgery and in orthopedics, since they do not require a second surgical event for removal.^{4,13,18} In that vein, non-biodegradable composites have some significant drawbacks, including an increase in hospitalization time, in healthcare cost and in the risk of infection.³³

Conclusions

The presence of HANPs in the composites could affect the surface roughness and increase the surface area. The incorporation of PLGA into the scaffold could increase the pore size and biodegradation rate of the composites as compared to those of PVA alone or HANP/PVA. The HANP/PLGA/PVA composites demonstrated optimal pore size, morphology and degradability, which indicates their high potential as an effective bone scaffold to repair the alveolar defect following tooth extraction or for alveolar preservation.

ORCID iDs

Feni Istikharoh <https://orcid.org/0000-0003-2816-1036>

Hidayat Sujuti <https://orcid.org/0000-0003-2542-8575>

Edi Mustamsir <https://orcid.org/0000-0002-8914-6166>

Astika Swastirani <https://orcid.org/0000-0003-3300-7631>

References

- Fithri Z, Rochim A, Cholid Z. Distribution of tooth extraction based on sociodemographic characteristic of Dental Hospital of University of Jember patients in January–December 2014 [in Indonesian]. *e-J Pustaka Kesehatan*. 2017;5(1):177–184.
- Hansson S, Halldin A. Alveolar ridge resorption after tooth extraction: A consequence of a fundamental principle of bone physiology. *J Dent Biomech*. 2012;3:1758736012456543.
- Mahyudin F, Utomo DN, Suroto H, Martanto TW, Edward M, Gaol IL. Comparative effectiveness of bone grafting using xenograft freeze-dried cortical bovine, allograft freeze-dried cortical New Zealand white rabbit, xenograft hydroxyapatite bovine, and xenograft demineralized bone matrix bovine in bone defect of femoral diaphysis of white rabbit: Experimental study in vivo. *Int J Biomater*. 2017;2017:7571523.
- Sheikh Z, Najeeb S, Khurshid Z, Verma V, Rashid H, Glogauer M. Biodegradable materials for bone repair and tissue engineering applications. *Materials (Basel)*. 2015;8(9):5744–5794.

5. Tian Q, Lin J, Rivera-Castaneda L, et al. Nano-to-submicron hydroxyapatite coatings for magnesium-based bioresorbable implants – deposition, characterization, degradation, mechanical properties, and cytocompatibility. *Sci Rep*. 2019;9:810.
6. Barretto Montandon AA, Zuza EP, Corrêa de Toledo BE. Prevalence and reasons for tooth loss in a sample from a dental clinic in Brazil. *Int J Dent*. 2012;2012:ID 719750.
7. Taşşöker M, Menziletoğlu D, Baştürk F, Karabekiroğlu S, Şener S. Investigation of tooth extraction reasons in patients who applied to a dental faculty. *Meandros Med Dent J*. 2018;19:219–225.
8. Hong CE, Lee JY, Choi J, Joo JY. Prediction of the alveolar bone level after the extraction of maxillary anterior teeth with severe periodontitis. *J Periodont Implant Sci*. 2015;45(6):216–222.
9. Moreno AR, Magdaleno MO, Islas MM, et al. Postextraction alveolar preservation and use of the crown of the extracted tooth as a temporary restoration. *Case Rep Dent*. 2019;2019:4262067.
10. Hämmerle CHF, Tarnow D. The etiology of hard- and soft-tissue deficiencies at dental implants: A narrative review. *J Clin Periodontol*. 2017;45(Suppl 20):S267–S277.
11. Avila-Ortiz G, Elangovan S, Kramer KWO, Blanchette D, Dawson DV. Effect of alveolar ridge preservation after tooth extraction: A systematic review and meta-analysis. *J Dent Res*. 2014;93(10):950–958.
12. Miyazaki T, Ishikawa K, Shirosaki Y, Ohtsuki C. Organic-inorganic composites designed for biomedical applications. *Biol Pharm Bull*. 2013;36(11):1670–1675.
13. Daud NM, Sing NB, Yusop AH, Abdul Majid FA, Hermawan H. Degradation and in vitro cell–material interaction studies on hydroxyapatite-coated biodegradable porous iron for hard tissue scaffolds. *J Orthop Transl*. 2014;2(4):177–184.
14. Kattimani VS, Kondaka S, Lingamaneni KP. Hydroxyapatite – past, present, and future in bone regeneration. *Bone Tissue Regener Insights*. 2016;7:8–19.
15. Loh QL, Choong C. Three-dimensional scaffolds for tissue engineering applications: Role of porosity and pore size. *Tissue Eng Part B Rev*. 2013;19(6):485–502.
16. Wang Q, Wang Q, Wan C. The effect of porosity on the structure and properties of calcium polyphosphate bioceramics. *Ceramics Silikaty*. 2011;55(1):43–48.
17. Ryan AJ, Gleeson JP, Matsiko A, Thompson EM, O'Brien FJ. Effect of different hydroxyapatite incorporation methods on the structural and biological properties of porous collagen scaffolds for bone repair. *J Anat*. 2015;227(6):732–745.
18. Ortega-Oller I, Padial-Molina M, Galindo-Moreno P, O'Valle F, Jódar-Reyes AB, Peula-García JM. Bone regeneration from PLGA micro-nanoparticles. *Biomed Res Int*. 2015;2015:415289.
19. Ma'ruf T, Siswomihardjo W, Soesatyo MHNE, Tontowi AE. Polyvinyl alcohol-hydroxyapatite composite reinforced with catgut fibers as biodegradable bone plates. *3rd International Conference on Instrumentation, Communications, Information Technology, and Biomedical Engineering (ICICI-BME)*. 2013:246–248.
20. Tontowi AE, Perkasa DP, Siswomihardjo W, Darwis D. Effect of polyvinyl alcohol (PVA) blending and gamma irradiation on compressive strength of FHAp/FGel composite as candidate of scaffold. *Int J Eng Technol*. 2016;8(1):108–116.
21. Kapoor DN, Bhatia A, Kaur R, Sharma R, Kaur G, Dhawan S. PLGA: A unique polymer for drug delivery. *Ther Deliv*. 2015;6(1):41–58.
22. Shibata A, Yada S, Terakawa M. Biodegradability of poly(lactic-co-glycolic acid) after femtosecond laser irradiation. *Sci Rep*. 2016;6:27884.
23. Makadia HK, Siegel SJ. Poly lactic-co-glycolic acid (PLGA) as biodegradable controlled drug delivery carrier. *Polymers (Basel)*. 2011;3(3):1377–1397.
24. Costa-Pinto AR, Martins AM, Castelhana-Carlos MJ, et al. In vitro degradation and in vivo biocompatibility of chitosan-poly(butylene succinate) fiber mesh scaffolds. *J Bioact Compat Polym*. 2014;29(2):137–151.
25. Istikharoh F, Sujuti H, Mustamsir E, Swastirani A, Milla LE. Poly(lactic-co-glycolic acid) enhance of biodegradability properties and pore size of hydroxyapatite nanoparticle/PVA composites for alveolar ridge preservation. *Malaysian J Med Health Sci*. 2019;15(Suppl 7):63.
26. Chang HI, Wang Y. Responses to surface and architecture of tissue engineering scaffolds. *Regenerative Medicine and Tissue Engineering – Cells and Biomaterials*. London, UK: IntechOpen Ltd.; 2011:569–589.
27. Zamani F, Amani-Tehran M, Latifi M, Shokrgozar MA. The influence of surface nanoroughness of electrospun PLGA nanofibrous scaffold on nerve cell adhesion and proliferation. *J Mater Sci Mater Med*. 2013;24(6):1551–1560.
28. Li L, Crosby K, Sawicki M, Shaw LL, Wang Y. Effects of surface roughness of hydroxyapatite on cell attachment and proliferation. *J Biotechnol Biomater*. 2012;2:6.
29. Bobbert FSL, Zadpoor AA. Effects of bone substitute architecture and surface properties on cell response, angiogenesis, and structure of new bone. *J Mater Chem B*. 2017;5(31):6175–6193.
30. Garg T, Singh O, Arora S, Murthy R. Scaffold: A novel carrier for cell and drug delivery. *Crit Rev Ther Drug Carrier Syst*. 2012;29(1):1–63.
31. Arsiccio A, Sparavigna AC, Pisano R, Barresi AA. Measuring and predicting pore size distribution of freeze-dried solutions. *Dry Technol*. 2019;37(4):435–447.
32. Assegehegn G, Brito-de la Fuente E, Franco JM, Gallegos C. The importance of understanding the freezing step and its impact on freeze-drying process performance. *J Pharm Sci*. 2019;108(4):1378–1395.
33. Iqbal N, Khan AS, Asif A, Yar M, Haycock JW, Rehman IU. Recent concepts in biodegradable polymers for tissue engineering paradigms: A critical review. *Int Mater Rev*. 2019;64(2):91–126.

Effect of photobiomodulation with 810 and 940 nm diode lasers on human gingival fibroblasts

Mohammd Ayoub Rigi Ladiz^{1,A,B,F}, Alireza Mirzaei^{2,A,B,F}, Seyedeh Sareh Hendi^{3,D–F}, Roya Najafi-Vosough^{4,C,F}, Amirarsalan Hooshyarfard^{5,E,F}, Leila Gholami^{5,A–C,E,F}

¹ Oral and Dental Research Center, Department of Periodontology, Faculty of Dentistry, Zahedan University of Medical Sciences, Iran

² Department of Periodontics, Faculty of Dentistry, University of Bonn, Germany

³ Department of Endodontics, School of Dentistry, Hamadan University of Medical Sciences, Iran

⁴ Department of Biostatistics, School of Public Health, Hamadan University of Medical Sciences, Iran

⁵ Dental Implant Research Center, Department of Periodontics, School of Dentistry, Hamadan University of Medical Sciences, Iran

A – research concept and design; B – collection and/or assembly of data; C – data analysis and interpretation;

D – writing the article; E – critical revision of the article; F – final approval of the article

Dental and Medical Problems, ISSN 1644-387X (print), ISSN 2300-9020 (online)

Dent Med Probl. 2020;57(4):369–376

Address for correspondence

Leila Gholami

E-mail: l.gholami@hotmail.com

Funding sources

None declared

Conflict of interest

None declared

Received on November 13, 2019

Reviewed on March 16, 2020

Accepted on May 21, 2020

Published online on December 31, 2020

Cite as

Rigi Ladiz MA, Mirzaei A, Hendi SS, Najafi-Vosough R, Hooshyarfard A, Gholami L. Effect of photobiomodulation with 810 and 940 nm diode lasers on human gingival fibroblasts. *Dent Med Probl.* 2020;57(4):369–376. doi:10.17219/dmp/122688

DOI

10.17219/dmp/122688

Copyright

© 2020 by Wrocław Medical University

This is an article distributed under the terms of the

Creative Commons Attribution 3.0 Unported License (CC BY 3.0)

(<https://creativecommons.org/licenses/by/3.0/>).

Abstract

Background. The growth and proliferation of gingival fibroblasts are important in the process of oral wound healing, and photobiomodulation (PBM) might be able to modify this process.

Objectives. The aim of the current study was to evaluate the biomodulatory effect of a single session of laser PBM by means of 810 nm and 940 nm diode lasers alone and their combined application with different fluencies on human gingival fibroblasts (HGFs).

Material and methods. Cells were provided by the Pasteur Institute, the National Cell Bank of Iran (NCBI) (C-165). Laser irradiation was carried out using 810 nm, 940 nm and 810 nm + 940 nm in the continuous wave (CW) mode, 100 mW, and energy densities of 0.5, 1.5 and 2.5 J/cm². Cell viability was evaluated at 24 h with the MTT assay. Trypan blue staining was used to evaluate proliferation 24, 48 and 72 h after laser therapy. Propidium iodine was used to stain DNA and the cell nucleus.

Results. Laser irradiation (810 nm, 0.5 J/cm²) increased the viability of gingival fibroblasts, while this dose had an inhibitory effect with 940 nm. No positive effect on cell viability was found with other settings at 24 h. The viability results were not statistically different from those of the control in the dual wavelength group. At all single-laser irradiation doses, the cell proliferation results were lower as compared to the control at 48 and 72 h. The dual wavelength group results were significantly better than those of the control for the 1.5 J/cm² and 2.5 J/cm² energy densities ($p < 0.001$). Propidium iodine staining showed no negative effect of laser irradiation on the cell nucleus in any of the groups.

Conclusions. Although a single irradiation dose of 810 nm, 0.5 J/cm², resulted in a positive effect on cell viability at 24 h, no statistically significant stimulatory effect on viability and proliferation was observed for the other single wavelength group. When a combination of the 2 wavelengths was used, better results were observed as compared to the control, which needs to be further investigated in future studies.

Key words: wound healing, cell proliferation, lasers, cell survival

Introduction

Wound healing is a complex physiological process involving biological clot formation, angiogenesis, granulation tissue formation, and re-epithelialization. The growth and proliferation of various types of cells, such as fibroblasts, play important roles in this process,¹ with fibroblasts having a key role and a critical anti-inflammatory effect. They are involved in the contraction of the wound and the production of collagen, elastin, fibronectin, and proteoglycans.² Unlike skin fibroblasts, adult gingival fibroblasts are much more similar to embryonic fibroblasts in terms of morphology, growth, migration ability, and cytokine production, which is probably the reason for the rapid improvement of oral ulcers with the lowest amount of scars.³ Therefore, their proliferation and migration are essential for accelerating wound healing, and success in increasing their proliferation can directly influence the healing results.^{4,5}

Low-level (intensity) laser therapy (LLLT, LILT), or better called photobiomodulation (PBM), refers to the use of photons to modulate biological activity.⁶ This type of therapy uses non-thermal laser light, mostly from the red and near-infrared region of the spectrum. Its ability to stimulate the proliferation of different cell types has been shown to be its most important physiological effect.⁷ The influence of LLLT on the migration of gingival fibroblasts and the synthesis of collagen as well as its anti-inflammatory effects, which are directly related to the wound healing process, have also been shown in previous studies.^{2,8–10}

Although the mechanisms behind the biomodulatory effects of different wavelengths require further investigation, studies have shown that visible to near-infrared light is thought to be absorbed by mitochondrial and non-mitochondrial photoacceptors. The best known ones are mitochondrial respiratory chain components, which cause an increase in reactive oxygen species (ROS) and adenosine triphosphate (ATP) or cyclic adenosine monophosphate (cAMP), and initiate a signaling cascade, thereby promoting cellular proliferation.^{7,11}

Most studies on wound healing have been conducted on skin fibroblasts or epithelial cells. In recent years, *in vitro* and *in vivo* studies have also evaluated the effect of phototherapy on oral wounds and gingival fibroblasts, with different devices and settings.^{2,3,10,12}

The laser effect depends on various parameters, such as wavelength, power, energy density, and the duration and schedule of laser irradiation. Despite various studies in this field, there is still no optimal protocol for the application of PBM in dental treatment due to inconsistencies in the study design, a wide range of parameters involved, and phenotypic and genotypic differences that might exist in the cell lines used. Previous studies have mostly focused on certain wavelengths of the laser in the range of 600–810 nm, with few comparisons of different wavelengths.^{2,4,12–15} Moreover, there are very few studies

evaluating the simultaneous application of 2 wavelengths, which seems to have the potential of a novel synergistic effect due to different penetration depths and absorption by specific chromophores.^{16–18}

Near-infrared laser dental devices with wavelengths of 810 nm and 940 nm have currently become popular adjunctive tools in different areas of dental practice (especially in periodontal treatment and soft-tissue oral surgery), and there is a limited number of studies comparing these wavelengths in order to find the ideal laser settings for adjunctive photobiostimulatory application in oral wound healing. This study was designed to evaluate the biomodulatory effect of a single irradiation session of these 2 lasers alone and their combined irradiation with different energy densities, chosen based on the previously reported suitable energy densities, on human gingival fibroblast (HGF) cells.

Material and methods

This study was approved by the ethics research committee of Zahedan University of Medical Sciences, Iran (IR.ZUMS.94.5.11-7347). Human gingival fibroblasts were provided by the Pasteur Institute, National Cell Bank of Iran (NCBI) (C-165; NCBI, Tehran, Iran). This cell line was cultured in the minimum essential medium α modification (α MEM) containing 10% of fetal bovine serum (FBS) (Gibco®, Grand Island, USA) in sterile flasks, in 5% CO₂ and at 37°C, in an incubator. After 2–3 days, the culture was replaced and after 1 week, the cells were passaged.

The third-passaged cells were cultured at 5×10^3 cells per well in 96-well plates (Zhejiang Sofra Life Sciences Co., Ltd., Zhongguan, China) and the type of treatment was identified according to numbering. Six wells were allocated for each energy density at each study time, and the average result was reported.

Laser irradiation

Diode lasers with wavelengths of 810 nm (Picasso®; AMD Lasers LLC, Indianapolis, USA) and 940 nm (Epic®10; Biolase, Irvine, USA) were used. A 400-micron fiber and an output power of 0.1 W were used for both lasers. The fiber tip was placed perpendicular to the bottom of each well at a fixed distance of 15 mm to produce an irradiation spot size of 0.8 cm in diameter to cover only 1 well of a 96-well plate.

In order to have 3 energy densities of 0.5, 1.5 and 2.5 J/cm², the cell culture wells were irradiated from underneath the plates for 2.5, 7.5 and 12.5 s, respectively. The output power was 100 mW and the power transmitted through the transparent, flat-bottom culture plates was checked with a power meter (Nova II®; Ophir Photonics, Jerusalem, Israel) before irradiation. An empty well was

placed between the cultured wells in order to prevent overtreatment. Wells other than the one being irradiated were covered with a black cardboard. In order to evaluate the combined effect of the 2 wavelengths, a third group was also assessed. For this purpose, in order to produce the same energy densities as in the case of the single wavelength groups, each energy density was reduced by 2 for each wavelength to achieve the same density together. The 810 nm wavelength was applied first, followed by the 940 nm wavelength. The irradiation process was conducted in a semi-dark room, with no ceiling light turned on over the counter where laser irradiation was performed. This was to limit unintentional light from the environment reaching the cells. The control wells received no laser irradiation, but their plates were also removed from the incubator for the same duration as the laser-irradiated group wells to provide the same situation for both groups.

Evaluation of cell survival

Cell viability was assessed by evaluating mitochondrial activity by means of the MTT colorimetric assay 24 h after irradiation with different lasers. In the MTT method, the mitochondrial succinate dehydrogenase enzyme causes a breakdown in the MTT ring solution to change it to insoluble blue formazan; then, using photometry, the amount of formazan is measured and the intensity of the produced color is related to the number of live cells. For this, we placed the cells in the incubator for 24 h. Then, 10 μL of the MTT solution and 90 μL of αMEM containing 10% FBS were added to each well and placed in the incubator for 3–4 h at 37°C. Formazan crystals were dissolved by adding dimethyl sulfoxide. Subsequently, spectrophotometry was used to measure the cell metabolism. Light absorption was read using the enzyme-linked immunosorbent assay (ELISA) with the ELx808™ absorbance microplate reader (BioTek Instruments GmbH, Bad Friedrichshall, Germany) at a wavelength of 540–690 nm. Results were reported as percentage, and the control of this test was considered as 100%.

Evaluation of cell proliferation

The trypan blue assay was used to evaluate the number of cells in the culture after the application of LLLT. The trypan blue dye can penetrate only the porous, permeable membranes of the lethally damaged (dead) cells, which is clearly detectable under optical microscopy (OM) and the total number of viable cells is counted. Cells in the amount of 5×10^3 were cultured in the wells of 96-well plates. Then, 24, 48 and 72 h after irradiation, the cell number was determined by counting the viable cells with the trypan blue dye exclusion assay. For each time period, the cells from 6 wells of each group were counted and their increased ratio was reported numerically in comparison with the baseline number of cells.

Propidium iodide staining

In order to study the effects of laser irradiation on the nucleus of the cultured cells, after 72 h, propidium iodide was prepared with 1 mg/mL phosphate-buffered saline (PBS) and 100 times diluted, and 10 μL of it was added to each well of the cell cultures. After 1–2 min, the samples were washed with the PBS solution and examined under a fluorescence phase contrast microscope (BX51; Olympus Corp., Tokyo, Japan) for the morphological changes of the nucleus (pyknotic nuclei and nuclear fragmentation).

Statistical analysis

The data was analyzed using Student's *t* test and subjected to the three-way analysis of variance (ANOVA). After that, Tukey's post-hoc test was used for further comparisons between the subgroups. All statistical analyses were performed at a significance level of 0.05 and expressed as mean (*M*) \pm standard deviation (*SD*) through graphics. The R statistical software, v. 3.3.3 (the R Project for Statistical Computing, Vienna, Austria; <http://www.r-project.org>), and SPSS for Windows, v. 16.0 (SPSS Inc., Chicago, USA) were used.

Results

Cell survival

The MTT assay was used to determine the effect of laser irradiation on cell survival at 24 h. (Fig. 1) Only the 810 nm 0.5 J/cm² group had better viability results, which was about 35% higher than the control and was statistically significant ($p = 0.013$). There was also a reduced viability for the 940 nm 0.5 J/cm² group as compared to the control ($p = 0.001$).

A statistically significant difference existed between the 810 nm 0.5 J/cm² group and the control; the former showed better viability results ($p = 0.013$). However,

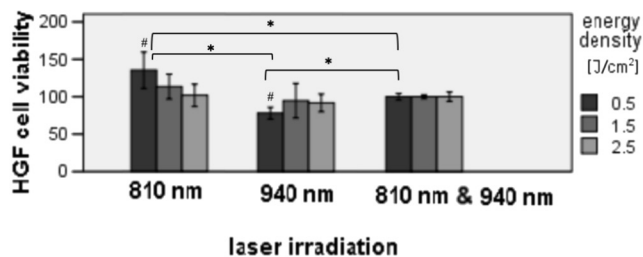


Fig. 1. Percentage of the viability of human gingival fibroblast (HGF) cells as compared to the control at 24 h after laser irradiation with 810 nm and 940 nm lasers and dual wavelength irradiation with energy densities of 0.5, 1.5 and 2.5 J/cm²

* significant differences between the groups; # significant differences as compared to the controls ($p < 0.05$).

the 940 nm 0.5 J/cm² irradiation provided lower viability results as compared to the control. The dual wavelength group showed no statistically significant difference as compared to its control.

When comparing the wavelengths with similar energy densities, the 810 nm 0.5 J/cm² group had a higher viability percentage as compared to the 940 nm laser group and the combined irradiation group (810 nm + 940 nm) with statistically significant differences ($p < 0.001$). There was a statistically significant difference between the combined irradiation group with the 0.5 J/cm² irradiation and the 940 nm laser group with the 0.5 J/cm² irradiation (Fig. 1)

Cell proliferation

The cell proliferation amounts were lower for the single wavelength irradiation groups as compared to the controls at 48 and 72 h, but the dual wavelength group results were significantly better than those of their control for the 1.5 J/cm² and 2.5 J/cm² energy densities ($p < 0.001$) (Table 1).

The three-way ANOVA was used to compare the effect of the laser wavelength, energy density and time on proliferation. The results of this test also showed that both laser and time factors affect proliferation ($p < 0.05$) (Table 2). In addition, the results of the study show that the laser effect depends on energy density and time ($p < 0.05$). Further two-fold comparisons between the groups were done using Tukey's test and the results are shown in Fig. 2.

When comparing different energy densities of the 810 nm laser, 0.5 J/cm² showed higher proliferation amounts as compared to 2.5 J/cm² at 24 h ($p = 0.002$) and 72 h ($p < 0.001$). The 810 nm 1.5 J/cm² laser also provided better results as compared to 2.5 J/cm² after 72 h ($p = 0.038$). There was only 1 statistically significant difference in the 940 nm group, which was between irradiation with the 0.5 J/cm² and 2.5 J/cm² energy densities at 72 h, with better results for the 2.5 J/cm² group ($p = 0.038$). Differences between the 3 energy densities of the combined irradiation group were statistically significant at all time points, with better results as the energy dose increased ($p \leq 0.001$) (Table 3).

Table 2. Results of the three-way analysis of variance (ANOVA)

Variable	df	F-value	p-value
Intercept	1	12,598.297	<0.0001*
Wave	2	23,380.106	<0.0001*
Power	2	338.679	<0.0001*
Time	3	19.819	<0.0001*
Wave*Power	4	849.839	<0.0001*
Wave*Time	6	35.599	<0.0001*
Power*Time	6	86.589	<0.0001*
Wave*Power*Time	12	7.399	<0.0001*

df – degrees of freedom; * statistically significant difference ($p < 0.05$).

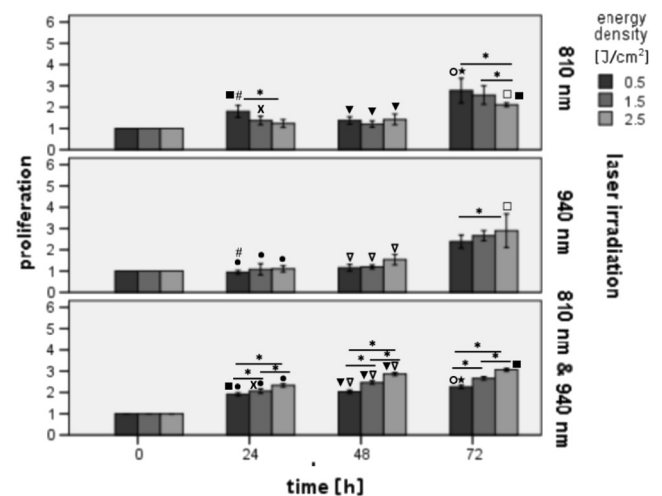


Fig. 2. Proliferation of HGF cells at 0, 24, 48, and 72 h after laser irradiation with 810 nm and 940 nm lasers and the combined wavelength irradiation with energy densities of 0.5, 1.5 and 2.5 J/cm²

* significant differences between different energy densities in the same laser treatment group at each time point; other matching symbols indicate significant differences between different wavelength groups with the same energy density at each time point ($p < 0.05$).

We also compared similar energy densities of different laser wavelengths. The 940 nm 2.5 J/cm² group had statistically significantly higher results as compared to 810 nm 2.5 J/cm² at 72 h ($p < 0.001$). The 810 nm 0.5 J/cm² group showed better proliferation results as compared to

Table 1. Comparative evaluation of the effect on the proliferation of HGF cells between different energy densities of the lasers and the controls after 24, 48 and 72 h

Time	810 nm laser							940 nm laser							810 nm + 940 nm laser						
	Control	0.5 J/cm ²		1.5 J/cm ²		2.5 J/cm ²		Control	0.5 J/cm ²		1.5 J/cm ²		2.5 J/cm ²		Control	0.5 J/cm ²		1.5 J/cm ²		2.5 J/cm ²	
		M ±SD	p-value	M ±SD	p-value	M ±SD	p-value		M ±SD	p-value	M ±SD	p-value	M ±SD	p-value		M ±SD	p-value	M ±SD	p-value	M ±SD	p-value
24 h	1.65 ±0.24	1.80 ±0.17	0.196	1.37 ±0.19	0.560	1.23 ±0.17	0.196	1.65 ±0.24	0.94 ±0.09	0.010*	1.08 ±0.21	0.089	1.10 ±0.13	0.058	1.71 ±0.07	1.91 ±0.07	0.001*	2.11 ±0.07	<0.001*	2.33 ±0.07	<0.001*
48 h	2.36 ±0.12	1.37 ±0.14	<0.001*	1.20 ±0.14	<0.001*	1.42 ±0.20	<0.001*	2.36 ±0.12	1.15 ±0.15	<0.001*	1.19 ±0.09	<0.001*	1.54 ±0.19	<0.001*	2.06 ±0.07	2.06 ±0.07	1.000	2.46 ±0.07	<0.001*	2.86 ±0.07	<0.001*
72 h	4.83 ±0.51	2.77 ±0.47	<0.001*	2.56 ±0.35	<0.001*	2.11 ±0.07	<0.001*	4.83 ±0.51	2.38 ±0.19	<0.001*	2.66 ±0.19	<0.001*	2.89 ±0.49	0.001*	2.31 ±0.07	2.26 ±0.07	0.242	2.66 ±0.07	<0.001*	3.06 ±0.07	<0.001*

M – mean; SD – standard deviation; * statistically significant difference ($p < 0.05$).

0.5 J/cm² of the 940 nm laser at 24 h ($p < 0.001$), but this difference was not significant at the 0.05 level after 48 and 72 h. The 1.5 J/cm² setting showed no statistical difference between the 2 lasers. The combined irradiation group with similar energy densities as compared to the 810 nm and 940 wavelengths applied individually presented significantly better results, except for comparisons with 810 nm 2.5 J/cm² at 24 h and 810 nm 1.5 J/cm² at 72 h. Differences between similar energy densities of the combined treatment and the 940 nm laser were also non-significant after 72 h (Table 4).

Propidium iodide staining

The cells were carefully evaluated after staining and no negative effect of laser irradiation on the cell nucleus was observed in any of the groups.

Discussion

Finding the appropriate PBM protocol for cells before clinical trials regarding wound healing is strongly recommended. Cell culture studies provide conditions which make it possible to better assess the effect of laser irradiation on cells by eliminating interventional factors in the clinic. However, differences should also be considered when translating the results of in vitro studies to clinical application.

The results obtained in the present study on gingival fibroblast cells showed that a single dose of 0.5 J/cm² with the 810 nm laser could slightly increase the viability of gingival fibroblasts measured at 24 h. Other energy densities of this laser and also the 940 nm laser did not show a positive effect on cell viability at 24 h. Differences

in the results of the same energy density between different wavelengths might be due to the fact that different wavelengths of the laser may operate through different mechanisms and each wavelength can be unique in terms of the chromophores it can stimulate, and also differences in their penetration depths can affect their results. This has been demonstrated in some studies.^{19–21} For example, in a study by Wang et al., different mechanisms of action were reported for 2 infrared wavelengths of 980 nm and 810 nm.²⁰ They were able to demonstrate that the 980 nm wavelength affects temperature-gated calcium ion channels, while the mitochondrial cytochrome c oxidase is the most probable target of the 810 nm laser.²⁰ Also, in a study on the effects of 2 wavelengths of red and near-infrared, Marques et al. observed different effects of laser wavelengths.¹⁹ According to their findings, an energy density of 5 J/cm² applied with the red laser increased cell viability and proliferation, while the same dose of the near-infrared laser led to negative effects.¹⁹

Based on these differences, we also evaluated the effect of the combined irradiation of 2 wavelengths on gingival fibroblast viability and proliferation. A synergistic effect of applying 2 different wavelengths has been previously reported in sparse in vitro and in vivo studies.^{16–18,22} We were also able to observe this effect. Based on our findings, the combined irradiation showed different results as compared to the separate application of each wavelength. This combined therapy seemed to have a better effect on proliferation than the lasers applied alone. It was also more effective in comparison with the control.

In a study by Fekrazad et al., the effects of the blue, green, red, and infrared lasers as well as their combination on the proliferation and differentiation of mesenchymal stem cells (MSCs) were assessed.¹⁸ They reported that some combinations, such as red + infrared, had negative

Table 3. Comparative evaluation of the effect of different energy densities of each laser wavelength on the proliferation of HGF cells after 24, 48 and 72 h (p -values)

Time	810 nm			940 nm			810 nm + 940 nm		
	0.5 J/cm ² vs 1.5 J/cm ²	0.5 J/cm ² vs 2.5 J/cm ²	1.5 J/cm ² vs 2.5 J/cm ²	0.5 J/cm ² vs 1.5 J/cm ²	0.5 J/cm ² vs 2.5 J/cm ²	1.5 J/cm ² vs 2.5 J/cm ²	0.5 J/cm ² vs 1.5 J/cm ²	0.5 J/cm ² vs 2.5 J/cm ²	1.5 J/cm ² vs 2.5 J/cm ²
24 h	0.099	0.002*	0.999	0.999	0.997	1.000	0.001*	<0.001*	0.001*
48 h	0.998	1.000	0.962	1.000	0.148	0.320	<0.001*	<0.001*	<0.001*
72 h	0.985	<0.001*	0.038*	0.856	0.038*	0.977	<0.001*	<0.001*	<0.001*

* statistically significant difference ($p < 0.05$).

Table 4. Comparative evaluation of the effect of similar energy densities of different irradiation wavelengths on the proliferation of HGF cells after 24, 48 and 72 h (p -values)

Time	810 nm vs 940 nm			810 nm vs (810 nm + 940 nm)			940 nm vs (810 nm + 940 nm)		
	0.5 J/cm ²	1.5 J/cm ²	2.5 J/cm ²	0.5 J/cm ²	1.5 J/cm ²	2.5 J/cm ²	0.5 J/cm ²	1.5 J/cm ²	2.5 J/cm ²
24 h	<0.001*	0.635	0.999	<0.001*	<0.001*	0.186	<0.001*	<0.001*	<0.001*
48 h	0.968	0.999	0.999	<0.001*	<0.001*	<0.001*	<0.001*	<0.001*	<0.001*
72 h	0.262	0.999	<0.001*	<0.001*	0.529	0.026*	0.430	0.976	0.192

* statistically significant difference ($p < 0.05$).

effects, but the blue + green laser combination was better than each one applied alone. However, the authors stated that they were still not able to reach a clear conclusion as to the effect of the combined irradiation on these cells.¹⁸ On the other hand, Zare et al. reported that in the combination treatment with 630 nm + 810 nm LLLT, 3 sessions of irradiation at 2.4 J/cm² resulted in an increase in the viability of human adipose stem cells (hASCs) as compared to the control cells and PBM-treated bone marrow-derived stem cells.¹⁶ However, this effect was not observed with 1 session of this combined treatment at 1.2 J/cm².¹⁶ In the present study, we only evaluated a single session of irradiation and we probably could have obtained different results with multiple sessions, which needs to be investigated in future studies.

Interesting positive effects were reported in a recent *in vivo* wound healing study for the simultaneous application of the 660 nm and 808 nm lasers as PBM therapy in infected pressure ulcers in mice, where this combined treatment accelerated healing and had antibacterial effects.²² In another study, the combination of 2 wavelengths – 660 nm and 808 nm – at a higher dose of 300 J/cm² applied twice a week was investigated clinically and was reported as effective treatment for oral mucosistis.¹⁷

It seems that the combined wavelength treatment may have many interesting synergistic effects, which need to be evaluated more precisely in further *in vitro* and *in vivo* studies with well controlled groups.

There are a number of studies on gingival fibroblasts, but mostly with many different wavelengths and laser parameters, showing a variation of results.^{2,23–25} We have only tried to focus on discussing the results of similar wavelengths with regard to the ones used in the present study to better elucidate their effects on these cells.

Although the results of the current study show a slight positive effect of a single dose of the 810 nm laser in the 0.5 J/cm² setting at 24 h, no irradiation was sufficient to result in increased proliferation rates during the 72 h of evaluation as compared to the control in the single wavelength groups; however, the dual wavelength results showed significantly better effects on proliferation as compared to the control. Similar to our results, low-level laser (LLL) irradiation with lower energy densities of <2.5 J/cm² in a recent study by Marques et al. was not able to promote the metabolic activity and proliferation of stem cells with red and near-infrared wavelengths.¹⁹ The same authors reported lesser cell proliferation in the 2.5 J/cm² 660 nm red laser group at 48 h based on the sulforhodamine B (SRB) assay, but not in the near-infrared irradiated group.¹⁹ In the present study, we observed a reduction in the proliferation of cells, yet only in the 810 nm group at the 48 h time point, which needs to be considered and better elucidated in future studies.

Frozanfar et al. investigated the effect of the low-power diode laser with a wavelength of 810 nm, an output power of 50 mW and an energy density of 4 J/cm², with 3 con-

secutive irradiation sessions, on the expression of type I collagen gene and the proliferation of HGF cells.²⁶ Their study revealed that laser irradiation increased the expression of type I collagen gene on the 3rd day and the fibroblast proliferation rate after 48 and 72 h.²⁶ It seems that the lower output power used in that study and the repeated delivery of laser radiation energy might have resulted in a cumulative positive effect, better in comparison with the one of the present study.

In a study by Kreisler et al., the 809 nm diode laser with a very low output power of 10 mW and energy densities of 1.96, 3.92 and 7.84 J/cm² was used for irradiation 2 and 3 times in 24-hour intervals.⁵ They reported an increase in the proliferation of gingival fibroblasts after 24 h. However, this increase of the proliferation gradient declined 48 and 72 h later, with a density-dependent pattern.⁵ The reason for this decrease can be explained by the gradual vanishing effect of the laser or the cells reaching the saturation point after 3 days of incubation. If the latter is the case, we might have achieved a different result by seeding a lower number of cells in each well. Interestingly, in a report by Moore et al., similar results to ours were reported.²⁷ They observed that although the proliferation of fibroblasts increased after a single irradiation session with red wavelengths, with a maximum effect in the case of the 665 nm and 675 nm wavelengths, a single dose of 810 nm low-power diode laser radiation (5 mW/cm, 10 J/cm²) resulted in an inhibitory effect. However, the energy density they utilized was much higher as compared to the ones in the present study and had a much lower output power.²⁷

Wavelengths of around 940 nm have also been studied in a few reports. Similar to the results of the present study, Hakki et al. reported that a single application of high-power 2 W and 1.5 W in the pulsed wave (PW) and low-power 0.3 W in the continuous wave (CW) of the 940 nm laser did not have any significant effects on the proliferation of fibroblasts.²⁸ However, they reported a significant increase in the insulin-like growth factor (IGF), vascular endothelial growth factor (VEGF) and transforming growth factor- β (TGF- β) mRNA expressions in all 3 laser setting groups as compared to the control group. An increase in the type I collagen mRNA expression was also observed, but only in the 0.3 W setting.²⁸

In another study, Pereira et al. evaluated the effect of using the 904 nm laser in 2 sessions of irradiation with a 6-hour interval on cell growth and the synthesis of procollagen in the cultured NIH-3T3 fibroblasts.²⁹ Cell stress was also simulated in this study. The cells were submitted to low-power laser irradiation with an output power of 120 mW and energy densities varying from 3 to 5 J/cm² over a period of 1–6 days. The results indicated that the 5 J/cm² irradiation had no effect on cell growth, but an energy density of 3 or 4 J/cm² caused a remarkable increase in the cell number; however, laser irradiation did not affect the synthesis of procollagen.²⁹ Following this study, Marques et al. performed another

study on HGF cells, using the same wavelength, and obtained similar results to ours.³⁰ They irradiated the cells at an output power of 120 mW and an energy density of 3 J/cm². A decrease in type I collagen was observed in the irradiated group, and also a change in the cytoplasmic matrix of the cells was noted. The irradiated cells became more electron-dense, which is similar to apoptosis. They suggested that laser irradiation has the potential to both stimulate cell division and sometimes result in the apoptosis of cells.³⁰

As it can be seen, PBM studies on gingival fibroblasts still vary regarding the irradiation protocols despite similarities in the cells and wavelengths studied.² On the other hand, one possible application of LLLT, connected to its potential inhibitory effects, is in the management of conditions with abnormal collagen or extracellular matrix deposition, in cases with the risk of keloid formation or conditions such as hereditary gingival fibromatosis.³⁰ The biological mechanisms of low-power laser radiation are not fully understood yet and more advanced molecular experiments are needed to help better understand laser–cell interactions and the mechanisms of different wavelengths in order to be able to design novel, more effective clinical applications for wound healing.

Conclusions

We have only studied the effect of a single session of laser irradiation with 2 laser devices which are normally used at a high output power in clinical practice. The comparison of the effects of single and multiple irradiation with these wavelengths is recommended in future studies. Also, it would be interesting to compare the effects of laser devices designed for PBM therapy (which can produce very low output powers) and of the devices used in the present study, which are usually used as adjunctive in dental practice. Moreover, we studied the effect of the combined laser irradiation provided on a different day than the lasers applied alone and suggest further investigations on this interesting dual wavelength therapy with the same control samples. According to the results of the present study, although a single irradiation dose of 810 nm 0.5 J/cm² resulted in a slight positive effect on cell viability at 24 h, no significant stimulatory effect on viability and proliferation was observed for other settings evaluated in this study. When the combination of the 2 wavelengths was used, better results were obtained as compared to the controls, which needs to be further investigated in future studies.

ORCID iDs

Mohammd Ayoub Rigi Ladiz  <https://orcid.org/0000-0001-9232-0404>
 Alireza Mirzaei  <https://orcid.org/0000-0003-4999-6462>
 Seyedeh Sareh Hendi  <https://orcid.org/0000-0003-2249-7006>
 Roya Najafi-Vosough  <https://orcid.org/0000-0003-2871-5748>
 Amirarsalan Hooshyarfard  <https://orcid.org/0000-0001-9567-9607>
 Leila Gholami  <https://orcid.org/0000-0001-5287-1754>

References

- Häkkinen L, Uitto VJ, Larjava H. Cell biology of gingival wound healing. *Periodontol* 2000. 2000;24:127–152.
- Ren C, McGrath C, Jin L, Zhang C, Yang Y. Effect of diode low-level lasers on fibroblasts derived from human periodontal tissue: A systematic review of in vitro studies. *Lasers Med Sci*. 2016;31(7):1493–1510.
- Pansani TN, Basso FG, Silveira Turrioni AP, Soares DG, Hebling J, de Souza Costa CA. Effects of low-level laser therapy and epidermal growth factor on the activities of gingival fibroblasts obtained from young or elderly individuals. *Lasers Med Sci*. 2017;32(1):45–52.
- Basso FG, Pansani TN, Turrioni APS, Bagnato VS, Hebling J, de Souza Costa CA. In vitro wound healing improvement by low-level laser therapy application in cultured gingival fibroblasts. *Int J Dent*. 2012;2012:719452.
- Kreisler M, Christoffers AB, Al-Haj H, Willershausen B, d'Hoedt B. Low level 809-nm diode laser-induced in vitro stimulation of the proliferation of human gingival fibroblasts. *Lasers Surg Med*. 2002;30(5):365–369.
- Anders JJ, Lanzafame RJ, Arany PR. Low-level light/laser therapy versus photobiomodulation therapy. *Photomed Laser Surg*. 2015;33(4):183–184.
- Gao X, Xing D. Molecular mechanisms of cell proliferation induced by low power laser irradiation. *J Biomed Sci*. 2009;16(1):PMC2644974.
- Basso FG, Soares DG, Pansani TN, et al. Proliferation, migration, and expression of oral-mucosal-healing-related genes by oral fibroblasts receiving low-level laser therapy after inflammatory cytokines challenge. *Lasers Surg Med*. 2016;48(10):1006–1014.
- Eslami H, Motahari P, Safari E, Seyyedi M. Evaluation effect of low level helium-neon laser and Iranian propolis extract on collagen type I gene expression by human gingival fibroblasts: An in vitro study. *Laser Ther*. 2017;26(2):105–112.
- Pansani TN, Basso FG, Silveira Turirioni AP, Kurachi C, Hebling J, de Souza Costa CA. Effects of low-level laser therapy on the proliferation and apoptosis of gingival fibroblasts treated with zole-dronic acid. *Int J Oral Maxillofac Surg*. 2014;43(8):1030–1034.
- Karu T. Primary and secondary mechanisms of action of visible to near-IR radiation on cells. *J Photochem Photobiol B*. 1999;49(1):1–17.
- Gkogkos AS, Karoussis IK, Prevezanos ID, Marcopoulou KE, Kyriakidou K, Vrotsos IA. Effect of Nd:YAG low level laser therapy on human gingival fibroblasts. *Int J Dent*. 2015;2015:258941.
- Almeida-Lopes L, Rigau J, Zângaro RA, Guidugli-Neto J, Marques Jaeger MM. Comparison of the low level laser therapy effects on cultured human gingival fibroblasts proliferation using different irradiance and same fluence. *Lasers Surg Med*. 2001;29(2):179–184.
- Azevedo LH, de Paula Eduardo F, Moreira MS, de Paula Eduardo C, Marques MM. Influence of different power densities of LILT on cultured human fibroblast growth: A pilot study. *Lasers Med Sci*. 2006;21(2):86–89.
- Basso FG, Soares DG, de Souza Costa CA, Hebling J. Low-level laser therapy in 3D cell culture model using gingival fibroblasts. *Lasers Med Sci*. 2016;31(5):973–978.
- Zare F, Moradi A, Fallahnezhad S, et al. Photobiomodulation with 630 plus 810 nm wavelengths induce more in vitro cell viability of human adipose stem cells than human bone marrow-derived stem cells. *J Photochem Photobiol B*. 2019;201:111658.
- Soares RG, Farias LC, da Silva Menezes AS, et al. Treatment of mucositis with combined 660- and 808-nm-wavelength low-level laser therapy reduced mucositis grade, pain, and use of analgesics: A parallel, single-blind, two-arm controlled study. *Lasers Med Sci*. 2018;33(8):1813–1819.
- Fekrazad R, Asefi S, Eslaminejad MB, Taghian L, Bordbar S, Hamblin MR. Photobiomodulation with single and combination laser wavelengths on bone marrow mesenchymal stem cells: Proliferation and differentiation to bone or cartilage. *Lasers Med Sci*. 2019;34(1):115–126.
- Marques NP, Lopes CS, Teixeira Marques NC, et al. A preliminary comparison between the effects of red and infrared laser irradiation on viability and proliferation of SHED. *Lasers Med Sci*. 2019;34(3):465–471.
- Wang Y, Huang YY, Wang Y, Lyu P, Hamblin MR. Photobiomodulation of human adipose-derived stem cells using 810 nm and 980 nm lasers operates via different mechanisms of action. *Biochim Biophys Acta Gen Subj*. 2017;1861(2):441–449.

21. Posten W, Wrone DA, Dover JS, Arndt KA, Silapunt S, Alam M. Low-level laser therapy for wound healing: Mechanism and efficacy. *Dermatol Surg.* 2005;31(3):334–340.
22. Cortez Thomé Lima AM, da Silva Sergio LP, da Silva Neto Trajano LA, et al. Photobiomodulation by dual-wavelength low-power laser effects on infected pressure ulcers. *Lasers Med Sci.* 2020;35(3):651–660.
23. Saygun I, Karacay S, Serdar M, Ural AU, Sencimen M, Kurtis B. Effects of laser irradiation on the release of basic fibroblast growth factor (bFGF), insulin like growth factor-1 (IGF-1), and receptor of IGF-1 (IGFBP3) from gingival fibroblasts. *Lasers Med Sci.* 2008;23(2):211–215.
24. Ogita M, Tsuchida S, Aoki A, et al. Increased cell proliferation and differential protein expression induced by low-level Er:YAG laser irradiation in human gingival fibroblasts: Proteomic analysis. *Lasers Med Sci.* 2015;30(7):1855–1866.
25. Damante CA, De Micheli G, Harumi Miyagi SP, Feist IS, Marques MM. Effect of laser phototherapy on the release of fibroblast growth factors by human gingival fibroblasts. *Lasers Med Sci.* 2009;24(6):885–891.
26. Frozanfar A, Ramezani M, Rahpeyma A, Khajehahmadi S, Arbab HR. The effects of low level laser therapy on the expression of collagen type I gene and proliferation of human gingival fibroblasts (Hgf3-Pi 53): In vitro study. *Iran J Basic Med Sci.* 2013;16(10):1071–1074.
27. Moore P, Ridgway TD, Higbee RG, Howard EW, Lucroy MD. Effect of wavelength on low-intensity laser irradiation-stimulated cell proliferation in vitro. *Lasers Surg Med.* 2005;36(1):8–12.
28. Hakki SS, Bozkurt SB. Effects of different setting of diode laser on the mRNA expression of growth factors and type I collagen of human gingival fibroblasts. *Lasers Med Sci.* 2012;27(2):325–331.
29. Pereira AN, de Paula Eduardo C, Matson E, Marques MM. Effect of low-power laser irradiation on cell growth and procollagen synthesis of cultured fibroblasts. *Lasers Surg Med.* 2002;31(4):263–267.
30. Marques MM, Pereira AN, Fujihara NA, Nogueira FN, Eduardo CP. Effect of low-power laser irradiation on protein synthesis and ultrastructure of human gingival fibroblasts. *Lasers Surg Med.* 2004;34(3):260–265.

Preparation and characterization of insulin-loaded injectable hydrogels as potential adjunctive periodontal treatment

Ali Raef Abboud^{1,A–D}, Ali Mohammad Ali^{2,A,C,E,F}, Tihama Youssef^{1,A,E,F}

¹ Department of Periodontics, Faculty of Dentistry, Tishreen University, Lattakia, Syria

² Department of Food Technology, Faculty of Technical Engineering, University of Tartous, Syria

A – research concept and design; B – collection and/or assembly of data; C – data analysis and interpretation;

D – writing the article; E – critical revision of the article; F – final approval of the article

Dental and Medical Problems, ISSN 1644-387X (print), ISSN 2300-9020 (online)

Dent Med Probl. 2020;57(4):377–384

Address for correspondence

Ali Raef Abboud

E-mail: ali.abboud90@gmail.com

Funding sources

None declared

Conflict of interest

None declared

Acknowledgements

We would like to thank the Faculty of Technical Engineering, University of Tartous, Syria.

Received on March 2, 2020

Reviewed on July 18, 2020

Accepted on July 23, 2020

Published online on December 31, 2020

Cite as

Abboud AR, Ali AM, Youssef T. Preparation and characterization of insulin-loaded injectable hydrogels as potential adjunctive periodontal treatment. *Dent Med Probl.* 2020;57(4):377–384. doi:10.17219/dmp/125658

DOI

10.17219/dmp/125658

Copyright

© 2020 by Wrocław Medical University

This is an article distributed under the terms of the

Creative Commons Attribution 3.0 Unported License (CC BY 3.0)

(<https://creativecommons.org/licenses/by/3.0/>).

Abstract

Background. The application of local drugs as adjunctive periodontal treatment is a topic of rapidly increasing interest. Consequently, new discoveries are arising, a noteworthy portion of which employ hydrogels as delivery systems due to their high biocompatibility with and similarity to human tissues. In the search for new therapeutic agents capable of aiding periodontal treatment, authors became interested in a unique concept investigated by very few in vitro or in vivo studies concerning the local application of insulin. These studies concluded that insulin promotes the recovery and regeneration of damaged soft and bone tissues.

Objectives. The aim of the study was an endeavor to design a linear hydrogel that is injectable into periodontal pockets, and is able to carry a small insulin load through physical bonds and provide sustained release.

Material and methods. The chitosan hydrogel as well as blends of polyvinyl pyrrolidone (PVP), polyvinyl alcohol (PVA) and polyethylene glycol (PEG) were prepared and characterized in terms of the hydrogel texture and injectability. Afterward, to study the insulin release kinetics, a specific amount of each formulation was loaded with insulin, and then incubated in phosphate-buffered saline (PBS). Specimens of the incubated samples were withdrawn daily to measure insulin concentrations by means of the ultraviolet (UV)-absorbance method; ultimately the cumulative release was calculated.

Results. Out of the 5 formulations, 4 had homogenous one-phasic texture and their insulin release profiles in vitro ranged from a few hours to about 2 weeks. The blend of 26.5 wt% PVP, 6.6 wt% PVA, 0.03 wt% calcium chloride dihydrate ($\text{CaCl}_2 \cdot 2\text{H}_2\text{O}$), and 66.8 wt% water, loaded with 2 IU/g of insulin, had favorable regular sustained release, approaching 13 days.

Conclusions. The composition of the hydrogel, the component ratio and the amount of loaded insulin were found to affect the release profile. A linear hydrogel of copolymerized PVP, PVA and $\text{CaCl}_2 \cdot 2\text{H}_2\text{O}$ can serve as a local vehicle for the sustained delivery of insulin inside periodontal pockets.

Key words: insulin, hydrogel, cumulative release, periodontal pockets, UV-absorbance

Introduction

Handling gingival and periodontal disease is not a simple mission. Plaque-induced gingivitis can be resolved by biofilm removal and scaling procedures. Still, to preserve healthy gingiva, the maintenance of self-performed oral hygiene is indispensable. Non-surgical periodontal therapy (NSPT), a cornerstone in managing periodontitis, precedes any additional therapy. To accomplish it, practitioners use scalers and pocket/root instrumentation in order to approximate the ultimate goal of the therapy, which is to remove microbial deposits and calculus from the supra- and infragingival areas.¹ Besides that, a variety of treatment strategies can modulate the patient's response to the management of periodontitis. This involves the local application of chemotherapeutic agents as an adjunct to NSPT, increasing its ability to ensure satisfactory outcomes. In the medical literature, most local drugs that are applied for treating periodontitis can be divided into antibiotics, antiseptics, anti-inflammatory drugs, growth factors, interleukins, and medicinal herbal products.^{2,3}

An ideal local drug delivery system (LDDS) should provide a gradual release of the active drug for a sensible period, and be biocompatible, bioadhesive and noncytotoxic.^{4–6} In patients with periodontitis, periodontal pockets themselves are available as natural reservoirs for LDDSs. At first, subgingival irrigating systems can supply therapeutic agents to the diseased area at effective concentrations, but conspicuous limitations arise from the continuous flow of the gingival crevicular fluid (GCF), which is replaced approx. 40 times per hour, leading to the rapid clearance of subgingivally placed drugs. Any added clinical advantage subgingival irrigation may have over NSPT is probably limited to drugs that can bind to the surface of the root and/or lining of the periodontal pocket, such as tetracyclines or chlorhexidine.¹

Recognizing that the potency of a locally applied medicine hinges on its relatively long-lasting availability at concentrations over the effective minimum, several forms of LDDSs have emerged. They include fibers, strips, films, gels, microparticles, and nanoparticles, all aiming to offer easy application, steadiness and uniform distribution inside periodontal pockets as well as controlled or sustained release. Local delivery systems for various drugs have been designed in *in vitro* and/or *in vivo* studies, and their drug release profiles, architecture and the clinical outcomes of their application have been described.^{7–9} Quite a number of efficiency-proven LDDSs are commercially available, and some are approved by the U.S. Food and Drug Administration (FDA). Actisite[®] is a non-resorbable fiber made of ethylene/vinyl acetate copolymer, measuring 23 cm in length and 0.5 mm in diameter, with evenly dispersed tetracycline hydrochloride (HCl).⁷ This product is now discontinued, probably because of difficulties in handling it during placement and its non-biodegradable nature. Recently, a product called Periodontal Plus AB[™] has been presented, containing 2 mg of evenly

impregnated tetracycline HCl in 25 mg of pure fibrillar collagen. Periodontal Plus AB releases tetracycline gradually and dissolves in 8–12 days.⁸ PerioChip[®] is an FDA-approved rectangular chip (5 mm × 4 mm × 0.3 mm) containing 2.5 mg of chlorhexidine gluconate, embedded in the matrix of a biodegradable polymer – gelatin.⁹

Gels combine the ease of fabrication and application, enough to have made them the most popular form of local drug carriers. For example, a xanthan gum-based gel containing 1.5% chlorhexidine, called Chlosite[®], is available in place of PerioChip. Ligosan[®] Slow Release is a hydrogel matrix loaded with 14% doxycycline (w/w). The matrix is composed of copolymerized polyglycolic acid and poly(poly(oxyethylene)-co-DL-lactic acid/glycolic acid).¹⁰ Delivery systems can be mixable before use, such as Atridox[®], an FDA-approved LDDS for doxycycline hyclate into the subgingival sites. One syringe contains the Atrigel[®] delivery system, which has 36.7% poly(DL-lactide) as a solute and 63.3% N-methyl-2-pyrrolidone as a solvent; another syringe holds 50 mg of doxycycline hyclate. Mixing the components from the 2 syringes results in a viscous liquid with 10% doxycycline hyclate, which solidifies quickly and begins controlled release. Periofilm T[®] is a local delivery system that consists of an antibiotic powder (100 mg of sodium piperacillin, 12.5 mg of sodium tazobactam) and a liquid (aminoalkyl methacrylate copolymer, ammonium methacrylate copolymer, 95% ethanol, and purified water).¹¹ The components should be mixed immediately before application. Gelatinous formulations for the delivery of minocycline HCl are also commercially available, e.g., Dentomycin[®] in the European Union and Periocline[®] in Japan.³ Elyzol[®] Dental Gel is a popular delivery system for metronidazole. It is composed of a semi-solid suspension of 25% metronidazole benzoate in the mixture of glyceryl monooleate and sesame oil; its viscosity should increase after placement.¹ One of the microparticle-based subgingival delivery systems is Arestin[™] – FDA-approved microspheres synthesized from poly(lactic-co-glycolic acid) (PLGA) for releasing minocycline HCl sustainably inside periodontal pockets.¹²

Human insulin – the hormone of β cells in the Langerhans islets of the pancreas – consists of 2 peptide chains called A and B, linked via 2 intermolecular disulfide bridges. Insulin receptors (IRs) are transmembrane receptors with tyrosine kinase activity, existing on almost every cell. The activation of the IR substrate by insulin binding initiates a signaling cascade regulating the transport and usage of glucose in the liver and other cells. Thereby, insulin stimulates sugar storage and amino acid synthesis in the liver. In addition, it controls ATP production and fatty acid synthesis in muscles and adipose tissue.¹³

Many scientists have long regarded insulin-like growth factors (IGFs) as major regulators of cell proliferation, survival and organism growth, while insulin has been considered a dominant controller of energy storage and usage. But some researchers deem this concept simplistic due to evidence that the roles of IGFs and insulin overlap

in several physiologic processes.¹⁴ In vitro studies have proven that insulin increases the proliferation and differentiation of wild-type osteoblasts by suppressing the Runx2 inhibitor Twist2,¹⁵ and simultaneously increases the markers of bone resorption.^{15,16}

The healing of the supporting alveolar bone, following surgical or non-surgical periodontal therapy, passes through 3 sequential phases – inflammation, repair and remodeling. During the inflammation phase, some events can be distinguished as preparation for repair. Cells from myeloid and mesenchymal cell lineages are attracted to the area, and begin to differentiate into osteoblasts and chondroblasts.¹ Evidence of IGF-1 having an anabolic role in bone is abundant in the literature, whereas evidence that its homolog – insulin – also plays such a role is still accumulating. Pre-osteoblasts and osteoblasts possess different isoforms of IR, where IR-A is expressed in pre-osteoblasts and IR-B is expressed in osteoblasts. This specificity supports the idea that insulin is a critical factor in the differentiation of osteoblasts from marrow stromal cells.¹⁷ Interleukin 6 (IL-6) contributes to the mediation of chronic low-grade inflammation (including chronic periodontitis). It has been found in vitro to induce cellular insulin resistance by inhibiting IR signal transduction,¹⁸ and increasing the expression and activity of insulin-degrading enzymes.¹⁹ Thrailkill et al. bred mice with the osteoprogenitor-selective ablation of IRs.²⁰ The prenatal elimination of IRs resulted in osteoblasts lacking 80% IRs, which in turn led to a decrease in the structural strength of the femur bone postnatally as compared with mice which had normal IRs. It therefore makes sense to investigate how effective the local delivery of insulin is in compensating for the cellular insulin resistance caused by periodontitis, which could enhance the quality of bone repair with a cost-effective method.

A few in vivo and clinical trials have studied the local application of insulin to determine its safety and influence on wound healing,^{21–24} recovery from decubitus ulcers,²⁵ bone healing and regeneration,^{26,27} and the osseointegration of titanium implants.²⁸ In these studies, researchers demonstrated that the local application of insulin correlated with statistically significant acceleration in the variables studied. At the same time, the studies noted no adverse effects or significant differences in blood glucose levels before and after application.^{16,21,23–25,29} Paglia et al. reported greater acceleration in the early phase of bone healing in a non-diabetic, fractured Wistar rat model after local injections of insulin.²⁷ Wang et al. cultured bone marrow stem cells within nano-hydroxyapatite/collagen/PLGA composite scaffolds, either loaded or not loaded with insulin, and observed higher rates of osteogenesis and mineralization in the insulin-loaded ones, especially at the primary bone formation stage.²⁶

The promising results of the local application of insulin mean it is a reasonable idea for us to design a delivery vehicle for insulin, with a view to investigating the effectiveness of insulin in promoting periodontal regeneration

after NSPT for periodontitis. Ideally, the vehicle should be capable of providing sustained release during the primary healing period after periodontal treatment (1–3 weeks³⁰).

Particular interest in hydrogels still prevails, as biomaterials benefit from high water retention, effective mass transfer, similarity to natural tissues, and the ability to form different shapes.³¹ We chose 3 synthetic medical polymers – polyvinyl pyrrolidone (PVP), polyvinyl alcohol (PVA) and polyethylene glycol (PEG) – and a natural polymer (chitosan) on the basis of the long-term historical usage of these polymers in the pharmaceutical industry, wound dressing and tissue engineering, which allows us to conclude that they meet the safety requirements, beside being bio-adhesive and biodegradable.^{32,33}

In light of the foregoing, the objectives of the present in vitro study were to prepare various hydrogel formulations, and then to define the following characteristics of each hydrogel after loading them with insulin: the hydrogel texture; syringeability; and the kinetics of insulin release from the hydrogel into phosphate-buffered saline (PBS) over time.

Material and methods

This research was conducted at the Faculty of Dentistry of Tishreen University in Lattakia, Syria, and the Faculty of Technical Engineering of the University of Tartous, Syria, between June and November 2019.

Material and equipment

Chitosan (molecular weight (MW): 100,000–300,000 Da), 87–89% hydrolyzed PVA (MW: ~31,000–50,000 Da) and PEG (average MW: 4,000 Da) were purchased from Acros Organics, Geel, Belgium. Protease-free PVP (MW: 40,000 Da) was purchased from Thermo Fisher Scientific, Waltham, USA. Polyethylene glycol (MW: 10,000 Da) was obtained from Alfa Aesar/Thermo Fisher (Kandel) GmbH, Kandel, Germany. The regular human insulin solution (100 IU/mL) was from ASIA Pharmaceutical Industries, Aleppo, Syria. All other chemicals used were of analytical grade and were purchased from Loba Chemie Pvt Ltd., Mumbai, India.

The equipment we used included the V-630 UV-Vis spectrophotometer (JASCO Corporation, Tokyo, Japan), the LMS-2003D digital hotplate & stirrer (LabTech SRL, Sorisole, Italy); the ED224S analytical laboratory balance (Sartorius Lab Instruments GmbH & Co. KG, Goettingen, Germany), the PURELAB® Option-Q DV25 water treatment system (ELGA LabWater, High Wycombe, UK), the Myr V1-R rotational viscometer (Viscotech Hispania SL, El Vendrell, Spain), the TopPette® single-channel pipettor, volume: 10–100 µL (Dragon Laboratory Instruments Ltd., Beijing, China), a pH meter, beakers, glass stirring rods, disposable syringes, and plastic specimen bottles.

Preparation of hydrogels

The chemicals underwent no further purification before usage. The chitosan hydrogel was prepared by scattering the precursor into distilled water during magnetic stirring; then drops of acetic acid were gradually added until chitosan completely dissolved. All the other hydrogels were blends of at least 2 polymers. Table 1 shows the components of each formulation as weight percentage (wt%). The blends were prepared by dissolving the polymers gradually one by one during magnetic stirring in heated water (60–90°C), which was left for half an hour after that to initiate copolymerization.

Table 1. Composition of the hydrogel formulations (approximate wt%)

Formulation	Water	Chitosan	PEG	PVP	PVA	CaCl ₂ ·2H ₂ O
F1	92.6	7.4	–	–	–	–
F2	78.1	–	10.9*	7.8	3.2	–
F3	71.4	–	–	14.3	14.3	–
F4	72.0	–	–	13.9	13.9	0.15**
F5	66.8	–	–	26.5	6.6	up to# 0.05**

PEG – polyethylene glycol; PVP – polyvinyl pyrrolidone; PVA – polyvinyl alcohol;
 * 7.8 wt% of PEG (MW: 4,000 Da) + 3.1 wt% of PEG (MW: 10,000 Da);
 ** weight percentage of pure CaCl₂·2H₂O; # blends with different weight percentages (0.006 wt%, 0.018 wt%, 0.03 wt%, and 0.05 wt%) were prepared.

Loading insulin into the hydrogels

After preparation, every hydrogel mixture was stored in a refrigerator (at a temperature of 2–8°C) for a minimum of 24 h to let it relax and to get rid of air bubbles. Then, insulin loading was done by adding a specific volume of the regular human insulin solution (100 IU/mL) to the hydrogel during magnetic stirring at ~250 rpm for 30 min. Hydrogel samples loaded with various insulin concentrations were prepared. Table 2 presents the concentrations of insulin in the samples of each formulation.

Table 2. Insulin concentrations in the samples of each hydrogel formulation

Formulation	Insulin concentration [IU/g]			
F1	2	3	4	5
F2	formulation excluded			
F3	–	3	–	–
F4	–	3	–	–
F5	2	3	4	5

Syringeability test

A sufficient amount of each formulation was pulled into a 5-milliliter disposable syringe. After that, a 20-gauge needle was installed. Finally, the plunger was pressed to release the hydrogel. A formulation was considered syringeable if it passed through the needle upon moderate pressure on the plunger.

Insulin release kinetics

We prepared PBS following the 2006 Cold Spring Harbor protocol.³⁴ Briefly, 8 g of NaCl, 0.2 g of KCl, 1.8 g of Na₂HPO₄, and 0.24 g of KH₂PO₄ were dissolved in 800 mL of distilled water. The pH was adjusted to ~7.4 (at a temperature of ~25°C) using the potassium hydroxide (KOH) solution. Finally, distilled water was added to reach a total volume of 1L.

The ultraviolet (UV)-absorbance method for determining and quantifying proteins is based on the absorbance of light at a wavelength of ~280 nm by the aromatic amino acids tryptophan and tyrosine, and by cysteine/disulfide-bonded cysteine residues in protein solutions.³⁵ Hence, simple spectrophotometry without reagents can be used for the quantification of insulin in pharmaceutical preparations.^{36,37} In our study, the wavelength corresponding to the maximum light absorbance by the insulin solute in PBS was determined from the UV-visible spectrum (the maximum absorbance was at 270 nm). After that, a calibration curve was drawn depending on the UV absorbed by gradually increasing insulin concentrations (0.5–4 IU/mL), measured at 270 nm. The concentrations of insulin in the samples were calculated by comparing their absorbance at 270 nm (A_{270}) with the calibration curve.

In order to characterize the cumulative release of the formulations, 4 g of each insulin-loaded formulation (the samples) and 4 g of the same formulation without insulin (the controls) were incubated separately in 15 mL of PBS in plastic bottles and stored in a refrigerator (at a temperature of 2–8°C). As the first step, the measurements of insulin release were taken at an average temperature of 5°C (the unified incubation condition) to compare the performance of different formulations. That was because storing regular insulin at 37°C, even for less than 1 month, can affect its stability.³⁸ Later, the samples of the formulation which showed the longest sustained-release interval (F5 loaded with 2 IU/g of insulin) were incubated at 37 ± 0.5°C and subjected to insulin release measurements. The release profiles for formulation F5 at the 2 incubation temperatures were compared schematically.

The measurements were performed as follows: after 1 day of incubation, 3 mL of both the control and the sample were withdrawn after rotating the bottles gently to measure A_{270} , and then the withdrawn amounts were returned. The procedure was repeated for each sample at a specified time every day until no more cumulative release was detectable. To calculate the UV absorbance of insulin (IA_{270}), the control A_{270} was subtracted from the sample A_{270} . The concentration of the released insulin in the sample (RIC) was calculated using equation (1) below, extracted from the calibration curve by applying the Beer–Lambert law:

$$RIC = (IA_{270} - 0.1)/0.4086 \text{ [IU/mL]} \quad (1)$$

where:

RIC – released insulin concentration [IU/mL];

IA_{270} – UV absorbance of insulin.

Assuming that the concentration of insulin in the sample after the loaded insulin had been completely released was FC ($FC = \text{insulin load} / \text{total sample volume [IU/mL]}$), then the insulin cumulative release (ICR) from the date of incubation until the date of measurement would be calculated from equation (2):

$$ICR = (RIC/FC) \times 100 \quad [\%] \quad (2)$$

where:

ICR – insulin cumulative release [%].

Results

Texture of the hydrogels

Formulations F1, F3, F4, and F5 were honeycomb-like, thick liquids with a one-phasic, deposit-free, yellowish, translucent appearance (Fig. 1). Formulation F2 was a bi-phasic, thick liquid and had the bottom layer more viscous than the upper one. Therefore, it was considered heterogeneous and excluded from further characterization. As F5 demonstrated the most favorable insulin release profile, it was submitted to viscosity tests at $5 \pm 1^\circ\text{C}$ and $37 \pm 1^\circ\text{C}$. The results were $1,630 \pm 40 \text{ mPa}\cdot\text{s}$ and $1,180 \pm 30 \text{ mPa}\cdot\text{s}$, respectively.

Syringeability

All the formulations passed through a 20-gauge needle upon moderate pressure on the plunger, so they were regarded as syringeable.

Insulin release kinetics

Calibration curve for the insulin solute in phosphate-buffered saline

For the absorbance values measured using a range of insulin concentrations between 0.5 and 4 IU/mL, the relation between the concentration and IA_{270} was linear (Fig. 2).

Table 3. Cumulative release of insulin over time for different hydrogel formulations

Formulation	Insulin load [IU/g]	Time [days]						
		1	2	4	6	8	10	12
		ICR [%]						
F1	2	44.00 ± 3.8	95.15 ± 2.3	100	–	–	–	–
	3	72.86 ± 2.9	90.44 ± 2.6	100	–	–	–	–
	4	98.34 ± 2.8	100	–	–	–	–	–
	5	81.65 ± 3.1	100	–	–	–	–	–
F2		formulation excluded						
F3	3	100	–	–	–	–	–	–
F4	3	18.70 ± 2.1	55.00 ± 3.5	89.30 ± 4.8	100	–	–	–
F5	2	UD	11.43 ± 1.8	–	44.5 ± 2.3	–	–	92.42 ± 3.6
	3	UD	13.47 ± 2.2	36.87 ± 5.1	–	80.00 ± 2.4	99.42 ± 1.0	
	4	UD	20.13 ± 5.0	60.26 ± 3.0	71.30 ± 3.1	98.60 ± 1.2	–	
	5	UD	26.60 ± 2.3	64.35 ± 4.6	78.23 ± 4.1	99.27 ± 0.8	–	

ICR – insulin cumulative release; UD – undetectable. The ICR data is presented as $M \pm SD$.



Fig. 1. Appearance of hydrogels F1, F3, F4, and F5

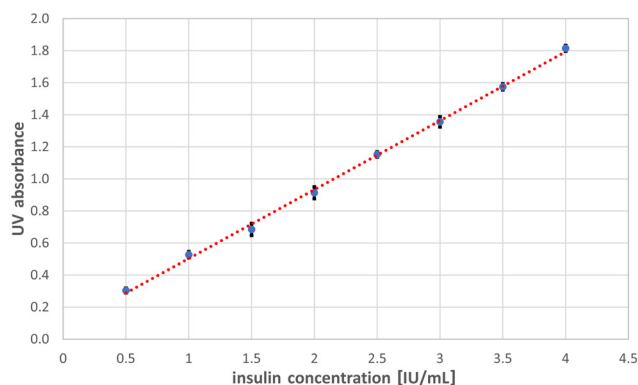


Fig. 2. Calibration curve for the insulin solute in phosphate-buffered saline (PBS) ($n = 3$)

The UV-absorbance data is presented as mean (M) ± standard deviation (SD).

In vitro release of insulin

The cumulative release of insulin over time for different formulations is shown in Table 3. Generally, for the F1 samples, the greater the insulin load, the faster the ICR was.

The longest release time (in the 3 IU/g sample) was less than 4 days (Fig. 3). Formulation F3 exhibited the complete release of the loaded insulin within 1 day, while F4 had a regular release profile up to 6 days (Fig. 4). The F5 samples with diverse insulin loads and 0.03 wt% of calcium chloride dihydrate ($\text{CaCl}_2 \cdot 2\text{H}_2\text{O}$) released insulin faster when the insulin load was bigger. The longest release time (13 days) was for 2 IU/g (Fig. 5).

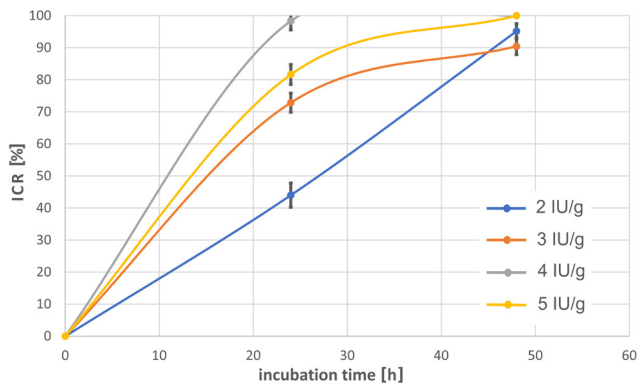


Fig. 3. Cumulative release profiles of insulin for the F1 samples with different insulin loads ($n = 3$). The ICR data is presented as $M \pm SD$.

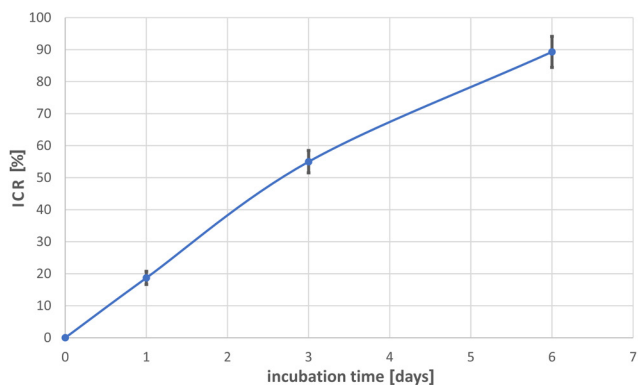


Fig. 4. Cumulative release profile of insulin for the F4 samples loaded with 3 IU/g of insulin ($n = 3$). The ICR data is presented as $M \pm SD$.

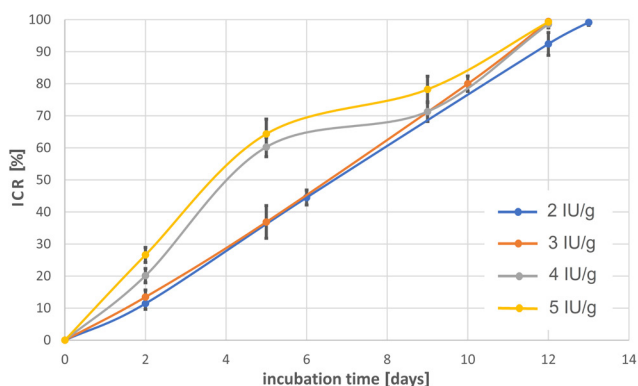


Fig. 5. Cumulative release profiles of insulin for the F5 samples with different insulin loads ($n = 3$). The ICR data is presented as $M \pm SD$.

The weight percentage of $\text{CaCl}_2 \cdot 2\text{H}_2\text{O}$ in formulation F5 had a significant effect on the insulin release profile. Among the percentages investigated in the present study, 0.03 wt% gave the longest and most regular release profile (Fig. 6).

Formulation F5 containing 0.03 wt% of $\text{CaCl}_2 \cdot 2\text{H}_2\text{O}$ and loaded with 2 IU/g of insulin showed a notable difference in the release kinetics in response to 2 different temperatures of incubation (5°C and 37°C), as illustrated in Fig. 7. At 37°C , the complete in vitro release of insulin was reached about 4 days faster (9 days compared to 13 days).

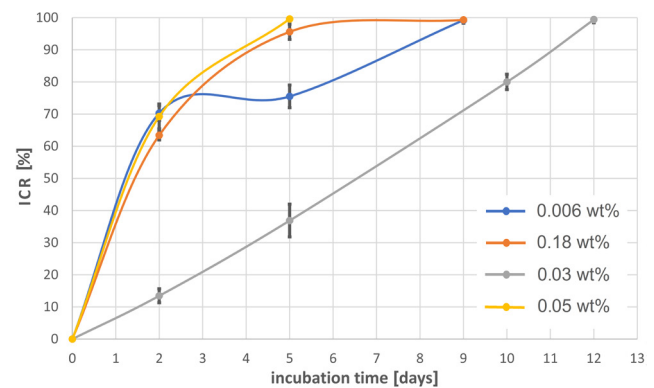


Fig. 6. Cumulative release profiles of insulin for the F5 samples with different $\text{CaCl}_2 \cdot 2\text{H}_2\text{O}$ contents, loaded with 3 IU/g of insulin ($n = 3$). The ICR data is presented as $M \pm SD$.

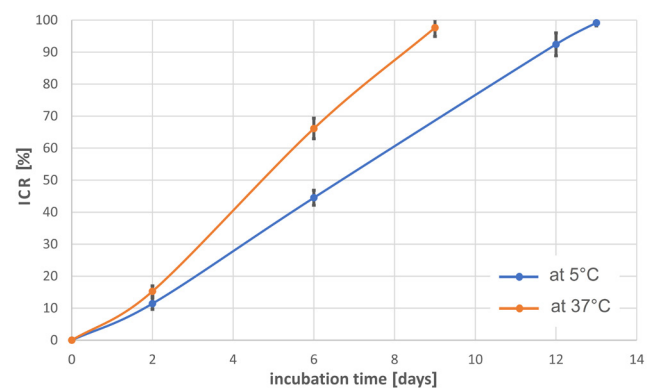


Fig. 7. Cumulative release profiles of insulin for the F5 samples (0.03 wt% $\text{CaCl}_2 \cdot 2\text{H}_2\text{O}$, 2 IU/g of insulin) at 2 different temperatures of incubation (5°C and 37°C) ($n = 3$). The ICR data is presented as $M \pm SD$.

Discussion

Drug release from a matrix takes place through one or more of the following mechanisms: diffusion, swelling, degradation, and erosion,^{39,40} which are matrix-affected. The kind and load of the drug are factors influencing drug release.⁴¹ No wonder, then, that available LDDSs for periodontal therapy have different drug release kinetics. Clinical studies on Actisite reported concentrations

of tetracycline HCl higher than 1,000 µg/mL for a period of 10 days.⁷ PerioChip showed the burst release of about 40% of the chlorhexidine content in the first 24 h after application, followed by constant release for 7 days.⁹ Ligosan is claimed to reach 12 days of doxycycline release subgingivally.¹⁰ The performance of Atridox in terms of chlorhexidine release was similar to PerioChip, as demonstrated by clinical studies with effective antimicrobial concentrations measured in GCF up to 7 days.⁴² The subgingival application of 0.05 mL of Dentomycin ointment in a clinical trial led to concentrations of minocycline in GCF reaching 1,300 µg/mL after 1 h, but reduced to 90 µg/mL after 7 h.⁴³ In a trial including 12 patients, Elyzol Dental Gel was applied once into pockets ≥5 mm and metronidazole was detectable in GCF for 36 h, but its concentration was higher than the minimum inhibitory concentration (1 µg/mL) for only 12 h.⁴⁴ Arestin achieved concentrations of minocycline in GCF >1 µg/mL up to 14 days.¹²

Local drug delivery systems that have higher cross-linked drug carrier matrices, such as non-absorbable LDDSs, films and chips, seem to achieve relatively longer release intervals. On the other hand, non-absorbable LDDSs need a second appointment for removal. Fibers, films and chips can be tricky to insert into some pockets. Many LDDSs offer initial burst release (e.g., PerioChip). The use of microparticle-based techniques (e.g., Arestin) can overcome these disadvantages, although they entail more complicated procedures, hence higher costs. A few LDDSs have short release intervals (e.g., Dentomycin and Elyzol). The LDDS designed in this study for the local delivery of insulin took good advantage of the abilities of the hydrogel to entrap and release materials, which can be modulated simply by physically blending many polymers and other additives together until the desired release profile is obtained.

Since sufficient viscosity is mandatory for hydrogels to be able to entrap molecules,⁴⁵ in addition to being needed to prevent the hydrogel from leaking from the injection site, we dissolved greater quantities of the precursor as a strategy to increase viscosity during the preparation of the hydrogel. However, the viscosity of the hydrogels was adjusted so that they were injectable. Also, blending many polymers together helped to fine-tune drug release kinetics. Still, the bi-phasic texture of F2 seems consistent with what Inamura et al. indicated about the repulsive interactions and incompatibility of the PEG/PVA and PEG/PVP polymer pairs in water,⁴⁶ which can eventually cause liquid-liquid phase separation in the solution.

The link between increased insulin loads and accelerated release could be explained by more insulin-to-insulin weak bonds forming at the expense of polymer-to-insulin bonds. The effect of the addition of CaCl₂·2H₂O on the insulin release profiles of PVP/PVA blends is similar to its influence posited by Rambabu and Velu on the dye rejection of polyethersulfone ultrafiltration membranes.⁴⁷

This may be ascribed to the steric hindrance initiated by polymer-to-calcium chloride bonds. Steric hindrance restricts the diffusion of the drug from the hydrogel. It also restricts the diffusion of water into the hydrogel, which is responsible for the hydrolysis of drug-to-polymer bonds. Another possible mechanism is that calcium ions form adsorption sites for insulin molecules, making their out-diffusion slower.

Conclusions

The results of the present study allow the authors to ratiocinate that a linear copolymer-hydrogel composed of PVP, PVA and CaCl₂·2H₂O can provide the sustained release of insulin (in vitro) for a reasonable period. Insulin release intervals can be fine-tuned by changing one or more of the following determinants, which were found to affect the insulin release profile: the hydrogel composition, the insulin load and the CaCl₂·2H₂O content. The design presented may perhaps be beneficial for the local delivery of insulin in patients with periodontitis, as an adjunct to NSPT.

ORCID iDs

Ali Raef Abboud  <https://orcid.org/0000-0002-0790-901X>
 Ali Mohammad Ali  <https://orcid.org/0000-0002-8906-1904>
 Tihama Youssef  <https://orcid.org/0000-0002-6687-4814>

References

- Lang NP, Lindhe J, eds. *Clinical Periodontology and Implant Dentistry*. 6th ed. Hoboken, USA: Wiley-Blackwell; 2015:749–761.
- Krayer JW, Leite RS, Kirkwood KL. Non-surgical chemotherapeutic treatment strategies for the management of periodontal diseases. *Dent Clin North Am*. 2010;54(1):13–33.
- Rajeshwari HR, Dhamecha D, Jagwani S, et al. Local drug delivery systems in the management of periodontitis: A scientific review. *J Control Release*. 2019;307:393–409.
- Joshi D, Garg T, Goyal AK, Rath G. Advanced drug delivery approaches against periodontitis. *Drug Deliv*. 2016;23(2):363–377.
- Thakur VK, Thakur MK, eds. *Handbook of Polymers for Pharmaceutical Technologies. Volume 2. Processing and Applications*. Austin, USA: Wiley-Scrivener Publishing; 2015:95–113.
- Javanbakht T, Bérard A, Tavares JR. Polyethylene glycol and poly(vinyl alcohol) hydrogels treated with photo-initiated chemical vapor deposition. *Can J Chem*. 2016;94(9):744–750.
- Litch JM, Encarnacion M, Chen S, Leonard J, Burkoth TL. Use of the polymeric matrix as internal standard for quantitation of in vivo delivery of tetracycline HCl from Actisite tetracycline fiber during periodontal treatment. *J Periodontol Res*. 1996;31(8):540–544.
- Kataria S, Chandrashekar KT, Mishra R, Tripathi V, Galav A, Sthapak U. Effect of tetracycline HCl (Periodontal Plus AB) on *Aggregatibacter actinomycetemcomitans* levels in chronic periodontitis. *Arch Oral Dent Res*. 2015;2(1):1–8.
- Paolantonio M, D'Angelo M, Grassi RF, et al. Clinical and microbiologic effects of subgingival controlled-release delivery of chlorhexidine chip in the treatment of periodontitis: A multicenter study. *J Periodontol*. 2008;79(2):271–282.
- Kiesow A, Buchholz M, Sarembe S, Mäder K, Kirchberg M, Eick S. Tetracycline complexes with sustained activity. <https://patentscope.wipo.int/search/en/detail.jsf?docId=WO2020089249&tab=PCTDESCRPTION>. Accessed June 11, 2020.
- Lauenstein M, Kaufmann M, Persson GR. Clinical and microbiological results following nonsurgical periodontal therapy with or without local administration of piperacillin/tazobactam. *Clin Oral Investig*. 2013;17(7):1645–1660.

12. Persson GR, Salvi GE, Heitz-Mayfield LJA, Lang NP. Antimicrobial therapy using a local drug delivery system (Arestin) in the treatment of peri-implantitis. I: Microbiological outcomes. *Clin Oral Implants Res.* 2006;17(4):386–393.
13. Kleine B, Rossmannith WG. *Hormones and the Endocrine System.* Cham, Switzerland: Springer International Publishing AG; 2016:89–92.
14. Fulzele K, Clemens TL. Novel functions for insulin in bone. *Bone.* 2012;50(2):452–456.
15. Fulzele K, Riddle RC, DiGirolamo DJ, et al. Insulin receptor signaling in osteoblasts regulates postnatal bone acquisition and body composition. *Cell.* 2010;142(2):309–319.
16. Ferron M, Wei J, Yoshizawa T, et al. Insulin signaling in osteoblasts integrates bone remodeling and energy metabolism. *Cell.* 2010;142(2):296–308.
17. Klein GL. Insulin and bone: Recent developments. *World J Diabetes.* 2014;5(1):14–16.
18. Senn JJ, Klover PJ, Nowak IA, Mooney RA. Interleukin-6 induces cellular insulin resistance in hepatocytes. *Diabetes.* 2002;51(12):3391–3399.
19. Kurauti MA, Costa-Júnior JM, Ferreira SM, et al. Interleukin-6 increases the expression and activity of insulin-degrading enzyme. *Sci Rep.* 2017;7:46750.
20. Thraillkill K, Bunn RC, Lumpkin C Jr., et al. Loss of insulin receptor in osteoprogenitor cells impairs structural strength of bone. *J Diabetes Res.* 2014;2014:703589.
21. Fai S, Ahem A, Mustapha M, Mohd Noh UK, Bastion MLC. Randomized controlled trial of topical insulin for healing corneal epithelial defects induced during vitreoretinal surgery in diabetics. *Asia Pac J Ophthalmol (Phila).* 2017;6(5):418–424.
22. Attia EAS, Belal DMI, El Samahy MH, El Hamamsy MH. A pilot trial using topical regular crystalline insulin vs aqueous zinc solution for uncomplicated cutaneous wound healing: Impact on quality of life. *Wound Repair Regen.* 2014;22(1):52–57.
23. Rezvani O, Shabbak E, Aslani A, Bidar R, Jafari M, Safarnezhad S. A randomized, double-blind, placebo-controlled trial to determine the effects of topical insulin on wound healing. *Ostomy Wound Manage.* 2009;55(8):22–28.
24. Zhang XJ, Wu X, Wolf SE, Hawkins HK, Chinkes DL, Wolfe RR. Local insulin-zinc injection accelerates skin donor site wound healing. *J Surg Res.* 2007;142(1):90–96.
25. Van Ort SR, Gerber RM. Topical application of insulin in the treatment of decubitus ulcers: A pilot study. *Nurs Res.* 1976;25(1):9–12.
26. Wang X, Zhang G, Qi F, et al. Enhanced bone regeneration using an insulin-loaded nano-hydroxyapatite/collagen/PLGA composite scaffold. *Int J Nanomedicine.* 2018;13:117–127.
27. Paglia DN, Wey A, Breitbart EA, et al. Effects of local insulin delivery on subperiosteal angiogenesis and mineralized tissue formation during fracture healing. *J Orthop Res.* 2013;31(5):783–791.
28. Han Y, Zhang XY, Ling EL, Wang DS, Liu HS. Sustained local delivery of insulin for potential improvement of peri-implant bone formation in diabetes. *Sci China Life Sci.* 2012;55(11):948–957.
29. Bartlett JD, Slusser TG, Turner-Henson A, Singh KP, Atchison JA, Pillion DJ. Toxicity of insulin administered chronically to human eye in vivo. *J Ocul Pharmacol.* 1994;10(1):101–107.
30. Emecen-Huja P, Eubank TD, Shapiro V, Yildiz V, Tatakis DN, Leblebicioglu B. Peri-implant versus periodontal wound healing. *J Clin Periodontol.* 2013;40(8):816–824.
31. Vedadghavami A, Minoeei F, Mohammadi MH, et al. Manufacturing of hydrogel biomaterials with controlled mechanical properties for tissue engineering applications. *Acta Biomater.* 2017;62:42–63.
32. Shi Y, Xiong DS, Peng Y, Wang N. Effects of polymerization degree on recovery behavior of PVA/PVP hydrogels as potential articular cartilage prosthesis after fatigue test. *EXPRESS Polym Lett.* 2016;10(2):125–138.
33. Ozdil D, Wimpenny L, Aydin M, Yang Y. Biocompatibility of biodegradable medical polymers. In: Zhang X, ed. *Science and Principles of Biodegradable and Bioresorbable Medical Polymers: Materials and Properties.* Cambridge, UK: Elsevier (Woodhead Publishing); 2017:379–414.
34. Chazotte B. Labeling Golgi with fluorescent ceramides. *Cold Spring Harb Protoc.* 2012;2012(8):pdb.prot070599.
35. Simonian MH. Spectrophotometric determination of protein concentration. *Curr Protoc Cell Biol.* 2002;15(1):A.3B.1–A.3B.7.
36. Yilmaz B, Kadioglu Y. Determination of human insulin in pharmaceutical preparation by zero, first and second order derivative spectrophotometric methods. *Intl R J Pharmaceut.* 2012;2(2):21–29.
37. Lassalle VL, Pirillo S, Rueda E, Ferreira ML. An accurate UV/visible method to quantify proteins and enzymes: Impact of aggregation, buffer concentration and the nature of the standard. *Curr Top Anal Chem.* 2011;3:83–93.
38. Vimalavathini R, Gitanjali B. Effect of temperature on the potency & pharmacological action of insulin. *Indian J Med Res.* 2009;130(2):166–169.
39. Muzzarelli RAA. Chitins and chitosans for the repair of wounded skin, nerve, cartilage and bone. *Carbohydr Polym.* 2009;76(2):167–182.
40. Pillai O, Panchagnula R. Polymers in drug delivery. *Curr Opin Chem Biol.* 2001;5(4):447–451.
41. Weiser JR, Saltzman WM. Controlled release for local delivery of drugs: Barriers and models. *J Control Release.* 2014;190:664–673.
42. Garrett S, Johnson L, Drisko CH, et al. Two multi-center studies evaluating locally delivered doxycycline hyclate, placebo control, oral hygiene, and scaling and root planing in the treatment of periodontitis. *J Periodontol.* 1999;70(5):490–503.
43. van Steenberghe D, Bercy P, Kohl J, et al. Subgingival minocycline hydrochloride ointment in moderate to severe chronic adult periodontitis: A randomized, double-blind, vehicle-controlled, multi-center study. *J Periodontol.* 1993;64(7):637–644.
44. Stoltze K. Concentration of metronidazole in periodontal pockets after application of a metronidazole 25% dental gel. *J Clin Periodontol.* 1992;19(9 Pt 2):698–701.
45. Talukdar MM, Vinckier I, Moldenaers P, Kinget R. Rheological characterization of xanthan gum and hydroxypropylmethyl cellulose with respect to controlled-release drug delivery. *J Pharm Sci.* 1996;85(5):537–540.
46. Inamura I, Akiyama K, Kubo Y. Polymer 2–polymer 3 interactions in water 1/polymer 2/polymer 3 ternary systems. *Polym J.* 1997;29(2):119–122.
47. Rambabu K, Velu S. Improved performance of CaCl₂ incorporated polyethersulfone ultrafiltration membranes. *Period Polytech Chem Eng.* 2016;60(3):181–191.

Salivary enzymatic antioxidant activity and dental caries: A cross-sectional study

Zakaria Vahabzadeh^{1,2,A–F}, Zahra Moaven Hashemi^{3,B}, Bijan Nouri^{4,C}, Fatemeh Zamani^{5,B}, Faranak Shafiee^{6,A–F}

¹ Liver and Digestive Research Center, Research Institute for Health Development, Kurdistan University of Medical Sciences, Sanandaj, Iran

² Department of Biochemistry, Faculty of Medicine, Kurdistan University of Medical Sciences, Sanandaj, Iran

³ Student Research Committee, Kurdistan University of Medical Sciences, Sanandaj, Iran

⁴ Social Determinants of Health Research Center, Research Institute for Health Development, Kurdistan University of Medical Sciences, Sanandaj, Iran

⁵ Cellular and Molecular Research Center, Research Institute for Health Development, Kurdistan University of Medical Sciences, Sanandaj, Iran

⁶ Department of Pediatric Dentistry, Faculty of Dentistry, Kurdistan University of Medical Sciences, Sanandaj, Iran

A – research concept and design; B – collection and/or assembly of data; C – data analysis and interpretation;

D – writing the article; E – critical revision of the article; F – final approval of the article

Dental and Medical Problems, ISSN 1644-387X (print), ISSN 2300-9020 (online)

Dent Med Probl. 2020;57(4):385–391

Address for correspondence

Faranak Shafiee

E-mail: faranakshafiee@gmail.com

Funding sources

This work, as a dentistry student's thesis, was supported financially by the Vice-Chancellor for Research of Kurdistan University of Medical Sciences in Sanandaj, Iran (grant No. IR.MUK.REC.1397/230).

Conflict of interest

None declared

Acknowledgements

We would like to thank the Heads of the Cellular and Molecular Research Center of Kurdistan University of Medical Sciences in Sanandaj, Iran, for their valuable assistance.

Received on June 7, 2020

Reviewed on July 5, 2020

Accepted on August 6, 2020

Published online on December 31, 2020

Cite as

Vahabzadeh Z, Hashemi ZM, Nouri B, Zamani F, Shafiee F. Salivary enzymatic antioxidant activity and dental caries: A cross-sectional study. *Dent Med Probl.* 2020;57(4):385–391. doi:10.17219/dmp/126179

DOI

10.17219/dmp/126179

Copyright

© 2020 by Wrocław Medical University

This is an article distributed under the terms of the

Creative Commons Attribution 3.0 Unported License (CC BY 3.0)

(<https://creativecommons.org/licenses/by/3.0/>).

Abstract

Background. Oxidative stress has been identified as a predisposing factor for dental caries. Saliva, as a rich source of antioxidants, plays an essential role in the protection against dental caries. Salivary enzymatic antioxidants include superoxide dismutase (SOD), catalase (CAT) and glutathione peroxidase (GPx).

Objectives. The aim of this study was to evaluate the correlation of salivary enzymatic antioxidant activity with different levels of dental caries in children.

Material and methods. In this cross-sectional study, 90 healthy children aged 7–12 years (36 girls, 54 boys) were investigated. Demographic information was gathered and dental examinations were provided for all participants. Then, unstimulated whole saliva samples were collected in the morning. The salivary SOD, CAT and GPx activity was measured spectrophotometrically. For statistical analysis, Spearman's correlation test, the Mann–Whitney *U* test and the Kruskal–Wallis test were used with the SPSS for Windows software, v. 16.

Results. Our results showed no significant correlation between SOD, CAT and GPx and the decayed, missing, filled teeth index for permanent/primary dentition (DMFT/dmft). The CAT activity was elevated in proportion to the number of decayed teeth. The SOD activity showed a positive correlation with the frequency of tooth brushing. The activity of SOD, CAT and GPx was higher in boys than in girls. An inverse relationship between enzymatic antioxidant activity and age was also observed.

Conclusions. Although enzymatic antioxidants had no positive correlation with DMFT/dmft, they were positively correlated with the number of decayed teeth and the improvement of oral hygiene.

Key words: dental caries, saliva, oral hygiene, enzymatic antioxidant

Introduction

Dental caries is a dynamic and continuous process. It involves repeated cycles of demineralization by the acidic metabolites produced through the fermentation process of dietary carbohydrates of microbial origin, followed by remineralization by salivary components. Bacterial infection is one of the main etiologic factors for dental caries. The substrate and the host are also crucial factors for the initiation of the caries process. Clinical studies have shown that saliva, as a host factor, plays an essential role in the progression or regression of oral diseases, and in some cases, it regulates them. It is well established that the salivary protective mechanisms control the process of dental caries to a great extent.¹ Saliva is a heterogeneous liquid and a multifunctional natural defense system. It is a rich source of antioxidants, which play an important role the protection against bacteria, viruses and fungi, also with regard to the mucosa and tooth surfaces.^{2,3}

Several studies have been done to identify the components of the natural defense system for the teeth and the oral mucosa.⁴⁻⁶ Oxidative stress occurs as a result of an imbalance between reactive oxygen species (ROS) and the antioxidant system. It has been identified as one of the essential predisposing factors for many oral inflammatory conditions.^{6,7} Oxidative stress directly affects the underlying mechanisms which induce the intracellular signals leading to the growth and differentiation of cariogenic bacteria.⁸ Recent studies provided documentation indicating the elevation of oxidative damage biomarkers in the saliva of patients with periodontal diseases and dental caries,² but it is not yet known whether the elevation of these biomarkers is due to the increased production of ROS or antioxidant deficiency. Interventional studies on humans and animal models showed the beneficial effect of supplementation with antioxidants to prevent or reduce the progression of periodontitis.^{3,5,9}

The salivary antioxidant system contains both enzymatic and non-enzymatic antioxidants. The enzymatic antioxidant defense system includes superoxide dismutase (SOD), catalase (CAT) and glutathione peroxidase (GPx).¹⁰ Enzymatic antioxidants make up the first line of antioxidant defense. They inhibit the release of primary free radicals and other following chemical chain reactions.¹⁰

Superoxide dismutase is an antioxidant enzyme that catalyzes 2 superoxide anion molecules to hydrogen peroxide (H₂O₂) and oxygen (O₂) molecules.¹⁰ This enzyme is essential for cellular health and body protection against free radicals. The SOD levels decrease with age. A daily intake of SOD supplements has been shown to improve the immune system potential and reduce the chances of disease.¹⁰

Glutathione peroxidase is another enzymatic antioxidant that plays an essential role in neutralizing H₂O₂ produced through the SOD dismutation process.¹¹

It is mainly found in mitochondria, and sometimes in cytosol. Glutathione peroxidase breaks down H₂O₂ into water as well as lipid peroxides into their relevant alcohols.¹² It also plays an important role in the prevention of cancer and cardiovascular diseases.¹⁰

Catalase is a ubiquitous antioxidant enzyme, found in almost all living organisms using oxygen. It has a secondary role in defense against peroxidative agents.¹³ This enzyme catalyzes H₂O₂ produced through the dismutation process to water and O₂ molecules, thus completing the detoxification process after SOD. Patients with CAT deficiency (acatalasemia) are more likely to develop type 2 diabetes mellitus.¹⁰

It has been shown that imbalances in the SOD, CAT and GPx ratios can lead to disease.¹³⁻¹⁵ Hendi et al. showed decreased SOD activity and increased CAT and GPx activity in children with dental caries as compared to those without caries.⁴ It has been suggested in recent years that salivary oxidative stress markers could be used to screen and control oral diseases, including dental caries.³ The evaluation of these salivary markers could help identify patients who are reluctant to undergo regular dental examinations or are at high risk for dental caries; additionally, these markers offer useful information concerning the development of new preventive and treatment modalities.^{3,5,6} Also, the availability and non-invasiveness of these techniques are good reason to use saliva as a diagnostic biological fluid to evaluate diseases.² Previous studies showed that the antioxidant status of saliva, especially in children, may reflect the risk for dental caries.¹⁶ Considering the relationship between antioxidants and the caries process, and the feasibility of the analysis of salivary enzymatic antioxidants, this study aimed to evaluate salivary enzymatic antioxidant levels in children with caries.

Material and methods

Patient selection

This cross-sectional study was carried out in 2019 in Sanandaj, Iran. Clinical unstimulated salivary samples were collected from 90 healthy children aged 7–12 years. This age group has more experience of dental caries.¹⁷ The sample size was determined based on previous studies.^{2,6} Children whose parents received a complete explanation about the aims and methods of the study, and then signed written consent were included in the study. The inclusion criteria of this study were similar to those previously reported by others.^{2,7} Children who had a history of a systemic or local disease affecting salivary secretion and/or received antifungal agents, antihistamines, corticosteroids, nonsteroidal anti-inflammatory drugs (NSAIDs), antimicrobial mouthwashes, or other long-term medications

or supplements for at least 1 month before the study were excluded. Demographic information was gathered and dental examinations were provided for all participants. The dental caries index was determined according to the World Health Organization (WHO) criteria using a dental mirror and an explorer 24 h before sampling.

This study was approved by the ethics committee of Kurdistan University of Medical Sciences in Sanandaj, Iran, under IR.MUK.REC.1397/230.

Collection of saliva

Unstimulated salivary samples were collected between 9 a.m. and 12 a.m., at least 2 h after the last episode of eating or drinking to reduce any variability resulting from the effect of the circadian rhythm or possible stimulation. Generally, unstimulated saliva contains basal and normal components of saliva that is secreted into the oral cavity during the day. The children were asked to rinse their mouths with distilled water to remove any food debris before the salivary samples were collected. They were also asked to sit quietly on a chair and bend their head slightly downward without any masticating movement to allow saliva to flow from the lower lip into sterile tubes passively. This draining protocol is more reliable and requires no stimulation.¹⁸ Finally, 5 mL of saliva was collected in appropriately numbered tubes by means of the abovementioned method. The tubes were then tightly sealed to prevent contamination or evaporation, placed on an ice pack and sent to the laboratory within an hour. The salivary samples were centrifuged at 4,000 rpm for 4 min at 4°C. The supernatants were divided in 2 aliquots, and then stored at –80°C until final analysis.

Measurement of enzymatic antioxidant activity

Superoxide dismutase activity

The SOD activity of the separated salivary samples was measured using an appropriate assay kit (CAT No. ZB-SOD-96A; ZellBio GmbH, Lonsee, Germany). In brief, in this method, H₂O₂ produced during the enzymatic reaction combines with the chromogen component of the kit to provide a complex. Its optical density (OD) was measured in the samples and blank at 420 nm within 0- and 2-minute time intervals with a microplate reader (Synergy HTX; BioTek Instruments Inc., Winooski, USA). Finally, the SOD activity in the subjects' salivary samples was reported in U/mL as mean (M) ± standard deviation (SD).

Catalase activity

The CAT activity of the separated salivary samples was measured using an appropriate assay kit

(CAT No. ZB-CAT-96A; ZellBio GmbH). In brief, in this method, a two-step reaction is used to measure the enzymatic activity. In the 1st step, the patients' and blank samples were incubated with a certain amount of H₂O₂ for 1 min. In this reaction, H₂O₂ dissociates into water and O₂. The rate of H₂O₂ dissociation was proportional to the CAT concentration in the samples. In the 2nd step, the residual H₂O₂ reacts with the existing chromogen to form a complex. Its OD was measured in the samples and blank at 405 nm after 1 min with a microplate reader (Synergy HTX; BioTek Instruments Inc.). Finally, the CAT activity in the subjects' salivary samples was reported in U/mL as $M \pm SD$.

Glutathione peroxidase activity

The GPx activity of the separated salivary samples was measured using an appropriate assay kit (CAT No. ZB-GPX-96A; ZellBio GmbH). In brief, in this method, a two-step reaction was used to measure the enzymatic activity. In the 1st step, the samples, control and blank were incubated with a certain amount of glutathione (GSH) for 5 min. In this reaction, GSH is oxidized to glutathione disulfide (GSSG) through the activity of GPx of the samples and control. The amount of the consumed GSH was proportional to the GPx concentration in the samples. In the 2nd step, the residual GSH reacts with the existing chromogen in the kit (Pierce Ellman's Reagent (DTNB); Thermo Fisher Scientific, Waltham, USA) to form a yellow complex. Its OD was measured at 412 nm after 1 min with a microplate reader (Synergy HTX; BioTek Instruments Inc.). Finally, the GPx activity in the salivary samples was reported in U/mL as $M \pm SD$.

Statistical analysis

Data was expressed as $M \pm SD$. Statistical analysis was performed using the SPSS for Windows software, v. 16.0 (SPSS Inc., Chicago, USA). For statistical analysis, Spearman's correlation test, the Mann–Whitney U test and the Kruskal–Wallis test were used with the software. Statistical significance was set at $p < 0.05$.

Results

In this cross-sectional study, 90 children aged 7–12 years participated. Thirty-six (40%) of them were girls and 54 (60%) were boys. Since the children had mixed dentition, the average caries index was calculated based on the sum of the decayed, missing, filled teeth in permanent/primary dentition (DMFT/dmft). This index was 7.17 ± 3.56 in our study. No significant correlation was established between the SOD, CAT and GPx activity and DMFT/dmft ($p > 0.05$) (Fig. 1A,1C,1E).

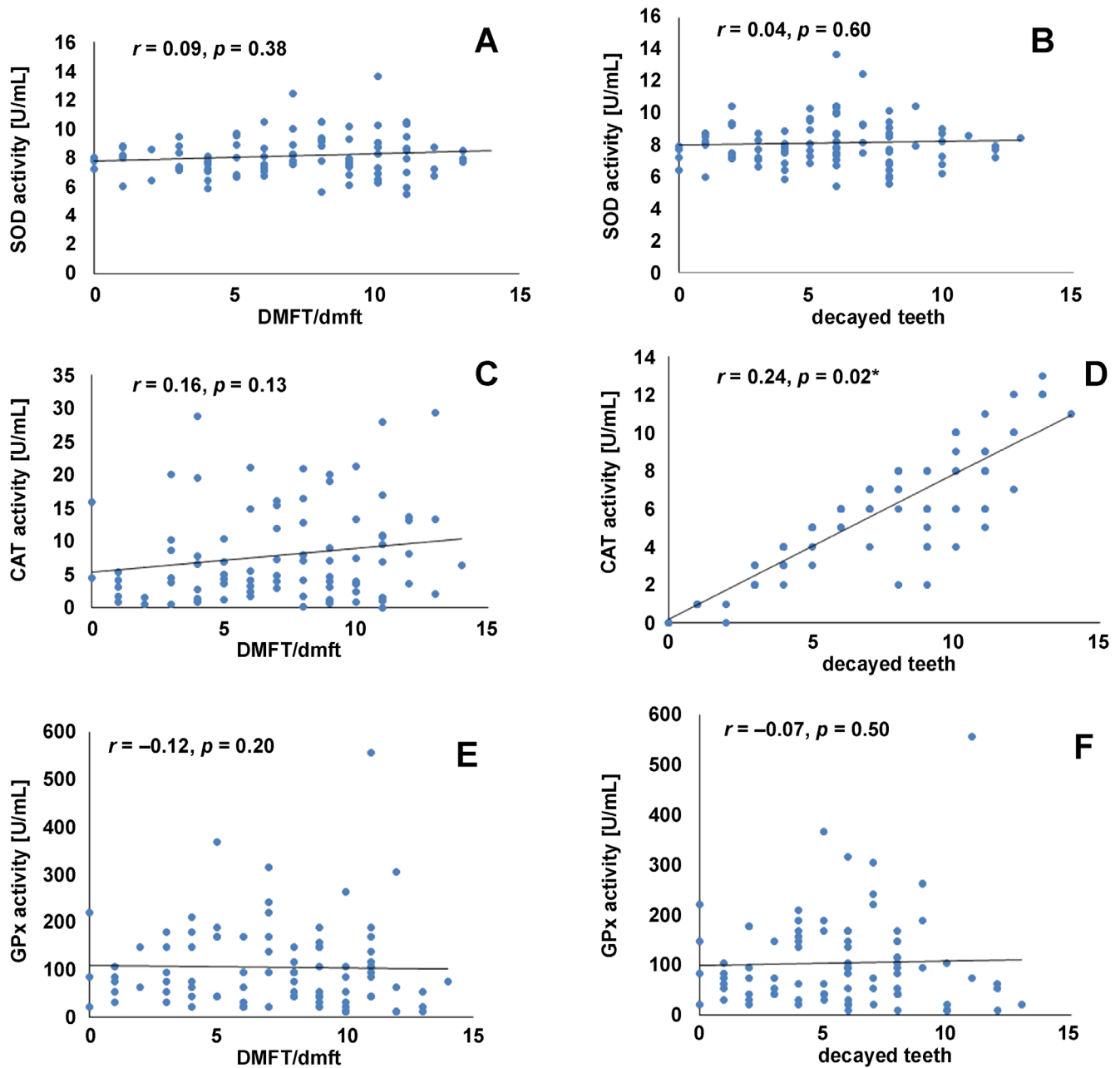


Fig. 1. Associations between salivary enzymatic antioxidants and the decayed, missing, filled teeth in permanent/primary dentition index (DMFT/dmft) as well as the decayed teeth

A – SOD activity and DMFT/dmft; B – SOD activity and the decayed teeth; C – CAT activity and DMFT/dmft; D – CAT activity and the decayed teeth; E – GPx activity and DMFT/dmft; F – GPx activity and the decayed teeth.

SOD – superoxide dismutase; CAT – catalase; GPx – glutathione peroxidase; * statistical significance ($p < 0.05$; Spearman's correlation test).

The CAT activity showed a positive correlation with the total number of decayed teeth ($r = 0.24$; $p = 0.02$) (Fig. 1D), but the SOD and GPx activity showed no correlation ($r = 0.04$; $p = 0.60$ and $r = -0.07$; $p = 0.50$, respectively) (Fig. 1B,1F).

Spearman's correlation test showed a positive correlation between the SOD activity and the frequency of tooth brushing; the positive direction of the relationship indicates that the SOD activity increases with increased tooth brushing frequency ($p = 0.03$) (Fig. 2A). The CAT and GPx

activity was not correlated with the frequency of tooth brushing ($p > 0.05$) (Fig. 2B,2C). The Mann–Whitney U test showed no significant differences in the activity of enzymatic antioxidants between genders ($p > 0.05$). The test showed higher values of the SOD, CAT and GPx activity in boys in comparison with girls, but the differences were statistically nonsignificant (Table 1). As shown in Fig. 3A–C, there was an inverse relationship between the SOD ($r = -0.04$; $p < 0.001$), CAT ($r = -0.07$; $p < 0.001$) and GPx ($r = -0.08$, $p < 0.001$) activity and age.

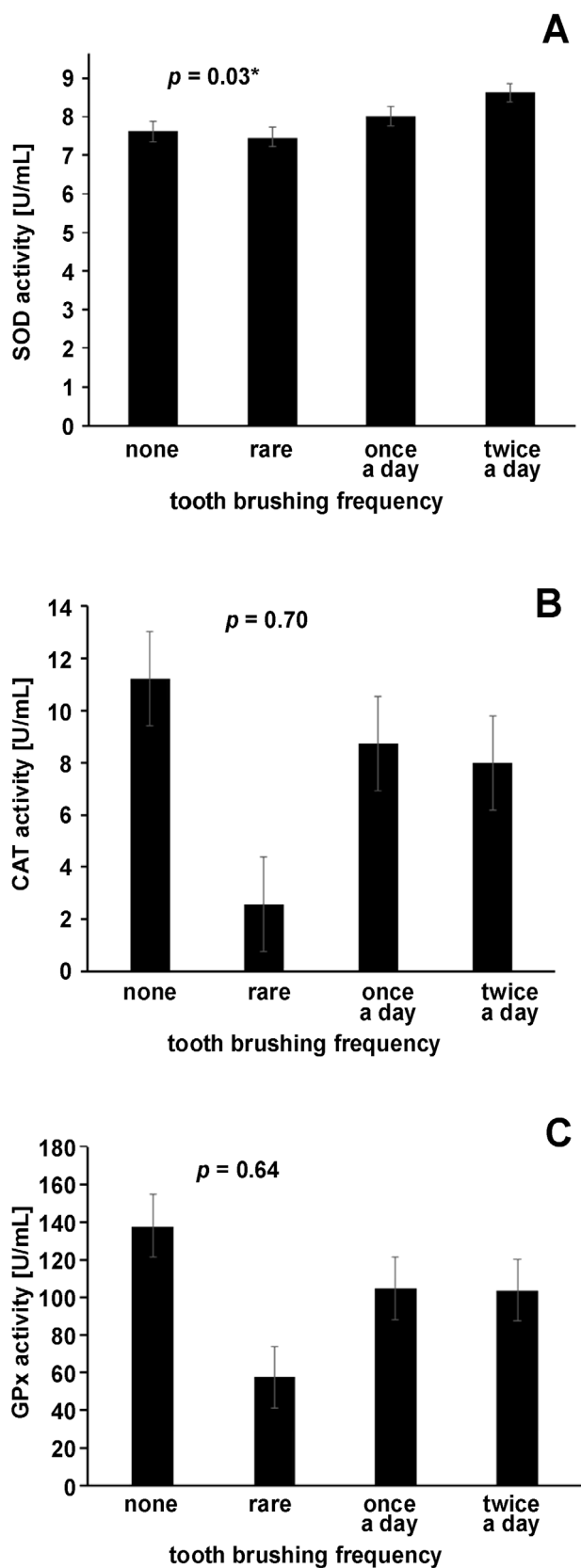


Fig. 2. Correlation between salivary enzymatic antioxidants and tooth brushing frequency

A – salivary SOD activity and tooth brushing frequency; B – salivary CAT activity and tooth brushing frequency; C – salivary GPx activity and tooth brushing frequency.

* statistical significance ($p < 0.05$; Spearman's correlation test).

Table 1. Comparison of the activity of the salivary antioxidants between the genders (Mann–Whitney U test)

Antioxidant	Male	Female	p -value
SOD [U/mL]	8.14 ± 1.49	8.05 ± 1.38	0.641
CAT [U/mL]	8.39 ± 7.26	7.06 ± 6.89	0.447
GPx [U/mL]	112.42 ± 103.37	90.08 ± 65.43	0.516

Data presented as mean (M) ± standard deviation (SD).

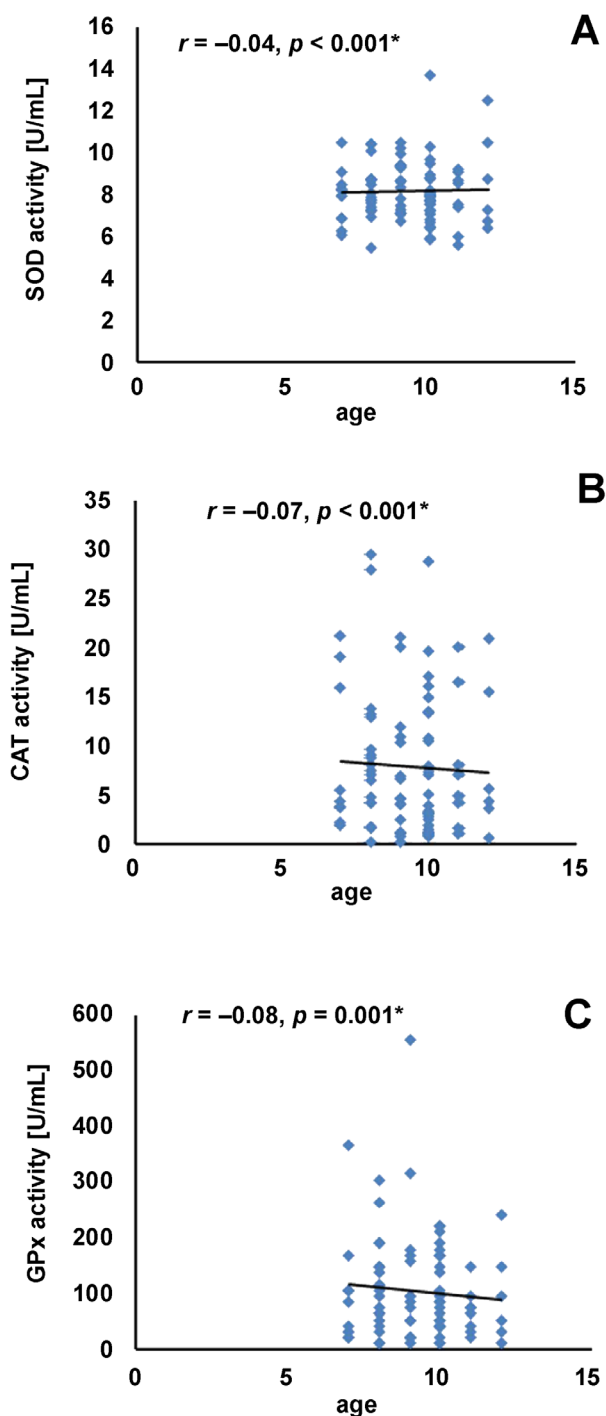


Fig. 3. Association between salivary enzymatic antioxidants and age

A – SOD activity and age; B – CAT activity and age; C – GPx activity and age.

* statistical significance ($p < 0.001$; Spearman's correlation test).

Discussion

In the present study, there was no significant relationship between the SOD activity and DMFT/dmft. Hendi et al. reported a decrease in the SOD activity in children with caries as compared to children without caries.⁴ In contrast, some studies showed that the salivary SOD activity in children with severe early childhood caries (S-ECC) is higher than in children without caries.^{2,6} Silva et al. showed that the salivary SOD activity in children with S-ECC was significantly higher than in children without caries.⁶ Hedge et al. reported a significant increase in the salivary SOD activity in the group with DMFT >10 as compared to DMFT = 0.² The most important reason for the differences between our results and the abovementioned studies might be the sampling methods and techniques used. In those case-control studies, the enzymatic activity was compared between 2 groups with great DMFT differences. This may explain their significant results.^{2,6} In contrast, in our cross-sectional study, children with varying degrees of dental caries were not divided into different groups due to the small sample size of the caries-free group.

In the present study, a significant and positive association was observed between the CAT activity and the number of decayed teeth, like in the study done by Hendi et al.⁴

Our results showed no significant relationship between the salivary GPx activity and DMFT/dmft. This finding is consistent with the results of Hedge et al.¹¹ They also observed no significant difference in the GPx activity of subgroups with different DMFT/dmft (DMFT < 3; 3 < DMFT < 10; and DMFT > 10). However, they showed a significant increase in the salivary GPx activity in the group with active caries as compared to the caries-free group.¹¹ In our study, such a comparison was not made due to the small number of caries-free subjects.

Previous studies reported a significant elevation of the salivary total antioxidant capacity (TAC) in patients with an advanced form of caries (cavitated lesions) in comparison with a non-caries group.^{2,8,19,20} Furthermore, the elevation of TAC in children with a high caries rate may be due to the colonization of microorganisms as well as the stimulation of the immune system, which consequently results in the body's compensatory reaction to reduce oxidative stress.⁶ Tóthová et al. showed that an improvement in the clinical parameters of the Oral Hygiene Index (OHI) reduced the concentrations of thiobarbituric acid reacting substances (TBARS) as markers for increasing TAC.³ In the present study, the SOD activity increased with the increased frequency of tooth brushing whereas there was no relationship between the CAT and GPx activity and the tooth brushing frequency.

Several studies have also shown a positive relationship between periodontal parameters and enzymatic antioxidants. Novaković et al. showed increased SOD and GPx activity in patients with chronic periodontitis

after non-surgical treatment.²¹ An *in vitro* study also showed that the SOD and CAT activity diminished with the increasing depth of the sulcus in periodontal patients.²² A medication with liposome-encapsulated SOD improves the healing process by reducing periodontal inflammatory reactions. However, such an effect was not observed in the case of liposome-encapsulated CAT.²²

Our study showed there was a reduction in the activity of SOD, CAT and GPx with age. This relationship is weaker for SOD in comparison with CAT and GPx. To support this finding, there are studies that show a positive relationship between age and TAC. For example, Tóthová et al.¹⁶ and Hedge et al.²³ showed the elevation of TAC with age in 4–18-year-old children and in children aged <71 months as well as in 6–12-year-olds, respectively. In contrast to the abovementioned studies, Kumar et al. showed no significant relationship between the children's age (age range: 3–5 years) and TAC.¹⁹

In our study, the activity of SOD, CAT and GPx was not significantly different between genders. In contrast to this finding, the results of Ahmadi-Motamayel et al. showed higher TAC in boys than in girls in the age range of 15–17 years.²⁴ Moreover, Hendi et al. reported lower CAT activity and higher GPx activity in the female group as compared to the male group.⁴ Since the performance of the antioxidant system generally depends on various factors, including TAC, the amount of the released free radicals, genetics, diet, age, hormones as well as individual stress,²⁵ differences in the results of various studies may be attributed to differences in those factors.²³ Finally, more clinical and laboratory studies are also needed to clarify the complete relationship between enzymatic antioxidants and dental caries.

Conclusions

In conclusion, since few studies have been carried out on enzymatic antioxidants and dental caries, the present study has provided new insights about the activity of enzymatic antioxidants in children with varying degrees of dental caries. The CAT activity increased with an increase in the number of decayed teeth. The SOD activity was positively correlated with the tooth brushing frequency. There was a decrease in the SOD, CAT and GPx activity with advancing age. The activity of SOD, CAT and GPx activity was higher in boys than in girls.

Since the frequency of tooth brushing was evaluated as one of the indicators of oral health, further studies are needed to determine the exact relationship between the salivary enzymatic antioxidant activity and the oral hygiene score. Also, further extensive studies with larger sample sizes are required, which might lead to some significant results. Moreover, case-control studies are suggested in the future.

ORCID iDs

Zakaria Vahabzadeh  <https://orcid.org/0000-0002-9854-9653>
 Zahra Moaven Hashemi  <https://orcid.org/0000-0001-5711-9094>
 Bijan Nouri  <https://orcid.org/0000-0002-2932-5058>
 Fatemeh Zamani  <https://orcid.org/0000-0002-0795-8276>
 Faranak Shafiee  <https://orcid.org/0000-0002-7280-2235>

References

1. Featherstone JDB. Dental caries: A dynamic disease process. *Aust Dent J.* 2008;53(3):286–291.
2. Hegde MN, Hegde ND, Ashok A, Shetty S. Biochemical indicators of dental caries in saliva: An in vivo study. *Caries Res.* 2014;48(2):170–173.
3. Tóthová L, Kamodyová N, Červenka T, Celec P. Salivary markers of oxidative stress in oral diseases. *Front Cell Infect Microbiol.* 2015;5:73.
4. Hendi SS, Goodarzi MT, Moghimbeigi A, Ahmadi-Motamayel F. Evaluation of the status of salivary antioxidants in dental caries. *Infect Disord Drug Targets.* 2019. doi:10.2174/1871526519666191031100432
5. Hegde MN, Attavar SH, Shetty N, Hegde ND, Hegde NN. Saliva as a biomarker for dental caries: A systematic review. *J Conserv Dent.* 2019;22(1):2–6.
6. Silva PVD, Troiano JA, Nakamune ACMS, Pessan JP, Antoniali C. Increased activity of the antioxidants systems modulate the oxidative stress in saliva of toddlers with early childhood caries. *Arch Oral Biol.* 2016;70:62–66.
7. Hegde MN, Hegde ND, Ashok A, Shetty S. Evaluation of total antioxidant capacity of saliva and serum in caries-free and caries-active adults: An in-vivo study. *Indian J Dent Res.* 2013;24(2):164–167.
8. Jurczak A, Kościelniak D, Skalniak A, Papież M, Vyhouskaya P, Krzyściak W. The role of the saliva antioxidant barrier to reactive oxygen species with regard to caries development. *Redox Rep.* 2017;22(6):524–533.
9. Lopes Castro MM, Duarte NN, Nascimento PC, et al. Antioxidants as adjuvants in periodontitis treatment: A systematic review and meta-analysis. *Oxid Med Cell Longev.* 2019;2019:9187978.
10. Ighodaro OM, Akinloye OA. First line defence antioxidants – superoxide dismutase (SOD), catalase (CAT) and glutathione peroxidase (GPX): Their fundamental role in the entire antioxidant defence grid. *Alexandria J Med.* 2018;54(4):287–293.
11. Hegde MN, Kumari S, Hegde ND, Shetty SS. Myeloperoxidase and glutathione peroxidase activity of saliva and serum in adults with dental caries: A comparative study. *J Free Radic Antioxid Photon.* 2013;139(2):175–180.
12. Góth L, Rass P, Páy A. Catalase enzyme mutations and their association with diseases. *Mol Diag.* 2004;8(3):141–149.
13. Karıncaoglu Y, Batcioglu K, Erdem T, Esrefoglu M, Genc M. The levels of plasma and salivary antioxidants in the patient with recurrent aphthous stomatitis. *J Oral Pathol Med.* 2005;34(1):7–12.
14. Weydert CJ, Cullen JJ. Measurement of superoxide dismutase, catalase and glutathione peroxidase in cultured cells and tissue. *Nat Protoc.* 2010;5(1):51–66.
15. Livnat G, Bentur L, Kuzmisky E, Nagler RM. Salivary profile and oxidative stress in children and adolescents with cystic fibrosis. *J Oral Pathol Med.* 2010;39(1):16–21.
16. Tóthová L, Celecová V, Celec P. Salivary markers of oxidative stress and their relation to periodontal and dental status in children. *Dis Markers.* 2013;34(1):9–15.
17. Dean J, ed. *McDonald and Avery's Dentistry for the Child and Adolescent.* 10th ed. St. Louis, MO: Mosby (Elsevier Health Sciences); 2016:135.
18. Yamuna Priya K, Muthu Prathibha K. Methods of collection of saliva – a review. *Int J Oral Health Dent.* 2017;3(3):149–153.
19. Kumar D, Pandey RK, Agrawal D, Agrawal D. An estimation and evaluation of total antioxidant capacity of saliva in children with severe early childhood caries. *Int J Paediatr Dent.* 2011;21(6):459–464.
20. Preethi BP, Reshma D, Anand P. Evaluation of flow rate, pH, buffering capacity, calcium, total proteins and total antioxidant capacity levels of saliva in caries free and caries active children: An in vivo study. *Indian J Clin Biochem.* 2010;25(4):425–428.
21. Novaković N, Cakić S, Todorović T, et al. Antioxidative status of saliva before and after non-surgical periodontal treatment. *Srp Arh Celok Lek.* 2013;141(3–4):163–168.
22. Trivedi S, Lal N. Antioxidant enzymes in periodontitis. *J Oral Biol Craniofac Res.* 2017;7(1):54–57.
23. Hegde AM, Rai K, Padmanabhan V. Total antioxidant capacity of saliva and its relation with early childhood caries and rampant caries. *J Clin Pediatr Dent.* 2009;33(3):231–234.
24. Ahmadi-Motamayel F, Goodarzi MT, Hendi SS, Kasraei S, Moghimbeigi A. Total antioxidant capacity of saliva and dental caries. *Med Oral Patol Oral Cir Bucal.* 2013;18(4):e553–e556.
25. Pereslegina IA. The activity of antioxidant enzymes in the saliva of normal children [in Russian]. *Lab Delo.* 1989;11(1):20–23.

Antibacterial activity of silver nanoparticles activated by photodynamic therapy in infected root canals

Hakan Aydın^{1,A–D}, Kürşat Er^{1,2,A–F}, Alper Kuştarıcı^{1,C,E}, Murat Akarsu^{3,A–D}, Gül Merve Gençer^{3,B,C}, Hakan Er^{4,5,B–D}, Rasih Felek^{6,B,C}

¹ Department of Endodontics, Faculty of Dentistry, Akdeniz University, Antalya, Turkey

² Department of Endodontics, Faculty of Dentistry, Alanya Alaaddin Keykubat University, Turkey

³ Department of Chemistry, Faculty of Arts and Science, Akdeniz University, Antalya, Turkey

⁴ Electron Microscopy Image Analyzing Unit, Faculty of Medicine, Akdeniz University, Antalya, Turkey

⁵ Department of Biophysics, Faculty of Medicine, Akdeniz University, Antalya, Turkey

⁶ Department of Microbiology, Faculty of Dentistry, Akdeniz University, Antalya, Turkey

A – research concept and design; B – collection and/or assembly of data; C – data analysis and interpretation;

D – writing the article; E – critical revision of the article; F – final approval of the article

Dental and Medical Problems, ISSN 1644-387X (print), ISSN 2300-9020 (online)

Dent Med Probl. 2020;57(4):393–400

Address for correspondence

Kürşat Er

E-mail: qursater@hotmail.com

Funding sources

The work was supported by the Scientific Research Projects Coordination Unit of Akdeniz University in Antalya, Turkey (grant No. TDH-2015-778).

Conflict of interest

None declared

Received on March 24, 2020

Reviewed on May 3, 2020

Accepted on June 6, 2020

Published online on December 31, 2020

Cite as

Aydın H, Er K, Kuştarıcı A, et al. Antibacterial activity of silver nanoparticles activated by photodynamic therapy in infected root canals. *Dent Med Probl.* 2020;57(4):393–400. doi:10.17219/dmp/123615

DOI

10.17219/dmp/123615

Copyright

© 2020 by Wrocław Medical University

This is an article distributed under the terms of the

Creative Commons Attribution 3.0 Unported License (CC BY 3.0)

(<https://creativecommons.org/licenses/by/3.0/>).

Abstract

Background. Root canal disinfection includes mechanical, chemical and biological struggle against microorganisms (MOs). Photodynamic therapy (PDT) and nanoparticle (NP) agents may be proposed as an alternative for use against intracanal infections due to their ability to disrupt biofilm and prevent bacterial adhesion to dentin. The use of NP agents in combination with light/photosensitizer (PS) agents increases the efficiency of PDT in root canal disinfection.

Objectives. The aim of the study was to evaluate the effect of light application – PDT – on the antibacterial activity of the combination of a PS agent (toluidine blue O –TBO) and an NP agent (silver nanoparticles – AgNPs) for the disinfection of the root canals inoculated with *Enterococcus faecalis* (*E. faecalis*).

Material and methods. In this study, concentrations of 20 ppm of TBO and 10 ppm of AgNPs, which showed the highest antibacterial activity against *E. faecalis* in the TBO/AgNPs combination, were used according to the preliminary studies. After instrumentation, 120 human, single-rooted, straight-canal mandibular premolars of a standard length of 13 mm were contaminated with bacteria, and experimental procedures were conducted against 21-day-old mature biofilm. The teeth were randomly divided into 5 main experimental groups: TBO/light; AgNPs; TBO/AgNPs; AgNPs/light; and TBO/AgNPs/light. Then, these main groups were divided into 2 subgroups each, according to the 2 application time periods (30 s and 60 s) ($n = 10$). The remaining 20 teeth constituted positive and negative control groups. The data was analyzed with the Kolmogorov–Smirnov test, one-way analysis of variance (ANOVA), Tukey's honestly significant difference (HSD) test, and the Bonferroni correction.

Results. The NaOCl group provided a bacterial reduction that was higher than in all other groups in a statistically significant manner. Light application on the TBO/AgNPs combination was the group that provided the highest bacterial reduction after NaOCl.

Conclusions. The photoactivation of the TBO/AgNPs combination led to an increase in the effect of PDT, and it has the potential to be used as an adjunct for disinfection of the root canal system.

Key words: silver nanoparticles, photodynamic therapy, root canal disinfection

Introduction

One of the main purposes of endodontic treatment is to completely eliminate microorganisms (MOs) from root canals.¹ Root canal disinfection with mechanical cleaning and irrigation with antimicrobial agents is important to achieve this aim. However, according to the literature, current disinfection techniques cannot completely eliminate the microbial flora from the infected areas.^{2–4} To improve the antimicrobial effect, innovative delivery systems are needed.

Since photodynamic therapy (PDT) increases microbial decontamination after chemomechanical preparation, it is recommended as an adjunct for endodontic treatment.^{5–8} Nontoxic photosensitizer (PS) agents, such as toluidine blue O (TBO), and irradiation at an appropriate wavelength are used in PDT.^{9–11} The photosensitizer, which is activated by irradiation, reacts with molecular oxygen in order to produce highly reactive oxygen species (ROS), which lead to the damage and death of MOs.¹² The photosensitizer binds to the cell membranes of the bacteria, then it leads to singlet oxygen generation as a result of irradiation, and bacterial death takes place as a result of the degradation of the bacterial wall with singlet oxygen.¹³

One of the subjects that researchers have recently focused on is the use of nanoparticles (NPs) for antimicrobial purposes, since endodontic treatment and novel techniques, such as PDT, cannot ensure complete success in bacterial elimination.^{14–17} Nanoparticles such as chitosan,¹⁸ magnesium oxide,¹⁹ zinc oxide,²⁰ quaternary ammonium polyethylenimine,²¹ poly(lactic-co-glycolic acid) (PLGA),²² and silver nanoparticles (AgNPs)^{15,16} have been researched in order to increase the efficacy of root canal disinfection.

Silver nanoparticles have at least 1 dimension that is between 1 and 100 nm, and the surface area–volume rate considerably increases with the decreasing particle dimension. This condition results in significant changes in physical, chemical and biological characteristics.²³ Its antimicrobial effect is attributed to the strong oxidative activity of the surfaces of AgNPs and the release of Ag ions (Ag⁺) in biological environments.²⁴ The antibacterial, antifungal, antiviral, and anti-inflammatory activity of AgNPs has recently attracted great attention in biomedical practices.²³

One of the most important advantages of nanomaterials is the potential for improving drug delivery in order to provide the maximum therapeutic effect in the target area.²⁵ Nanoparticles that are functionalized with PSs enable physicochemical advantages, such as target cell selectivity, increasing the uptake of PS in cells, reducing the leakage of PS from the target cells, and allowing the controlled release of ROS.¹⁴ Combinations such as chitosan NPs functionalized with rose bengal (RB), which is a PS agent,¹⁴ and methylene blue (MB)-loaded PLGA NPs²²

have been used for this purpose. However, to the best of our knowledge, there is no study assessing the effect of photoactivation on the combination of TBO and AgNPs in the literature.

The aim of this study was to research the amount of antibacterial activity increment achieved through light application on the combination of a PS agent – TBO and an NP agent – AgNPs on the 3-week-old mature *Enterococcus faecalis* (*E. faecalis*) biofilm formed experimentally on the extracted human teeth. The study hypothesis was that light application on the TBO and AgNPs combination does not have any additional antibacterial effect as compared to the separate usage of PDT and AgNPs.

Material and methods

Ethical approval for this study was obtained from the Research Ethics Committee of Akdeniz University in Antalya, Turkey (No. 70904504/147).

Synthesis and characterization of silver nanoparticles

A total of 0.21 g of highly pure silver nitrate (Merck, Kenilworth, USA) was dissolved in 20.79 g of distilled water, and then diluted with 44.8 g of distilled water. An amount of 0.68 g of the diluted polyvinylpyrrolidone (Sigma-Aldrich, St. Louis, USA) solution (10 wt%, diluted with water) was added dropwise into the Ag solution. An amount of 0.1568 g of potassium bromide (Sigma-Aldrich) was dissolved in 66.52 g of distilled water in a separate container, and then added dropwise into the Ag-polyvinylpyrrolidone solution; the obtained mixture was stirred for 5 h at room temperature. This final mixture had an Ag concentration of 1,000 ppm and was used as a basis to prepare solutions in the subsequent experiments. Distilled and sterilized water was used to dilute the main 1,000 ppm AgNPs solution.

Preliminary studies

Toluidine blue O, AgNPs and their combination were used in the operation of the experimentally infected root canals of the extracted teeth. Before the experiment, preliminary studies were performed in order to determine which concentration produced the optimum effect of the photoactivation of each combination. Antibacterial efficacy was tested on a planktonic *E. faecalis* culture (ATCC 29212). Primarily, in order to determine to what extent NPs were superior to Ag⁺, 10 ppm of the Ag⁺-containing silver nitrate solution (in distilled water) and 10 ppm of the AgNPs solution were prepared, and efficacy tests were done. It was found that when PDT was not applied to the samples with a bacterial density of 1×10^4 CFU/mL, the antibacterial activity of AgNPs was about 6% lower

than that of Ag⁺ and, on the contrary, when PDT was applied with a 30-second duration, the activity of AgNPs was about 20% higher than in the case of Ag⁺.

Subsequently, the TBO/AgNPs rates to be used with PDT were studied. When the concentration of AgNPs in the 20 ppm TBO solution was increased from 5 ppm to 10 ppm, a reduction in the bacterial load rose from 99.7% to 99.9%. On the other hand, when the concentration of AgNPs was increased to 20 ppm, a reduction in the bacterial load fell to 91%. As expected, in the control samples there was not any reduction. In preliminary trials, due to the highest amount of reduction being achieved with 20 ppm TBO + 10 ppm AgNPs, it was decided to continue further studies with this TBO/AgNPs rate.

Selection and preparation of tooth samples

One hundred and thirty mature mandibular premolars with straight root canals, extracted for periodontal and/or prosthetic reasons, were obtained with written informed consent. Digital radiographs were taken from mesiodistal and buccolingual directions in order to check if the teeth had the desired anatomic structures, and it was confirmed that they had single canals. The teeth were stored in the thymol solution until required.

The crowns of the teeth were removed under water with a low-speed diamond saw (Komet USA, Rock Hill, USA) to obtain a root height of 13 mm. This standard length allowed root canal shaping and disinfection strategies to be performed under similar conditions for all samples. A K-file size 10 (Micro-Mega, Besançon, France) was inserted into the root canal until the tip of the file was visible at the apical foramen, and the working length (WL) was determined by subtracting 1 mm from this length. The preparation of root canals was performed with the ProTaper® Universal nickel-titanium rotary files (Dentsply Maillefer, Ballaigues, Switzerland) in accordance with the manufacturer's instructions, using the crown-down preparation technique. Files SX, S1, S2, F1, F2, F3, and F4 were used respectively according to the recommended speed and torque adjustments. Root canal shaping was completed when the master apical file was F4. During shaping, root canals were irrigated with 2.5 mL of 2.5% NaOCl after each file change, using a standard dental needle with a 27-gauge tip. Final irrigation was performed using 5 mL of 17% EDTA solution (Calasept EDTA; Nordiska Dental, Ängelholm, Sweden) for 2 min, 2 mL of 2.5% NaOCl and 5 mL of saline. The teeth were maintained in saline for 5 days to eliminate residual NaOCl. Root canals were dried with the ProTaper F4 paper points (Dentsply Maillefer). The apical foramina of the teeth were sealed with light-polymerized flowable composite resin (CLEARFIL MAJESTY™ Flow; Kuraray Noritake Dental Inc., Okayama, Japan) in order to prevent bacterial leakage and irrigant overflow. Two layers of nail polish were rigorously applied on the root

surfaces of the teeth. Then, the samples were sterilized in ethylene oxide. After sterilization, 5 samples were randomly selected in order to confirm the complete elimination of bacteria and the removal of smear layers with scanning electron microscopy (SEM).

Cultivation of *Enterococcus faecalis* and root canal contamination

All microbiological procedures in this study were conducted under aseptic conditions and in a laminar flow cabinet. An *E. faecalis* strain (ATCC 29212) was used as the test bacteria in the study. The *E. faecalis* were taken from frozen stocks. The cultures were maintained by being subcultured in broth that contained trypticase soy agar, and the strain was inoculated in blood agar. The cultures were prepared by being incubated for 24 h at 37°C in a micro-aerophilic environment. The number of cells was adjusted in a spectrometer device (the Cary 5000 Bio UV-Vis spectrophotometer; Varian Medical Systems, Palo Alto, USA) according to their optical density so that 10⁸ cells in every mL of the broth were included. These measurements were performed at a wavelength of 600 nm.

Each one of the 125 teeth was transferred to sterile 1.5-milliliter Eppendorf tubes. Following the injection of 1 mL of the brain-heart infusion (BHI) broth (Merck), containing 10⁸ *E. faecalis* cells, to the prepared root canals with insulin injectors, each sample was entirely submerged in the BHI broth.²⁶ It was incubated for the formation of the *E. faecalis* biofilm in an incubator at 37°C for 21 days. The broth in each tube was refreshed every day. Following the incubation period, the mediums in the tubes were aseptically aspirated and the residual mediums were eliminated from root canals by means of paper points.

Photosensitizer and a light source

A light-emitting diode (LED) device (FotoSan®; CMS Dental, Copenhagen, Denmark) was used as a light source in the experimental procedures. The output power of the system was 2,000–4,000 mW/cm², and its wavelength spectrum was between 620 and 640 nm. Although there was TBO at a concentration of 0.1 mg/mL as a PS agent in the system, 0.02 mg/mL of TBO was used according to the aforementioned preliminary study results. The endodontic tip was introduced as deeply as possible into the root canal without applying pressure.

SEM preparation and analysis

Five samples were analyzed with SEM (the Zeiss Leo 1430 scanning electron microscope; Carl Zeiss, Oberkochen, Germany) in order to verify the formation of the *E. faecalis* biofilm. Five random teeth were selected from among the samples. Longitudinal grooves

were carved on the root surfaces without invading the inner part of the root canal with a high-speed diamond bur (Komet USA). Afterward, the roots were divided into 2 parts through these grooves with the help of a stainless steel chisel. The samples were irrigated with saline in order to remove cells that were not bound to the biofilm. The samples were fixed in 10% formalin for 24 h, then incubated for 20 min in a graded series of ethanol concentrations (50%, 70%, 90%, and 100%, twice) and left to dry in the air at room temperature during the night. Later, they were mounted on the aluminum stubs of the scanning electron microscope, sputter coated with a 300-angstrom gold-palladium alloy under vacuum and analyzed at 15 kV. The SEM images of the apical, middle and coronal thirds and fracture surfaces were taken.

Experimental procedures

The remaining 120 teeth were randomly divided into 5 main experimental groups ($n = 20$). Then, these main groups were divided into 2 subgroups ($n = 10$). In total, there were 10 experimental groups:

- group 1A: TBO at a concentration of 0.02 mg/mL (20 ppm) was injected into root canals and agitated with a K-file size 15; it was left in root canals for 1 min, and then activated for 30 s with the help of the 0.5-millimeter tip of the FotoSan light delivery system;
- group 1B: the same procedures as in group 1A were applied, but following a 30-second break, another 30 s of light application was performed; photoactivation was performed for a total of 60 s;
- group 2A: AgNPs at a concentration of 10 ppm were injected into root canals and left for 30 s after being agitated with a hand file size 15;
- group 2B: AgNPs at a concentration of 10 ppm were injected into the root canals and left for 60 s after being agitated with a hand file size 15;
- group 3A: the homogeneous distribution of the mixture of 20 ppm of TBO and 10 ppm of AgNPs was ensured; later, this was placed into root canals and kept for 30 s;
- group 3B: the same procedures as in group 3A were applied, but for 60 s;
- group 4A: AgNPs at a concentration of 10 ppm were injected into root canals and photoactivation was performed for 30 s;
- group 4B: AgNPs at a concentration of 10 ppm were injected into root canals and photoactivation was performed for 60 s;
- group 5A: the mixture of 20 ppm of TBO and 10 ppm of AgNPs was injected into root canals; it was kept for 1 min for its distribution into the root canal system, and then photoactivation was performed for 30 s;
- group 5B: the mixture of 20 ppm of TBO and 10 ppm of AgNPs was injected into root canals; it was kept for 1 min for its distribution into the root canal system, and then photoactivation was performed for 60 s.

The remaining 20 teeth constituted positive and negative control groups. The samples were irrigated with 2 mL of 2.5% NaOCl for 1 min in the positive control group ($n = 10$). The teeth in the positive control group were irrigated with 5 mL of 5% sodium thiosulphate for 1 min in order to inactivate the NaOCl remaining in the canal.²⁶ The samples were irrigated with 2 mL of 0.9% saline solution for 1 min in the negative control group ($n = 10$).

Microbiological analysis

The microbiological analysis was conducted in all experimental and control groups before and just after the treatment regimens. After the treatment regimens, root canals were irrigated with 1 mL of saline in order to remove the agents. As in the method used by Souza et al.,²⁷ root canals were filled with saline in the sampling procedures and samples were taken with 3 sterile paper points in order. These paper points were combined to count CFU. Paper points were introduced up to WL in root canals for 1 min. Before placing paper points for the microbiological sampling following the treatment, root canals were filed vigorously with an H-file size 25.¹¹ This procedure allowed the biofilm to deteriorate and the bacteria which were left in the biofilm and could not be reached with paper points to be obtained. The bacterial CFU were counted and the actual counts were determined based on the known dilution factors.

Statistical analysis

The statistical analyses of the results were carried out using IBM SPSS Statistics for Windows, v. 20.0 (IBM Corp., Armonk, USA). The reduction percentages in the data obtained by counting CFU after the treatment were transformed into logarithmic (\log_{10}) values. The Kolmogorov–Smirnov test, the one-way analysis of variance (ANOVA) and Tukey's honestly significant difference (HSD) test were used to carry out the statistical analyses of the study data. After the Bonferroni correction, $p < 0.004$ was taken as the level of statistical significance.

Results

Characterization of nanoparticles

The dimension distributions of the synthesized AgNPs were measured using the Nano-Z device of the Zetasizer® Nano series (Malvern Panalytical, Malvern, UK), which operates based on the principle of dynamic light scattering. The average size of the particles which were synthesized according to the measurements was 52 nm. The effect of the synthesized AgNPs on TBO absorption was analyzed using ultraviolet-visible (UV-Vis) spectroscopy. When the UV-Vis spectra of the 20 ppm of TBO,

20 ppm of TBO + 10 ppm of AgNPs and 10 ppm of AgNPs solutions were examined, it was observed that only the solution containing AgNPs did not lead to any absorption in the visible area. On the other hand, TBO led to a maximum absorption of approx. 600 nm. The addition of AgNPs to the TBO solution did not change this maximum absorption.

SEM analysis

The SEM images which were examined to verify the complete elimination of smear layers and bacteria before the canal systems were contaminated with *E. faecalis*, following the preparation of the root samples, showed clean dentin surfaces with open dentinal tubules (Fig. 1).

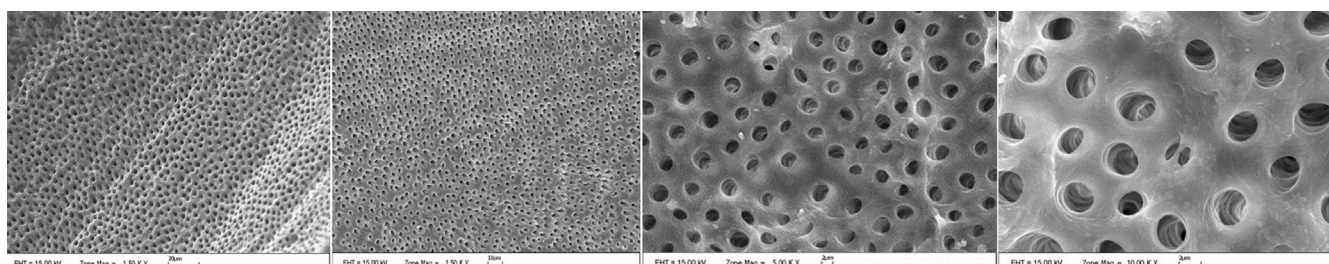


Fig. 1. Clean dentinal tubules with no smear layers

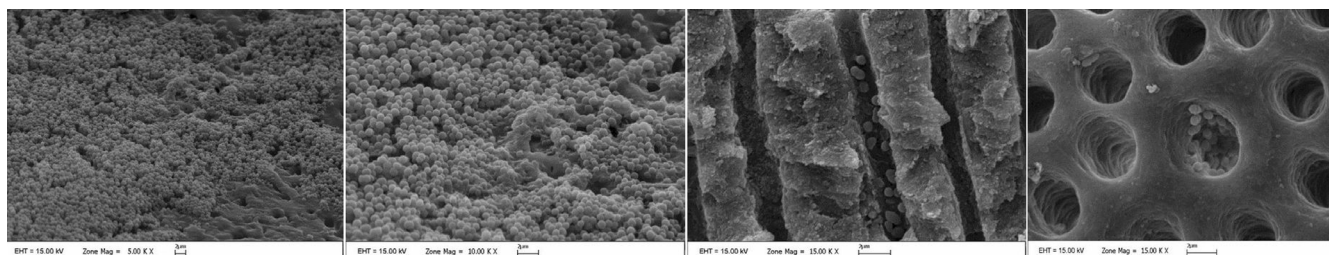


Fig. 2. Root canal walls heavily colonized with bacteria; bacterial cells observed in dentinal tubules

Table 1. Average logarithmic and percentage values of bacterial reduction in all groups

Groups	<i>n</i>	<i>M</i> ± <i>SD</i> [log ₁₀]	Range	<i>M</i> ± <i>SD</i> [%]	Range
TBO/light 30 s ^{a-j,k}	10	1.63 ± 0.23	1.23–1.97	97.34 ± 1.56	94.13–98.92
TBO/light 60 s ^{b-k,m}	10	2.03 ± 0.19	1.64–2.29	98.98 ± 0.51	97.72–99.49
AgNPs 30 s ^{c-j,k}	10	1.61 ± 0.43	1.24–2.71	96.80 ± 1.84	94.20–99.80
AgNPs 60 s ^{d-k,m}	10	1.95 ± 0.29	1.52–2.38	98.65 ± 0.88	97.00–99.58
TBO/AgNPs 30 s ^{e-j,k}	10	1.80 ± 0.58	1.11–2.94	97.28 ± 2.35	92.15–99.88
TBO/AgNPs 60 s ^{f-k,m}	10	1.93 ± 0.55	0.83–2.80	97.36 ± 4.40	85.31–99.84
AgNPs/light 30 s ^{g-j,k}	10	1.84 ± 0.19	1.51–2.13	98.41 ± 0.73	96.94–99.26
AgNPs/light 60 s ^{h-k,m}	10	2.10 ± 0.31	1.55–2.49	98.96 ± 0.90	97.16–99.68
TBO/AgNPs/light 30 s ^{i-k,m}	10	2.14 ± 0.26	1.89–2.80	99.18 ± 0.34	98.71–99.84
TBO/AgNPs/light 60 s ^{j-a,c,e,g,k,m}	10	2.71 ± 0.60	1.74–3.85	99.61 ± 0.52	98.18–99.99
Positive control ^{k-a,b,c,d,e,f,g,h,i,j,m}	10	4.29 ± 0.96	2.95–6.00	99.98 ± 0.03	99.89–100.00
Negative control ^{m-b,d,f,h,i,j,k}	10	1.02 ± 0.20	0.71–1.40	89.70 ± 4.49	80.63–96.05

TBO – toluidine blue O; AgNPs – silver nanoparticles; *M* – mean; *SD* – standard deviation; ^a TBO/light 30 s; ^b TBO/light 60 s; ^c AgNPs 30 s; ^d AgNPs 60 s; ^e TBO/AgNPs 30 s; ^f TBO/AgNPs 60 s; ^g AgNPs/light 30 s; ^h AgNPs/light 60 s; ⁱ TBO/AgNPs/light 30 s; ^j TBO/AgNPs/light 60 s; ^k positive control; ^m negative control. Superscript letters show significant differences between the related group and the other groups.

The SEM images verified the presence of 21-day-old mature biofilm before the treatment protocols were performed (Fig. 2). The root canal walls were densely colonized by *E. faecalis* cells. In some areas, the cells were organized in biofilm and observed to have penetrated dentinal tubules.

Bacteriological analysis

Table 1 illustrates average reduction percentages and average reduction amounts as logarithmic values after the treatment in all groups. The initial and post-treatment average NaOCl group provided a bacterial reduction that was higher than in all other groups in a statistically significant manner; it was the group which displayed the highest

antibacterial activity. Increasing the treatment time from 30 s to 60 s caused an increase in antibacterial activity; however, it was not statistically significant. The saline group was the least successful one; yet, no significant difference was found between groups 1A, 2A, 3A, and 4A. Light application on the TBO/AgNPs combination was the group that provided the highest bacterial reduction after NaOCl.

Discussion

The present study analyzed the antibacterial activity obtained by light application on the combination of a PS agent – TBO and an NP agent – AgNPs on the 3-week-old mature *E. faecalis* biofilm formed experimentally on the extracted human teeth, and compared it to the same combination without photoactivation, light application on TBO, the separate use of AgNPs, and light application on AgNPs. The teeth treated with saline and NaOCl served as control groups.

The study consisted of 2 stages. At the 1st stage, a preliminary study was conducted to establish at which concentrations the procedures of combining TBO and AgNPs as well as applying light on this combination showed the best results. It was observed that the combination of 20 ppm of TBO and 10 ppm of AgNPs showed the most effective antibacterial activity against the suspension containing *E. faecalis*. Hence, these concentrations were used in the experiment conducted on the prepared root samples. In the analysis of the UV-Vis spectra, it was noted that the solution containing AgNPs did not lead to absorption and TBO resulted in absorption at approx. 600 nm. The addition of AgNPs to the TBO solution did not change the maximum absorption. Based on these results, the FotoSan device, which provided light at a wavelength of approx. 600 nm, was preferred as the source of light to be used in the experiment.

Enterococcus faecalis was used in this study, as it is generally believed that these bacteria are one of the most common isolated MOs found in infected root canals and has a higher prevalence in secondary infections as compared to primary infections.²⁸ Despite having various virulence factors, their capability of causing periradicular diseases arises from being persistent and protected from the effects of the root canal treatment procedures, applied in the root canals and dentinal tubules of the tooth.²⁹ In addition, MOs in biofilm have a stronger pathogenic potential as compared to planktonic MOs.^{30,31} Clinically, they are of particular importance due to their higher capability of protecting themselves from host defense mechanisms and therapeutic approaches, such as chemical and mechanical antimicrobial treatment procedures.³² The presence of mature biofilm was detected in the SEM images taken before performing the treatment regimens. This provided for the method of the infected dentin model to be used; colonization was present in the canal lumens and dentinal tubules,

the possible relationship between the applied agents and dentin was taken into consideration, the effects related to the penetration and distribution of agents in a closed environment, such as the root canal system, were taken into consideration, a dark environment was provided during light application, and the administration and duration of agents were similar to those met in clinical conditions. Thus, the conditions closest to the clinical ones were obtained.

NaOCl is suggested as the primary irrigation solution in endodontics due to its wide-spectrum antimicrobial efficiency as well as its capability of dissolving organic substances.³³ Photodynamic therapy is antimicrobial treatment on which numerous studies have been conducted^{7,34–36} and the efficiency of which has been proven in endodontics. Eliminating the bacteria selectively without affecting other normal tissue and damaging surrounding tissues is among its advantages.³⁷ In studies conducted on PDT, some researchers have found PDT to be more successful than NaOCl^{11,38} or as efficient as NaOCl,³⁹ while others found it to be less successful and reported contradictory results.^{40,41} The reason for these reported differences is associated with the methodologies used, NaOCl concentrations and the diversity of PDT procedures. Hecker et al. asserted that PDT was ineffective in ensuring sufficient disinfection.³⁴

It is difficult to make comparisons between studies conducted on the efficiency of PDT. This is because different PSs, PS concentrations, light parameters, irradiation durations, and light delivery systems were used. In this study, the NaOCl group displayed statistically significantly higher antibacterial efficiency as compared to PDT and the other groups. Despite a significant decrease in the number of bacteria, complete elimination was not achieved with PDT. In their study conducted on teeth with pulpal necrosis and periapical pathology, Ng et al. applied PDT after the chemomechanical cleaning of canals and found that the bacterial load decreased with PDT.⁴² However, they construed that the failure to obtain complete elimination was associated with the incomplete penetration of PS into dentinal tubules due to bonding through the interaction of PS with dentin components, the failure of the penetration of PS into the canal biofilm and the insufficient amount of oxygen.⁴²

In a micro-environment with low oxygen levels, such as the closed environment surrounded by dentinal tubules, molecular oxygen is quickly depleted, and singlet oxygen-mediated damage is prevented or minimized. It is recommended to fractionate light delivery and apply irradiation once again after some time in order to overcome the problem of oxygen consumption.⁴³ In the current study, the application of PDT was performed once again after 30 s. The efficacy of PDT increased, although the rise was not statistically significant.

Silver nanoparticles have attracted a great deal of attention in biomedical applications recently, since they show antibacterial, antifungal, antiviral, and anti-inflammatory activity.²³ They lead to apoptosis and necrosis by stimulating potent oxidative damage to organelles such as the cell

membrane, lysosome, mitochondrion, and nucleus.⁴⁴ Biological cellular proteins are negatively charged due to their side chains, which may contain carboxyl and sulfhydryl groups, and the high affinity of Ag for negatively charged molecules in the cells of bacteria inactivates the critical functions of bacterial cells, and prevents bacterial growth and biofilm formation.⁴⁵ Therefore, positively charged NPs have more antibacterial effects than negatively charged and neutral NPs.¹⁷

Abbaszadegan et al. evaluated the antibacterial activity and cytotoxicity of stable AgNPs synthesized with different surface charges (neutral, positive and negative), and compared them with the NaOCl and chlorhexidine (CHX) solutions.¹⁷ Silver nanoparticles with a positive surface charge were effective at considerably low concentrations as compared to other agents.¹⁷ Similarly, Lotfi et al. demonstrated that AgNPs could have the same bactericidal effect as 5.25% NaOCl at considerably low concentrations.⁴⁶ In their study, 70 times higher NaOCl concentration was required to obtain the equivalent antibacterial effect of AgNPs.⁴⁶ Contrary to the results of these studies, Wu et al. compared the antibacterial effect of the 0.1% AgNPs solution with 2% NaOCl and saline in dentin samples.¹⁵ In the study in which they evaluated the residual biofilm structure with SEM and confocal laser scanning microscopy (CLSM), irrigation was performed for 2 min with 6 mL of the solutions. The 0.1% AgNPs solution did not disrupt the structure of the *E. faecalis* biofilm, but provided a significant biofilm bacteria death. NaOCl was found to be more successful than the other groups.¹⁵ The results of this study are similar to ours. However, our study was aimed at improving disinfection before canal filling, with the AgNPs solution not as an irrigation solution. Therefore, our study enabled a comparison with the PDT group, and displayed similar antibacterial efficiency of AgNPs and PDT.

One of the most important advantages of nanomaterials is the potential for improving drug delivery in order to ensure the maximum therapeutic effect in the target area.²⁵ However, in PDT, PSs have insufficient water solubility and tend to cluster in an aqueous environment under physiological conditions.⁴⁷ In order to overcome this problem, an advanced non-invasive light-activated disinfection procedure that consists of 2 stages has been suggested; the 1st stage consists in using PS that is dissolved in a formulation, which increases its photochemical characteristics and allows a better diffusion of PS to the anatomical complexities of the root canal system. Then, the 2nd stage facilitates light distribution in the irradiation phase and an oxygen-carrying solution is applied, which increases the amount of oxygen.⁴⁸ Another method is to increase the solubility of hydrophobic PS through the use of NP agents as carriers in drug delivery in order to improve the transfer of PS to the target tissue.⁴⁷ Nanoparticles that are functionalized with PSs enable physicochemical advantages, such as target cell selectivity, increasing the uptake of PS in cells, reducing the leakage of PS from the target cells, increasing

the stability of PS molecules after conjugation, preventing the physical quenching caused by PS aggregation, and allowing the controlled release of ROS.¹⁴

In a study using chitosan NPs functionalized with RB, which is a xanthen PS dye, antibiofilm efficiency in the multiple-species biofilm formed in dentin was investigated, and increased affinity to bacterial cell membrane, more penetration into the biofilm structure and more bacterial elimination were obtained.¹⁴ Shrestha and Kishen evaluated the antibacterial efficiency of this conjugation in the presence of tissue inhibitors in root canals.⁴⁹ The synergistic antibacterial effect of chitosan NPs and singlet oxygen released from RB after photoactivation ensured a significant antibacterial efficiency potential for this conjugation, even in the presence of tissue inhibitors.⁴⁹ Pagonis et al. examined the antibacterial efficiency of MB-loaded PLGA NPs and their photoactivation against *E. faecalis*.²² After keeping the solution in the canal for 15 min, irradiation was performed with the help of a diode laser for 5 min. After irradiation, a significant decrease in the CFU values was found.²² In the present study, antibacterial efficiency was increased by means of light application on the TBO and AgNPs combination, and this was the most successful group after NaOCl. Thus, the null hypothesis was rejected.


This study has several limitations. Firstly, to the best of our knowledge, there is still no information in the literature concerning the photoactivation of the combination of TBO and AgNPs. Therefore, making a comparison is not possible. Secondly, only 1 bacterial strain was evaluated, while endodontic infections are polymicrobial. Thirdly, various possible light sources and wavelength ranges can change the antimicrobial effects of PSs or AgNPs. Currently, there is a lack of an established protocol for adjunctive PDT for root canal disinfection.


Conclusions


All the treatment protocols used in this study displayed strong antibacterial efficiency on mature *E. faecalis* biofilm. The photoactivation of the TBO/AgNPs combination led to an increase in the effect of PDT, and only the 2.5% NaOCl group was more effective. The use of NP agents in combination with light/PS agents plays an important role in increasing the efficiency of PDT in root canal disinfection. It is required for future studies to research the effect of this combination on multiple-species biofilm, its cytotoxicity and its efficacy in the presence of tissue inhibitors.


ORCID iDs

Hakan Aydın  <https://orcid.org/0000-0003-3597-0843>


Kürşat Er  <https://orcid.org/0000-0002-0667-4909>

Alper Kuştarıcı  <https://orcid.org/0000-0002-4942-3739>

Murat Akarsu  <https://orcid.org/0000-0002-2114-7904>

Gül Merve Gençer  <https://orcid.org/0000-0001-7087-609X>

Hakan Er  <https://orcid.org/0000-0001-7739-4712>

Rasih Felek  <https://orcid.org/0000-0002-5722-1176>

References

- Nair PNR. Pathogenesis of apical periodontitis and the causes of endodontic failures. *Crit Rev Oral Biol Med*. 2004;15(6):348–381.
- Siqueira JF Jr., de Uzeda M. Disinfection by calcium hydroxide pastes of dentinal tubules infected with two obligate and one facultative anaerobic bacteria. *J Endod*. 1996;22(12):674–676.
- Siqueira JF Jr., Magalhães KM, Rôças IN. Bacterial reduction in infected root canals treated with 2.5% NaOCl as an irrigant and calcium hydroxide/camphorated paramonochlorophenol paste as an intracanal dressing. *J Endod*. 2007;33(6):667–672.
- Siqueira JF Jr., Rôças IN, Paiva SSM, Guimarães-Pinto T, Magalhães KM, Lima KC. Bacteriologic investigation of the effects of sodium hypochlorite and chlorhexidine during the endodontic treatment of teeth with apical periodontitis. *Oral Surg Oral Med Oral Pathol Oral Radiol Endod*. 2007;104(1):122–130.
- Soukos NS, Chen PSY, Morris JT, et al. Photodynamic therapy for endodontic disinfection. *J Endod*. 2006;32(10):979–984.
- Garcez AS, Ribeiro MS, Tegos GP, Núñez SC, Jorge AOC, Hamblin MR. Antimicrobial photodynamic therapy combined with conventional endodontic treatment to eliminate root canal biofilm infection. *Lasers Surg Med*. 2007;39(1):59–66.
- Fimple JL, Fontana CR, Foschi F, et al. Photodynamic treatment of endodontic polymicrobial infection in vitro. *J Endod*. 2008;34(6):728–734.
- Garcez AS, Nuñez SC, Hamblin MR, Suzuki H, Ribeiro MS. Photodynamic therapy associated with conventional endodontic treatment in patients with antibiotic-resistant microflora: A preliminary report. *J Endod*. 2010;36(9):1463–1466.
- Benov L. Photodynamic therapy: Current status and future directions. *Med Princ Pract*. 2015;24 Suppl 1(Suppl 1):14–28.
- Williams JA, Pearson GJ, Colles MJ. Antibacterial action of photo-activated disinfection (PAD) used on endodontic bacteria in planktonic suspension and in artificial and human root canals. *J Dent*. 2006;34(6):363–371.
- Bago I, Plečko V, Gabrić Pandurić D, Schauerperl Z, Baraba A, Anić I. Antimicrobial efficacy of a high-power diode laser, photo-activated disinfection, conventional and sonic activated irrigation during root canal treatment. *Int Endod J*. 2013;46(4):339–347.
- Demidova TN, Hamblin MR. Photodynamic therapy targeted to pathogens. *Int J Immunopathol Pharmacol*. 2004;17(3):245–254.
- Komine C, Tsujimoto Y. A small amount of singlet oxygen generated via excited methylene blue by photodynamic therapy induces the sterilization of *Enterococcus faecalis*. *J Endod*. 2013;39(3):411–414.
- Shrestha A, Kishen A. Antibacterial efficacy of photosensitizer functionalized biopolymeric nanoparticles in the presence of tissue inhibitors in root canal. *J Endod*. 2014;40(4):566–570.
- Wu D, Fan W, Kishen A, Gutmann JL, Fan B. Evaluation of the antibacterial efficacy of silver nanoparticles against *Enterococcus faecalis* biofilm. *J Endod*. 2014;40(2):285–290.
- Javidi M, Afkhami F, Zarei M, Ghazvini K, Rajabi O. Efficacy of a combined nanoparticle/calcium hydroxide root canal medication on elimination of *Enterococcus faecalis*. *Aust Endod J*. 2014;40(2):61–65.
- Abbaszadegan A, Nabavizadeh M, Gholami A, et al. Positively charged imidazolium-based ionic liquid-protected silver nanoparticles: A promising disinfectant in root canal treatment. *Int Endod J*. 2015;48(8):790–800.
- Kishen A, Shi Z, Shrestha A, Neoh KG. An investigation on the antibacterial and antibiofilm efficacy of cationic nanoparticulates for root canal disinfection. *J Endod*. 2008;34(12):1515–1520.
- Monzavi A, Eshraghi S, Hashemian R, Momen-Heravi F. In vitro and ex vivo antimicrobial efficacy of nano-MgO in the elimination of endodontic pathogens. *Clin Oral Investig*. 2015;19(2):349–356.
- Shrestha A, Shi Z, Neoh KG, Kishen A. Nanoparticulates for antibiofilm treatment and effect of aging on its antibacterial activity. *J Endod*. 2010;36(6):1030–1035.
- Kesler Shvero D, Abramovitz I, Zaltsman N, Perez Davidi M, Weiss El, Beyth N. Towards antibacterial endodontic sealers using quaternary ammonium nanoparticles. *Int Endod J*. 2013;46(8):747–754.
- Pagonis TC, Chen J, Fontana CR, et al. Nanoparticle-based endodontic antimicrobial photodynamic therapy. *J Endod*. 2010;36(2):322–328.
- Ge L, Li Q, Wang M, Ouyang J, Li X, Xing MMQ. Nanosilver particles in medical applications: Synthesis, performance, and toxicity. *Int J Nanomedicine*. 2014;9:2399–2407.
- He W, Zhou YT, Wamer WG, Boudreau MD, Yin JJ. Mechanisms of the pH dependent generation of hydroxyl radicals and oxygen induced by Ag nanoparticles. *Biomaterials*. 2012;33(30):7547–7555.
- Paszko E, Ehrhardt C, Senge MO, Kelleher DP, Reynolds JV. Nanodrug applications in photodynamic therapy. *Photodiagnosis Photodyn Ther*. 2011;8(1):14–29.
- Christo JE, Zilm PS, Sullivan T, Cathro PR. Efficacy of low concentrations of sodium hypochlorite and low-powered Er,Cr:YSGG laser activated irrigation against an *Enterococcus faecalis* biofilm. *Int Endod J*. 2016;49(3):279–286.
- Souza LC, Brito PRR, Machado de Oliveira JC, et al. Photodynamic therapy with two different photosensitizers as a supplement to instrumentation/irrigation procedures in promoting intracanal reduction of *Enterococcus faecalis*. *J Endod*. 2010;36(2):292–296.
- Pinheiro ET, Gomes BPPA, Ferraz CCR, Sousa ELR, Teixeira FB, Souza-Filho FJ. Microorganisms from canals of root-filled teeth with periapical lesions. *Int Endod J*. 2003;36(1):1–11.
- Stuart CH, Schwartz SA, Beeson TJ, Owatz CB. *Enterococcus faecalis*: Its role in root canal treatment failure and current concepts in retreatment. *J Endod*. 2006;32(2):93–98.
- Lewis K. Riddle of biofilm resistance. *Antimicrob Agents Chemother*. 2001;45(4):999–1007.
- Chafas R, Wójcik-Chęcińska I, Woźniak MJ, Grzonka J, Świąszkowski W, Kurzydowski KJ. Dental plaque as a biofilm – a risk in oral cavity and methods to prevent [in Polish]. *Postepy Hig Med Dosw (Online)*. 2015;69:1140–1148.
- Costerton JW, Stewart PS, Greenberg EP. Bacterial biofilms: A common cause of persistent infections. *Science*. 1999;284(5418):1318–1322.
- Zehnder M. Root canal irrigants. *J Endod*. 2006;32(5):389–398.
- Hecker S, Hiller KA, Galler KM, Erb S, Mader T, Schmalz G. Establishment of an optimized ex vivo system for artificial root canal infection evaluated by use of sodium hypochlorite and the photodynamic therapy. *Int Endod J*. 2013;46(5):449–457.
- Stojicic S, Amorim H, Shen Y, Haapasalo M. Ex vivo killing of *Enterococcus faecalis* and mixed plaque bacteria in planktonic and biofilm culture by modified photoactivated disinfection. *Int Endod J*. 2013;46(7):649–659.
- Schiffner U, Cachovan G, Bastian J, Sculean A, Eick S. In vitro activity of photoactivated disinfection using a diode laser in infected root canals. *Acta Odontol Scand*. 2014;72(8):673–680.
- Bhatti M, MacRobert A, Meghji S, Henderson B, Wilson M. Effect of dosimetric and physiological factors on the lethal photosensitization of *Porphyromonas gingivalis* in vitro. *Photochem Photobiol*. 1997;65(6):1026–1031.
- Garcez AS, Núñez SC, Lage-Marques JL, Cardoso Jorge AO, Ribeiro MS. Efficiency of NaOCl and laser-assisted photosensitization on the reduction of *Enterococcus faecalis* in vitro. *Oral Surg Oral Med Oral Pathol Oral Radiol Endod*. 2006;102(4):e93–e98.
- Yildirim C, Karaarslan ES, Ozsevik S, Zer Y, Sari T, Usumez A. Antimicrobial efficiency of photodynamic therapy with different irradiation durations. *Eur J Dent*. 2013;7(4):469–473.
- Rios A, He J, Glickman GN, Spears R, Schneiderman ED, Honeyman AL. Evaluation of photodynamic therapy using a light-emitting diode lamp against *Enterococcus faecalis* in extracted human teeth. *J Endod*. 2011;37(6):856–859.
- Lim Z, Cheng JL, Lim TW, et al. Light activated disinfection: An alternative endodontic disinfection strategy. *Aust Dent J*. 2009;54(2):108–114.
- Ng R, Singh F, Papamanou DA, et al. Endodontic photodynamic therapy ex vivo. *J Endod*. 2011;37(2):217–222.
- Singh S, Nagpal R, Manuja N, Tyagi SP. Photodynamic therapy: An adjunct to conventional root canal disinfection strategies. *Aust Endod J*. 2015;41(2):54–71.
- Zhang T, Wang L, Chen Q, Chen C. Cytotoxic potential of silver nanoparticles. *Yonsei Med J*. 2014;55(2):283–291.
- Bhardwaj SB, Mehta M, Gauba K. Nanotechnology: Role in dental biofilms. *Indian J Dent Res*. 2009;20(4):511–513.
- Lotfi M, Vosoughhosseini S, Ranjkesh B, Khani S, Saghiri M, Zand V. Antimicrobial efficacy of nanosilver, sodium hypochlorite and chlorhexidine gluconate against *Enterococcus faecalis*. *Afr J Biotechnol*. 2011;10(35):6799–6803.
- Yin R, Agrawal T, Khan U, et al. Antimicrobial photodynamic inactivation in nanomedicine: Small light strides against bad bugs. *Nanomedicine (Lond)*. 2015;10(15):2379–2404.
- George S, Kishen A. Augmenting the antibiofilm efficacy of advanced noninvasive light activated disinfection with emulsified oxidizer and oxygen carrier. *J Endod*. 2008;34(9):1119–1123.
- Shrestha A, Kishen A. Antibiofilm efficacy of photosensitizer-functionalized bioactive nanoparticles on multispecies biofilm. *J Endod*. 2014;40(10):1604–1610.

Maximum equivalent stress induced and the displacement of the developing permanent first molars after the premature loss of primary second molars: A finite element analysis

Arghavan Kamali Sabeti^{A,C,E}, Zahra Karimizadeh^{A,B,D,F}, Rezvan Rafatjou^{A,C}

Department of Pediatric Dentistry, Dental School, Hamadan University of Medical Sciences, Iran

A – research concept and design; B – collection and/or assembly of data; C – data analysis and interpretation; D – writing the article; E – critical revision of the article; F – final approval of the article

Dental and Medical Problems, ISSN 1644-387X (print), ISSN 2300-9020 (online)

Dent Med Probl. 2020;57(4):401–409

Address for correspondence

Zahra Karimizadeh
E-mail: Zahra_kmz69@yahoo.com

Funding sources

None declared

Conflict of interest

None declared

Received on January 13, 2020

Reviewed on April 1, 2020

Accepted on May 5, 2020

Published online on December 31, 2020

Cite as

Kamali Sabeti A, Karimizadeh Z, Rafatjou R. Maximum equivalent stress induced and the displacement of the developing permanent first molars after the premature loss of primary second molars: A finite element analysis. *Dent Med Probl.* 2020;57(4):401–409. doi:10.17219/dmp/122041

DOI

10.17219/dmp/122041

Copyright

© 2020 by Wrocław Medical University

This is an article distributed under the terms of the Creative Commons Attribution 3.0 Unported License (CC BY 3.0) (<https://creativecommons.org/licenses/by/3.0/>).

Abstract

Background. The use of a space maintainer during the deciduous dentition period at a proper time can prevent the consequences of the loss of the arch length in the future. There is controversy over the use of space maintainers.

Objectives. The aim of this study was to evaluate the magnitude of stresses exerted on immature permanent molar teeth, and the extent of displacement of these teeth when the adjacent teeth are missing, but after placing a space maintainer. Studies carried out to date have used clinical measurements, e.g., X-rays and dental casts.

Material and methods. The finite element model (FEM) was used for modeling the maxillary and mandibular teeth and the bone structure. A space maintainer (band and loop) was also designed for modeling. Force was applied and a finite element analysis (FEA) was carried out in 6 states in the maxilla and in the mandible to evaluate the distribution of stresses and the amount of displacement of immature permanent first molar teeth in the presence or absence of deciduous second molar teeth and a space maintainer.

Results. During mastication, when the deciduous second molar tooth was absent, the maximum stress was transferred to incomplete roots. When there was a space maintainer, stress was transferred to the space maintainer itself and to the distal side of the deciduous first molar tooth. The displacement of permanent first molar teeth was minimal in the presence of all teeth; in the absence of the deciduous second molar tooth, this displacement increased 4–5-fold, which decreased again almost to the level of the 1st/4th state (intact arch) in the presence of the space maintainer.

Conclusions. The results showed the importance of the use of space maintainers, as they significantly decrease the momentary displacement of the teeth as well as the stress exerted on the developing permanent first molar teeth.

Key words: finite element analysis, space maintenance, mesial tooth movement

Introduction

Space management is a crucial issue in pediatric dentistry.¹ Local or systemic factors can lead to the early loss of deciduous teeth, including tooth extractions due to caries, traumatic injuries, and premature exfoliation resulting from abnormal root resorption and systemic disorders. Space reduction after the premature loss of primary second molars is one of the important factors affecting the occurrence of malocclusion, often increasing a demand for orthodontic treatment.² The premature loss of deciduous second molars has the most significant effect on the dental arch, and the maximum space loss is due to the mesial drift of permanent first molar teeth.³ The use of a space maintainer during the deciduous dentition period at a proper time can prevent the consequences of the loss of the arch length in the future.⁴ It has been reported that the space change after the premature loss of a primary second molar in 3 weeks is statistically significant.⁵ A primary second molar is an eruption guide for a permanent first molar, so with the early loss of this guidance, a severe space loss will occur. The fastest and the greatest space closure occurs in the maxilla, followed by the mandible.⁶

There is controversy over the use of space maintainers. Some researchers believe that space maintainers are not useful and have detrimental effects in 19% of cases.⁷ There are a number of ill effects of conventional band and loop space maintainers – they lead to plaque retention, which causes gingivitis, the blanching of the gingivae due to band displacement, mucosal overgrowth, and loop impingement on the mucosa, causing pain and ulceration.⁸ Bilateral space maintainers may have questionable efficacy, and in case of the loss of multiple molars in the same quadrant, their use should be weighed against the risk of unwanted tooth movements, the loss of a removable space maintainer or no space maintenance at all.⁴

Space maintainers are mostly prescribed at a young age; their use is associated with some problems as a result of the patients' poor compliance, the possible manipulation of these appliances, and even the risk of swallowing a separated segment of the wires used as well as with economic problems. Therefore, in some cases, parents are not interested in the use of such appliances.⁹

The masticatory force is defined as a force that is created through the dynamic action of the masticatory muscles during the act of chewing.¹⁰ The force of mastication depends on many factors, including age, gender, tooth developmental stage, and hardness of food. This force is maximum in the molar area. The alveolar bone is immature and more elastic in children, less calcified, and has fewer trabeculae and larger bone marrow spaces as compared to adults. In addition, the lamina dura is thinner and the interdental crest is flatter than in the case of adults.¹¹ In the mixed dentition period, permanent first molar teeth in the maxilla and the mandible are still

developing and erupting; the roots of these teeth are not completely mature, making them very different from mature teeth. When a tooth is subjected to the physiologic force of mastication, stresses are transferred to the underlying bone through the periodontal ligament (PDL). Mature teeth with their long roots provide a large area to transfer these stresses and they are distributed on all root surfaces. However, in teeth that are still developing, only a small surface area of the root is available for transferring similar forces to the underlying bone. Therefore, it is expected that higher stresses will be induced in PDL.¹² The analysis of the biomechanical properties of the tooth can help us understand the pattern of functioning of the periodontal tissue during mastication, and in general, the masticatory function. Therefore, it is necessary to construct a model to unify the structural geometry of the teeth, the tissue characteristics and the forces applied to the jaws. It is now well established that a model accurately simulating all the above variables is able to provide very accurate results.¹³ Currently, the need for a model such as the finite element model (FEM) has attracted attention. So far, no study has evaluated the magnitude of stresses exerted on immature permanent molar teeth with short roots and open apices, and the extent of displacement of these teeth when the adjacent teeth are missing; in addition, this displacement has not been evaluated after placing a space maintainer. Studies carried out to date have used clinical measurements, and none of them have made accurate evaluations with the use of a finite element analysis (FEA). Furthermore, studies using FEA have been very limited, especially in children during the mixed dentition period on immature molars. The stresses considered normal for mature teeth might be different for an immature, developing tooth; in addition, there are differences between maxillary and mandibular first molars in terms of the extent of displacement and bodily movement of the teeth.

The aim of this study was to evaluate the magnitude of stresses exerted on immature permanent molar teeth, and the extent of displacement of these teeth when the adjacent teeth are missing after a space maintainer was placed. Studies carried out to date have used clinical measurements, such as X-rays and plaster models (dental casts).

Material and methods

A finite element analysis was designed and applied in the present study to evaluate stresses and the displacement of maxillary and mandibular first molars in the mixed dentition period under normal masticatory forces in the presence or absence of deciduous second molar teeth and a space maintainer. To this end and to carry out the study on both jaws, three-dimensional (3D) models of the teeth, the jaws and a band and loop space maintainer were constructed as follows.

Preparation of a 3D model of the teeth

A 3D model was designed using the cone-beam computed tomography (CBCT) images of a 6-year-old child whose permanent first molar teeth had erupted recently and established in the occlusal relationship (Fig. 1).

The model was designed accurately in its geometric dimensions, and deciduous first and second molars as well as permanent first molars were included in the model. The CBCT images were entered into a computer for processing 3D images, which converts CBCT and magnetic resonance imaging (MRI) data to 3D computer-aided design (CAD) models, and then the teeth were constructed. All tooth surface curves were recorded during the designing process, which resulted in an improvement in the accuracy of calculations in this model.

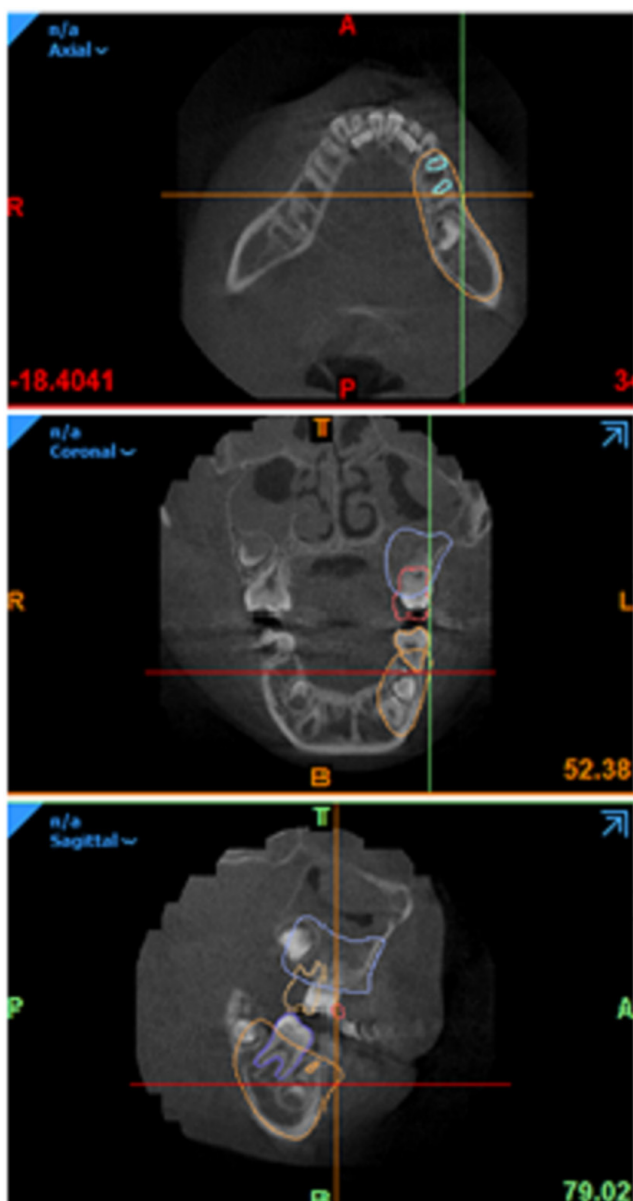


Fig. 1. Cone-beam computed tomography (CBCT) images of a 6-year-old child's dentition

Preparation of a 3D model of the periodontal ligament

After constructing a 3D model of the teeth, a 3D model of PDL was constructed with a thickness of 0.25 mm,^{14,15} along the anatomic roots (Fig. 2). The periodontal ligament was considered as a uniform mass with linear behavior. Although such a structure does not conform with the real biologic behavior of PDL, various studies have shown that this assumption, i.e., a uniform linear structure, is very valuable for assessing orthodontic forces and appears to be sufficient to explain the initial tooth movements.

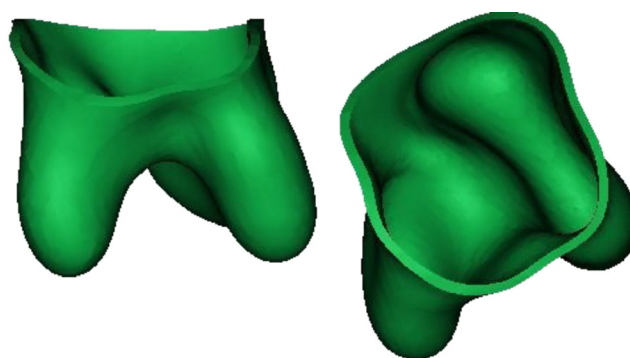


Fig. 2. A three-dimensional (3D) model of the periodontal ligament (PDL) with a thickness of 0.25 mm

Preparation of the bone surrounding the tooth

The geometry of the maxilla and the mandible was constructed using the CBCT images of a 6-year-old child, and materials were assigned to the spongy- and compact-bone compartments. To design and construct the bone, it was considered as a solid and rigid body. Then, the tooth root–PDL complex was eliminated from this volume by using a complex process with the 'subtract' command (Fig. 3).

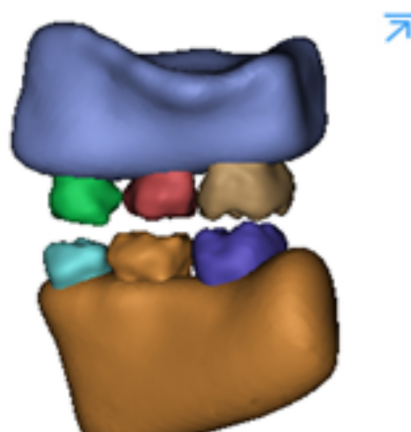


Fig. 3. Geometric model of the maxillary and mandibular bone and the teeth

Incorporation of the model for drawing

Geometric software was used to divide the teeth, which were in the form of surfaces, into solid segments. The 3D model was extracted in the SAT format, which could be read in the Essence milieu. With the FE package, point cloud data was converted into 3D volumes, and then all components were converted into the STP format for FEA.

Preparation of a model of a space maintainer

A band and loop space maintainer was used to this end. The geometry of the space maintainer was designed in the form of a 0.180 × 0.005-inch stainless steel band and a 0.36-inch stainless steel loop (Fig. 4).

To prepare a geometric model for applying boundary conditions, and for meshing and loading, it is necessary to enter the characteristics of the materials forming each component into a computer. Table 1 presents the physical properties of the materials used in the present study.¹⁶

The contact between the components was considered complete and tie-bonded. The coefficient of friction between the tooth and the space maintainer was assumed to be 0.2.¹⁶

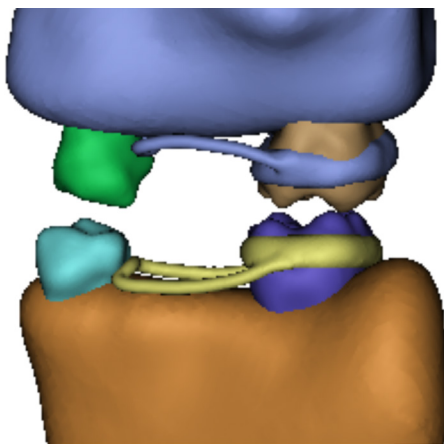


Fig. 4. Geometric model of a band and loop space maintainer

Table 2. Component characteristics

Component	Element type	Number of nodes	Number of elements
Maxillary cortical bone	tetrahedral	12,002	5,240
Maxillary spongy bone	tetrahedral	10,911	6,501
Maxillary first and second primary molars and first permanent molars	tetrahedral	9,173	5,198
PDL of maxillary first and second primary molars and first permanent molars	tetrahedral	14,482	7,085
Maxillary space maintainer	tetrahedral	6,174	2,906
Mandibular cortical bone	tetrahedral	12,185	6,264
Mandibular spongy bone	tetrahedral	13,457	8,218
Mandibular first and second primary molars and first permanent molars	tetrahedral	8,277	4,674
PDL of mandibular first and second primary molars and first permanent molars	tetrahedral	14,696	7,183
Mandibular space maintainer	tetrahedral	5,693	2,705

Table 1. Properties of the materials used in the finite element analysis (FEA) model

Component	Material	Young's modulus [MPa]	Poisson's ratio
Cortical bone	elastic, isotropic	13,700	0.30
Spongy bone	elastic, isotropic	1,370	0.30
PDL	elastic, isotropic	0.05	0.30
Tooth	elastic, isotropic	20,000	0.30
Space maintainer	stainless steel	193,000	0.31

PDL – periodontal ligament.

Automatic meshing

All the components of the 3D model were divided into smaller components (Fig. 5). In addition, the areas subject to the concentration of tensions, such as the apical and alveolar crest areas, were constructed of smaller components to improve the accuracy of these points. The elements were constructed in the form of a tetrahedron. Table 2 presents the approximate number of knots in each component.

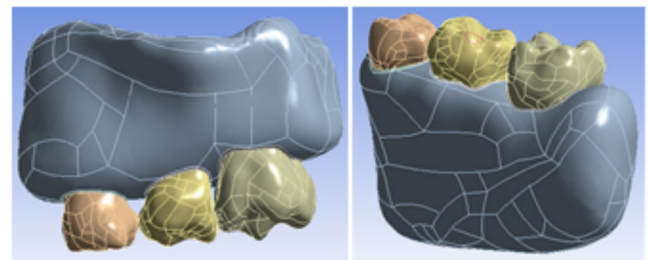


Fig. 5. Automatic meshing of the geometric model

Application of force

Seventy-newton vertical forces (almost equal to the normal masticatory force) were applied to the mesiopalatal cusp of the maxillary permanent first molar and to the distobuccal cusp of the mandibular permanent first molar (Fig. 6).

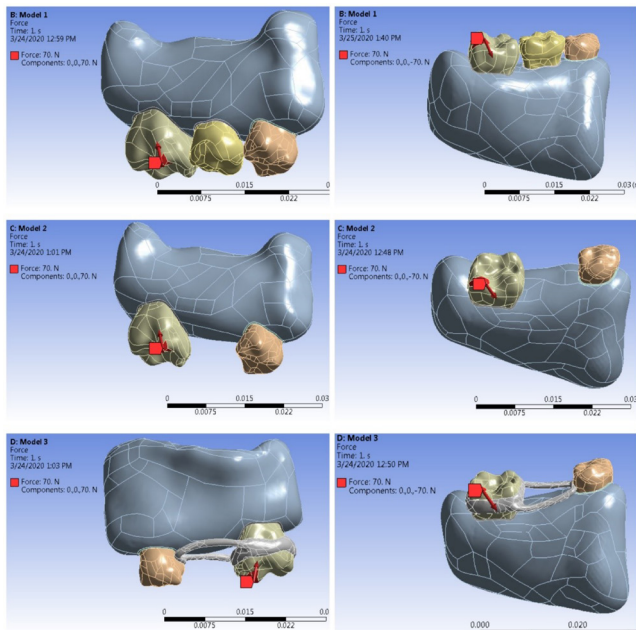


Fig. 6. Load application on the functional cusps of mandibular and maxillary permanent first molars

The different states of the model components were as follows:

- 1 – the maximum equivalent stress induced and the amount of displacement of the maxillary first molar in an intact arch in the presence of the deciduous second molar;
- 2 – the maximum equivalent stress induced and the amount of displacement of the maxillary first molar in the absence of the deciduous second molar;
- 3 – the maximum equivalent stress induced and the amount of displacement of the maxillary first molar in the presence of the space maintainer;
- 4 – the maximum equivalent stress induced and the amount of displacement of the mandibular first molar in an intact arch in the presence of the deciduous second molar;
- 5 – the maximum equivalent stress induced and the amount of displacement of the mandibular first molar in the absence of the deciduous second molar;
- 6 – the maximum equivalent stress induced and the amount of displacement of the mandibular first molar in the presence of the space maintainer.

Results

A static FEA was carried out in 6 states in the maxilla and the mandible to evaluate the distribution of stresses and the amount of displacement of immature permanent first molar teeth in the presence or absence of deciduous second molar teeth and a space maintainer.

The maximum equivalent stress and displacement of the permanent maxillary first molar are presented in Table 3.

When a 70-N force was applied to the mesiopalatal cusp of the maxillary permanent first molar tooth in the presence of the deciduous second molar tooth, the maximum equivalent stress was recorded at the mesial contact of the crown at 50 MPa, and the other parts of the crown and PDL did not exhibit a considerable stress (Fig. 7). The amount of displacement of the permanent first molar was only 0.5 μm (Fig. 8).

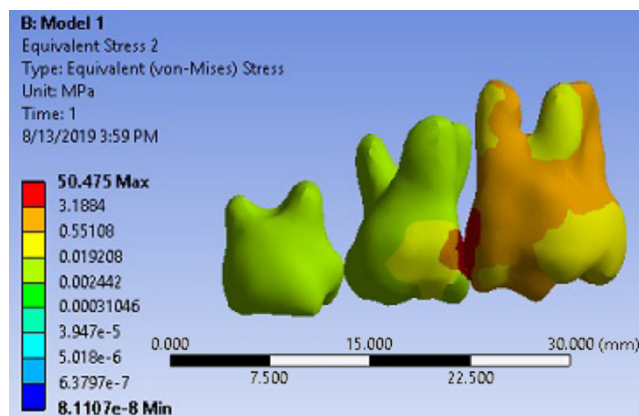


Fig. 7. Pattern of equivalent stress distribution in the maxillary permanent first molar with mesial constraint (distobuccal view)

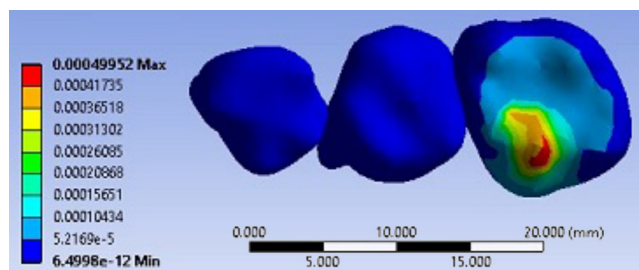


Fig. 8. Displacement pattern in the maxillary permanent first molar with mesial constraint (occlusal view)

Table 3. Maximum equivalent stress and displacement in the crown and roots of the permanent maxillary first molar

Particulars	Presence of the deciduous second molar	Absence of the deciduous second molar	Presence of the space maintainer
Maximum equivalent stress in the mesiobuccal root [MPa]	3.15	2.45	2.58
Maximum equivalent stress in the distobuccal root [MPa]	0.50	2.45	0.50
Maximum equivalent stress in the palatal root [MPa]	3.15	12.22	2.04
Maximum equivalent stress in the crown [MPa]	50.00 (the mesial contact of the crown)	2.45 (the mesiopalatal cusp)	10.00 (broad area)
Maximum displacement [μm]	0.5	6.5	0.6

In the 2nd state, a 70-N force was applied in the absence of the deciduous second molar tooth. In this state, the maximum equivalent stress was recorded in the palatal root of the permanent first molar tooth at 12–16 MPa. The crown and the 2 other roots had a low level of stress (Fig. 9). The displacement of the permanent first molar tooth increased in this state and was 6.5 μm in the mesio-palatal direction (Fig. 10).

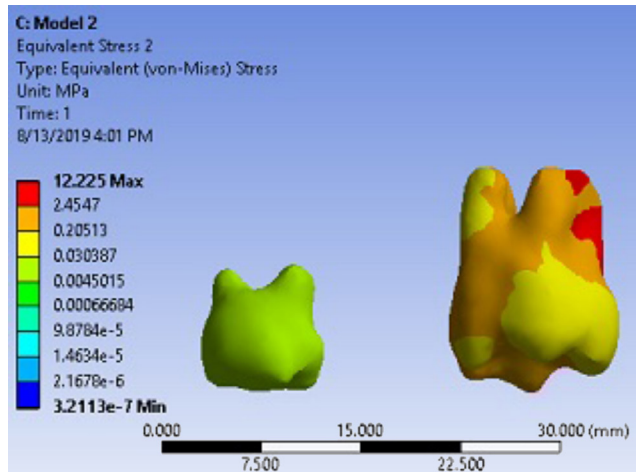


Fig. 9. Pattern of equivalent stress distribution in the maxillary permanent first molar without mesial constraint (distobuccal view)

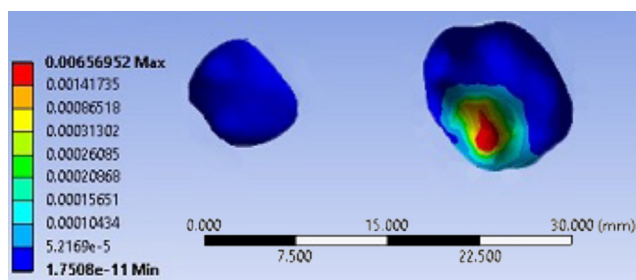


Fig. 10. Displacement pattern in the maxillary permanent first molar without mesial constraint (occlusal view)

In the 3rd state, the force was applied in the presence of the space maintainer. In this state, the maximum equivalent stress on the permanent first molar tooth was recorded on the whole surface of the crown at 10–15 MPa, while the stress in PDL decreased. The maximum equivalent stress in this state was recorded on the surface of the space maintainer and on the distal aspect of the crown of the deciduous first molar tooth (94 MPa) (Fig. 11). A displacement of 0.6 μm was recorded in this state (Fig. 12).

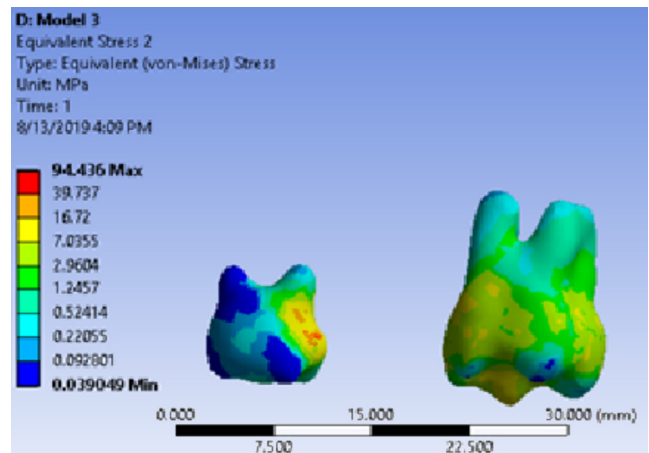


Fig. 11. Pattern of equivalent stress distribution in the maxillary permanent first molar with space maintenance (distobuccal view)

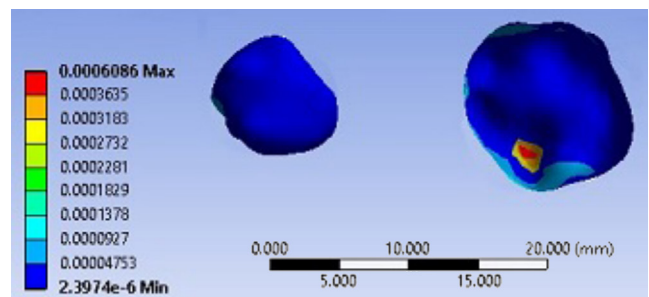


Fig. 12. Displacement pattern in the maxillary permanent first molar with space maintenance (occlusal view)

The maximum equivalent stress and displacement of the permanent mandibular first molar are presented in Table 4.

When a 70-N force was applied to the distobuccal cusp of the mandibular permanent first molar tooth in the 4th state, i.e., in the presence of the deciduous second molar tooth, the maximum equivalent stress was recorded at the mesial contact of the crown at 75.5 MPa. The stress in the roots was similar at 5–6 MPa (Fig. 13). Displacement in this state was 0.8 μm (Fig. 14).

The force was applied in the 5th state, i.e., in the absence of the deciduous second molar tooth. In this state, the maximum equivalent stress at the cervical area of the mesial root was 14 MPa (Fig. 15). Displacement in this state was 7.8 μm in the mesial direction (Fig. 16).

Table 4. Maximum equivalent stress and displacement in the crown and roots of the permanent mandibular first molar

Particulars	Presence of the deciduous second molar	Absence of the deciduous second molar	Presence of the space maintainer
Maximum equivalent stress in the mesial root [MPa]	5.50	14.00	5.40
Maximum equivalent stress in the distal root [MPa]	5.50	14.00	5.40
Maximum equivalent stress in the crown [MPa]	75.50 (the mesial contact of the crown)	6.35 (the distobuccal cusp)	12.00 (broad area)
Maximum displacement [μm]	0.8	7.8	0.7

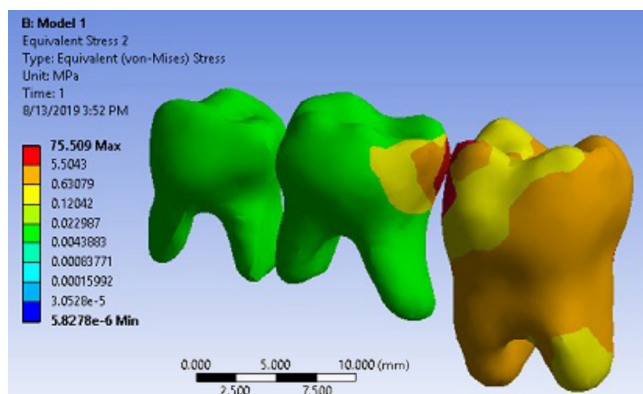


Fig. 13. Pattern of equivalent stress distribution in the mandibular permanent first molar with mesial constraint (distobuccal view)

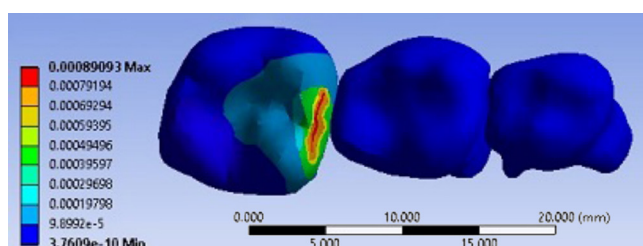


Fig. 14. Displacement pattern in the mandibular permanent first molar with mesial constraint (occlusal view)

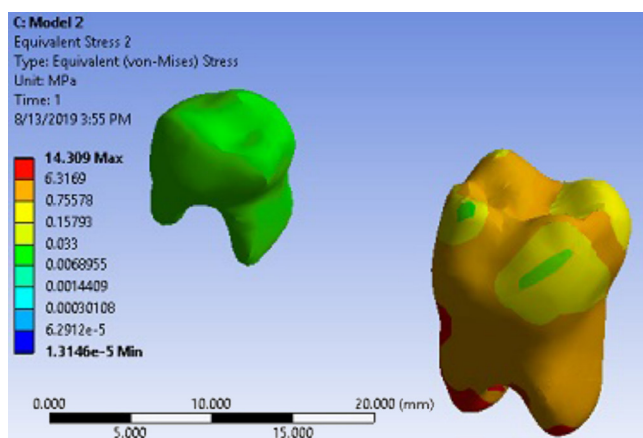


Fig. 15. Pattern of equivalent stress distribution in the mandibular permanent first molar without mesial constraint (distobuccal view)

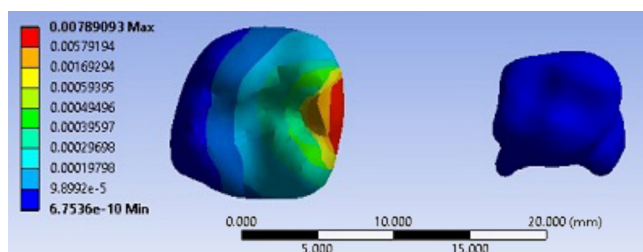


Fig. 16. Displacement pattern in the mandibular permanent first molar without mesial constraint (occlusal view)

In the 6th state, in which the force was applied in the presence of the space maintainer, the maximum equivalent

stress on the entire crown surface was 10–12 MPa, while the root stress decreased to 5–6 MPa. In the mandible, too, a high rate of stress was applied to the space maintainer and the distal area of the crown of the deciduous first molar tooth (98 MPa) (Fig. 17). Displacement in this state was 0.7 μ m (Fig. 18).

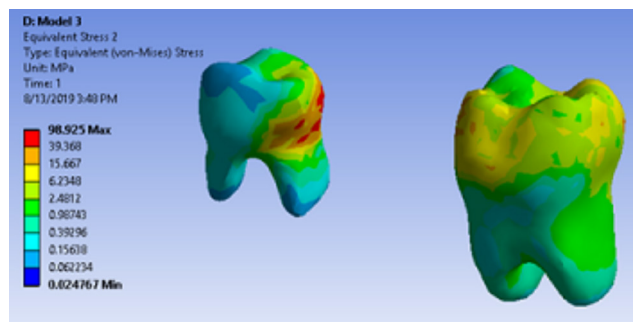


Fig. 17. Pattern of equivalent stress distribution in the mandibular permanent first molar with space maintenance (distobuccal view)

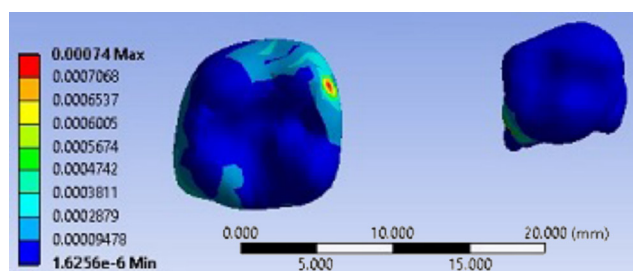


Fig. 18. Displacement pattern in the mandibular permanent first molar with space maintenance (occlusal view)

Discussion

In FEA, maxillary and mandibular permanent first molars were used to construct a model and simulate changes in the equivalent stress distribution pattern and displacement in the presence and absence of deciduous second molar teeth and a space maintainer.

This analysis is independent of time and shows changes on the spot. However, it is possible to determine changes in the shape of the models in terms of a time factor with the use of some frameworks. This analysis has some obvious advantages, including the fact that it can provide data consistent with real and clinical conditions, and confirm or refute it. Furthermore, it can measure some variables that cannot be observed and measured in real and clinical conditions.¹⁷

The normal masticatory force is significantly lower than the maximum bite force. The maximum bite force is defined as the maximum force that an individual can apply with their teeth, and is different from the normal masticatory force. In a normal child, this masticatory force is approx. 78 N.¹⁸ In the present study, this force for a 6-year-old child was considered at 70 N.

In an intact dental arch with all the teeth present in both jaws, the maximum equivalent stress was detected at the mesial contact of the permanent first molar tooth, which was transferred to the tooth mesial to the first molar, rather than to its roots. The tooth root, PDL and all the other areas of the tooth crown exhibited much lower stresses, which is consistent with the results of a study by Southard et al., who reported that the anterior component of the occlusal force (ACF) was transferred to the mesial teeth by a proximal contact and could even pass the midline.¹⁹ Chauhan et al. also reported similar results.¹²

The application of force resulted in the minor displacement of the roots of permanent first molars, and the tooth crown also exhibited a displacement of 0.5–1 μm , which is not clinically important and can be considered the physiological displacement of the tooth during mastication. This finding is consistent with the results of clinical studies which showed that in the presence of all teeth, no significant displacement could take place.²⁰

In the 2nd/5th state, in which deciduous second molars were not present in the dental arch, the maximum equivalent stresses in both arches were transferred to the roots, with higher stresses in the palatal root of the maxillary tooth, followed by the mesiobuccal root. In the mandible, the mesial aspect of the mesial root exhibited the maximum equivalent stress, followed by the mesial aspect of the distal root. These stresses were maximum in the cervical area and the apical area of the roots, which is consistent with the results of a study by Dejak et al., who reported that the maximum stresses during mastication were produced in the occlusal area and in the cervical area of the lingual aspect of permanent first molars in the mandible.²¹ In addition, Petcu et al. carried out a study on subjects during the mixed dentition period and reported that the maximum stress was detected in the cemento-enamel junction (CEJ) area and in the coronal third of the root.¹⁷ Such a discrepancy between the results of studies might be attributed to differences in the anatomy of the teeth and the different developmental stages of immature permanent first molar teeth.

In this state, the maximum equivalent stresses were recorded in the mandibular permanent first molar as compared to the maxilla.

When a permanent first molar tooth is not in contact with a deciduous second molar tooth, the momentary tooth displacement increases 4–5-fold, which is mostly visible in the crown area, while the roots are displaced at a lower rate. Therefore, both maxillary and mandibular permanent first molars tend to tip mesially, rather than move bodily, which was confirmed in the present study and reported in previous clinical studies.²² In studies by Chauhan et al.¹² and Kojima and Fukui,²³ the FEA of maxillary permanent first molar teeth showed that the mesial tipping of these teeth was greater than their bodily movement. In the present study, such displacement of maxillary first molars was observed in the mesiopalatal direction, with only mesial displacement in the case of mandibular first molars.

The comparison of displacement between the 2 jaws showed that the displacement of the lower first molar was greater than that of the upper first molar, which does not coincide with the results of previous clinical studies.^{1,5} It can be concluded that, although momentary displacement in the mandible is greater than in the maxilla, more displacement will occur in the maxilla over time due to the more spongy nature of the maxillary bone.

The amount of displacement of the roots was much smaller than that of the tooth crown, and the displacement of the roots of the mandibular first molar was lesser than in the case of the maxillary first molar, indicating much fewer bodily movements in the mandible as compared to the maxilla. Chauhan et al. also recorded some bodily movement in maxillary first molar teeth.¹²

When the force was applied in the presence of the space maintainer, stresses on the crown and the roots decreased significantly, and were transferred to the space maintainer itself. In addition, high stresses were recorded in the distal aspect of the crowns of deciduous first molars. In the present study, stresses in the distal aspect of the deciduous mandibular first molar were higher than those in the distal aspect of the corresponding tooth in the maxilla. Such a difference might be explained by differences in the anatomy of the teeth between the 2 jaws.

The amount of tooth displacement that was recorded in this state decreased almost to that from the 1st/4th state in an intact arch, and tooth tipping, which was observed in the absence of second primary molars and without mesial constraint, decreased significantly. However, a small amount of root displacement is not clinically important.²⁴

The results of the present study showed that when a permanent first molar tooth erupts, if a deciduous second molar tooth is not in contact with the mesial aspect of the erupting tooth, a large amount of the arch length will be lost and the space will be closed over time. No study to date has evaluated the equivalent stresses exerted on the tooth, the space maintainer and the distal aspect of the deciduous second molar tooth. The results of the present study showed the pattern of distribution of the equivalent stress during mastication; the results also showed that space maintainers are useful in preventing the momentary displacement of the teeth.

Conclusions

The results showed the importance of the use of space maintainers, as they significantly decrease the momentary displacement of the teeth as well as the stress exerted on the developing permanent first molar teeth.

ORCID iDs

Arghavan Kamali Sabeti  <https://orcid.org/0000-0003-4862-1116>
Zahra Karimizadeh  <https://orcid.org/0000-0002-2960-9210>
Rezvan Rafatjou  <https://orcid.org/0000-0002-3333-1725>

References

1. Pokorná H, Marek I, Kucera J, Hanzelka T. Space reduction after premature loss of a deciduous second molar – retrospective study. *IOSR J Dent Med Sci*. 2016;15(11):1–8.
2. Smith SL, Buschang PH. Growth in root length of the mandibular canine and premolars in a mixed-longitudinal orthodontic sample. *Am J Hum Biol*. 2009;21(5):623–634.
3. Ciftci V, Uzel A, Dogan MC. Evaluation of skeletal and dental effects of lower lingual arches. *J Clin Pediatr Dent*. 2018;42(6):469–474.
4. Ahmad A, Parekh S, Ashley PF. Methods of space maintenance for premature loss of a primary molar: A review. *Eur Arch Paediatr Dent*. 2018;19(5):311–320.
5. Bindaýel NA. Clinical evaluation of short term space variation following premature loss of primary second molar, at early permanent dentition stage. *Saudi Dent J*. 2019;31(3):311–315.
6. Srivastava N, Grover J, Panthri P. Space maintenance with an innovative “Tube and Loop” space maintainer (Nikhil appliance). *Int J Clin Pediatr Dent*. 2016;9(1):86–89.
7. Gray S, Stacknik S, Farella M. Space maintenance: An overview for clinicians. *NZ Dent J*. 2016;112(3):76–80.
8. Chandra HS, Krishnamoorthy SH, Johnson JS, Prabhu S. III effects of conventional band and loop space maintainers: Time to revolutionise. *Int Dent Med J Adv Res*. 2018;4:1–3.
9. Rajah LD. Clinical performance and survival of space maintainers: Evaluation over a period of 5 years. *ASDC J Dent Child*. 2002;69(2):156–160.
10. Zhang YR, Du W, Zhou XD, Yu HY. Review of research on the mechanical properties of the human tooth. *Int J Oral Sci*. 2014;6(2):61–69.
11. Parcha E, Bitsanis E, Halazonetis DJ. Morphometric covariation between palatal shape and skeletal pattern in children and adolescents: A cross-sectional study. *Eur J Orthod*. 2017;39(4):377–385.
12. Chauhan SP, Sharma DS, Jain M. Initial stresses induced in permanent maxillary first molar in mixed dentition under normal masticatory forces: A finite element study. *J Clin Pediatr Dent*. 2016;40(4):334–340.
13. Zhang H, Cui JW, Lu XL, Wang MQ. Finite element analysis on tooth and periodontal stress under simulated occlusal loads. *J Oral Rehabil*. 2017;44(7):526–536.
14. Heravi F, Salari S, Tanbakuchi B, Loh S, Amiri M. Effects of crown–root angle on stress distribution in the maxillary central incisors’ PDL during application of intrusive and retraction forces: A three-dimensional finite element analysis. *Prog Orthod*. 2013;14:26.
15. Hedayati Z, Shomali M. Maxillary anterior en masse retraction using different antero-posterior position of mini screw: A 3D finite element study. *Prog Orthod*. 2016;17(1):31.
16. Tominaga J, Ozaki H, Chiang PC, et al. Effect of bracket slot and archwire dimensions on anterior tooth movement during space closure in sliding mechanics: A 3-dimensional finite element study. *Am J Orthod Dentofacial Orthop*. 2014;146(2):166–174.
17. Petcu A, Bălan A, Haba D, Dumitraş C. Importance of the mathematical model in the premature loss of the lower temporary molar. *Pediatr Dent*. 2014;18(4):296–300.
18. Castelo PM, Duarte Gavião MB, Pereira LJ, Bonjardim LR. Masticatory muscle thickness, bite force, and occlusal contacts in young children with unilateral posterior crossbite. *Eur J Orthod*. 2007;29(2):149–156.
19. Southard TE, Behrents RG, Tolley EA. The anterior component of occlusal force. Part 1. Measurement and distribution. *Am J Orthod Dentofacial Orthop*. 1989;96(6):493–500.
20. Natali AN, Pavan PG, Scarpa C. Numerical analysis of tooth mobility: Formulation of a non-linear constitutive law for the periodontal ligament. *Dent Mater*. 2004;20(7):623–629.
21. Dejak B, Młotkowski A, Romanowicz M. Finite element analysis of stresses in molars during clenching and mastication. *J Prosthet Dent*. 2003;90(6):591–597.
22. Lin YT, Lin WH, Lin YJT. Immediate and six-month space changes after premature loss of a primary maxillary first molar. *J Am Dent Assoc*. 2007;138(3):362–368.
23. Kojima Y, Fukui H. Effects of transpalatal arch on molar movement produced by mesial force: A finite element simulation. *Am J Orthod Dentofacial Orthop*. 2008;134(3):335.e1–e7;discussion 335–336.
24. Mühlemann HR. Tooth mobility: A review of clinical aspects and research findings. *J Periodontol*. 1967;38(6)Suppl.:686–713.

Orthodontic-care burden for patients with unilateral and bilateral cleft lip and palate

Sylwia Roguzińska^{A–D,F}, Anna Pelc^{A,D–F}, Marcin Mikulewicz^{D–F}

Division of Facial Abnormalities, Department of Dentofacial Orthopedics and Orthodontics, Wrocław Medical University, Poland

A – research concept and design; B – collection and/or assembly of data; C – data analysis and interpretation;
D – writing the article; E – critical revision of the article; F – final approval of the article

Dental and Medical Problems, ISSN 1644-387X (print), ISSN 2300-9020 (online)

Dent Med Probl. 2020;57(4):411–416

Address for correspondence

Sylwia Roguzińska
E-mail: s.roguzinska@gmail.com

Funding sources

None declared

Conflict of interest

None declared

Received on June 3, 2020
Reviewed on June 14, 2020
Accepted on July 30, 2020

Published online on December 31, 2020

Abstract

Background. Cleft lip and palate (CLP) cause severe malocclusion, which requires numerous orthodontic interventions in specialized centers. There is little literature regarding the overall orthodontic burden of care for these patients.

Objectives. The aim of the study was the evaluation of orthodontic-care burden for patients treated in the Division of Facial Abnormalities at the Department of Dentofacial Orthopedics and Orthodontics of Wrocław Medical University in Poland.

Material and methods. The medical data of patients with complete unilateral and bilateral cleft lip and palate (ULCP and BCLP) who finished orthodontic treatment between 2012 and 2019 was evaluated. The duration of orthodontic treatment, the number of removable appliances, the number of kilometers traveled as well as the number of visits and surgical procedures performed were recorded. The sample was divided into 2 groups according to the World Health Organization (WHO) International Classification of Diseases (ICD-10) diagnosis codes. All data was subjected to statistical analysis.

Results. For the UCLP patients ($n = 54$), the mean time of orthodontic treatment was 9.24 years, the mean number of orthodontic appointments was 62.91, the mean number of removable appliances was 4.12, the mean number of surgical procedures was 3.35, and the mean distance traveled to visit the center for orthodontic appointments was 5,466.95 km. For the BCLP patients ($n = 19$), the mean time of orthodontic treatment was 10.16 years, the mean number of orthodontic appointments was 66.26, the mean number of removable appliances was 4.12, the mean number of surgical procedures was 4.05, and the mean distance traveled to visit the center for orthodontic appointments was 3,758.23 km.

Conclusions. The orthodontic treatment of patients with UCLP and BCLP is very burdensome for the patients. However, the burden of care in the Division of Facial Abnormalities at the Department of Dentofacial Orthopedics and Orthodontics of Wrocław Medical University in Poland is not greater than in other European countries.

Key words: orthodontics, cleft lip, cleft palate, burden of care

Cite as

Roguzińska S, Pelc A, Mikulewicz M. Orthodontic-care burden for patients with unilateral and bilateral cleft lip and palate. *Dent Med Probl.* 2020;57(4):411–416. doi:10.17219/dmp/125874

DOI

10.17219/dmp/125874

Copyright

© 2020 by Wrocław Medical University
This is an article distributed under the terms of the
Creative Commons Attribution 3.0 Unported License (CC BY 3.0)
(<https://creativecommons.org/licenses/by/3.0/>).

Introduction

The main purpose of cleft palate orthodontic treatment is to minimize craniofacial growth dysfunction and to achieve correct pronunciation in the patient. The achievement of this goal requires interdisciplinary treatment by specialists of many fields, including neonatologists, pediatricians, orthodontists, maxillofacial surgeons, plastic surgeons, laryngologists, phoniatricians, speech therapists, pediatric dentists, prosthetists, and psychologists. This results in treatment lasting from childhood to adulthood and is very burdensome for the patient and their parents.

The term 'burden of care' is commonly used nowadays in medical care. It refers to a balance between the compromises the patient and their family need to make and the benefits the child receives. The burden of care in this specific case refers to the total number of surgeries, treatment episodes, appointments, and procedures during the patient's whole multidisciplinary rehabilitation.¹ Many centers where children with similar defects are treated have analyzed orthodontic-care burden for their patients and they strive to minimize it, while maintaining the best treatment results.²

The importance of the topic is emphasized by the fact that it has been discussed at World Health Organization (WHO) Meetings on International Collaborative Research on Craniofacial Anomalies. The WHO has even created strategies to reduce the health-care burden of craniofacial anomalies.¹ However, despite the systematic introduction of these strategies, the burden of treatment remains a huge problem for patients and their families. In 2002, a study comparing the treatment burden of unilateral cleft lip and palate (UCLP) in 5 European centers was carried out.³ The average length of orthodontic treatment varied up to 5 years between the centers. At this time, there is only 1 report (from the UK) taking into account the orthodontic-care burden for patients with bilateral cleft lip and palate (BCLP).⁴ Bearing in mind that BCLP causes greater impairment than UCLP,⁵ it can be expected that its treatment might be longer and more demanding, and therefore more burdensome for the patient.

This study aimed to assess the orthodontic-care burden for patients with UCLP and BCLP from a single center in Poland.

Material and methods

All the data necessary to carry out the analysis was obtained by reviewing the existing medical records at the Academic Dental Policlinic in Wrocław, Poland. For the purposes of the research, all patients of both sexes who met the following inclusion criteria were enrolled: UCLP or BCLP (according to the WHO International

Classification of Diseases (ICD-10); Q37.1 and Q37.0, respectively), patients who underwent orthodontic treatment in 1 center – the Division of Facial Abnormalities, Department of Dentofacial Orthopedics and Orthodontics, Wrocław Medical University, Poland – and finished the therapy between 2012 and 2019. The following information was retrospectively obtained from the patients' existing records: sex, date of birth, place of residence, cleft side (in the case of UCLP), age at registration at the Academic Dental Policlinic, age at the beginning and ending of orthodontic treatment, number of all visits at the clinic, number of visits forced by the damage of the appliance, age at the beginning and ending of treatment with a mobile and permanent appliance with the number of the related follow-up visits, number of removable appliances in use, age during the lip and palate surgery, age during bone grafting to the alveolar process, number of all operations related to the defect, and total number of days spent in the hospital. The distance traveled for treatment at the clinic was calculated by multiplying the number of all visits by the distance from the patient's place of residence to the clinic based on the fastest suggested route according to Google Maps.

The data was described using individual descriptive statistics, such as central tendency (mean – M and median – Me) and measures of variability (standard deviation – SD , the minimum and maximum values of the variables).

Results

The sample consisted of 73 patients, including 54 with one-sided cleft (18 women and 36 men) and 19 patients with bilateral cleft (10 women and 9 men). For UCLP, no statistically significant difference was observed in the mean treatment duration for both sexes. Women's therapy was 51.1 days longer. This is a relatively small difference as compared to the total length of treatment. However, in the case of BCLP, the difference was significant. The average length of treatment for women was 11.6 years, and for men only 8.56 years.

All data was statistically analyzed with the determination of a 95% confidence interval (CI). Table 1 shows the results for the patients with UCLP. Complete orthodontic treatment took a mean time of 9.24 years. The mean number of orthodontic appointments was 62.91. The mean total distance traveled for the patient/family to attend orthodontic appointments at the clinic was 5,466.95 kilometers. Table 2 shows the results for the patients with BCLP. Complete orthodontic treatment took a mean time of 10.16 years. The mean number of orthodontic appointments was 66.26. The mean total distance traveled for the patient/family to attend orthodontic appointments at the clinic was 3,758.23 km.

Table 1. Results for the patients with unilateral cleft lip palate (UCLP) (Q37.1) ($n = 54$)

Data analyzed	<i>M</i>	<i>Me</i>	<i>SD</i>	Min	Max	95% <i>CI</i>
Age at registration at the center [years]	4.83	3	5.07	0	18	1.35
Age at the start of treatment [years]	8.54	8	3.79	3	18	1.01
Age at the end of treatment [years]	17.78	18	1.89	13	21	0.50
Total treatment length [years]	9.24	10	3.65	2	16	0.97
Total number of appointments	62.91	62	30.62	14	153	8.17
Distance traveled [km]	5,466.95	2,890	7,836.99	0	36,408	2,090.26
Age at the start of treatment with a removable appliance ($n = 49$) [years]	7.94	7	3.44	3	17	0.92
Length of treatment with a removable appliance ($n = 49$) [years]	5.31	5	2.43	1	10	0.65
Number of removable appliances ($n = 49$)	4.12	4	2.67	1	16	0.71
Number of control appointments with a removable appliance ($n = 49$)	25.74	24	17.00	1	76	4.53
Age at the start of treatment with a fixed appliance ($n = 52$) [years]	13.21	13	2.15	7	18	0.57
Length of treatment with a fixed appliance ($n = 52$) [years]	3.10	3	1.83	1	9	0.49
Number of control appointments with a fixed appliance ($n = 52$)	22.81	23	10.67	6	66	2.85
Number of additional appliances	0.45	0	0.72	0	2	0.19
Number of missing teeth	0.11	1	0.32	0	1	0.08
Number of appointments caused by the damage of the appliance	1.13	1	1.63	0	6	0.43
Age at lip repair [months]	6.96	6	5.07	3	36	1.35
Age at palate repair [months]	18.09	12	13.85	5	96	3.69
Age at the alveolar bone grafting [years]	9.88	10	2.88	3	19	0.77
Number of oral surgical procedures	3.35	3	0.78	2	5	0.21
Number of days spent in the hospital	18.24	15	10.75	5	44	2.87

M – mean; *Me* – median; *SD* – standard deviation; min – minimum; max – maximum; *CI* – confidence interval.

Table 2. Results for the patients with bilateral cleft lip palate (BCLP) (Q37.0) ($n = 19$)

Data analyzed	<i>M</i>	<i>Me</i>	<i>SD</i>	Min	Max	95% <i>CI</i>
Age at registration at the center [years]	4.53	5	4.36	0	13	1.92
Age at the start of treatment [years]	7.26	7	2.98	3	15	1.34
Age at the end of treatment [years]	17.42	18	3.45	10	24	1.55
Total treatment length [years]	10.16	11	5.06	2	19	2.27
Total number of appointments	66.26	73	35.89	14	140	16.14
Distance traveled [km]	3,758.23	2,199	3,979.69	0	15,120	1,789.45
Age at the start of treatment with a removable appliance ($n = 17$) [years]	6.53	7	2.07	3	10	0.93
Length of treatment with a removable appliance ($n = 17$) [years]	5.65	6	2.03	2	9	0.91
Number of removable appliances ($n = 17$)	4.24	3	2.99	1	11	1.34
Number of control appointments with a removable appliance ($n = 17$)	27.29	26	18.65	4	77	8.39
Age at the start of treatment with a fixed appliance ($n = 16$) [years]	12.94	13	1.39	11	16	0.62
Length of treatment with a fixed appliance ($n = 16$) [years]	3.50	3	1.82	1	8	0.82
Number of control appointments with a fixed appliance ($n = 16$)	21.06	23	8.79	2	32	3.95
Number of additional appliances	0.58	0	0.69	0	2	0.31
Number of missing teeth	0.21	1	0.53	0	2	0.24
Number of appointments caused by the damage of the appliance	0.42	0	1.02	0	4	0.45
Age at lip repair [months]	9.42	7	5.53	6	24	2.49
Age at palate repair [months]	23.37	24	9.14	12	48	4.11
Age at the alveolar bone grafting [years]	11.33	11	2.10	9	15	0.95
Number of oral surgical procedures	4.05	3	1.96	1	7	0.88
Number of days spent in the hospital	30.42	29	20.89	2	60	9.39

From among all the analyzed cases with UCLP, 9% were treated without a mobile appliance, and 4% without a fixed appliance. In BCLP, these results were 11% and 16%, respectively. The lack of treatment with a mobile appliance was in most cases caused by the late beginning of treatment. The average age at registration at the clinic was around 4 years in both groups; however, the maximum age was as much as 18 years old.

Discussion

The treatment of patients with CLP is long-lasting and requires a lot of commitment from both parents and patients. The initial malformation as well as the subsequent surgical procedures – the stitching of the fissure within the lip and the palate – lead to scars that cause three-dimensional disorders in the development of the maxilla, which causes complex malocclusion. The treatment of patients with clefts consists of surgical and orthodontic procedures. The most commonly used surgical protocol is two-stage treatment – the suturing of cleft lip at around 6 months of age and of cleft palate at around 12–18 months of age. There is also a single-stage treatment protocol, in which the suturing of the lip and the palate is performed simultaneously. In Poland, both surgical treatment protocols are used, depending on the center where the treatment is carried out. Orthodontic treatment can be divided into early orthopedic treatment before cleft lip correction, orthodontic treatment during the period of primary dentition and treatment with mixed and permanent dentition. Early pre-surgical treatment aims to bring the split tissues closer together and to minimize the extent of the subsequent surgery. Taping, McNeil's plates and nasolabial molding (NAM) plates are used at this stage. After the treatment, the child is under the constant care of the orthodontist, who monitors the eruption of the teeth in order to intervene at the right time. The postoperative scar of the jaw often disturbs the growth of the maxilla, which makes it necessary to use rapid maxillary expansion and a facial mask. This usually takes place during the period of mixed dentition. After obtaining the correct bite, we align the teeth with a fixed appliance. Meanwhile, surgical and prosthetic interventions due to hypodontia, hyperdontia and the deformation of individual teeth proceed.^{6,7} The same protocol of treatment is followed in Australia.⁸

Many centers around the world have analyzed the effects of the orthodontic treatment of people with CLP in terms of treatment burden for patients. In the comparative study of 5 treatment centers from Northern Europe mentioned in the introduction, the length of orthodontic treatment with the correlated total number of appointments as well as the number of days spent in the hospital were analyzed.³ Their results were very divergent. The length of treatment varied even 5.2 years between

the centers, and the number of visits varied from 49 to even 96. The number of days spent in the hospital varied from 24 to 60. In another study, conducted in Oslo, patients with ULCP spent an average of 24.1 days in the hospital; orthodontic treatment with permanent dentition lasted 2.4 years.⁹ Outside Europe, a similar analysis was carried out in Brazil, where orthodontic treatment lasted on average 11.68 years and required 61.89 visits.¹⁰ The data which we analyzed was age at the time of the surgeries, the total number of surgeries and the total number of days spent in the hospital. Patients suffering from UCLP spent fewer days in the hospital (*M*: 18.24 days) than patients with BCLP (*M*: 30.42 days). This was due to the fact that UCLP required fewer surgical procedures as compared to BCLP (*M*: 3.35 and *M*: 4.05, respectively).

A large number of surgical procedures results from the fact that some of them must be repeated. Scientific research shows that in the case of the split lip surgery, the procedure must be repeated within a year in up to 36% of patients.¹¹ But according to the results of the Americleft study project, the use of secondary surgery did not lead to a significantly better nasolabial appearance than what was achieved in children who underwent only primary surgery.^{12,13} The Americleft study project also showed that children with UCLP had fewer surgeries in the United States than in Europe; the mean number varied from 1 to 4.¹⁴ In Europe, the average number of days spent in the hospital by children with UCLP varied from 24 to 60, depending on the center.^{3,15} Our results also show that the procedures were performed earlier in children with UCLP than in those with BCLP. The mean age at lip repair for UCLP was 6.96 months old, and for BCLP 9.42 months old. The mean age at palate repair was 18.09 and 23.37 months old, respectively.

The orthodontic treatment protocol used at the Division of Facial Abnormalities, Wrocław Medical University, includes treatment with a removable appliance, maxillary expansion if the patient requires it (according to other authors, up to 70% of patients need it¹⁶), and then treatment with a fixed appliance. If bone grafting to the alveolar process is needed, it is most often performed before or after maxillary expansion, considering that the appliance can be fixed only after about 3 months post bone grafting, but not later than 6 months.¹⁷ The average length of treatment with fixed appliances in patients with unilateral cleft was 3.1 years, which does not differ from the results from other centers. For example, in Oslo, the average duration of treatment with permanent dentition was 2.4 years.⁹ One of the hospitals in the UK has an average score of 3.0 years.⁴ For comparison, the treatment of people without cleft with full dentition lasts on average 19.9 months.¹⁸

In a study whose goal was to calculate the amount of treatment and the associated travel experienced by 5 groups of patients treated at different centers, the average duration of the entire orthodontic treatment

ranged from 3.3 to 8.5 years.¹⁵ With these results, the average of 9.24 years obtained in our results does not look satisfactory. One of the reasons may be the fact that patients treated at the center are included in the Program of Orthodontic Care for Children with Facial Abnormalities. Due to the program, parents do not bear the costs of treatment. However, in the years 2002–2004, the program was not implemented, which raises the presumption that some parents could not afford to continue treatment. This is only the authors' supposition, but taking this thesis into account would explain the extension of the treatment time.

Outside Europe, a similar retrospective study was conducted in Brazil. There, the average duration of the entire orthodontic treatment was even longer – 11.68 years.¹⁰ The comparison of the average values obtained in our research vs other countries' research is presented in Table 3. On the issue of BCLP, we can only compare our results with a London hospital. As initially assumed, in both studies, the results showed that the treatment of bilateral cleft was longer than in the case of UCLP. According to the data from the present study, the average duration of treatment with a removable appliance was 5.65 years, and with a fixed appliance 3.5 years. The total length of treatment was 10.16 years. In the study presented by Hameed et al., the mean time length values were 1 year for a removable appliance, 3 years for a fixed appliance and 3.5 years for total treatment.⁴ It is easy to notice that treatment with a removable appliance lasted much longer in Wrocław than in London. This data is not sufficient to draw conclusions, but it is alarming information supporting the need to carry out analyses in other centers. Conducting tests in several centers on larger groups of patients would make it possible to assess whether the problem really exists and to verify the possible causes of the prolonged treatment

with removable appliances. Some authors think that there is an association between the treatment outcome and intensity; thus, a simple protocol with minimum economic burden can provide better or equally good outcomes with less burden of care.¹⁹

The analysis of the number of visits and the distance traveled by the patient for treatment at the clinic shows that for patients with BCLP, the number of visits was higher in proportion to the duration of treatment (M : 66.26). However, this does not coincide at all with the distance traveled, with its average being 1,708.72 km higher for UCLP, despite a smaller number of visits (M : 62.91). The distance the patient had to travel was very small as compared to patients from Brazil (M : 38,978.58 km).¹⁰ This is due to the high availability in Poland of clinics covered by the Program of Orthodontic Care for Children with Facial Abnormalities – there are 16 such clinics (data from the National Health Fund).

Conclusions

The orthodontic treatment of patients with UCLP and BCLP is long-lasting and very burdensome for the patients. The treatment of BCLP lasts longer and requires more procedures than in the case of UCLP. The orthodontic-care burden of patients UCLP and BCLP treated at the Division of Facial Abnormalities, Wrocław Medical University, does not differ from that in other European countries. Therefore, considering that the estimation of the burden of care depends on the results obtained, it should be remembered that a positive objective assessment of treatment may not be synonymous with a subjective assessment by the patient,²⁰ which requires further research.


Table 3. Comparison of own research results with those from other countries (the mean values for UCLP)

Data analyzed	Wrocław	Eurocleft study ³					Oslo ⁹	São Paulo ¹⁰	London ⁴
		A	B	D	E	F			
Age at registration at the center [years]	4.83	no data	no data	no data	no data	no data	no data	0.29	no data
Age at the start of treatment [years]	8.54	no data	no data	no data	no data	no data	no data	8.84	13.4
Total treatment length [years]	9.24	5.6	3.3	8.5	3.5	4.0	3.0	11.68	3.5
Total number of appointments	62.91	63	64	96	49	72	24.3	61.89	no data
Distance traveled [km]	5,466.95	no data	no data	no data	no data	no data	no data	38,978.58	no data
Length of treatment with a removable appliance [years]	5.31	no data	no data	no data	no data	no data	no data	no data	1.0
Number of removable appliances	4.12	no data	no data	no data	no data	no data	no data	11.01	no data
Age at the start of treatment with a fixed appliance [years]	13.21	no data	no data	no data	no data	no data	12.7	no data	no data
Length of treatment with a fixed appliance [years]	3.10	no data	no data	no data	no data	no data	2.4	no data	3.0
Age at the alveolar bone grafting [years]	9.88	no data	no data	no data	no data	no data	9.7	13.36	no data
Age at lip repair [months]	6.96	no data	no data	no data	no data	no data	no data	9.86	no data
Age at palate repair [months]	18.09	no data	no data	no data	no data	no data	no data	25.16	no data
Number of oral surgical procedures	3.35	4.8	3.8	6.0	4.4	3.5	4.8	6.23	no data
Number of days spent in the hospital	18.24	33.0	31.0	60.0	24.0	26.0	24.1	no data	no data

ORCID iDs

Sylwia Rogużińska  <https://orcid.org/0000-0001-9062-4156>

Anna Pelc  <https://orcid.org/0000-0001-6788-6422>

Marcin Mikulewicz  <https://orcid.org/0000-0001-5754-0284>

References

- WHO Human Genetics Programme, WHO Meeting on International Collaborative Research on Craniofacial Anomalies (1st: 2000: Geneva, Switzerland) & WHO Meeting on International Collaborative Research on Craniofacial Anomalies (2nd: 2001: Park City, Utah, USA). *Global Strategies to Reduce the Health-Care Burden of Craniofacial Anomalies: Report of WHO Meetings on International Collaborative Research on Craniofacial Anomalies, Geneva, Switzerland, 5–8 November 2000; Park City, Utah, USA, 24–26 May 2001*. Geneva, Switzerland: World Health Organization; 2002.
- Murthy J. Burden of care: Management of cleft lip and palate. *Indian J Plast Surg*. 2019;52(3):343–348.
- Semb G, Brattström V, Mølsted K, Prah-Andersen B, Shaw WC. The Eurocleft study: Intercenter study of treatment outcome in patients with complete cleft lip and palate. Part 1: Introduction and treatment experience. *Cleft Palate Craniofac J*. 2005;42(1):64–68.
- Hameed O, Amin N, Haria P, Patel B, Hay N. Orthodontic burden of care for patients with a cleft lip and/or palate. *J Orthod*. 2019;46(1):63–67.
- Holmes LB. *Common Malformations*. New York, USA: Oxford University Press; 2013:70–87.
- Vig KWL, Mercado AM. Overview of orthodontic care for children with cleft lip and palate, 1915–2015. *Am J Orthod Dentofacial Orthop*. 2015;148(4):543–556.
- Greyson BH, Maull D. Nasoalveolar molding for infants born with clefts of the lip, alveolus, and palate. *Clin Plast Surg*. 2004;31(2):149–158.
- Schnitt DE, Agir H, David DJ. From birth to maturity: A group of patients who have completed their protocol management. Part I. Unilateral cleft lip and palate. *Plast Reconstr Surg*. 2004;113(3):805–817.
- Semb G, Rønning E, Åbyholm F. Twenty-year follow-up of 50 consecutive patients born with unilateral complete cleft lip and palate treated by the Oslo Cleft Team, Norway. *Semin Orthod*. 2011;17(3):207–224.
- Alberconi TF, Clavasio Siqueira GL, Sathler R, Kelly KA, Garib DG. Assessment of orthodontic burden of care in patients with unilateral complete cleft lip and palate. *Cleft Palate Craniofac J*. 2018;55(1):74–78.
- Sitzman TJ, Coyne SM, Britto MT. The burden of care for children with unilateral cleft lip: A systematic review of revision surgery. *Cleft Palate Craniofac J*. 2016;53(4):84–94.
- Sitzman TJ, Mara CA, Long RE Jr., et al. The Americleft project: Burden of care from secondary surgery. *Plast Reconstr Surg Glob Open*. 2015;3(7):e442.
- Trotman CA, Faraway JJ, Phillips C, van Aalst J. Effects of lip revision surgery in cleft lip/palate patients. *J Dent Res*. 2010;89(7):728–732.
- Long RE Jr., Hathaway R, Daskalogiannakis J, et al. The Americleft study: An inter-center study of treatment outcomes for patients with unilateral cleft lip and palate part 1. Principles and study design. *Cleft Palate Craniofac J*. 2011;48(3):239–243.
- Shaw WC, Dahl E, Asher-McDade C, et al. A six-center international study of treatment outcome in patients with clefts of the lip and palate: Part 5. General discussion and conclusions. *Cleft Palate Craniofac J*. 1992;29(5):413–418.
- Meazzini MC, Capello AV, Ventrini F, et al. Long-term follow-up of UCLP patients: Surgical and orthodontic burden of care during growth and final orthognathic surgery need. *Cleft Palate Craniofac J*. 2015;52(6):688–697.
- Uzel A. Orthodontics in relation with alveolar bone grafting in CLP patients. In: Aslan BI, Uzuner FD, eds. *Current Approaches in Orthodontics*. Ankara, Turkey: IntechOpen; 2019:157–173.
- Tsichlaki A, Chin SY, Pandis N, Fleming PS. How long does treatment with fixed orthodontic appliances last? A systematic review. *Am J Orthod Dentofacial Orthop*. 2016;149(3):308–318.
- Sallis JF, Owen N, Fisher EB. Ecological models of health behavior. In: Glanz K, Rimer BK, Viswanath K, eds. *Health Behavior and Health Education: Theory, Research, and Practice*. 4th ed. San Francisco, USA: Jossey-Bass; 2008:465–495.
- Semb G, Brattström V, Mølsted K, et al. The Eurocleft study: Intercenter study of treatment outcome in patients with complete cleft lip and palate. Part 4: Relationship among treatment outcome, patient/parent satisfaction, and the burden of care. *Cleft Palate Craniofac J*. 2005;42(1):83–92.

Comparison of the marginal discrepancy of PFM crowns in the CAD/CAM and lost-wax fabrication techniques by triple scanning

Elham Ahmadi^{1,2,A,E}, Masoumeh Hasani Tabatabaei^{1,2,A,F}, Sina Mohammadi Sadr^{1,B-D}, Faezeh Atri^{1,3,B,D}

¹ Dental Research Center, Dentistry Research Institute, Tehran University of Medical Sciences, Iran

² Department of Operative Dentistry, School of Dentistry, Tehran University of Medical Sciences, Iran

³ Department of Prosthodontics, School of Dentistry, Tehran University of Medical Sciences, Iran

A – research concept and design; B – collection and/or assembly of data; C – data analysis and interpretation;

D – writing the article; E – critical revision of the article; F – final approval of the article

Dental and Medical Problems, ISSN 1644-387X (print), ISSN 2300-9020 (online)

Dent Med Probl. 2020;57(4):417–422

Address for correspondence

Faezeh Atri

E-mail: f-atr@sina.tums.ac.ir

Funding sources

This study was part of a thesis supported by Dental Research Center, Dentistry Research Institute, Tehran University of Medical Sciences, Iran (grant No. 37544).

Conflict of interest

None declared

Received on March 16, 2020

Reviewed on April 28, 2020

Accepted on July 19, 2020

Published online on December 31, 2020

Cite as

Ahmadi E, Hasani Tabatabaei M, Sadr SM, Atri F. Comparison of the marginal discrepancy of PFM crowns in the CAD/CAM and lost-wax fabrication techniques by triple scanning. *Dent Med Probl.* 2020;57(4):417–422. doi:10.17219/dmp/125532

DOI

10.17219/dmp/125532

Copyright

© 2020 by Wrocław Medical University

This is an article distributed under the terms of the

Creative Commons Attribution 3.0 Unported License (CC BY 3.0)

(<https://creativecommons.org/licenses/by/3.0/>).

Abstract

Background. Computer-aided design/computer-aided manufacturing (CAD/CAM) systems are widely used for the fabrication of porcelain-fused-to-metal (PFM) crowns.

Objectives. This study was conducted to compare PFM crowns through triple scanning in terms of marginal discrepancy between the CAD/CAM and lost-wax fabrication techniques.

Material and methods. Twenty uniform resin dies of a prepared maxillary first molar were randomly divided into 2 groups: conventional lost-wax; and milling. Marginal discrepancy was evaluated at the framework and porcelain steps through triple scanning and direct visualization under a stereomicroscope. Then, the crowns were cemented to the related die and the marginal gap was measured with triple scanning, direct visualization under a stereomicroscope and scanning electron microscopy (SEM). The data was analyzed using the independent *t* test and the one-way analysis of variance (ANOVA). The significance level was set at 0.05.

Results. Differences in the mean marginal gap were measured by the various evaluation methods. Triple scanning and stereomicroscopy identified increasing discrepancy during the fabrication process. According to the results of the independent *t* test, stereomicroscopy showed no difference after cementation between the CAD/CAM and lost-wax groups ($p > 0.05$), triple scanning showed higher fitness in the CAD/CAM group ($p < 0.05$), and SEM showed better adaptation in the lost-wax group ($p < 0.05$); however, there was a positive correlation between the findings of stereomicroscopy and SEM ($p < 0.05$).

Conclusions. The cobalt-chromium crowns had clinically acceptable marginal fitness from both the CAD/CAM and lost-wax techniques; however, the lost-wax group showed lower marginal discrepancy after cementation according to SEM.

Key words: computer-aided design, crown, dental marginal adaptation, metal-ceramic alloys

Introduction

The clinical durability of porcelain-fused-to-metal (PFM) restorations stems from their exact adaptation to the abutment teeth.¹ In the case of a misfit, some complications would occur, such as dental caries,¹ periodontal disease,^{2–5} dental pulpitis,³ reduced long-term success of the PFM crown,³ and cement loss.⁴

Nickel-chromium and cobalt-chromium are popular alloys in PFM restorations. Due to nickel allergy and the toxicity of beryllium, cobalt-chromium alloys are considered the better alternative.⁴ They have some characteristics, such as a relatively low cost,^{5,6} stability in biological environments, corrosion resistance,^{4–6} and the ease of use in computerized milling methods.⁵ Cobalt-chromium alloys are used in the lost-wax and computer-aided design/computer-aided manufacturing (CAD/CAM) methods.^{4–6}

Metal frameworks are conventionally fabricated using the lost-wax and casting technique, in which certain drawbacks – such as the large number of laboratory steps^{2,5} and the lack of a standard cement thickness – can increase the technical sensitivity and the number of errors. Digital methods and CAD/CAM systems have become popular, as they reduce the number of laboratory steps, have a simple fabrication procedure¹ and are cost-effective.⁶ It seems that the CAD/CAM method, with its fewer steps and less human interference, could lower the number of errors and enhance the fitness of restorations.

A marginal gap of less than 120 μ is clinically acceptable for long-term durability and restoration success according to a study by McLean and von Fraunhofer.⁷ An increased gap size exposes the cement and bonding materials in the oral cavity, which gradually dissolve, producing a space for tiny microorganisms to penetrate, and even larger ones over time. This process results in restoration loss and tooth caries. Moreover, plaque accumulation increases and gingival health is endangered.^{8–10}

The methods of evaluating the marginal gap could be categorized as either destructive or non-destructive. Restorations cannot be used after applying destructive methods like sectioning and scanning electron microscopy (SEM).¹¹ Non-destructive methods are commonly used and are classified into two-dimensional (2D) (like direct visualization under a stereomicroscope, profilometry and the replica technique)¹² and three-dimensional (3D) (like micro-computed tomography (micro-CT)¹³ and triple scanning¹⁴) methods.

Several studies have compared marginal adaptation between 2 techniques of fabrication of PFM restorations – lost-wax and CAD/CAM – using different evaluation methods^{1–6}; however, the results are controversial and there is no consensus. The purpose of the present study was to evaluate the marginal adaptation of cobalt-chromium PFM crowns fabricated with the lost-wax and CAD/CAM techniques through direct visualization under a stereomicroscope and triple scanning at the framework and porcelain stages as well as after cementation.

After cementation, all of the samples were evaluated using SEM as the gold standard.

The null hypotheses were as follows:

- the marginal adaptation of PFM crowns is similar in both fabrication methods (lost-wax and CAD/CAM);
- the marginal adaptation of PFM crowns is similar at all fabrication steps (framework, porcelain and after cementation).

Material and methods

Preparation of the samples

In this *in vitro* experiment, 20 uniform resin models of a maxillary first molar were milled from a single scan of a prepared tooth for metal-ceramic restorations with the following features: a 1.5-millimeter radial shoulder finish line, an axial convergence of 6°, and an occlusal reduction of 1.5 mm in the non-functional cusp and of 2 mm in the functional cusp at a level of 45°. In each model, some notches were prepared in the base part and outside of the finish line as reference points.

Impressions were made from all samples with the one-stage putty and light-bodied wash technique using polyvinyl-siloxane (Panasil®; Kettenbach, Eschenburg, Germany), then poured with type IV stone. The stone dies were randomly divided into 2 groups: conventional lost-wax; and CAD/CAM.

Framework fabrication

In the 1st group, a 30-micron spacer (Renfert® die:master system; Renfert, Hilzingen, Germany) was uniformly applied to the stone dies up to 1 mm from the finish line. The frameworks were waxed with 0.5-millimeter uniform wax (Renfert) with a lingual shoulder position 1 mm wide and 2 mm high. The wax patterns were then cylindered with an investment material (the Z4 universal investment; Neiryneck & Vogt N.V., Schelle, Belgium), poured with a cobalt-chromium alloy (Wirobond® 280; Bego, Bremen, Germany), polished, and finished.

In the 2nd group, the stone dies were scanned using a laboratory scanner (an optical 3D scanner; Open Technologies, Rezzato, Italy). The frameworks were designed using the exocad® software (www.exocad.com), considering the same features as in the 1st group. The frameworks were milled from a cobalt-chromium block (ARUM Dentistry, Seoul, South Korea), using a milling machine (ARUM Dentistry).

Framework fitness evaluation

Stereomicroscopy: In both groups, the framework was seated on the related die and marginal discrepancy was observed under a stereomicroscope (SZX16; Olympus,

Tokyo, Japan) at $\times 10$ magnification. Photographs of the samples were taken and the gap size was measured in microns using the AxioVision Microscopic Imaging software (release 4.8; Carl Zeiss, Oberkochen, Germany) at the following points: 4 line angles; and the midpoints of the buccal, palatal, mesial, and distal margins. The mean values of these measurements were then compared.

Triple scanning method: In both groups, scan powder (Renfert® scan spray 1 \times 200 mL (6.8 fl. oz.); Renfert) was sprayed onto the stone dies, the internal and external surfaces of the frameworks, and then all of the surfaces were scanned. Each framework was seated on the related die for the next scan. These scans were merged automatically in the software by reference points. After registration, marginal discrepancy was measured at the above points (Fig. 1).

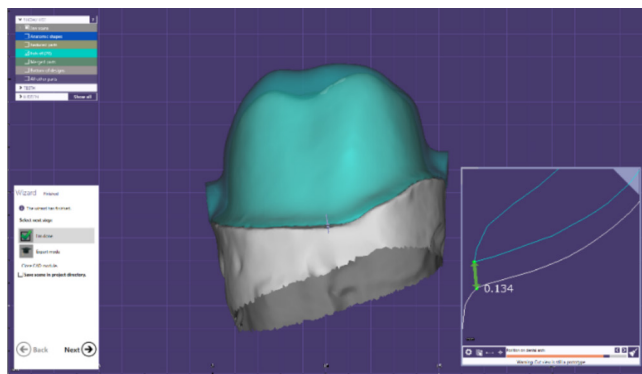


Fig. 1. Discrepancy measurement at the mid-buccal point of the margin

Porcelain application and fitness evaluation

In the next step, porcelain (Kuraray Noritake Dental Inc., Chiyoda-ku, Japan) with the same silicon index was applied in both groups by means of the layering technique (opaque, dentin and enamel) according to the manufacturer's instructions. The prepared crowns were evaluated for marginal discrepancy with stereomicroscopy and triple scanning as mentioned above.

Cementation and fitness evaluation

In the final step, all of the crowns were cemented to the related dies with zinc phosphate (Hoffmann, Berlin, Germany) under a 10-newton load, using a 1-kilogram weight. The cemented crowns were evaluated in terms of marginal discrepancy with stereomicroscopy and triple scanning. All crowns were then embedded in polyester and sectioned mesiodistally with a cutting machine (MECATOME® T 201 A; PRESI, Grenoble, France). The sectioned samples were evaluated under an electron microscope (Nova NanoSEM™ 450; FEI, Hillsboro, USA) at $\times 800$ magnification. Marginal discrepancy was measured at 2 axial points and the mean value was used for comparison (Fig. 2).

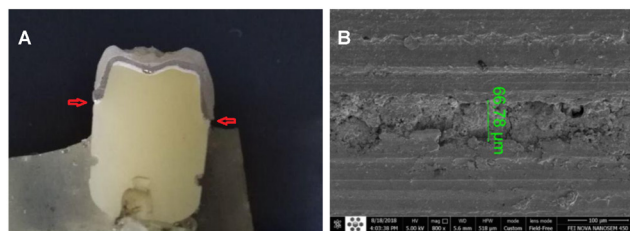


Fig. 2. Cross-sectional view of the cemented crown and marginal discrepancy measured at the 2 depicted points (A); evaluation at $\times 800$ magnification, using the QUANTAX micro X-ray fluorescence (micro-XRF) software (www.bruker.com)

Data analysis and statistics

The statistical analysis was performed using IBM SPSS Statistics for Windows, v. 22.0 (IBM Corp., Armonk, USA). The independent *t* test was used to compare the different fabrication methods at each step (framework, porcelain and cementation). The one-way analysis of variance (ANOVA) was used to evaluate the discrepancy at different steps in each group (lost-wax and milling). The significance level was set at 0.05.

Results

Marginal discrepancy was measured at each fabrication step (framework, porcelain and cementation) in both study groups.

Framework

According to the independent *t* test results, triple scanning showed a smaller marginal gap in the CAD/CAM group ($p < 0.001$), while stereomicroscopy revealed no significant difference between the 2 groups ($p > 0.05$) (Table 1).

Table 1. Mean marginal gap of the crowns fabricated with the computer-aided design/computer-aided manufacturing (CAD/CAM) and lost-wax techniques at the framework step

Evaluation method	Study groups	Marginal gap [μ]	<i>p</i> -value
Stereomicroscopy	CAD/CAM	94.44 \pm 22.02	0.970
	lost-wax	94.70 \pm 12.29	
Triple scanning	CAD/CAM	57.75 \pm 9.61	<0.001
	lost-wax	82.93 \pm 13.85	

Data presented as mean (*M*) \pm standard deviation (*SD*).

Porcelain

After porcelain application, neither stereomicroscopy nor triple scanning showed significant differences in marginal discrepancy between the study groups ($p > 0.05$) (Table 2).

Table 2. Mean marginal gap of the crowns fabricated with the CAD/CAM and lost-wax techniques at the porcelain step

Evaluation method	Study groups	Marginal gap [μ]	<i>p</i> -value
Stereomicroscopy	CAD/CAM	100.81 \pm 19.52	0.690
	lost-wax	104.12 \pm 16.87	
Triple scanning	CAD/CAM	102.20 \pm 26.20	0.090
	lost-wax	118.32 \pm 12.27	

Data presented as *M* \pm *SD*.

Cementation

According to the independent *t* test results, a smaller marginal gap was visible in the CAD/CAM group with triple scanning ($p < 0.05$), while stereomicroscopy did not reveal any significant difference between the 2 groups ($p > 0.05$). By contrast, SEM showed a smaller marginal gap in the lost-wax group as compared to the CAD/CAM group ($p < 0.05$) (Table 3).

Table 3. Mean marginal gap of the crowns fabricated with the CAD/CAM and lost-wax techniques after cementation

Evaluation method	Study groups	Marginal gap [μ]	<i>p</i> -value
Stereomicroscopy	CAD/CAM	119.87 \pm 30.76	0.730
	lost-wax	123.75 \pm 17.46	
Triple scanning	CAD/CAM	116.86 \pm 11.76	0.049
	lost-wax	131.28 \pm 17.07	
SEM	CAD/CAM	91.09 \pm 63.98	0.030
	lost-wax	40.60 \pm 20.85	

Data presented as *M* \pm *SD*.

SEM – scanning electron microscopy.

Marginal discrepancy changes at the fabrication steps

The mean marginal gap was calculated at each step, for both methods and all samples. The results are presented below.

Triple scanning

Based on the triple scanning evaluation of the steps, the marginal gap was 71.00 μ for the framework step, 110.69 μ for the porcelain step and 124.45 μ for the cementation step. The difference was significant according to the one-way ANOVA ($p < 0.05$).

Stereomicroscopy

Based on the stereomicroscopic evaluation of each step, the marginal gap was 94.58 μ for the framework step, 102.55 μ for the porcelain step and 121.91 μ for the cementation step. The difference was significant according to the one-way ANOVA ($p < 0.05$).

Correlation of different measurement methods

Pearson's correlation test was used to evaluate the correlation of the results of triple scanning, stereomicroscopy and SEM at different steps:

- framework: there was no significant correlation between triple scanning and stereomicroscopy (correlation: -0.22 ; $p > 0.05$);
- porcelain: there was a moderate negative correlation between triple scanning and stereomicroscopy (correlation: -0.561 ; $p < 0.05$);
- cementation: there was no significant correlation between triple scanning and stereomicroscopy (correlation: -0.296 ; $p > 0.05$); a moderate positive correlation was found between stereomicroscopy and SEM (correlation: 0.546 ; $p < 0.05$), but there was no significant correlation between triple scanning and SEM (correlation: -0.417 ; $p > 0.05$).

Discussion

The purpose of this study was to compare the marginal fitness of PFM crowns between the lost-wax and CAD/CAM fabrication methods at different stages of the process (framework, porcelain and cementation), using 3 evaluation methods – triple scanning, stereomicroscopy and SEM. The null hypotheses were rejected. After cementation, SEM – as the gold standard method – revealed significantly higher marginal adaptation in the lost-wax group, and the marginal gap increased significantly through the fabrication steps (from framework to porcelain to cementation).

Stereomicroscopy

No difference was found between the CAD/CAM and lost-wax methods at the framework step. This finding was consistent with studies conducted by Gunsoy and Ulusoy¹⁵ and Jung,¹ but it was in contrast to the results of studies performed by Nesse et al.⁵ and Kim et al.⁶ In 2015, Nesse et al. reported better marginal adaptation in the CAD/CAM group. The difference could be due to the evaluation method, since Nesse et al. observed the replica under a microscope, which is more sensitive than direct visualization.⁵ In 2017, Kim et al. found higher marginal fitness in the lost-wax group. They used implant abutments as samples, and the detection of gaps under a microscope could have been more difficult due to the loss of adequate contrast between the framework and the abutment.⁶

No difference was found between the CAD/CAM and lost-wax methods at the porcelain step, which was not consistent with the results of a study by Shokry et al., who reported lower marginal fitness in the lost-wax group.⁹

Differences in the finish line, die material and CAD/CAM system could have caused these inconsistent results.

No difference was found between the CAD/CAM and lost-wax techniques after cementation; this finding was not consistent with a study by Kaleli and Saraç, who reported significantly higher marginal fitness in the CAD/CAM group.² This difference could be due to the use of different CAD/CAM systems, alloys and cementation procedures, or other unknown confounding factors.

The comparison of the marginal gap through different fabrication steps by means of stereomicroscopy revealed a gradual increase in both the CAD/CAM and lost-wax groups. This finding was consistent with studies conducted by Kaleli and Saraç,² Shokry et al.⁹ and Hafezeqoran et al.¹⁰

Triple scanning

According to the results of triple scanning, significantly higher marginal fitness was observed in the CAD/CAM group at the framework step, no significant difference was found between the 2 groups at the porcelain step and significantly higher marginal fitness was noted in the CAD/CAM group after cementation. The comparison of the marginal gap through different fabrication steps by means of triple scanning revealed a gradual increase in the gap size in both groups.

Scanning is a non-destructive 3D measurement method. In 2011, Holst et al. described the triple scanning method, tested it in 50 samples, and suggested it as a reliable and repeatable technique.¹⁴

In 2015, Kuhn et al. used a charge-coupled device (CCD) camera to digitize a die with and without a respective replica.¹² The scans were recorded with a direct registration tool in the same alignment, and the difference in the point cloud of the die with and without the replica represented the gap space. They claimed that a digital, computer-based method could be beneficial for a 3D analysis, without information loss.¹²

Furthermore, Kane et al. used a 5-axis laser scanner to produce 3D models of dies with and without a replica, and evaluated marginal and internal fitness by superimposing 2 scans.⁴ This method has the sensitivity of the replica technique, but may lead to silicon tearing and scan errors.

In 2017, Park et al. used an intraoral scanner and software for the 3D analysis of fitness.¹⁶ In their recommended technique, an intra-coronal, ceramic-type restoration was used, which has less reflection and does not require the application of powder. Moreover, registration and superimposition were performed through intact nearby teeth. The authors only suggested the method and no further research was done regarding its accuracy.¹⁶

In 2017, Dahl et al. used the triple scanning method as used in the present study to compare the internal fitness of single crowns (made of ceramic and cobalt-chromium) fabricated with different methods.¹⁷ This study found

that lost-wax and conventional casting resulted in better adaptation than CAD/CAM (the ceramic and metal framework),¹⁷ which was in contrast to the results of the triple scanning method in the present study. The difference could be due to the smaller sample size of the former study and the different scanners and software used.

Scanning electron microscopy

The SEM evaluation after cementation showed better marginal fitness in the lost-wax group as compared to the CAD/CAM group.

It is worth noting that the mean marginal gap was clinically acceptable in both the CAD/CAM (91.09 μ) and lost-wax (40.60 μ) groups according to McLean and von Fraunhofer, who considered a gap size of less than 120 μ as a criterion for long-term stability and success.⁷

Comparison of different evaluation methods

Scanning electron microscopy is considered a valid and reliable method and the gold standard, as it is based on different conductivities of elements and is more accurate. However, this method is not routinely used, because it requires advanced equipment and gold coating, and is therefore costly.³ It is destructive and evaluation is limited to the sectioned area.

Stereomicroscopy correlated with the gold standard, SEM. It is a non-destructive method and can be performed in all the parts of the margin. However, it is unable to evaluate the internal fitness and horizontal discrepancy.¹⁴ The following points are important in stereomicroscopy: fixing the samples during photography; setting the same angle in all samples; setting the appropriate image contrast in the software; avoiding human error in determining the points for gap measurement; and calibrating the measurement software.

Triple scanning showed no correlation with SEM and stereomicroscopy. One reason could be the inability to apply a uniform layer of the scan powder (especially on the inner surfaces of the crowns), which affects the accuracy of scans. Furthermore, difficult access to some areas (undercuts and fissures) should be considered.¹² Moreover, optical scanners cannot detect the thin edges or margins of the framework, which may result in the incorrect interpretation of large discrepancy.

The application of titanium oxide powder to scan the reflective intaglio surface of the crown would produce a model that has a tighter fit than in reality because of the powder thickness. Holst et al.¹⁴ and Matta et al.¹⁸ found that this error was insignificant whereas it resulted in a major inaccuracy in the present study. In the current study, the intaglio surface was registered as tighter, overlapping and passing the die surface in some areas after superimposition, and the cement space was omitted,

resulting in negative discrepancy. According to the results, the discrepancy measured by this method did not correlate with direct visualization under a stereomicroscope or SEM.


After scanning, the data should be recorded. This can be performed by superimposing points or surfaces to position the data in the same coordinates. This is one of the key steps of a 3D analysis. This step is also prone to some errors.¹⁹ We believe that triple scanning may not be trusted yet, and that more research is needed.

Conclusions

The cobalt-chromium crowns had a clinically acceptable marginal fitness from both the CAD/CAM and lost-wax methods; however, the lost-wax method was associated with lower marginal discrepancy after cementation. According to the results, triple scanning could not be trusted with regard to evaluating the fitness of PFM crowns.

ORCID iDs

Elham Ahmadi  <https://orcid.org/0000-0002-3428-1045>

Masoumeh Hasani Tabatabaei  <https://orcid.org/0000-0001-8318-0163>

Sina Mohammadi Sadr  <https://orcid.org/0000-0003-1073-350X>

Faezeh Atri  <https://orcid.org/0000-0002-4334-6154>

References

- Jung JK. An evaluation of the gap sizes of 3-unit fixed dental prostheses milled from sintering metal blocks. *BioMed Res Int.* 2017;2017:7847930.
- Kaleli N, Saraç D. Influence of porcelain firing and cementation on the marginal adaptation of metal-ceramic restorations prepared by different methods. *J Prosthet Dent.* 2017;117(5):656–661.
- Nawafleh NA, Mack F, Evans J, Mackay J, Hatamleh MM. Accuracy and reliability of methods to measure marginal adaptation of crowns and FDPs: A literature review. *J Prosthodont.* 2013;22(5):419–428.
- Kane LM, Chronaios D, Sierraalta M, George FM. Marginal and internal adaptation of milled cobalt-chromium copings. *J Prosthet Dent.* 2015;114(5):680–685.
- Nesse H, Ulstein DMÅ, Vaage MM, Øilo M. Internal and marginal fit of cobalt-chromium fixed dental prostheses fabricated with 3 different techniques. *J Prosthet Dent.* 2015;114(5):686–692.
- Kim MJ, Choi YJ, Kim SK, Heo SJ, Koak JY. Marginal accuracy and internal fit of 3-D printing laser-sintered Co-Cr alloy copings. *Materials (Basel).* 2017;10(1):93.
- McLean JW, von Fraunhofer JA. The estimation of cement film thickness by an in vivo technique. *Br Dent J.* 1971;131(3):107–111.
- Tinschert J, Natt G, Mautsch W, Spiekermann H, Anusavice KJ. Marginal fit of alumina- and zirconia-based fixed partial dentures produced by a CAD/CAM system. *Oper Dent.* 2001;26(4):367–374.
- Shokry TE, Attia M, Mosleh I, Elhosary M, Hamza T, Shen C. Effect of metal selection and porcelain firing on the marginal accuracy of titanium-based metal ceramic restorations. *J Prosthet Dent.* 2010;103(1):45–52.
- Hafezeqoran A, Koodaryan R, Esmaili A, Noori H, Shahbaz A. Marginal adaptation of metal ceramic crowns cast from four different base metal alloys before and after porcelain application. *Adv Biosci Clin Med.* 2015;3(2):30–36.
- Groten M, Girthofer S, Pröbster L. Marginal fit consistency of copy-milled all-ceramic crowns during fabrication by light and scanning electron microscopic analysis in vitro. *J Oral Rehabil.* 1997;24(12):871–881.
- Kuhn K, Ostertag S, Ostertag M, Walter MH, Luthardt RG, Rudolph H. Comparison of an analog and digital quantitative and qualitative analysis for the fit of dental copings. *Comput Biol Med.* 2015;57:32–41.
- Brenes C. *Micro-CT Evaluation of the Marginal Fit of CAD/CAM All Ceramic Crowns* [doctoral dissertation]. Chapel Hill, USA: University of North Carolina at Chapel Hill; 2014.
- Holst S, Karl M, Wichmann M, Matta RET. A new triple-scan protocol for 3D fit assessment of dental restorations. *Quintessence Int.* 2011;42(8):651–657.
- Gunsoy S, Ulusoy M. Evaluation of marginal/internal fit of chrome-cobalt crowns: Direct laser metal sintering versus computer-aided design and computer-aided manufacturing. *Niger J Clin Pract.* 2016;19(5):636–644.
- Park JM, Hämmerle CHF, Benic GI. Digital technique for in vivo assessment of internal and marginal fit of fixed dental prostheses. *J Prosthet Dent.* 2017;118(4):452–454.
- Dahl BE, Ronold HJ, Dahl JE. Internal fit of single crowns produced by CAD-CAM and lost-wax metal casting technique assessed by the triple-scan protocol. *J Prosthet Dent.* 2017;117(3):400–404.
- Matta RE, Schmitt J, Wichmann M, Holst S. Circumferential fit assessment of CAD/CAM single crown – a pilot investigation on a new virtual analytical protocol. *Quintessence Int.* 2012;43(9):801–809.
- Rudolph H, Salmen H, Moldan M, et al. Accuracy of intraoral and extraoral digital data acquisition for dental restorations. *J Appl Oral Sci.* 2016;24(1):85–94.

Impact of periodontitis on the Oral Health Impact Profile: A systematic review and meta-analysis

Barbara Paśnik-Chwalik^{B–D}, Tomasz Konopka^{A,E,F}

Department of Periodontology, Wrocław Medical University, Poland

A – research concept and design; B – collection and/or assembly of data; C – data analysis and interpretation; D – writing the article; E – critical revision of the article; F – final approval of the article

Dental and Medical Problems, ISSN 1644-387X (print), ISSN 2300-9020 (online)

Dent Med Probl. 2020;57(4):423–431

Address for correspondence

Barbara Paśnik-Chwalik
E-mail: barbara.pasnik-chwalik@umed.wroc.pl

Funding sources

None declared

Conflict of interest

None declared

Received on June 8, 2020
Reviewed on June 22, 2020
Accepted on July 7, 2020

Published online on December 2, 2020

Cite as

Paśnik-Chwalik B, Konopka T. Impact of periodontitis on the Oral Health Impact Profile: A systematic review and meta-analysis. *Dent Med Probl.* 2020;57(4):423–431. doi:10.17219/dmp/125028

DOI

10.17219/dmp/125028

Copyright

© 2020 by Wrocław Medical University
This is an article distributed under the terms of the Creative Commons Attribution 3.0 Unported License (CC BY 3.0) (<https://creativecommons.org/licenses/by/3.0/>).

Abstract

Background. Periodontitis, being a chronic and multifactorial disease, affects oral health, and consequently, the patient's quality of life (QoL). The assessment of the oral health-related quality of life (OHRQoL) is possible with the Oral Health Impact Profile-14 (OHIP-14) questionnaire comprising 7 subdomains: functional limitation, physical pain, psychological discomfort, physical disability, psychological disability, social disability, and handicap.

Objectives. The aim of this study was to conduct a systematic review of cross-sectional or case–control studies concerning the impact of periodontitis on QoL measured with OHIP-14. The outcomes of the studies were subjected to a meta-analysis.

Material and methods. On the basis of a survey of databases (MEDLINE, Scopus, Google Scholar, and Polish Medical Bibliography – PBL), 1,346 titles related thematically to the impact of periodontitis on QoL were obtained and analyzed. Ten studies were considered eligible for evaluation (8 cross-sectional ones and 2 case–control ones).

Results. All studies indicated a significant influence of periodontitis on the deterioration of the OHIP-14 values. This relationship was shown to be directly modified in proportion to the degree of the advancement of the periodontal disease and to the extent of periodontal tissue damage. Our own meta-analysis confirmed the correlation between the prevalence of periodontitis and increased OHIP-14 scores with a cumulative odds ratio (OR) of 1.33, demonstrated a moderately significant deterioration of the OHIP-14 scores by 4.2 points in the group with periodontitis as compared to the control group, and assessed the probability of OHIP-14 deterioration to be 3.5 times greater in severe periodontitis.

Conclusions. The impact of periodontitis on the deterioration of OHRQoL is quite clearly explained by the clinical symptoms of periodontitis. According to patients, the most important problems that periodontitis may cause include psychological discomfort, stress, problems in interpersonal relations, or even difficulties in daily activities. This indicates the need for more of a holistic approach in planning the goals of the periodontal therapy, taking into account the psychological and social aspects of the patient's perception of the disease.

Key words: periodontitis, meta-analysis, oral health, quality of life

Introduction

Periodontitis is a chronic, multifactorial inflammatory disease associated with the dysbiosis of the bacterial biofilm in periodontal pockets, which leads to damage to the attachment apparatus through an inappropriate, usually excessive, host immune inflammatory response.¹ Risk factors affecting the initiation and progression of periodontitis can be divided into 2 categories: non-modifiable (age, gender, race, and genotype) and modifiable (poor oral hygiene, presence of periopathogens in the biocenosis of the oral cavity, nicotine dependence syndrome, selected general diseases – uncontrolled diabetes, obesity or osteoporosis – low socioeconomic status, poor dietary quality, and stress).² The clinical consequences of this progressive damage to periodontal tissues have an impact on the health of the oral cavity in the physiological, psychological and social aspects, which affects the patient's quality of life (QoL).³

The current definition of oral health stresses the interaction between 3 basic elements: the impact of the extent and severity of the disease on the patient's health; the physiological functions of speaking, smiling, chewing, and swallowing; and the social functions enabling unhindered social coexistence.⁴ It also draws attention to the need to determine the impact of oral health on QoL (oral health-related quality of life – OHRQoL).^{4,5}

The ability to measure OHRQoL allows oral health to be linked to both the subjective assessment of the patient's wellbeing and potential limitations in social life. The assessment of OHRQoL enables patient-centered care and helps to identify the needs for health promotion and prevention programs.⁶ It is important, therefore, to demonstrate whether and to what extent periodontitis and its severity affects the QoL of the population exposed to it, since it is second only to caries in terms of prevalence.

A psychometric test of QoL involves the patient filling out a questionnaire, which has been analyzed and validated beforehand. In modern dental epidemiology, it is possible to make the overall assessment of OHRQoL through such multiple indicators and indices as the Oral Impact on Daily Performance (OIDP), the Oral Health Index (OHX), the Geriatric Oral Health Assessment Index (GOHAI), the Liverpool Oral Rehabilitation Questionnaire (LORQ), and the Subjective Oral Health Status Indicators (SOHSI). Another group consists of indicators that estimate the impact of specific conditions affecting the sensation of oral health, such as the Xerostomia-Related Quality of Life Scale (XeQoLS), the Dentin Hypersensitivity Experience Questionnaire (DHEQ) and the Quality of Life With Implant Prosthesis (QoLIP-10). In addition, there are health-related quality of life (HRQoL) indicators that assess the physical, psychological and social impact of health conditions on an individual's wellbeing, e.g., the European Quality of Life (EuroQol) instrument, the 36-Item Short-Form Survey (SF-36), the World Health Organization's Quality

of Life (WHOQOL) instrument, and the Sickness Impact Profile (SIP).⁷ One of the most popular questionnaires for the overall OHRQoL assessment is the Oral Health Impact Profile (OHIP-49)⁸ and its shortened version – OHIP-14.⁹ It is based on Locker's model, which assumes a hierarchical impact of the effects of the disease and a sequential association with 7 dimensions of QoL. This questionnaire assesses the patient's perception of the impact of oral health on the social aspect of their wellbeing.⁸ In the shortened version of OHIP, 14 questions are divided into 7 subdomains: functional limitation, physical pain, psychological discomfort, physical disability, psychological disability, social disability, and handicap.⁹ The answers are structured on the basis of a 5-point Likert scale, indicating how often the oral cavity problems described in the questions have occurred (from 0 – never to 4 – very often). The score is the total of the answers to all questions, ranging from 0 to 56; the higher the score, the more negative the perception of the impact of oral health on the patient's QoL. The OHIP-14 questionnaire has been validated and translated into many languages, allowing its scores to be compared between specific populations. The Oral Health Impact Profile makes it possible to relate the scores to the clinical parameters of an oral health examination or sociodemographic factors. Based on the original OHIP questionnaire, attempts have been made to create specialized questionnaires on specific conditions that affect oral health, including OHIP-Esthetics, OHIP-EDENT (for edentulous patients), OHIP-TMDs (for patients with temporomandibular disorders), OHIP-PD (for patients with the periodontal disease),¹⁰ and OHIP-CP (for patients with chronic periodontitis).¹¹ The last 2 questionnaires are designed for people with periodontitis, and the questions included in them concern the most common symptoms and their impact on the patient's wellbeing.

The aim of the study was to conduct a literature review on the impact periodontitis has on the most frequently used OHRQoL assessment indicator, which is the shortened OHIP-14. The review includes the best studies that assessed the impact of periodontitis along with its severity and extent on the scores of this profile as well as the relationship between the subdomains of this indicator and the diagnosis of periodontitis. The combined effect of these studies was assessed in a meta-analysis.

Methods

The following databases were thoroughly surveyed for articles published through May 1, 2020: MEDLINE; Scopus; Google Scholar; and the Polish Medical Bibliography (PBL). Bibliographic lists were searched after the following terms had been entered: 'periodontitis', 'periodontal disease', 'quality of life', 'oral-health-related quality of life', and 'oral health impact profile', which corresponds to the Medical Subject Headings (MeSH) key word database.

The initial identification included the titles and abstracts of articles on the impact of periodontitis on QoL. This resulted in 1,346 titles. Selection was then made by rejecting the titles of articles not related to the literature review. Subsequently, the number of titles was reduced by selecting original observational studies published in English, German, Russian, or Polish. Further selection required both reviewers (BPC and TK) to read the full text of a given article and take into account the following criteria:

- the use of the shortened OHIP-14 version in a national language;
- the application of the definition of periodontitis based on the measurements of pocket depth (PD) and clinical attachment loss (CAL) or bone loss (BL) in radiographs;
- a control group, defined as individuals with a clinically healthy periodontium or with gingivitis, not with periodontitis;
- a full periodontal examination of all teeth with at least 4 measurement points;
- observations among adults aged 18–70 years;
- a cross-sectional or case–control study including confounding variables;
- the estimation of the strength of the relationship between periodontitis and OHIP-14 with the mean difference (*MD*), relative risk (*RR*) or odds ratio (*OR*); alternatively, available data to calculate one of these measures; and
- for studies from the same country, the later one was taken into account, with a preference for data from a national survey.

The following information was gathered about the studies eligible for the final analysis: the authors; the country and year of publication; the number and age of the participants; the definition of periodontitis; the estimation of the link along with the confounding variables taken into consideration; a significant demonstration of the relationship between the OHIP-14 subdomains and periodontitis; and the authors' final conclusions.

To determine the combined effect of studies reporting on the impact of periodontitis on the assessed Quality of Life Index (QLI), a model with a variable effect was chosen (the DerSimonian and Lard method). For the combined studies, the total *RR* or raw mean difference (*RMD*) was determined along with the corresponding confidence interval (*CI*). A significance level of $p < 0.05$ was adopted. The heterogeneity of the selected studies was assessed using the *Q* test and I^2 statistics, assuming a significance level of $p < 0.05$. The cumulative impact of the severity of periodontitis (mild, moderate or severe) on the OHIP-14 values was analyzed as well. The publication bias was assessed with Egger's test (with a significance level of $p < 0.05$) and by creating a funnel plot. All analyses were carried out using the analysis kit of Statistica, v. 13.1 (StatSoft, Kraków, Poland).

Results

There were 53 original observational studies with the assessment of the OHIP-14 index in individuals with the periodontal disease (Fig. 1). They were conducted from 2006 to 2020 in the following countries: Brazil ($n = 11$; Haye Biazevic et al.,¹² da Silva Araújo et al.,¹³ Cohen-Carneiro et al.,¹⁴ Bandéca et al.,¹⁵ de Freitas Borges et al.,¹⁶ Palma et al.,¹⁷ Batista et al.,¹⁸ Meusel et al.,¹⁹ de Vasconcelos Maia et al.,²⁰ Llanos et al.,²¹ and de Santana Passos-Soares et al.²²); India ($n = 5$; Acharya,²³ Fotedar et al.,²⁴ Sanadhya et al.,²⁵ Grover et al.,²⁶ and Yadav et al.²⁷); the UK ($n = 5$; Jowett et al.,²⁸ Bernabé and Marcenés,²⁹ White et al.,³⁰ Masood et al.,³¹ and Fuller et al.³²); Turkey ($n = 4$; Eltas et al.,³³ Balci et al.,³⁴ Ustaoglu et al.,³⁵ and Beşiroğlu and Lütfoğlu³⁶); China ($n = 1$; He et al.³⁷); Hong Kong ($n = 1$; Ng and Leung³⁸); New Zealand ($n = 1$; Lawrence et al.³⁹); Australia ($n = 2$; Mariño et al.⁴⁰ and Slade and Sanders⁴¹); Sweden ($n = 2$; Jansson et al.⁴² and Kato et al.⁴³); Germany ($n = 2$; Brauchle et al.⁴⁴ and Sonnenschein et al.⁴⁵); Norway ($n = 1$; Holde et al.⁴⁶); Spain ($n = 2$; Montero-Martín et al.⁴⁷ and Montero et al.⁴⁸); Belgium ($n = 1$; Carvalho et al.⁴⁹); the USA ($n = 2$; Cunha-Cruz et al.⁵⁰ and Wright et al.⁵¹); Mexico ($n = 1$; Rodríguez Franco and de la Rubia⁵²); Israel ($n = 1$; Levin et al.⁵³); Jordan ($n = 1$; Al Habashneh et al.⁵⁴); Sudan ($n = 1$; Khalifa et al.⁵⁵); Nigeria ($n = 1$; Lawal et al.⁵⁶); Jamaica, the Dominican Republic and Puerto Rico ($n = 1$; Collins et al.⁵⁷); Malaysia ($n = 1$; Sulaiman et al.⁵⁸); Nepal ($n = 1$; Goel and Baral⁵⁹); Sri Lanka ($n = 1$; Wellapuli and Ekanayake⁶⁰); Taiwan ($n = 1$; Wang et al.⁶¹); Poland ($n = 1$; Wąsacz et al.⁶²); Romania ($n = 1$; Grigoras et al.⁶³); and

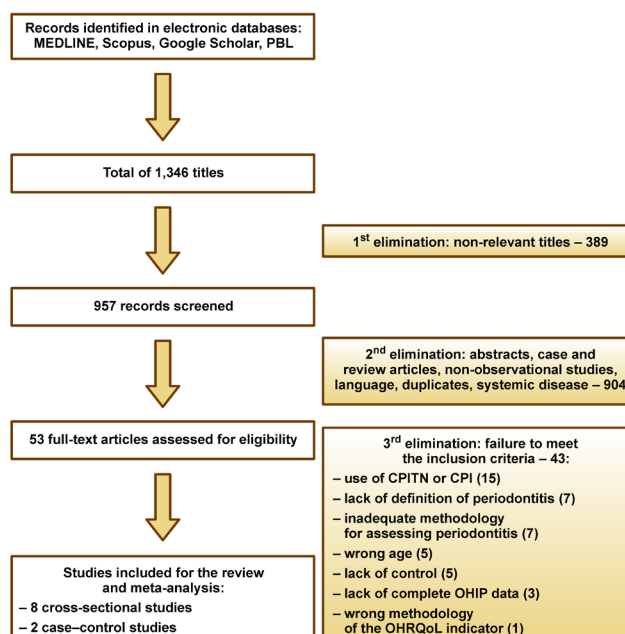


Fig. 1. Flow chart of the study selection process for the systematic review
PBL – Polish Medical Bibliography; CPITN – Community Periodontal Index of Treatment Needs; CPI – Community Periodontal Index; OHIP – Oral Health Impact Profile; OHRQoL – oral health-related quality of life.

Russia ($n = 1$; Drachev et al.⁶⁴). Forty-three studies did not meet the inclusion criteria and were not part of the review and meta-analysis. The reasons for eliminating these studies were as follows: the use of the Community Periodontal Index of Treatment Needs (CPITN) or the Community Periodontal Index (CPI) to assess the clinical condition of periodontitis ($n = 15$)^{13–15,18,20,24,25,28,31,33,44,47,48,55,56}, no adopted definition of periodontitis ($n = 7$)^{21,26,34,45,57,62,63}, the use of an outdated definition of periodontitis from 1999 or before ($n = 7$)^{16,17,23,38,40,51,52}, the assessment of individuals who were too old or too young ($n = 5$)^{12,30,43,49,64}, no control group ($n = 5$)^{19,27,58,60,61}, a lack of complete OHIP data ($n = 3$)^{36,46,59}, and an inadequate methodology of the OHRQoL indicator.⁵⁰

Ten studies (8 cross-sectional and 2 case-control; 8 local and 2 national) were eligible for the review and meta-analysis (Table 1).^{22,29,32,35,37,39,41,42,53,54} All of them showed a significant impact of the diagnosis of periodontitis (defined by the measurements of PD and CAL) on the deterioration of OHIP-14. In addition, the studies indicated that the association between the prevalence of periodontitis and OHRQoL was directly modified by the stage and extent of periodontal tissue damage^{32,37,54} relative to the number of preserved teeth.⁴² The quality of the selected articles is evidenced by the number of variables taken into account, related to both periodontitis and OHRQoL, which distorted these observations. The most frequently assessed confounding factors were age ($n = 8$), gender ($n = 8$), the markers of the socioeconomic status ($n = 7$), nicotine use ($n = 6$), and the number of teeth ($n = 6$). Eight observations recorded the effect of periodontitis on the OHIP-14 subdomains.^{22,32,35,37,39,42,53,54} Seven of them showed a significant impact on psychological and physical disability, 6 of them showed an impact on psychological discomfort, social disability and handicap, and 5 on functional limitation and physical pain.

In 5 of the studies eligible for the meta-analysis, in which the relationship between periodontitis and OHIP-14 was expressed with the adjusted odds ratio (*aOR*), a statistically significant relationship was shown, although not a very strong one.^{22,29,32,37,39} The strongest correlation was in the Chinese report – *aOR* for severe periodontitis was 1.63 with 95% *CI* ranging from 1.41 to 1.98.³⁷ The relatively weakest correlation, although also statistically significant, was found in the New Zealand study, in which *OR*, adjusted by only 3 confounding variables, was 1.49 with a fairly wide 95% *CI*: 1.01–2.19.³⁹ In our own meta-analysis of these 5 studies, involving a total of 1,869 individuals with periodontitis and 2,805 individuals in the control group from 4 countries (New Zealand, the UK, Brazil, and China), the relationship between the prevalence of periodontitis and an increase in the OHIP-14 index had a cumulative *OR* of 1.33 (95% *CI*: 1.25–1.43); $p < 0.001$ (Fig. 2). The analysis of heterogeneity of these 5 studies did not confirm this relationship ($Q = 3.66$; $p = 0.45$; $I^2 = 0\%$; 95% *CI*: 0–78.6).

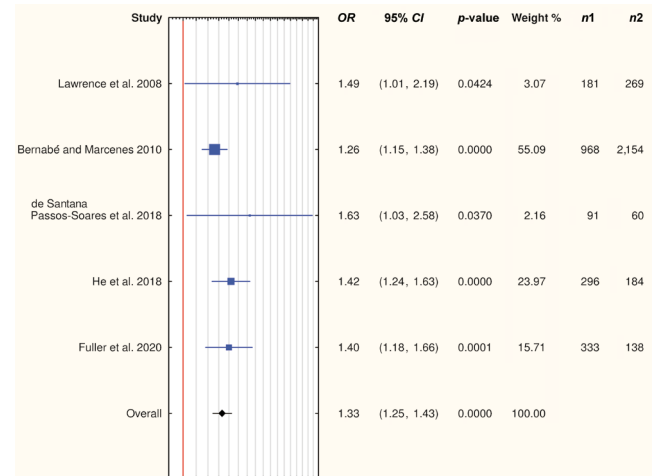


Fig. 2. Forest plot of the adjusted odds ratio (*aOR*) of the Oral Health Impact Profile-14 (OHIP-14) in periodontitis

$n1$ – size of the periodontitis group; $n2$ – size of the control group.

In the case of 7 studies eligible for the meta-analysis in which the difference between the periodontitis group and the control group was assessed through a difference in the mean values of the OHIP-14 index, in each study, the mean OHIP-14 value was significantly higher with exposure to periodontitis.^{22,32,35,41,42,53,54} These differences were quite diverse, ranging from 9.7 points for severe periodontitis in a recent English study³² to only 2.8 points in an Australian study.⁴¹ The meta-analysis of these 7 studies, including a total of 1,981 individuals with periodontitis and 3,472 individuals in the control group from 7 countries (Australia, Jordan, Sweden, Brazil, Israel, Turkey, and the UK) showed a moderately significant deterioration of the OHIP-14 index by 4.2 points (95% *CI*: 3.10–5.31); $p < 0.0001$ (Fig. 3). The results were heterogeneous ($Q = 36.95$; $p < 0.001$; $I^2 = 83.76\%$; 95% *CI*: 68.1–91.7).

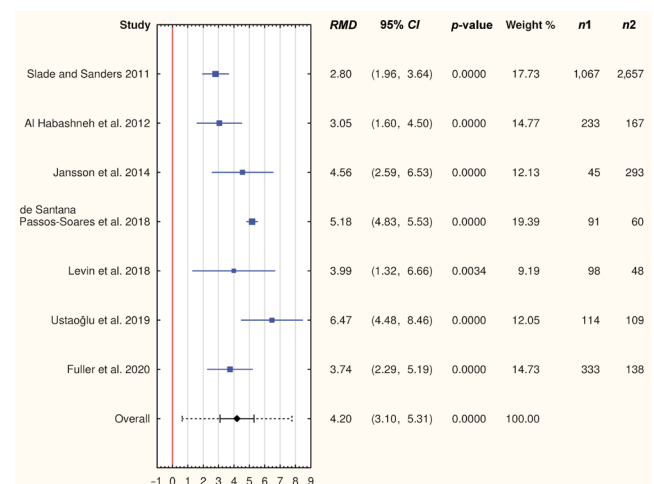


Fig. 3. Forest plot of the raw mean difference (*RMD*) in the Oral Health Impact Profile-14 (OHIP-14) in periodontitis

RMD – raw mean difference.

Table 1. Characteristics of the selected studies

Author, year, country	Number (age [years]) of the participants	Definition of periodontitis	Confounding variables assessed	Effect of periodontitis on OHIP-14	Subdomains relevant for periodontitis	Main conclusion
Lawrence et al. ³⁹ 2008, New Zealand cross-sectional, local study	PG – 181 (32) C (no P) – 269 (32)	1 site with PD ≥ 4 mm and 2 sites with CAL ≥ 4 mm	– age – gender – socioeconomic status	PG – OR: 1.49 (95% CI: 1.01–2.19) <i>p</i> = 0.0424	– physical pain – psychological discomfort – physical disability	a significant impact of periodontitis on the deterioration of OHRQoL
Bernabé and Marcenes ²⁹ 2010, the UK cross-sectional, national study	PG – 968 C (no P) – 2,154 average age for the whole group – 41.2 years	1 interdental site with PD ≥ 4 mm and 2 interdental sites with CAL ≥ 4 mm	– age – gender – number of teeth – education – income – place of residence	PG – RR: 1.26 (95% CI: 1.15–1.38) <i>p</i> < 0.001	NR	a significant impact of periodontitis on the deterioration of OHRQoL
Slade and Sanders ⁴¹ 2011, Australia cross-sectional, national study	PG – 1,067 (54.6) C (no P) – 2,657 (39.4)	2 sites with PD ≥ 5 mm or 2 sites with CAL ≥ 4 mm	– number of teeth	average OHIP-14 score: 9.5 ± 13.1 vs 6.7 ± 11.3 <i>p</i> < 0.001	NR	a significant impact of moderate and severe periodontitis on the deterioration of OHRQoL
Al Habashneh et al. ⁵⁴ 2012, Jordan cross-sectional, local study	PG – 233 (18–60) C (G) – 167 (18–60)	4 teeth with 1 site with PD ≥ 4 mm and CAL ≥ 3 mm	– age – gender – number of teeth – education – income – general diseases – nicotine	sP: 15.57 ± 7.5 vs 9.50 ± 7.1 <i>p</i> < 0.001 mP: 12.55 ± 7.4 vs 9.50 ± 7.1 <i>p</i> < 0.050 mP: NS	– physical pain – physical disability – psychological disability – social disability – handicap	a significant impact of periodontitis on the deterioration of OHRQoL; the more severe periodontitis, the greater the impact
Jansson et al. ⁴² 2014, Sweden cross-sectional, local study	IP – 83 (59.9) gP – 45 (64.4) C (no P) – 293 (42.5)	PD ≥ 4 mm and BL ≥ 33% of the root length; IP < 30% of the teeth with BL ≥ 33% of the root length, gP ≥ 30% of the teeth with BL ≥ 33% of the root length	– age – gender – number of teeth – education – nicotine	average OHIP-14 score: gP: 8.47 ± 10.4 vs 3.91 ± 5.4 <i>p</i> < 0.001 IP vs C: NS	– functional limitation – psychological discomfort – physical disability – psychological disability – social disability – handicap	a significant impact of severe and generalized periodontitis on the deterioration of OHRQoL
de Santana Passos- Soares et al. ²² 2018, Brazil cross-sectional, local study	PG – 91 (NA) C (no P) – 60 (NA)	4 teeth with at least 1 site with PD ≥ 4 mm and CAL ≥ 3 mm	– age – gender – education – nicotine	average OHIP-14 score: 13.15 ± 1.1 vs 7.97 ± 1.0 <i>p</i> < 0.010 PG – OR: 1.63 (95% CI: 1.03–2.58) <i>p</i> = 0.0370	– psychological discomfort – psychological disability	a significant impact of the co-occurrence of periodontitis and caries on the deterioration of OHRQoL
Levin et al. ⁵³ 2018, Israel case–control, local study	PG – 98 (38.8) C (no P) – 48 (37.7)	PD ≥ 4 mm and BL ≥ 3 mm	– age – gender – nicotine	average OHIP-14 score: 10.65 ± 8.5 vs 6.66 ± 5.8 <i>p</i> = 0.004	– functional limitation – physical disability – psychological disability – social disability – handicap	a significant impact of periodontitis on the deterioration of OHRQoL
He et al. ³⁷ 2018, China cross-sectional, local study	PG – 296 (35–74) C (no P) – 184 (35–74)	at least 2 interdental sites with PD ≥ 4 mm and CAL ≥ 3 mm or 1 site with PD ≥ 5 mm; def. acc. CDC/AAP	– age – gender – number of teeth – education – income – place of birth – nicotine	sP – OR: 1.63 (95% CI: 1.41–1.98) <i>p</i> < 0.010 mP – OR: 1.42 (95% CI: 1.24–1.63) <i>p</i> < 0.010 mP: NS	– functional limitation – physical pain – psychological discomfort – physical disability – psychological disability – social disability – handicap	a significant impact of periodontitis on the deterioration of OHRQoL; the more severe periodontitis, the greater the impact
Ustaoglu et al. ³⁵ 2019, Turkey cross-sectional, local study	PG – 114 (39.2) C (G) – 109 (23.7)	4 teeth in the mandible and maxilla with at least 1 site with PD ≥ 5 mm and CAL ≥ 4 mm	– general diseases	average OHIP-14 score: 13.53 ± 9.4 vs 7.06 ± 5.0 <i>p</i> < 0.001	– functional limitation – physical pain – psychological discomfort – physical disability – psychological disability – social disability – handicap	a significant impact of generalized periodontitis on the deterioration of OHRQoL
Fuller et al. ³² 2020, the UK case–control, local study	PG – 333 (25–50) C (no P) – 138 (24–64)	at least 1 site with PD ≥ 5 mm and CAL > 0 mm	– age – gender – race – number of teeth – socioeconomic status – BMI – general diseases – nicotine	average OHIP-14 score: sP: 14.89 ± 10.8 vs 5.20 ± 6.6 <i>p</i> < 0.001 mP: 8.94 ± 7.6 vs 5.20 ± 6.6 <i>p</i> < 0.05 PG – OR: 1.40 (95% CI: 1.18–1.66) <i>p</i> < 0.001	– functional limitation – physical pain – psychological discomfort – physical disability – psychological disability – social disability – handicap	a significant impact of periodontitis (classification from 1999 and 2007) on the deterioration of OHRQoL; the more severe periodontitis, the greater the impact

PG – periodontitis group; C – control; P – periodontitis; G – gingivitis; IP – localized periodontitis; gP – generalized periodontitis; NA – not available; PD – pocket depth; CAL – clinical attachment loss; BL – bone loss; CDC/AAP – the Centers for Disease Control/American Academy of Periodontology; BMI – body mass index; CI – confidence interval; RR – relative risk; sP – severe periodontitis; mP – moderate periodontitis; mP – mild periodontitis; NS – nonsignificant; OR – odds ratio; NR – not reported.

The meta-analysis of 3 studies in which the impact of the severity of periodontitis on the probability of OHIP-14 deterioration was assessed was also carried out (Fig. 4).^{32,37,54} Mild periodontitis did not change the likelihood of OHRQoL deterioration, while moderate periodontitis significantly increased this probability by 64% (95% CI: 1.12–2.40); $p = 0.012$, and severe periodontitis increased the probability by approx. 3.5 times (95% CI: 1.32–9.73); $p = 0.012$. The higher OR values in this meta-analysis in relation to the one shown in Fig. 2 result from combining the unadjusted and converted measures of MD for 2 observations.^{32,54}

The visual analysis of the funnel plot (Fig. 5), the noticeable symmetry of the distribution of the 7 points representing the results of the meta-analysis shown in the forest plot in Fig. 3 and the insignificance of Egger's test ($b_0: -1.6$; 95% CI: $-5.28-2.08$; $p = 0.31$) indicate an insignificant publication bias. Out of the 7 studies analyzed with the funnel plot, 3 of them are outside 95% CI, which indicates a large variety of these results.

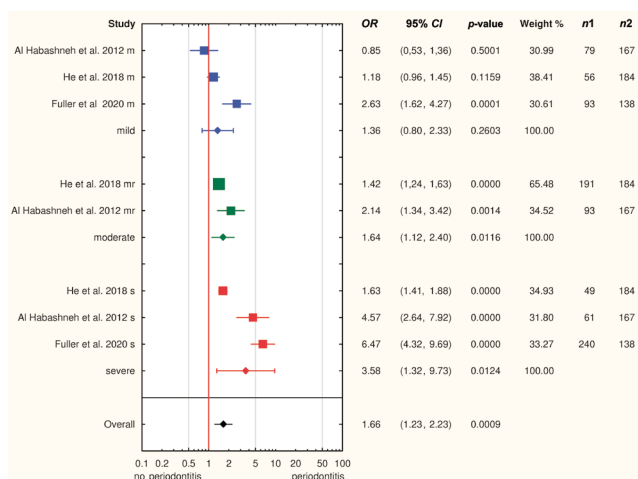


Fig. 4. Forest plot of the odds ratio (OR) of the Oral Health Impact Profile-14 (OHIP-14) in mild, moderate or severe periodontitis

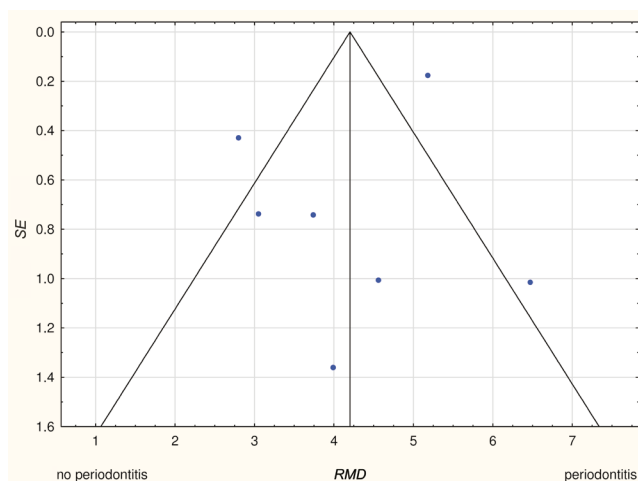


Fig. 5. Funnel plot with pseudo 95% confidence intervals (CIs)
SE – standard error.

Discussion

For the review and meta-analysis of studies on the link between periodontitis and QoL assessed with the most commonly used OHIP-14 index, articles of the best possible methodological quality were selected. The quality assessment of the 2 included case-control studies^{32,53} according to the Newcastle-Ottawa Scale (NOS)⁶⁵ indicated an average quality (7 stars). An important inclusion criterion was the definition of periodontitis using the measurements of PD and CAL, which is consistent with the current views on the assessment of the periodontal status for epidemiological and clinical purposes. Studies that considered the impact of confounding variables by applying multiple or logistic regression were also included. The introduction of a range limit for age in which periodontitis is one of the most common oral diseases, while minimizing the impact of tooth loss, was of great importance as well.

In all of these studies, a significant deterioration of OHRQoL under the influence of periodontitis was found, and this impact increased with the severity and extent of periodontopathy. This was reflected in the meta-analysis – periodontitis increased the probability of OHRQoL deterioration by 33%, and a significant impact of moderate and severe periodontitis was 64% and 358%, respectively. No reference was found in the available literature for our own meta-analysis. The unambiguity of these findings is distorted only by the heterogeneity of studies in which the correlation measure was expressed with MD (Fig. 3). This was probably due to the type of research conducted as well as to subjective differences in emotional patterns for experiencing discomfort, disability and pain among populations from different continents (East and West Asia, Oceania, Europe, and South America). Three systematic literature reviews (SLRs) on the impact of periodontitis on OHRQoL are not as unambiguous as our review.^{66–68} In the first one, Al-Harathi et al. indicated that 3 out of 4 studies showed a significant relationship between periodontitis and OHIP-14.⁶⁶ This was not confirmed in the Australian study by Marinõ et al.⁴⁰ In another review, Buset et al. selected 15 studies on this relationship and its significance was confirmed in 12 of them.⁶⁷ No such relationship was found by Marinõ et al.,⁴⁰ Montero-Martín et al.⁴⁷ or Bandéca et al.¹⁵ In the latest available SLR on the impact of periodontitis on OHIP-14, a significant relationship was found in 18 out of 22 of the selected observational studies.⁶⁸ This was not confirmed in the study by Bandéca et al.,¹⁵ another Brazilian study by Batista et al.,¹⁸ an Indian study by Sanadhya et al.,²⁵ or the study in our own review, regarding the observations among homeless people in Hong Kong (the study was excluded on the 3rd stage of selection).⁶⁹ All of those observations, in which this significant relationship was not found, combined 2 methodological characteristics – the assessment of the condition of the

periodontium and a definition of the periodontal disease based on CPI as well as a partial protocol for oral health testing. It seems that an incorrect determination of the rate of prevalence for periodontitis and a lack of the assessment of the periodontal status for all teeth may interfere with observations regarding the impact of periodontitis on OHRQoL.

The impact of periodontitis on the deterioration of OHRQoL is quite clearly explained by the influence of clinical symptoms such as gingival redness and swelling, bleeding while brushing the teeth, gingival recessions, often associated with the excessive sensitivity of the exposed dentin, tooth mobility, pathological tooth migration (PTM), or recurrent halitosis on the dysfunctions of the stomatognathic system, red complex esthetics and self-assessment. These symptoms should be associated only with the periodontal disease; thus, in observational studies, they should be controlled for by taking into account many local factors that may distort them, e.g., caries, mouth and facial pain, an increased tooth sensitivity, or the loss of tooth functionality (less than 10 interdental contact points) and severe tooth loss (less than 10 teeth).


In the last 3 studies included in the final part of our literature review,^{32,35,37} a significant relationship was confirmed between all subdomains of the OHIP-14 index and periodontitis. The consideration of earlier studies indicated psychological limitation (embarrassment, difficulty in being relaxed) and physical limitation (difficulty in toothbrushing and eating) as subdomains most frequently associated with periodontitis. In turn, pain, discomfort and functional limitation were indicated relatively rarely. The predominance of the impact of periodontitis on the psychological and social subdomains of OHRQoL was also noted by Buset et al. in their literature review.⁶⁷ This indicates the predominance of problems experienced by periodontal patients which very often go unnoticed during treatment, which is usually provided only to inhibit functional limitation, eliminate pain and improve an esthetic effect. However, in the patients' perception, the most important problems that periodontitis may cause are psychological discomfort, embarrassment, stress, problems in interpersonal relations, and even difficulties in everyday activities. This shows the need for even greater holistic planning as regards periodontal therapy goals. Lawrence et al. found that the severity of periodontitis led to an increase in the values of only some subdomains, not to an increase in all subdomains that showed incorrect values.³⁹ This may indicate that the progression of periodontitis affects the quality of particular OHRQoL subdomains and does not affect them all. He et al., on the other hand, showed that with an increase in the severity of periodontitis, there is a significant increase in the highest-scoring answers to the questions in all subdomains.³⁷ These differences may be caused by national, racial or socioeconomic discrepancies.


The literature review and the resulting meta-analysis have a number of limitations. Firstly, there is a risk of selection bias. Only in 5 of the selected studies was randomized sampling performed.^{29,37,41,42,54} A lack of the random selection of individuals for an epidemiological inquiry runs the risk of it being unrepresentative of the general or local population. This particularly concerns surveying individuals in academic centers. Secondly, not all confounding variables can be controlled for. In 4 studies, only 1–3 confounding variables were taken into account.^{35,39,41,53} Many of these studies show that general diseases associated with periodontitis and OHRQoL, such as diabetes, metabolic syndrome, osteoporosis, and local clinical conditions, e.g., caries, odontogenic pain and discomfort associated with prosthetic restorations, are not controlled for. Thirdly, the nature of an observational study in the form of a cross-sectional or case–control study does not unequivocally establish that exposure to periodontitis results in a reduced sense of QoL, since OHRQoL before periodontopathy is unknown. In addition, cross-sectional studies are highly exposed to the risk of selection bias. Fourthly, there is a possibility of observer bias. This is often the case when there is no process of calibrating examiners, or assessing inter- or intra-examiner reproducibility, especially in the clinical assessment of CAL. In the studies included in our review, such a procedure was performed only in 5 of them.^{22,29,35,37,54} The possibility of making a diagnostic error can come from adopting different definitions of periodontitis based on PD and CAL measurements. Currently, the definition of periodontitis by Eke et al.,⁷⁰ subsequently adopted by the Centers for Disease Control/American Academy of Periodontology (CDC/AAP), is considered to be the gold standard for epidemiological periodontal research. This literal definition was used only in the study by He et al.³⁷ Finally, there are limitations due to the use of the OHIP-14 index and varying methodologies for a subjective psychometric test. The questions contained in this questionnaire do not relate directly to the condition of the periodontium, which may lead to incorrect answers, especially when the questionnaire is self-administered. To reduce memory bias, one should limit the timeframe of the events being asked about. The best solution is to appoint a second examiner for a psychometric test who is blinded to the clinical condition of the periodontium, or to conduct such tests before the clinical examination. In the vast majority of studies eligible for this review, the psychometric test process was not described in sufficient detail.

This literature review and innovative meta-analysis provides further evidence on the relationship between periodontitis and OHRQoL, with a strong influence of the severity and extent of periodontopathy of a dose-effect type. The impact of periodontitis on the psychological and social aspects of the patient's perception of the disease has been shown, which should be taken into account for treatment purposes. Recommendations for further studies on

the relationship between periodontitis and OHRQoL indicators include conducting more high-quality European (including Polish) studies in this area, using QoL indicators profiled for periodontitis, using a comprehensive protocol for oral health testing as well as defining the prevalence rate, severity and extent of periodontitis according to CDC/AAP, controlling for the widest possible spectrum of local and general confounding factors, and conducting randomized, controlled studies on the impact of non-surgical and/or surgical treatment on OHRQoL indicators.

ORCID iDs

Barbara Paśnik-Chwalik  <https://orcid.org/0000-0002-2279-7458>

Tomasz Konopka  <https://orcid.org/0000-0002-8808-2893>

References

- Meyle J, Chapple I. Molecular aspects of the pathogenesis of periodontitis. *Periodontol 2000*. 2015;69(1):7–17.
- Genco RJ, Borgnakke WS. Risk factors for periodontal disease. *Periodontol 2000*. 2013;62(1):59–94.
- Needleman I, McGrath C, Floyd P, Biddle A. Impact of oral health on the life quality of periodontal patients. *J Clin Periodontol*. 2004;31(6):454–457.
- Hescot P. The new definition of oral health and relationship between oral health and quality of life. *Chin J Dent Res*. 2017;20(4):189–192.
- Glick M, Williams DM, Kleinman DV, Vujicic M, Watt RG, Weyant RJ. A new definition for oral health developed by the FDI World Dental Federation opens the door to a universal definition of oral health. *J Am Dent Assoc*. 2016;147(12):915–917.
- Sischo L, Broder HL. Oral health-related quality of life: What, why, how, and future implications. *J Dent Res*. 2011;90(11):1264–1270.
- Haag DG, Peres KG, Balasubramanian M, Brennan DS. Oral conditions and health-related quality of life: A systematic review. *J Dent Res*. 2017;96(8):864–874.
- Slade GD, Spencer AJ. Development and evaluation of the Oral Health Impact Profile. *Community Dent Health*. 1994;11(1):3–11.
- Slade GD. Derivation and validation of a short-form Oral Health Impact Profile. *Community Dent Oral Epidemiol*. 1997;25(4):284–290.
- Rodríguez NI, Moral J. Adaptation and content validity by expert judgment of the Oral Health Impact Profile applied to Periodontal Disease. *J Oral Res*. 2017;6(4):92–96.
- He S, Wang J, Wei S, Ji P. Development and validation of a condition-specific measure for chronic periodontitis: Oral Health Impact Profile for Chronic Periodontitis. *J Clin Periodontol*. 2017;44(6):591–600.
- Haye Biazevic MG, Rissotto RR, Michel-Crosato E, Amorim Mendes LA, Amorim Mendes MO. Relationship between oral health and its impact on quality of life among adolescents. *Braz Oral Res*. 2008;22(1):36–42.
- da Silva Araújo AC, Gusmão ES, Mazza Batista JE, Cimeiros R. Impact of periodontal disease on quality of life. *Quintessence Int*. 2010;41(6):e111–e118.
- Cohen-Carneiro F, Bessa Rebelo MA, Souza-Santos R, Bovi Ambrosano GM, Salino AV, Pontes DG. Psychometric properties of the OHIP-14 and prevalence and severity of oral health impacts in a rural riverine population in Amazonas State, Brazil. *Cad Saude Publica*. 2010;26(6):1122–1130.
- Bandéca MC, Nadalin MR, Calixto LR, Saad JRC, da Silva SRC. Correlation between oral health perception and clinical factors in a Brazilian community. *Community Dent Health*. 2011;28(1):64–68.
- de Freitas Borges T, Regalo SC, Taba M Jr, Siéssere S, Mestriner W Jr, Semprini M. Changes in masticatory performance and quality of life in individuals with chronic periodontitis. *J Periodontol*. 2013;84(3):325–331.
- Palma PV, Caetano PL, Gonçalves Leite IC. Impact of periodontal diseases on health-related quality of life of users of the Brazilian Unified Health System. *Int J Dent*. 2013;2013:150357.
- Batista MJ, Rihs Perianes LB, Hilgert JB, Hugo FN, de Sousa MdLR. The impacts of oral health on quality of life in working adults. *Braz Oral Res*. 2014;28(1):1–6.
- Meusel DRDZ, Ramacciato JC, Motta RHL, Brito RB Jr, Flório FM. Impact of the severity of chronic periodontal disease on quality of life. *J Oral Sci*. 2015;57(2):87–94.
- de Vasconcellos Maia C, Mendes FM, Normando D. The impact of oral health on quality of life of urban and riverine populations of the Amazon: A multilevel analysis. *PLoS One*. 2018;13(11):e0208096.
- Llanos AH, Benítez Silva CG, Ichimura KT, et al. Impact of aggressive periodontitis and chronic periodontitis on oral health-related quality of life. *Braz Oral Res*. 2018;32:e006.
- de Santana Passos-Soares J, de Souza Santos LP, da Cruz SS, et al. The impact of caries in combination with periodontitis on oral health-related quality of life in Bahia, Brazil. *J Periodontol*. 2018;89(12):1407–1417.
- Acharya S. Oral health-related quality of life and its associated factors in an Indian adult population. *Oral Health Prev Dent*. 2008;6(3):175–184.
- Fotedar S, Sharma KR, Fotedar V, Bhardwaj V, Chauhan A, Manchanda K. Relationship between oral health status and oral health related quality of life in adults attending H.P. Government Dental College, Shimla, Himachal Pradesh – India. *Oral Health Dent Manag*. 2014;13(3):661–665.
- Sanadhya S, Aapaliya P, Jain S, Sharma N, Choudhary G, Dobaria N. Assessment and comparison of clinical dental status and its impact on oral health-related quality of life among rural and urban adults of Udaipur, India: A cross-sectional study. *J Basic Clin Pharm*. 2015;6(2):50–58.
- Grover V, Malhotra R, Dhawan S, Kaur G, Kapoor A. Comparative assessment of oral health related quality-of-life between rural and urban chronic periodontitis patients. *Saudi J Oral Sci*. 2015;2(1):19–24.
- Yadav T, Chopra P, Kapoor S. Association between chronic periodontitis and oral health-related quality of life in Indian adults. *J Int Oral Health*. 2019;11(5):280–286.
- Jowett AK, Orr MTS, Rawlinson A, Robinson PG. Psychosocial impact of periodontal disease and its treatment with 24-h root surface debridement. *J Clin Periodontol*. 2009;36(5):413–418.
- Bernabé E, Marcenes W. Periodontal disease and quality of life in British adults. *J Clin Periodontol*. 2010;37(11):968–972.
- White DA, Tsakos G, Pitts NB, et al. Adult Dental Health Survey 2009: Common oral health conditions and their impact on the population. *Br Dent J*. 2012;213(11):567–572.
- Masood M, Younis LT, Masood Y, Bakri NN, Christian B. Relationship of periodontal disease and domains of oral health-related quality of life. *J Clin Periodontol*. 2019;46(2):170–180.
- Fuller J, Donos N, Suvan J, Tsakos G, Nibali L. Association of oral health-related quality of life measures with aggressive and chronic periodontitis. *J Periodontol Res*. 2020;55(4):574–580. doi: 10.1111/jre.12745
- Eltas A, Uslu MO, Eltas SD. Association of oral health-related quality of life with periodontal status and treatment needs. *Oral Health Prev Dent*. 2016;14(4):339–347.
- Balci N, Alkan N, Gurgan CA. Psychometric properties of a Turkish version of the Oral Health Impact Profile-14. *Niger J Clin Pract*. 2017;20(1):19–24.
- Ustaoglu G, Bulut DG, Gümüş KÇ, Ankarali H. Evaluation of the effects of different forms of periodontal diseases on quality of life with OHIP-14 and SF-36 questionnaires: A cross-sectional study. *Int J Dent Hyg*. 2019;17(4):343–349.
- Beşiroğlu E, Lütfoğlu M. Relations between periodontal status, oral health-related quality of life and perceived oral health and oral health consciousness levels in a Turkish population. *Int J Dent Hyg*. 2020;18(3):251–260. doi: 10.1111/idh.12443
- He S, Wei S, Wang J, Ji P. Chronic periodontitis and oral health-related quality of life in Chinese adults: A population-based, cross-sectional study. *J Periodontol*. 2018;89(3):275–284.
- Ng SKS, Leung WK. Oral health-related quality of life and periodontal status. *Community Dent Oral Epidemiol*. 2006;34(2):114–122.
- Lawrence HP, Thomson WM, Broadbent JM, Poulton R. Oral health-related quality of life in a birth cohort of 32-year olds. *Community Dent Oral Epidemiol*. 2008;36(4):305–316.

40. Mariño R, Schofield M, Wright C, Calache H, Minichiello V. Self-reported and clinically determined oral health status predictors for quality of life in dentate older migrant adults. *Community Oral Dent Epidemiol.* 2008;36(1):85–94.
41. Slade GD, Sanders AE. The paradox of better subjective oral health in older age. *J Dent Res.* 2011;90(11):1279–1285.
42. Jansson H, Wahlin Å, Johansson V, et al. Impact of periodontal disease experience on oral health-related quality of life. *J Periodontol.* 2014;85(3):438–445.
43. Kato T, Abrahamsson I, Wide U, Hakeberg M. Periodontal disease among older people and its impact on oral health-related quality of life. *Gerodontology.* 2018;35(4):382–390.
44. Brauchle F, Noack M, Reich E. Impact of periodontal disease and periodontal therapy on oral health-related quality of life. *Int Dent J.* 2013;63(6):306–311.
45. Sonnenschein SK, Betzler C, Kohnen R, Krisam J, Kim TS. Oral health-related quality of life in patients under supportive periodontal therapy. *Acta Odontol Scand.* 2018;76(8):572–579.
46. Holde GE, Baker SR, Jönsson B. Periodontitis and quality of life: What is the role of socioeconomic status, sense of coherence, dental service use and oral health practices? An exploratory theory-guided analysis on a Norwegian population. *J Clin Periodontol.* 2018;45(7):768–779.
47. Montero-Martín J, Bravo-Pérez M, Albaladejo-Martínez A, Hernández-Martín LA, Rosel-Gallardo EM. Validation the Oral Health Impact Profile (OHIP-14sp) for adults in Spain. *Med Oral Patol Oral Cir Bucal.* 2009;14(1):E44–E50.
48. Montero J, Albaladejo A, Zalba JI. Influence of the usual motivation for dental attendance on dental status and oral health-related quality of life. *Med Oral Patol Oral Cir Bucal.* 2014;19(3):e225–e231.
49. Carvalho JC, Mestrinho HD, Stevens S, van Wijk AJ. Do oral health conditions adversely impact young adults? *Caries Res.* 2015;49(3):266–274.
50. Cunha-Cruz J, Hujuel PP, Kressin NR. Oral health-related quality of life of periodontal patients. *J Periodontol Res.* 2007;42(2):169–176.
51. Wright CD, McNeil DW, Edwards CB, et al. Periodontal status and quality of life: Impact of fear of pain and dental fear. *Pain Res Manag.* 2017;2017:5491923.
52. Rodríguez Franco NI, de la Rubia JM. Oral Health Impact Profile scale applied to Periodontal Disease: Relationship with sociodemographic variables in general population and clinic samples from Monterrey, Mexico. *Open Dent J.* 2018;12:1152–1161.
53. Levin L, Zini A, Levine J, et al. Demographic profile, Oral Health Impact Profile and Dental Anxiety Scale in patients with chronic periodontitis: A case–control study. *Int Dent J.* 2018;68(4):269–278.
54. Al Habashneh R, Khader YS, Salameh S. Use of the Arabic version of Oral Health Impact Profile-14 to evaluate the impact of periodontal disease on oral health-related quality of life among Jordanian adults. *J Oral Sci.* 2012;54(1):113–120.
55. Khalifa N, Allen PF, Abu-bakr NH, Abdel-Rahman ME. Psychometric properties and performance of the Oral Health Impact Profile (OHIP-14s-ar) among Sudanese adults. *J Oral Sci.* 2013;55(2):123–132.
56. Lawal FB, Taiwo JO, Arowojolu MO. How valid are the psychometric properties of the Oral Health Impact Profile-14 measure in adult dental patients in Ibadan, Nigeria? *Ethiop J Health Sci.* 2014;24(3):235–242.
57. Collins JR, Elías AR, Brache M, et al. Association between gingival parameters and oral health-related quality of life in Caribbean adults: A population-based cross-sectional study. *BMC Oral Health.* 2019;19(1):234.
58. Sulaiman L, Saub R, Baharuddin NA, et al. Impact of severe chronic periodontitis on oral health-related quality of life. *Oral Health Prev Dent.* 2019;17(4):365–373.
59. Goel K, Baral D. A comparison of impact of chronic periodontal diseases and nonsurgical periodontal therapy on oral health-related quality of life. *Int J Dent.* 2017;2017:9352562.
60. Wellapuli N, Ekanayake L. Association between chronic periodontitis and oral health-related quality of life in Sri Lankan adults. *Int Dent J.* 2016;66(6):337–343.
61. Wang TF, Fang CH, Hsiao KJ, Chou C. Effect of a comprehensive plan for periodontal disease care on oral health-related quality of life in patients with periodontal disease in Taiwan. *Medicine (Baltimore).* 2018;97(5):e9749.
62. Wąsacz K, Pac A, Darczuk D, Chomyszyn-Gajewska M. Validation of a modified Oral Health Impact Profile scale (OHIP-14) in patients with oral mucosa lesions or periodontal disease. *Dent Med Probl.* 2019;56(3):231–237.
63. Grigoras S, Mărtu S, Balcos C. Quality of life regarding patients with periodontal disease in Iasi, Romania. *Procedia Soc Behav Sci.* 2014;127:15–20.
64. Drachev SN, Brenn T, Trovik TA. Oral health-related quality of life in young adults: A survey of Russian undergraduate students. *Int J Environ Res Public Health.* 2019;15(4):719.
65. Wells GA, Shea B, O’Connell D, et al. The Newcastle-Ottawa Scale (NOS) for assessing the quality of nonrandomised studies in meta-analyses. http://www.ohri.ca/programs/clinical_epidemiology/oxford.asp. Accessed May 20, 2020.
66. Al-Harathi LS, Cullinan MP, Leichter JW, Thomson WM. The impact of periodontitis on oral health-related quality of life: A review of the evidence from observational study. *Aust Dent J.* 2013;58(3):274–277; quiz 384.
67. Buset SL, Walter C, Friedmann A, Weiger R, Borgnakke WS, Zitzmann NU. Are periodontal diseases really silent? A systematic review of their effect on quality of life. *J Clin Periodontol.* 2016;43(3):333–344.
68. Ferreira MC, Dias-Pereira AC, Branco-de-Almeida LS, Martins CC, Paiva SM. Impact of periodontal disease on quality of life: A systematic review. *J Periodontol Res.* 2017;54(4):651–665.
69. Luo Y, McGrath C. Oral health and its impact on the life quality of homeless people in Hong Kong. *Community Dent Health.* 2008;25(2):137–142.
70. Eke PI, Dye BA, Wei L, et al. Prevalence of periodontitis in adults in the United States: 2009 and 2010. *J Dent Res.* 2012;91(10):914–920.

Relationship of the rs10850110 and rs11611277 polymorphisms of the *MYO1H* gene with non-syndromic mandibular prognathism in the Iranian population

Kazem Dalaie^{1,A,D,F}, Vahid Reza Yassaee^{2,A,C,E,F}, Mohammad Behnaz^{1,A,D}, Mohsen Yazdani^{3,A,D}, Farbod Jafari^{4,B,D}, Reza Morvaridi Farimani^{1,A,D}

¹ Dentofacial Deformities Research Center, Research Institute of Dental Sciences, Shahid Beheshti University of Medical Sciences, Tehran, Iran

² Genomic Research Center, Shahid Beheshti University of Medical Sciences, Tehran, Iran

³ Research Center for Prevention of Oral and Dental Diseases, Baqiyatallah University of Medical Sciences, Tehran, Iran

⁴ Department of Oral and Maxillofacial Surgery, School of Dentistry, Islamic Azad University, Tehran, Iran

A – research concept and design; B – collection and/or assembly of data; C – data analysis and interpretation;

D – writing the article; E – critical revision of the article; F – final approval of the article

Dental and Medical Problems, ISSN 1644-387X (print), ISSN 2300-9020 (online)

Dent Med Probl. 2020;57(4):433–440

Address for correspondence

Reza Morvaridi Farimani

E-mail: Morvaridi.reza@gmail.com

Funding sources

School of Dentistry, Shahid Beheshti University of Medical Sciences, Tehran, Iran.

Conflict of interest

None declared

Received on February 10, 2020

Reviewed on March 15, 2020

Accepted on May 4, 2020

Published online on December 31, 2020

Cite as

Dalaie K, Yassaee VR, Behnaz M, Yazdani M, Jafari F, Morvaridi Farimani R. Relationship of the rs10850110 and rs11611277 polymorphisms of the *MYO1H* gene with non-syndromic mandibular prognathism in the Iranian population. *Dent Med Probl.* 2020;57(4):433–440. doi:10.17219/dmp/122004

DOI

10.17219/dmp/122004

Copyright

© 2020 by Wrocław Medical University

This is an article distributed under the terms of the

Creative Commons Attribution 3.0 Unported License (CC BY 3.0)

(<https://creativecommons.org/licenses/by/3.0/>).

Abstract

Background. The myosin 1H (*MYO1H*) gene, located on chromosome 12, encodes the unconventional MYO1H protein, which is involved in the intracellular movement and morphology of chondrocytes, and plays a vital role in the prognathism or retrognathism of the mandible.

Objectives. The objective of this study was to assess the relationship between the polymorphisms of the *MYO1H* gene and mandibular prognathism in the Iranian population.

Material and methods. The current project evaluated 64 patients with mandibular prognathism requiring orthognathic surgery and 60 controls with skeletal class I occlusion. Genome amplification was performed using specific primer pairs to assess the rs10850110 and rs11611277 polymorphisms of the *MYO1H* gene through the polymerase chain reaction (PCR). The restriction fragment length polymorphism (RFLP) technique was used to detect single-nucleotide polymorphisms. The data was analyzed using the χ^2 test.

Results. The patient and control groups were not significantly different in terms of age or gender ($p > 0.05$). In all, 3.1% of patients and 6.7% of controls had the rs10850110 polymorphism ($p = 0.680$), and 1.6% of patients and 5% of controls had the rs11611277 polymorphism ($p = 0.602$).

Conclusions. No significant correlation was noted between the rs10850110 and rs11611277 polymorphisms of the *MYO1H* gene and mandibular prognathism in the Iranian population. However, the lower frequency of these polymorphisms in the patient group suggests a possible association with mandibular retrognathism, which needs to be investigated with a larger sample size.

Key words: polymorphism, class III malocclusion, *MYO1H* gene, single-nucleotide polymorphism, prognathism

Introduction

Several environmental and genetic factors are implicated in the development of malocclusion. Despite a high prevalence of craniofacial disorders,¹ the role of genetic factors in their occurrence is not well understood.

Skeletal class III malocclusion can be caused by mandibular prognathism, maxillary deficiency or the combination of both, and is among the most severe skeletal deformities in orthodontics.² Class III malocclusion can cause both functional and social disabilities.^{3–5} It is believed to be a polygenetic disorder, which occurs as the result of the interaction of genetic and environmental factors.⁶ Genes play a prominent role in mandibular prognathism.⁷ Evidence shows that the prevalence of mandibular prognathism is the highest in East Asia (15–23%), moderate in Africa (3–8%) and the lowest in the European ethnicity (0.48–4%).^{8,9} The prominent role of genes in the class III phenotype has been documented, and human studies have demonstrated an autosomal dominant genetic pattern in class III malocclusion.¹⁰ The myosin 1H (*MYO1H*) gene encodes a protein that plays a role in the cellular movement, phagocytosis and the vesicular transfer. This gene is composed of 107,121 base pairs and is located on human chromosome 12. It is also involved in the mandibular growth by producing cartilage at the condylar head and determining the morphology of chondrocytes.^{11,12} Moreover, the expression of this gene in the masseter muscle of patients with class II malocclusion is higher than its expression in the masseter muscle of class III patients.¹³

Tassopoulou-Fishell et al. were the first to report an association between mandibular prognathism and *MYO1H* (rs10850110) in a Hispanic group.¹⁴ This association was also confirmed by Cruz et al. and Burnheimer et al. in Brazilian and African American groups.^{15,16}

However, recent studies by Cunha et al. and Arun et al. could not find any significant association between rs10850110 and mandibular prognathism and retrognathism in Brazilian and Hispanic populations.^{17,18}

Since the original linkage result, which pointed to the *MYO1H* locus as associated with skeletal malocclusion, referred to a group of Hispanic families,¹⁴ the aim of this project was to evaluate this result in the Iranian population.

Material and methods

Subjects of both sexes between 16 and 30 years of age were included in this study. This case–control study evaluated skeletal class III malocclusion patients (41 females and 23 males) who were candidates for orthognathic surgery, and were selected from among those presenting to the university hospitals affiliated to the Shahid Beheshti University of Medical Sciences in Tehran, Iran,

and 5 orthodontic clinics. The control subjects (38 females and 22 males) were skeletal class I occlusion patients who were apparently healthy and had a socioeconomic status comparable to that of the patient group. Patients were recruited for this study from January 2015 to January 2017. This study was approved by the ethics committee of the Shahid Beheshti University of Medical Sciences (IR.SBMU.RIDS.REC.1396.49).

The inclusion criteria for the patient group were as follows: patients >16 years old whose growth and development had been terminated; and skeletal class III malocclusion patients with mandibular prognathism (SNB > 82°).

The exclusion criteria for the patient group were as follows: patients with other types of malocclusion, syndromic and metabolic conditions or endocrine disorders; patients with skeletal class III malocclusion due to maxillary retrognathism; and patients with dental class III malocclusion.

The inclusion criteria for the control group were the following: patients aged >16 years with class I occlusion or malocclusion and the orthognathic profile; patients without syndromic, congenital, systemic, or endocrine anomalies; ANB of 2–4°; and the Wits appraisal of 0–2 mm.

Subjects were selected using convenience sampling. The minimum sample size was calculated to be 60, assuming $\alpha = 0.05$ and a study power of 80%.

The demographic information about the patients and the controls was collected using a questionnaire. The patients and the controls were briefed about the study and written informed consent was obtained from them. Next, 5 mL of peripheral venous blood was obtained from the subjects and collected in tubes containing ethylenediaminetetraacetic acid (EDTA).

Extraction of genomic DNA

DNA was extracted from the peripheral blood samples using the salting-out technique.

Quantitative and qualitative assessment of the extracted DNA

After the extraction of DNA, its quality and quantity were evaluated using BioPhotometer® (Eppendorf AG, Hamburg, Germany). Table 1 presents the names and sequences of the specific primers used. Using primer pairs, the *MYO1H* gene was amplified with the polymerase chain reaction (PCR) program.

Assessment of the quality of the PCR products on 1.5% agarose gel

The PCR products along with the markers were electrophoresed to assess their quality, size and quantity. If the PCR products had favorable quality and the respective segment had been amplified, they were

Table 1. Sequences of the primers used for the amplification of the rs10850110 and rs11611277 polymorphisms

Primer name	Sequence	Length	Annealing	Extension	Product size [bp]
Sau96I	TCTTAACAGTGTCTTCTAATGAG	23	58°C	72°C	380
	GATTGTCTAAAGCCAGGAGTTG	22	30 s	40 s	
Hpy188I	TCCCAGGGTTTAGCATCTTG	20	60°C	72°C	386
	GAGTGGCGCCTCAGTATCTC	20	30 s	40 s	

subjected to sequencing. The PCR restriction fragment length polymorphism (RFLP) technique was then employed to detect the genotypes.

Statistical analysis

Eventually, a cephalometric analysis was performed to determine SNA, SNB, ANB, and the Wits appraisal in the patient and control groups.

The data was analyzed using IBM SPSS Statistics for Windows, v. 22.0 (IBM Corp., Armonk, USA) with the *t* test and the χ^2 test. The level of significance was set at $p < 0.05$.

Results

A total of 64 patients and 60 controls were evaluated. Table 2 presents the cephalometric findings as well as the sex and mean age of the subjects. According to the *t* test, the 2 groups were significantly different in terms of SNA, SNB, ANB, and Wits appraisal ($p < 0.001$). Table 3 presents

the frequency of different genotypes with respect to the 2 polymorphisms in the 2 groups. In all, 3.1% of patients and 6.7% of controls had the rs10850110 polymorphism ($p = 0.680$), and 1.6% of patients and 5% of controls had the rs11611277 polymorphism ($p = 0.602$). The χ^2 test revealed no significant differences in the frequency of the polymorphisms between the 2 groups. In other words, the 2 polymorphisms showed no significant correlation with mandibular prognathism ($p > 0.05$).

Figures 1 and Figures 2 show the PCR products of *MYO1H* on 1.5% agarose gel for the detection of the rs10850110 and rs11611277 polymorphisms, respectively. As shown, the PCR products had acceptable quality and quantity, and were selected for sequencing. The rs10850110 polymorphism was not detected in the majority of the subjects except for 2 patients and 4 controls. Figure 3 shows the PCR products of *MYO1H* on 1.5% agarose gel for the detection of the rs11611277 polymorphism in the control group. Figures 4–8 show the chromatography results of the sequencing of the *MYO1H* gene containing the rs10850110 and rs11611277 polymorphisms.

Table 2. Cephalometric findings, and the sex and mean age of the subjects

Data	Group	<i>n</i>	<i>M</i> ± <i>SD</i>	<i>p</i> -value
Wits appraisal [mm]	case	64	−6.70 ± 4.32468	<0.001*
	control	60	0.76 ± 0.76495	
ANB [°]	case	64	−3.20 ± 2.28129	<0.001*
	control	60	1.03 ± 0.61753	
SNA [°]	case	64	83.40 ± 4.37822	<0.001*
	control	60	80.90 ± 0.81184	
SNB [°]	case	64	86.60 ± 3.82949	<0.001*
	control	60	80.01 ± 0.60013	
Age [years]	case	64	24.64 ± 5.86	–
	control	60	22.41 ± 7.40	
Sex	case	41F + 23M	–	–
	control	38F + 22M		

M – mean; *SD* – standard deviation; F – female; M – male; * statistically significant.

Table 3. Frequency of different genotypes with respect to the 2 polymorphisms in the 2 groups

Polymorphism	Genotype	Case group <i>n</i> (%)	Control group <i>n</i> (%)	<i>p</i> -value
rs10850110	GG	40 (62.5)	37 (61.7)	0.680
	GA	22 (34.4)	19 (31.7)	
	AA	2 (3.1)	4 (6.7)	
rs11611277	CC	40 (62.5)	37 (61.7)	0.602
	CA	23 (35.9)	20 (33.3)	
	AA	1 (1.6)	3 (5.0)	

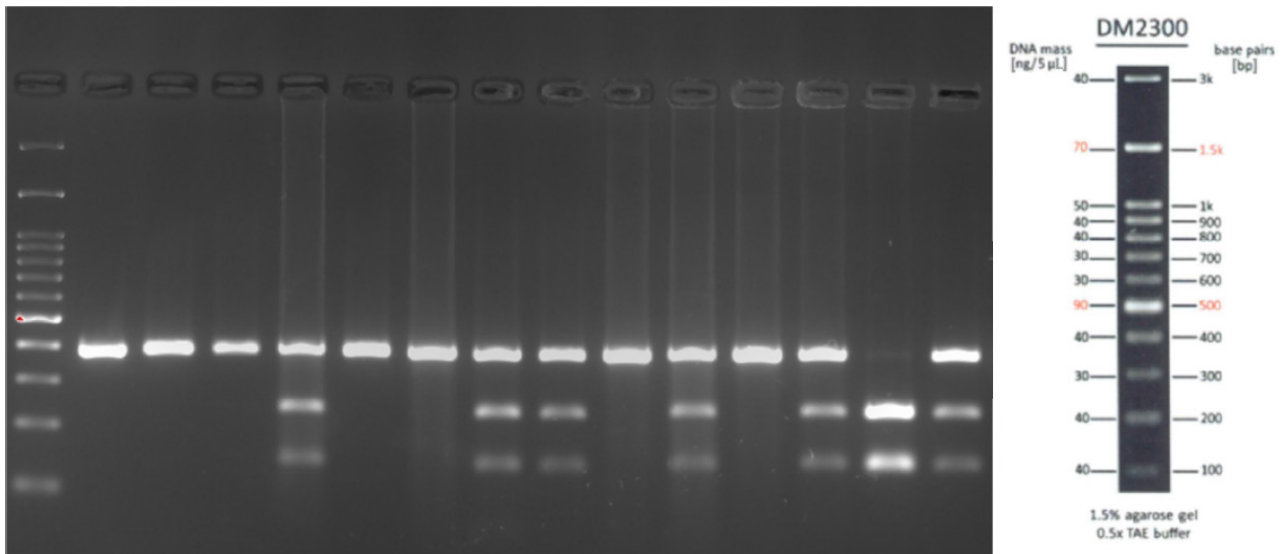


Fig. 1. Polymerase chain reaction (PCR) products of the *MYO1H* gene on 1.5% agarose gel for the detection of the rs10850110 polymorphism in the patient group TAE – tris-acetate-EDTA.

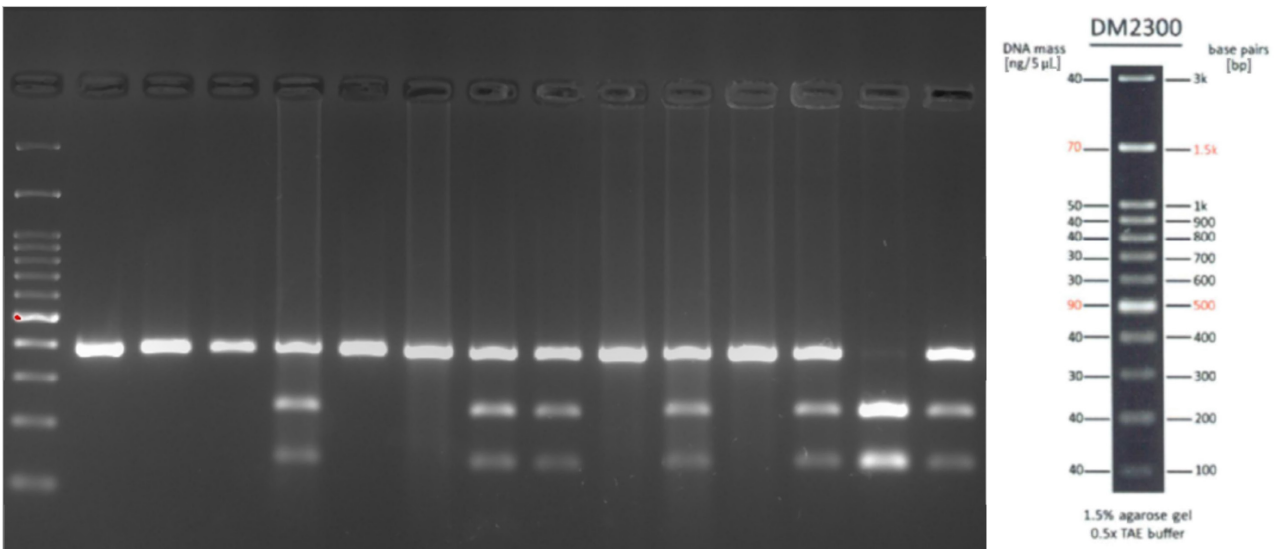


Fig. 2. PCR products of the *MYO1H* gene on 1.5% agarose gel for the detection of the rs11611277 polymorphism in the patient group

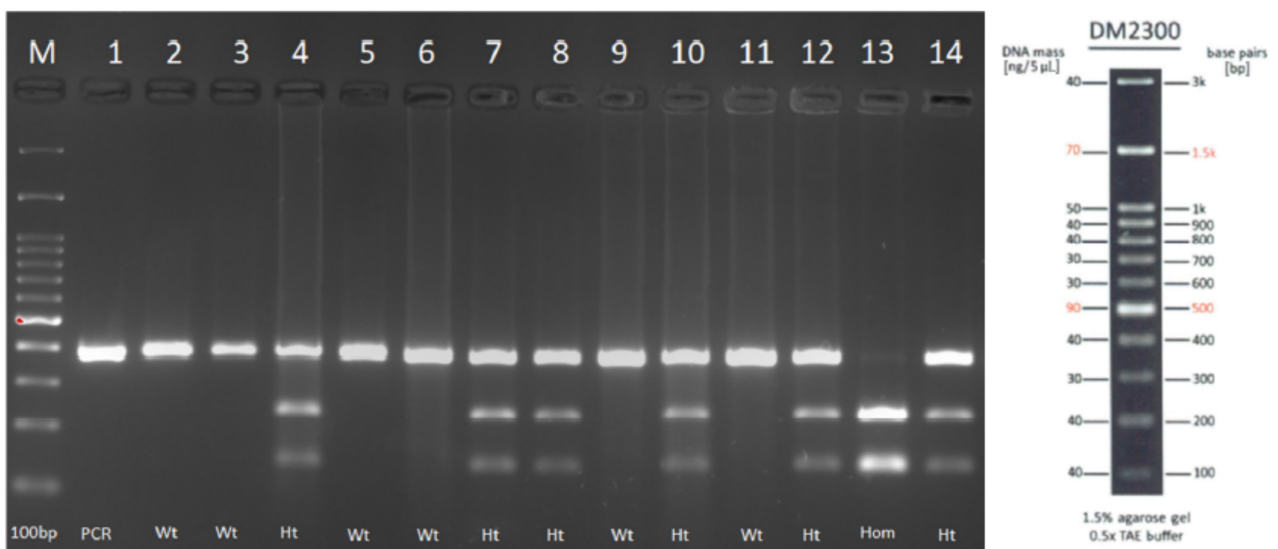


Fig. 3. PCR products of the *MYO1H* gene on 1.5% agarose gel for the detection of the rs11611277 polymorphism in the control group

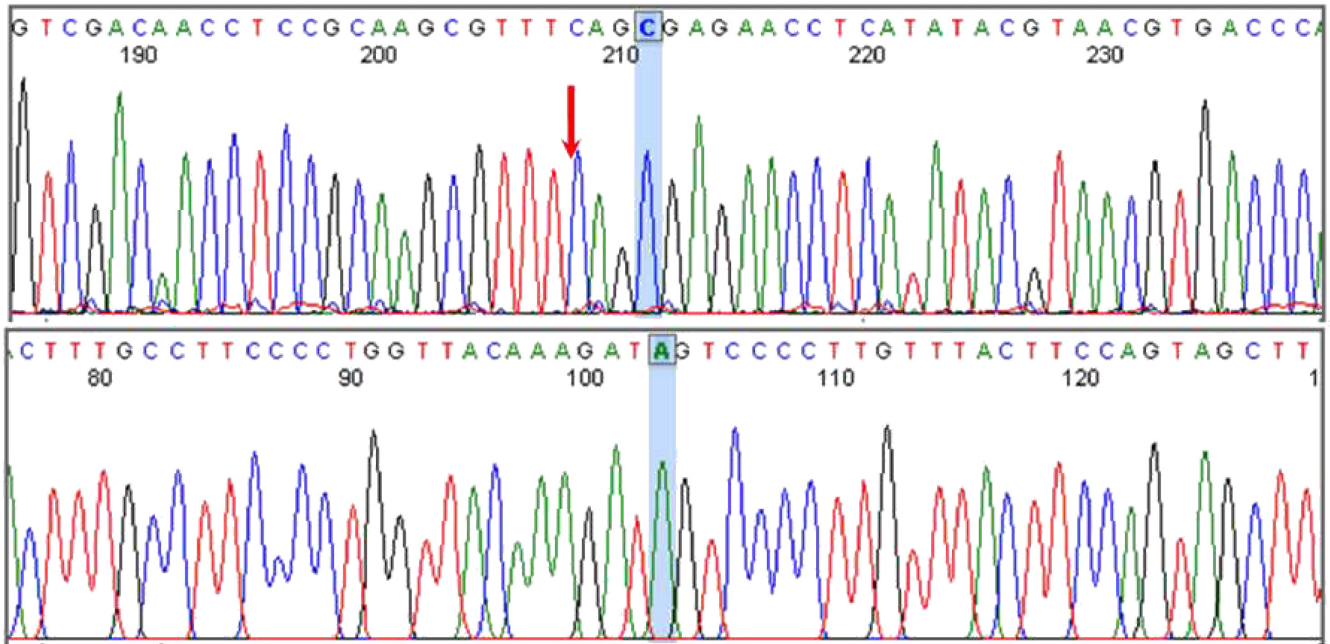


Fig. 4. DNA sequencing chromatogram of the *MYO1H* gene containing the sites of the rs10850110 and rs11611277 polymorphisms

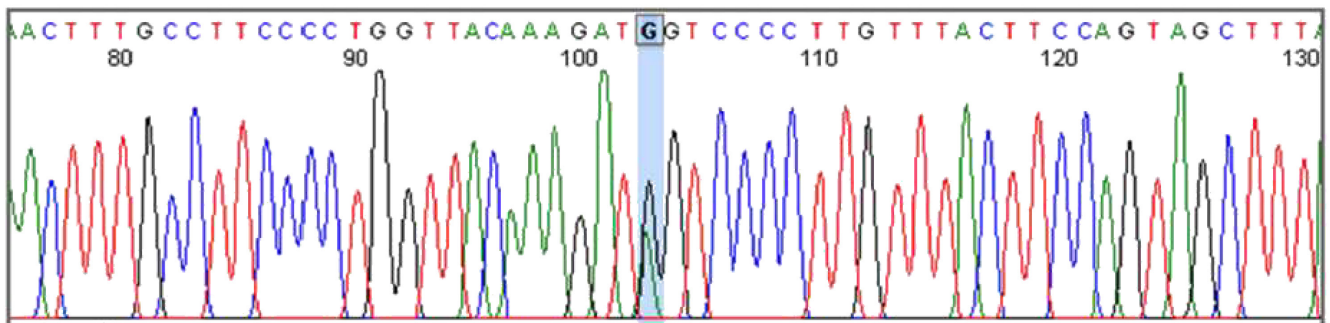


Fig. 5. DNA sequencing chromatogram of the heterozygote rs10850110 polymorphism

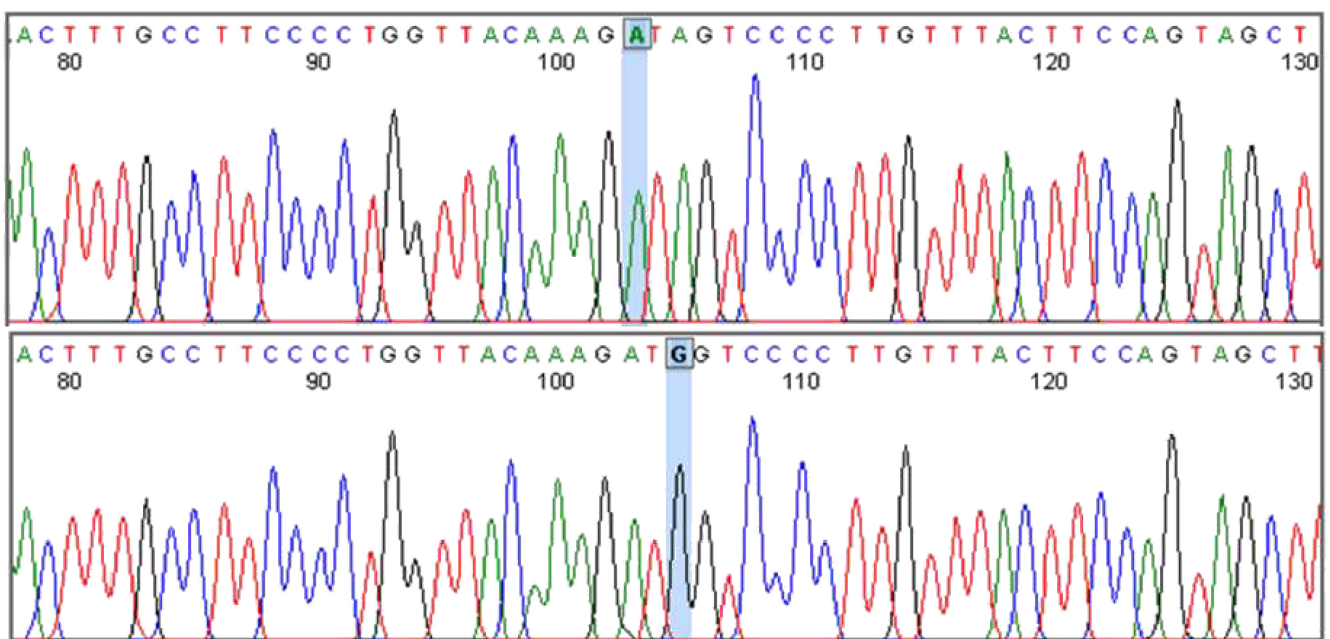


Fig. 6. DNA sequencing chromatogram of the normal heterozygote rs10850110 polymorphism

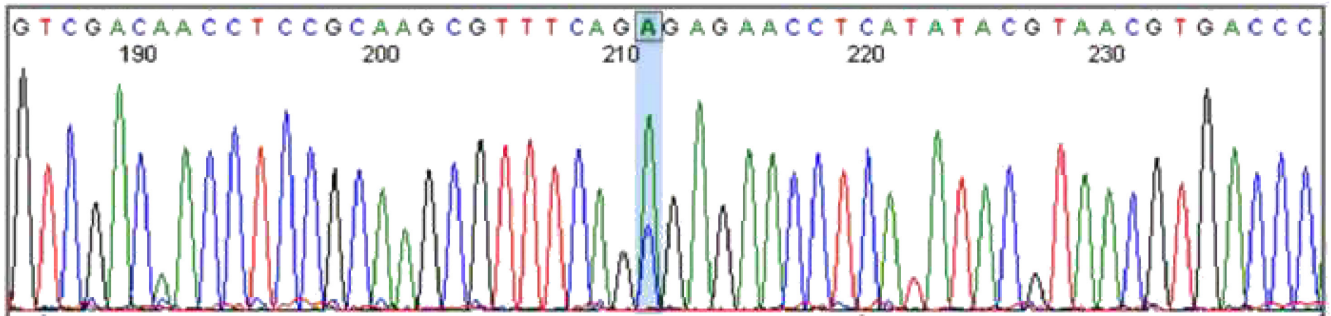


Fig. 7. DNA sequencing chromatogram of the heterozygote rs11611277 polymorphism

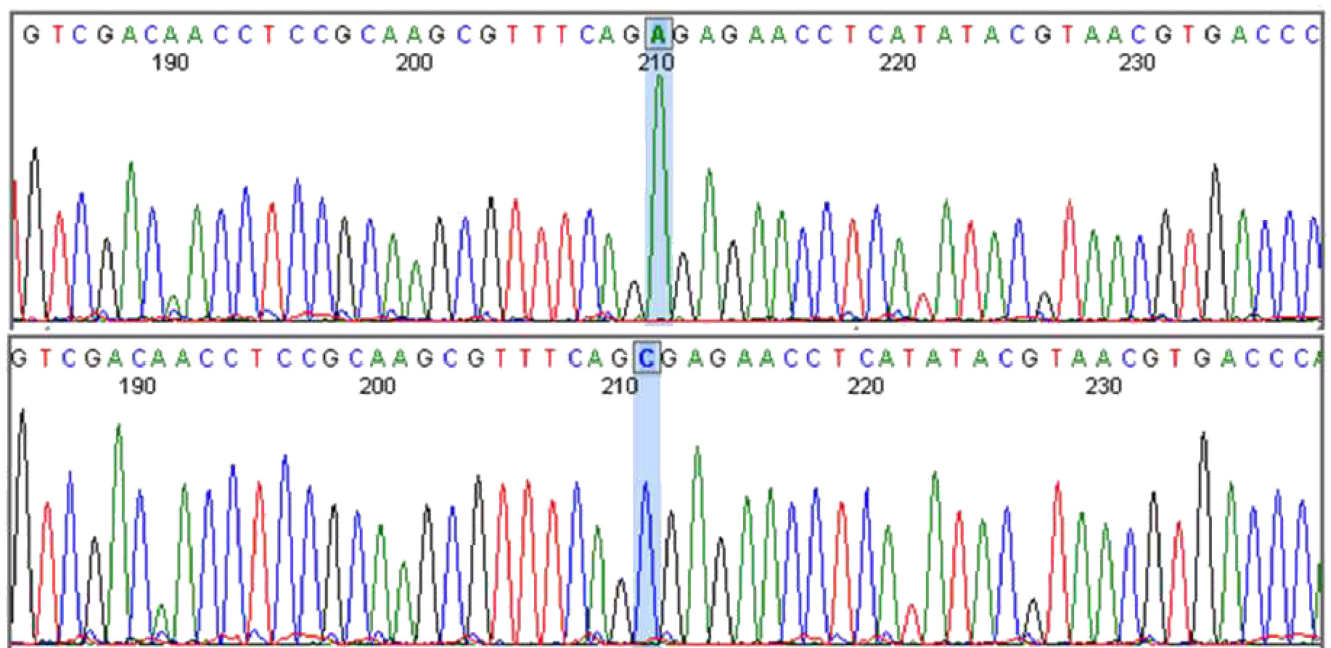


Fig. 8. DNA sequencing chromatogram of the normal heterozygote rs11611277 polymorphism

Discussion

The role of genetic factors in mandibular prognathism has been documented and the single-nucleotide polymorphisms of different genes may play a part in this respect. The *GHR* and *MYO1H* genes are 2 examples of such genes. This study aimed to assess the relationship between the rs10850110 and rs11611277 polymorphisms of the *MYO1H* gene and mandibular prognathism in the Iranian population.

Sun et al. used the whole-mount in situ hybridization (WISH) technique to analyze the pattern of expression of *MYO1H*.¹⁹ They concluded that *MYO1H* plays an important role in the mandibular growth, which was expected, considering the involvement of this gene in the proliferation and morphology of the mandibular condyle chondrocytes. They also found an association between the rs3825393 polymorphism and mandibular prognathism.¹⁹ Cruz et al. used the TaqMan method of the real-time PCR to amplify the genome, and demonstrated that the *MYO1H*, *GHR* and *FGF* genes play a role in

mandibular prognathism and maxillomandibular discrepancies.¹⁵ Tassopoulou-Fishell et al. used PCR along with TaqMan chemistry to amplify the genome and trace polymorphisms.¹⁴ They found no significant correlation between the rs2503243, rs972054, rs1413533, rs1490055, rs2101560, rs1601948, rs1387168, rs2940913, rs7718944, rs3016534, and rs9458378 polymorphisms and mandibular prognathism, but confirmed a correlation between the rs10850110 polymorphism of the *MYO1H* gene and mandibular prognathism in their study population.¹⁴ Arun et al. evaluated the rs10850110, rs11611277 and rs3825393 polymorphisms of the *MYO1H* gene and their correlation with mandibular retrognathism.¹⁸ The researchers extracted DNA by means of the modified salting-out method. They used the same enzymes as we did, and no cephalometric variable or growth measure showed a statistical difference between the genotypes for the rs10850110 and rs11611277 single-nucleotide polymorphisms in both studies. They confirmed a correlation between the rs3825393 polymorphism of the *MYO1H* gene and mandibular retrognathism.¹⁸ Cunha et al. studied

the relationship between *ACTN3* and *MYO1H* (rs10850110) and facial patterns on 4 different Brazilian samples with the TaqMan method of the real-time PCR.¹⁷ There was no significant correlation between *MYO1H* and mandibular prognathism in any sample, but in 1 of the 4 samples, they confirmed an association between *MYO1H* (rs10850110) and class II skeletal pattern.¹⁷ Ghergie et al. confirmed a correlation between the rs10850110 polymorphism of the *MYO1H* gene and mandibular prognathism.²⁰ Considering all the above, a significant correlation exists between the rs10850110 polymorphism and mandibular prognathism in the Romanian²⁰ and American⁹ populations, while no such correlation was noted in the Brazilian sample¹⁷ and our Iranian population. The controversy regarding the results of Arun et al.¹⁸ and Sun et al.¹⁹ is also understandable, considering their different study populations and sample sizes. Arun et al. found a strong correlation between the rs3825393 polymorphism and mandibular retrognathism,¹⁸ while Sun et al. found a strong correlation between the rs3825393 polymorphism and mandibular prognathism in a larger population.¹⁹ Future studies with larger sample sizes on both class II and class III patients from different populations are required to better elucidate the relationship between the rs3825393 polymorphism of the *MYO1H* gene and the position of the mandible. It should be noted that the genetic correlations found in a certain population cannot be generalized to other populations due to inherently different genetic backgrounds.²¹

In total, it should be emphasized that the *MYO1H* gene plays a fundamental role in the growth of the mandibular condyle cartilage, and there is evidence regarding the effect of the muscular system on the skeletal growth of the maxillofacial region. The rate of expression of this gene in the masseter muscle also affects the mandibular growth and development.^{22,23} Evidence shows a higher expression of this gene in the masseter muscle of distal occlusion subjects as compared to its expression in mesial occlusion individuals. In other words, the upregulation of this gene is more often noted in the masseter muscle of class II patients in comparison with class III individuals.^{24,25} It is assumed that *MYO1H* may take part in the intracellular transport of glucose with *MYO1C* to influence the masseter metabolism and fiber types. It, therefore, plays a role in the development of class I, II and III malocclusion.²⁶ Although the prognathic and retrognathic facial phenotypes may be similar vertically, the masseter muscle gene expression levels of the myosin heavy chain genes *MYH1*, *MYH2*, *MYH3*, *MYH6*, *MYH7*, and *MYH8* demonstrated that the prognathic and retrognathic facial phenotypes had different gene expression profiles.²⁷

Our study had some limitations. For instance, we evaluated only 1 city and 1 ethnic group of patients, and therefore the effect of ethnicity could not be evaluated. Also, we assessed the rs10850110 and rs11611277 polymorphisms of the *MYO1H* gene, while other polymorphisms


related to this gene were not evaluated. Future multicenter studies with larger sample sizes are required on different races and ethnic groups. Other single-nucleotide polymorphisms of this gene should also be assessed in future studies.


Conclusions


No significant correlation was noted between the rs10850110 and rs11611277 polymorphisms of the *MYO1H* gene and mandibular prognathism in the Iranian population. However, the lower frequency of the polymorphisms in the patient group suggests a possible association with mandibular retrognathism, which needs to be investigated with a larger sample size.


ORCID iDs


Kazem Dalaie  <https://orcid.org/0000-0002-5430-3301>

Vahid Reza Yassaee  <https://orcid.org/0000-0002-1879-3905>

Mohammad Behnaz  <https://orcid.org/0000-0002-2793-3292>

Mohsen Yazdani  <https://orcid.org/0000-0002-9109-8968>

Farbod Jafari  <https://orcid.org/0000-0003-3899-4891>

Reza Morvaridi Farimani  <https://orcid.org/0000-0002-6697-6837>

References

- Harris EF, Johnson MG. Heritability of craniometric and occlusal variables: A longitudinal sib analysis. *Am J Orthod Dentofacial Orthop.* 1991;99(3):258–268.
- Bayram S, Basciftci FA, Kurar E. Relationship between P561T and C422F polymorphisms in growth hormone receptor gene and mandibular prognathism. *Angle Orthod.* 2014;84(5):803–809.
- Bui C, King T, Proffit W, Frazier-Bowers S. Phenotypic characterization of Class III patients. *Angle Orthod.* 2006;76(4):564–569.
- Frazier-Bowers S, Rincon-Rodriguez R, Zhou J, Alexander K, Lange E. Evidence of linkage in a Hispanic cohort with a Class III dentofacial phenotype. *J Dent Res.* 2009;88(1):56–60.
- Kataoka K, Ekuni D, Mizutani S, et al. Association between self-reported bruxism and malocclusion in university students: A cross-sectional study. *J Epidemiol.* 2015;25(6):423–430.
- Ko JM, Suh YJ, Hong J, Paeng JY, Baek SH, Kim YH. Segregation analysis of mandibular prognathism in Korean orthognathic surgery patients and their families. *Angle Orthod.* 2013;83(6):1027–1035.
- Xue F, Wong RWK, Rabie ABM. Genes, genetics, and Class III malocclusion. *Orthod Craniofac Res.* 2010;13(2):69–74.
- Wolff G, Wienker TF, Sander H. On the genetics of mandibular prognathism: Analysis of large European noble families. *J Med Genet.* 1993;30(2):112–116.
- Cruz RM, Krieger H, Ferreira R, Mah J, Hartsfield J Jr., Oliveira S. Major gene and multifactorial inheritance of mandibular prognathism. *Am J Med Genet A.* 2008;146A(1):71–77.
- El-Gheriani AA, Maher BS, El-Gheriani AS, et al. Segregation analysis of mandibular prognathism in Libya. *J Dent Res.* 2003;82(7):523–527.
- Xue F, Rabie ABM, Luo G. Analysis of the association of *COL2A1* and *IGF-1* with mandibular prognathism in a Chinese population. *Orthod Craniofac Res.* 2014;17(3):144–149.
- Yamaguchi T, Park SB, Narita A, Maki K, Inoue I. Genome-wide linkage analysis of mandibular prognathism in Korean and Japanese patients. *J Dent Res.* 2005;84(3):255–259.
- Desh H, Gray SL, Horton MJ, et al. Molecular motor *MYO1C*, acetyltransferase *KAT6B* and osteogenic transcription factor *RUNX2* expression in human masseter muscle contributes to development of malocclusion. *Arch Oral Biol.* 2014;59(6):601–607.
- Tassopoulou-Fishell M, Deeley K, Harvey EM, Sciote J, Vieira AR. Genetic variation in myosin 1H contributes to mandibular prognathism. *Am J Orthod Dentofacial Orthop.* 2012;141(1):51–59.

15. Cruz CV, Mattos CT, Maia JC, et al. Genetic polymorphisms underlying the skeletal Class III phenotype. *Am J Orthod Dentofacial Orthop.* 2017;151(4):700–707.
16. Burnheimer J, Deeley K, Vieira AR. Myosin 1H and the soft tissue profile of African American females with mandibular prognathism. *Revista Científica do CRO-RJ (Rio de Janeiro Dent J).* 2019;4(2):35–41.
17. Cunha A, Nelson-Filho P, Marañón-Vásquez GA, et al. Genetic variants in *ACTN3* and *MYO1H* are associated with sagittal and vertical craniofacial skeletal patterns. *Arch Oral Biol.* 2019;97:85–90.
18. Arun RM, Lakkakula BVKS, Chitharanjan AB. Role of myosin 1H gene polymorphisms in mandibular retrognathism. *Am J Orthod Dentofacial Orthop.* 2016;149(5):699–704.
19. Sun R, Wang Y, Jin M, Chen L, Cao Y, Chen F. Identification and functional studies of *MYO1H* for mandibular prognathism. *J Dent Res.* 2018;97(13):1501–1509.
20. Ghergie M, Feștilă D, Kelemen B, Lupan I. *Myo1H* gene single nucleotide polymorphism rs10850110 and the risk of malocclusion in the Romanian population. *Acta Medica Transilvanica.* 2013;2(4):281–281.
21. Frazer KA, Murray SS, Schork NJ, Topol EJ. Human genetic variation and its contribution to complex traits. *Nat Rev Genet.* 2009;10(4):241–251.
22. Mew JR. Factors influencing mandibular growth. *Angle Orthod.* 1986;56(1):31–48.
23. Ueda HM, Ishizuka Y, Miyamoto K, Morimoto N, Tanne K. Relationship between masticatory muscle activity and vertical craniofacial morphology. *Angle Orthod.* 1998;68(3):233–238.
24. Gedrange T, Büttner C, Schneider M, Oppitz R, Harzer W. Myosin heavy chain protein and gene expression in the masseter muscle of adult patients with distal or mesial malocclusion. *J Appl Genet.* 2005;46(2):227–236.
25. Gedrange T, Büttner C, Schneider M, et al. Change of mRNA amount of myosin heavy chain in masseter muscle after orthognathic surgery of patients with malocclusion. *J Craniomaxillofac Surg.* 2006;34(Suppl 2):110–115.
26. Stedman HH, Kozyak BW, Nelson A, et al. Myosin gene mutation correlates with anatomical changes in the human lineage. *Nature.* 2004;428(6981):415–418.
27. Moawad HA, Sinanan ACM, Lewis MP, Hunt NP. Grouping patients for masseter muscle genotype-phenotype studies. *Angle Orthod.* 2012;82(2):261–266.

Current trends in craniofacial distraction: A literature review

Farheen Fatima^{1,A-F}, Waqar Jeelani^{2,A-F}, Maheen Ahmed^{2,B-F}

¹ Department of Orthodontics, Bahria University Medical and Dental College, Karachi, Pakistan

² Department of Orthodontics, Bakhtawar Amin Medical and Dental College, Multan, Pakistan

A – research concept and design; B – collection and/or assembly of data; C – data analysis and interpretation; D – writing the article; E – critical revision of the article; F – final approval of the article

Dental and Medical Problems, ISSN 1644-387X (print), ISSN 2300-9020 (online)

Dent Med Probl. 2020;57(4):441–448

Address for correspondence

Waqar Jeelani
E-mail: wjeelani@gmail.com

Funding sources

None declared

Conflict of interest

None declared

Received on April 9, 2020
Reviewed on May 4, 2020
Accepted on May 18, 2020

Published online on December 31, 2020

Abstract

The techniques and procedures involved in craniofacial distraction are constantly evolving. The understanding of histological and biochemical response at the distraction site is now improved. The cascade of events in distraction osteogenesis (DO) differs significantly from the typical fracture healing, and a better knowledge about these events has helped us identify suitable candidates for DO, make appropriate modifications to the distraction protocols and minimize the risk of complications. Recent advances in the manufacturing techniques have also facilitated the availability of distractors of various shapes and designs, which are now changing the way different craniofacial defects are being treated. Small but rigid intraoral distractors now enable easy placement, are well tolerated by patients and allow for a long consolidation period. The introduction of newer approaches toward treatment, together with the simultaneous management of different craniofacial defects at multiple osteotomy sites and enhanced surgical accuracy with the help of digital imaging, have made treatment outcomes more predictable.

Key words: distraction, repair, Ilizarov technique, craniofacial syndrome, computer-assisted three dimensional imaging

Cite as

Fatima F, Jeelani W, Ahmed M. Current trends in craniofacial distraction: A literature review. *Dent Med Probl.* 2020;57(4):441–448. doi:10.17219/dmp/122579

DOI

10.17219/dmp/122579

Copyright

© 2020 by Wrocław Medical University
This is an article distributed under the terms of the
Creative Commons Attribution 3.0 Unported License (CC BY 3.0)
(<https://creativecommons.org/licenses/by/3.0/>).

Introduction

Distraction osteogenesis (DO) is a well-established technique in the field of orthopedics, as it has been used for several decades for limb lengthening and the repair of long-bone defects. The standard protocol of DO is based on careful planning, with special attention being paid to the anatomy and blood supply of the osteotomy site, the patient's general health, and the design and mechanical properties of the distractor device.

The procedure is commenced with an osteotomy, followed by the insertion of a distractor. The osteotomy site is allowed to mature for a few days (the latency period); then, the distraction phase begins. The distractor is opened at a specific rate and rhythm so that the proximal and distal fragments of the bone start separating, leading to the mechanical induction of new bone formation between the bony surfaces at the osteotomy site.¹ Once the desired lengthening of the bone is achieved, the process of distraction is stopped and the newly formed non-mineralized bone (callus) is allowed to mature for a period of several weeks to several months as part of the consolidation phase (Fig. 1).¹

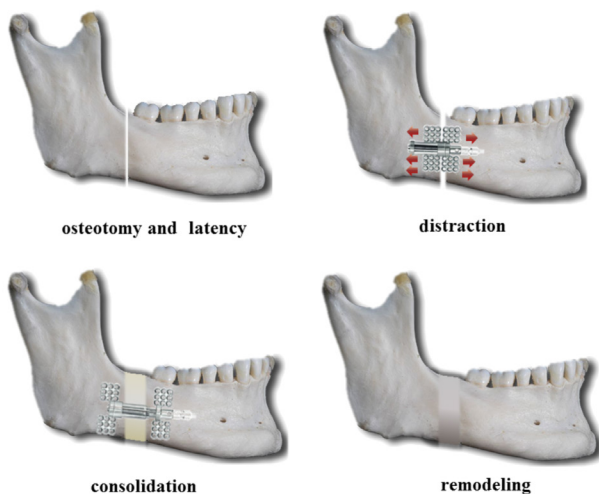


Fig. 1. Phases of distraction osteogenesis (DO)

Insights into the biological basis of craniofacial distraction

Histologically, the latency phase of DO closely resembles typical fracture healing, which involves hematoma formation, local inflammatory response and the influx of mesenchymal stem cells.^{2,3} During rapid bone formation in the latency period, endochondral bone formation is observed along the periosteum. The region in the middle of the healing callus, regarded as a fibrous interzone (FIZ), is rich in fibroblasts, chondrocytes, and cells that have the morphological features of both chondroblasts and fibroblasts.^{4,5} The process of ossification starts from the area adjacent to the bone and FIZ ossifies the last.^{5,6}

The predominant mechanism of bone formation is intramembranous, characterized by the formation of type-I collagen; however, a zone of endochondral bone formation is frequently observed.⁷⁻⁹ This process differs from the typical endochondral bone formation, as there is no capillary ingrowth in this cartilaginous matrix and the formation of type-II collagen by these chondroblast-like cells switches over to the production of type-I collagen. This process has been named as 'transchondroid bone formation'.¹⁰

The molecular expression during DO shows certain differences when compared to the molecular expression during fracture healing. Interleukin-6 (IL-6) concentration is increased not only during the initial inflammatory phase, but also when the distraction phase is started. Cho et al. showed that IL-6 could significantly enhance intramembranous ossification and had an overall anabolic effect during DO, contrary to its catabolic effect during fracture healing.¹¹ The members of the transforming growth factor beta (TGF- β) superfamily are other important mediators associated with DO, the expression of which is greater at the distracted osteotomy sites as compared to the non-distracted osteotomy or fracture sites. The expression of TGF- β is positively correlated with the rate of distraction, which promotes new bone formation through osteoblastic proliferation.^{2,12} A similar pattern of expression has been described for bone morphogenic protein (BMP)-2 and BMP-4.^{13,14} In the absence of mechanical strain, they gradually disappear from the distraction site. Moreover, the addition of BMP-2 has been shown to reduce the latency period, and thus may be used to reduce the overall treatment time.¹⁵ Other important growth factors that play a role during different phases of DO include insulin-like growth factor-1 (IGF-1) and fibroblast growth factor (FGF)-2.¹⁶

Angiogenesis is an essential part of DO, in the absence of which non-bony union occurs. Angiogenesis during DO is more intense as compared to that during fracture healing, with studies reporting about a ten-fold increase in the blood flow during the distraction phase as compared to the normal blood flow.⁵ Similarly, since maximum bone formation occurs during the consolidation period, the maximum increase in the vessel volume has also been found during this period. The experimental inhibition of vascular endothelial growth factor (VEGF)-mediated angiogenesis also results in reduced osteogenesis activity.¹⁷ Although new vessel formation begins during activation, the maximum increase in the vessel volume occurs during consolidation, suggesting a link between angiogenesis and bone formation.¹⁷⁻¹⁹

Evolution of distractor designs and techniques

The evolution of distractor devices goes along with the evolution in the DO techniques. The concept of intraoral and extraoral distractor devices goes back to the era

of McCarthy, when he used unidirectional extraoral distractors to lengthen the mandibles of patients suffering from congenital mandibular deficiencies in 1989.^{20,21} The following year, Guerrero reported the use of an intraoral tooth-borne distractor for mandibular symphyseal distraction.²²

Evolution of distractors for maxillomandibular distraction

Generally, mandibular distractors can be categorized into extraoral and intraoral ones, intraoral distractors being tooth-borne, bone-borne or hybrid. On the other hand, extraoral distractors are always bone-borne (Fig. 2). These distractors allow vector adjustment during distraction. However, the 2 major drawbacks of these distraction devices were the uniplanar control of the vector and extraoral placement. A common type of extraoral distractor is a two-pin distractor, which offers the advantage of easy placement in situations where minimal bone mass is available, without compromising the quality of callus formation and bone healing. Soon after the introduction of unidirectional distractors, it was realized that most of the defects were three-dimensional (3D) and linear distractors failed to completely restore them. When distractors were applied to different parts of the ramus, angle and body of the mandible, the results were rarely ideal and never precise enough to achieve optimal dental occlusion. In 1995, Molina and Ortiz Monasterio²³ demonstrated the use of bidirectional distractors by creating 2 osteotomy sites in the affected mandibles (Fig. 3), which further led to the development of multidirectional distraction devices, such as the ACE/Normed multidimensional distractor and the multi-vector mandibular distractor of McCarthy.²⁴



Fig. 2. Rigid external distractor

Another major leap in the evolution of distractors was the introduction of intraoral distractors, which were less conspicuous, easy to tolerate, socially acceptable, and free of the risk of facial scars. The realization of intraoral distractors was possible due to a significant reduction in the size of distractors

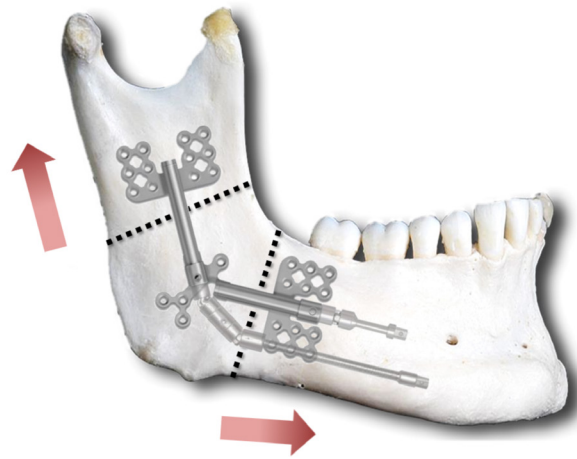


Fig. 3. Bidirectional distractor

and alteration in the distraction design. They were initially stock made, which meant they could be used for a specific bony location in any patient, as reported by Diner et al.,²⁵ or were universal in nature and could be placed on any site at the discretion of the surgeon, like the Dynaform Intraoral Distractor.²⁶ A newer category of distractors were custom made and designed according to the needs of a specific patient. Razdolsky's tooth-borne and hybrid ROD devices are examples of distractors that allow the preprogrammed fabrication of the device along the predetermined axis of distraction according to the needs of the patient.^{27,28}

The need for multidirectional or curvilinear distraction is often appreciated by oral and maxillofacial surgeons and orthodontists (Fig. 4). Multidirectional distractors are often large in size and need to be placed extraorally. A curvilinear distractor was described by Seldin²⁹ in 1999 on animal models (Fig. 5). The curved design allows for the simultaneous lengthening of the mandibular body and ramus along a curved path, which is very similar to the pattern of natural growth of the mandible.^{30–32} In addition, this pattern of mandibular lengthening is favorable for the correction of an anterior open bite, a common iatrogenic condition during mandibular distraction.³³

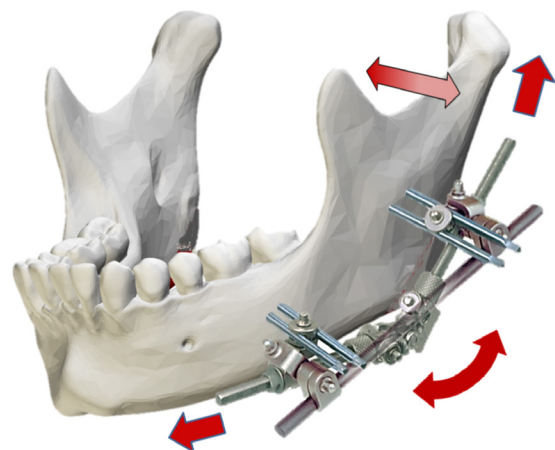


Fig. 4. Multidirectional distractor

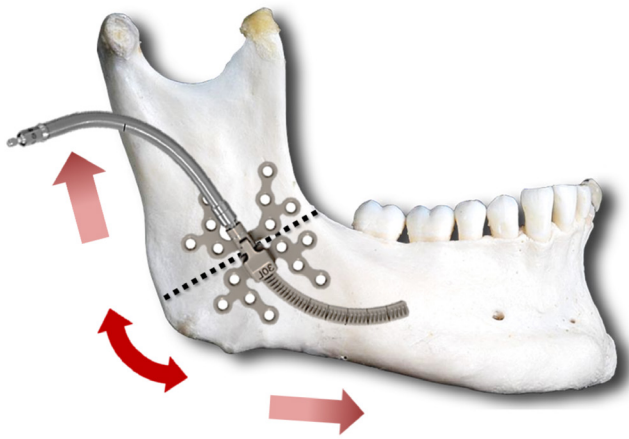


Fig. 5. Curvilinear distractor

A general concept that DO allows greater mid-facial advancement than the conventional orthognathic surgeries has been verified by a retrospective single-center study.³⁴ Bone healing in the maxilla is relatively faster. Studies have shown that the traditional consolidation phase duration of 8 weeks or longer can be shortened without compromising stability.^{35,36} Though these devices have served the specialty well, there is still a need to develop an appliance system that would carry out automated and continuous distraction. It is not uncommon to find that many patients could not adhere to the distraction protocol – intentionally, due to the pain or discomfort associated with activation, or unintentionally, when they failed to comprehend or remember the distraction protocol. Recently, newer devices with hydraulic, motor-driven or spring-mediated mechanisms are being developed. The first reports on animal models are satisfactory, but significant improvement in the device design is needed, along with the need to include a distraction protocol that is compatible with human body, before these devices could be used for routine patient care.^{37,38} Despite these deficiencies, it is expected that soon these appliances will become common, and thus will simplify the distraction process for patients and parents.

Evolution of distractors for cranial and craniofacial defects

In patients with differential dysmorphism involving the axial and sagittal planes, the en bloc movement using Le Fort III osteotomy may treat the position, but the axial dimension may remain untreated. The bipartition monobloc advancement using vertical osteotomy in the midline to pull the central face gives effective correction in midface concavity.³⁶ Greater soft-tissue resistance laterally as compared to the center of the face during advancement results in a more convex shape of the sagittal facial profile. The separation of the zygoma after Le Fort III osteotomy at the zygomaticomaxillary suture also

aids in differential advancement and the repositioning of the midface in the desired position relative to the corneal surface.

In patients with a shortened skull, DO allows correction over large distances, with the gradual movement and changes of the soft-tissue matrix. The contemporary distraction technique allows for the distraction of the cranium and skull base. The expansion of the anterior cranial fossa could also be performed, either in isolation or with the subcranial movement using the monobloc procedure, with the latter technique allowing for the simultaneous advancement of the inferior orbital rim, an increase in the dimension of the nasopharynx and overjet correction. The monobloc craniofacial advancement of the midface along with the anterior cranial vault is usually carried out at the age of 7–9 years, when the growth of the midface is almost complete.³⁹ However, this procedure may involve a significant risk, as the sinus–brain barrier in the anterior cranial vault can be violated. This has resulted in a reduction in the frequency of using this procedure, which is usually limited to cases with circumorbital symmetric retrusion, in which the conventional staged advancement of the midface and the anterior cranial vault is not possible.^{40,41} Contrary to this approach, gradual expansion and advancement with DO minimizes the risk of the creation of dead space, and the subsequent morbidity associated with it.⁴² Though some authors have advocated the use of frontofacial monobloc distraction at the age of 1 year, the long-term results as well as the final esthetic and functional outcomes are yet to be investigated.⁴³ In this regard, the use of early monobloc distraction is usually limited to life-threatening dysostosis, e.g., Pfeiffer type-II deformity.⁴⁴

Stimulation of bone repair

To minimize the duration of bone repair during DO, various surgical and non-surgical strategies have been implemented. Non-surgical strategies include electric and electromagnetic stimulation, injecting growth hormones, cytokines and BMPs, and the use of low-level laser therapy (LLLT) and low-intensity pulse ultrasound (LIPUS).

The acceleration of bone repair and the modification of the period of inflammation with biological stimulation can be achieved by means of lasers.^{45–48} Low-level laser therapy was used in the past for the treatment of unhealed ulcers.⁴⁹ It promotes osteoblastic activity during bone repair, which enhances the rate of bone healing.⁵⁰ The factors affecting the laser dose may result in variations in the effectiveness of LLLT. These include power output and the duration of the applied therapy. The doses recommended by various studies vary from 10–112.5 J/cm²^{51–53} to 0.03–3 J/cm².^{54–56} Another important criterion that affects the effectiveness of the therapy is the type of the target tissue, as this may result in variations in the depth

of penetration. Mucosa is more susceptible to penetration as compared to fat and muscle tissues. Depending on the dose, the therapy may cause biostimulation or bioinhibition.^{57,58} Therefore, low doses (3–5 J/cm²) are recommended rather than high doses (50–100 J/cm²) to prevent the destructive effect.⁵⁹

Ultrasound therapy produces micromechanical vibrations similar to physiological stress. The piezoelectric and angiogenic effects of ultrasound on bone apparently produce the therapeutic effect the therapy.⁶⁰ The application of ultrasound has been reported in mandibular fractures in rabbits.⁶¹ Harris treated mandibular osteoradionecrosis with ultrasound in humans.⁶² An increased healing ratio of 88% has been reported when using ultrasound with the conventional therapy in 1,317 fracture cases in human subjects.⁶³ With the application of LIPUS for 20 min/day, following DO for 10 days to lengthen the right tibia of rabbits, improved bone mineral density (BMD) at callus with increased stiffness and fracture strength have been observed.⁶¹ The application of 20–50 mW/cm² LIPUS results in a rise in tissue temperature <1°C. This brings about significant changes during bone formation and in the amount of enzymes.^{64,65} The tissue changes include a decrease in edema through the stimulation of mast cells.⁶⁶ Furthermore, an increase in the adhesion of leukocytes to endothelium during the inflammation period causes the increased release of macrophages, fibroblasts and VEGF, and the stimulation of collagen synthesis from fibroblasts during the healing phase has been reported in various studies.^{67–70} Increased BMD was reported in a study conducted on dogs, which received 40 mW/cm² LIPUS for 20 min/day during the distraction phase at a 2-week interval.⁷¹

Both LLLT and LIPUS have been reported to be safe and non-invasive to improve the outcome of the DO treatment.⁷² Kocyigit et al. investigated the effects of ultrasound stimulation (LIPUS) and laser therapy (LLLT) on the BMD of the bone formed during DO with the use of dual energy X-ray absorptiometry.⁷² Both methods showed improvement in healing after DO and greater BMD in the exposed groups (LIPUS or LLLT) as compared to the controls.⁷²

To improve the process of healing during and after distraction, several novel techniques are being implemented. A recent study investigated the effect of stem cells from human exfoliated deciduous teeth (SHED) on healing after DO.⁷³ The results were quite promising, denoting significantly greater bone formation in the SHED-transplanted groups, thus improving the quality of union and the speed of bone maturation.⁷³

Scientists are trying to explore the effects of different growth factors and biochemical mediators on DO. The role of BMPs and FGFs has long been documented. Recently, the positive effects of recombinant human erythropoietin (rhEPO) and platelet-rich plasma (PRP) have also been documented.^{74,75}

Recombinant human erythropoietin has been shown to increase the number of osteoblasts and blood vessels, and reduce the number of osteoclasts, leading to a larger area of bone formation.⁷⁵

These innovations in the science of DO can have significant clinical implication in the future. These methods may help reduce the latency and consolidation periods, improve bone strength after DO, improve the vascularity of tissues, and reduce the risk of complications.

Virtual surgical simulation and three-dimensional distraction osteogenesis

The process of DO in the craniofacial region consists of both linear and rotational movements as opposed to only linear movements in the case of epiphyseal lengthening. This is because of the morphology of the structures present in the head and the neck region. The vector produced by the distraction device is based on its position in relation to the surrounding bony structures.⁷⁶

Hence, for advances the desired movement, the careful planning of the osteotomy cuts and the accurate placement of the device are fundamental. Innovations in 3D imaging techniques in the current era have enabled the accurate visualization of the craniofacial structures in all 3 planes of space.⁷⁷

Recent advances in the virtual planning software have overcome some limitations, including achieving the desirable occlusal, functional and esthetic outcomes of two-dimensional (2D)-based DO. Intraoral distractors can produce movement only in a single direction; the accurate vector is dependent on the position of the device. Furthermore, intraoral devices are indicated for smaller defects, which make their placement more challenging due to a limited working field. The accurate placement and positioning of the device becomes even more important with intraoral distractors.⁷⁸

Hence, the accurate transfer of the surgical procedure planned with the aid of 3D software is mandatory for achieving the desired results. Another advantage of the virtual planning software is that multiple treatment simulations can be performed to determine the most feasible plan in terms of risks, benefits and cost, which can be set for a specific patient. The surrounding structures, including the developing tooth germs, may be taken into consideration when planning the osteotomy cuts. With the introduction of rapid prototyping machines and 3D printers, the desired surgical stent and distractor templates can be computer-aided design/computer-aided manufacturing (CAD-CAM)-fabricated to further increase the accuracy of the planned surgical procedure.^{79,80} Lastly, distractors may be modified to adapt to the bony segments on models to reduce the intraoperative surgical time and inconvenience.

The following are the basic guidelines for 3D-based DO and the fabrication of the surgical stent (Fig. 6):

- data acquisition: 3D imaging techniques, such as cone-beam computed tomography (CBCT), computed tomography (CT), magnetic resonance imaging (MRI), etc., have been used for data acquisition; these, along with the virtual models, are correlated on a common Cartesian system to construct a 3D model;
- data analysis and the determination of skeletal discrepancy: the exact skeletal discrepancy in all planes is computed using the 3D model; based on this, the exact amount and direction of movement of the bony segment is determined;
- determination of the position and angulation of the distractor: the vector is one of the significant factors for the achievement of the planned movement; this vector is determined by the position and angulation of the device on the bony segment, and the type of distractor used. With a unilateral distractor, the position and angulation becomes even more significant, as the distractor can be moved only in 1 plane. Various mathematical formulae can be used to calculate the required length and angle with respect to the bony bases by measuring the angle between the horizontal and vertical vectors^{81,82};
- treatment simulation: the osteotomy cuts are planned according the vector direction, taking into consideration the surrounding soft and hard structures. Usually, the osteotomy line is perpendicular to the vector distraction. The osteotomy cuts are simulated and the device is placed on the virtual models. If the movement is not satisfactory, an alternative plan may be simulated. An advantage of the virtual treatment planning software is the possibility of altering the position and angulation of the device until the desired result is achieved;

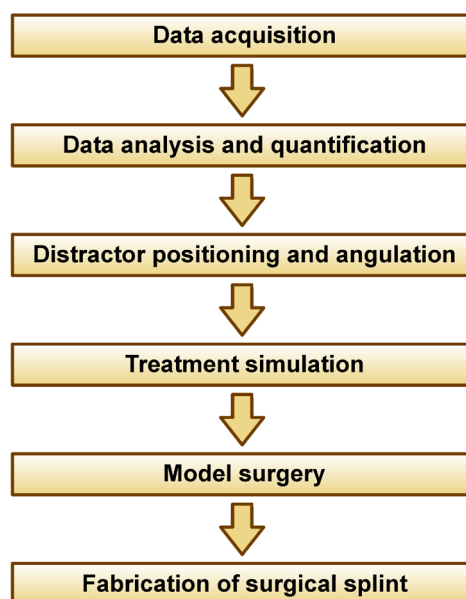


Fig. 6. Guidelines for three-dimensional (3D)-based DO

- model surgery and the fabrication of the surgical stent: various types of rapid prototyping, such as stereolithography and fused deposition modeling, may be used to fabricate models.^{83,84} The planned surgery is then performed on these models and a template distractor can be adapted to assess the feasibility of the treatment plan. Impressions of both the device and the bony surface are taken for the fabrication of the surgical stent. This stent is then used to transfer the planned surgery to the operating room.

Discussion

Recent advances have profoundly extended the scope of craniofacial DO. The incorporation of new diagnostic and treatment planning tools have improved the predictability of outcomes, providing the possibilities of using DO not only for deformity correction, but also in other situations.⁷⁷ Osteodistraction may help the orthodontist to treat crowded dental arches with non-extraction therapy by improving the arch length and perimeter in severely crowded cases.²² Also, the regeneration of the alveolar bone for the placement of implants in patients with atrophic bone may be possible with this technique, which would be preferable to tissue reaction and rejection, as in the case of artificial bone used for the augmentation purpose. In the cases of ankylosis and discrepancy in vertical height, treatment with distraction may also help the tooth attain an esthetic and functional position.


The application of the concept of acceleration in the healing process has also helped in reducing the duration of the consolidation period, offering a great advantage to the clinician and patients,^{51,60} and distraction histogenesis occurring during DO allows for larger skeletal corrections with a lower risk of relapse due to soft tissue adaptation. Moreover, advances in the designs of distractors have improved the efficiency of treatment in achieving functional and esthetic results.


Conclusions

Distraction techniques have established themselves as a highly efficient and practical mode of treating craniofacial defects. Newer techniques are making distraction a routine procedure with a long-term follow-up now available in the published literature. Orthodontists need to keep themselves updated to the latest advances in the field of craniofacial distraction to be able to offer the most suitable treatment to their patients.

ORCID iDs

Farheen Fatima  <https://orcid.org/0000-0001-5945-7185>

Waqar Jeelani  <https://orcid.org/0000-0003-0109-3117>

Maheen Ahmed  <https://orcid.org/0000-0003-0806-7739>

References

- Cope JB, Samchukov ML, Cherkashin AM. Biologic basis of new bone formation under the influence of tension stress. In: Samchukov ML, Cope JB, Cherkashin AM, eds. *Craniofacial Distraction Osteogenesis*. St. Louis, USA: Mosby; 2001:21–36.
- McCarthy JG, Stelnicki EJ, Mehrara BJ, Longaker MT. Distraction osteogenesis of the craniofacial skeleton. *Plast Reconstr Surg*. 2001;107(7):1812–1827.
- Ai-Aql ZS, Alagl AS, Graves DT, Gerstenfeld LC, Einhorn TA. Molecular mechanisms controlling bone formation during fracture healing and distraction osteogenesis. *J Dent Res*. 2008;87(2):107–118.
- Vauhkonen M, Peltonen J, Karaharju E, Aalto K, Alitalo I. Collagen synthesis and mineralization in the early phase of distraction bone healing. *Bone Miner*. 1990;10(3):171–181.
- Aronson J. Temporal and spatial increases in blood flow during distraction osteogenesis. *Clin Orthop Relat Res*. 1994;(301):124–131.
- Sato M, Yasui N, Nakase T, et al. Expression of bone matrix proteins mRNA during distraction osteogenesis. *J Bone Miner Res*. 1998;13(8):1221–1231.
- Ilizarov GA. The tension-stress effect on the genesis and growth of tissues. Part II. The influence of the rate and frequency of distraction. *Clin Orthop Relat Res*. 1989;(239):263–285.
- Ilizarov GA. The tension-stress effect on the genesis and growth of tissues. Part I. The influence of stability of fixation and soft-tissue preservation. *Clin Orthop Relat Res*. 1989;(238):249–281.
- Karaharju EO, Aalto K, Kahri A, et al. Distraction bone healing. *Clin Orthop Relat Res*. 1993;(297):38–43.
- Yasui N, Sato M, Ochi T, et al. Three modes of ossification during distraction osteogenesis in the rat. *J Bone Joint Surg Br*. 1997;79(5):824–830.
- Cho TJ, Kim JA, Chung CY, et al. Expression and role of interleukin-6 in distraction osteogenesis. *Calcif Tissue Int*. 2007;80(3):192–200.
- Farhadieh RD, Dickinson R, Yu Y, Gianoutsos MP, Walsh WR. The role of transforming growth factor-beta, insulin-like growth factor I, and basic fibroblast growth factor in distraction osteogenesis of the mandible. *J Craniofac Surg*. 1999;10(1):80–86.
- Sato M, Ochi T, Nakase T, et al. Mechanical tension-stress induces expression of bone morphogenetic protein (BMP)-2 and BMP-4, but not BMP-6, BMP-7, and GDF-5 mRNA, during distraction osteogenesis. *J Bone Miner Res*. 1999;14(7):1084–1095.
- Rauch F, Lauzier D, Croteau S, Travers R, Glorieux FH, Hamdy R. Temporal and spatial expression of bone morphogenetic protein-2, -4, and -7 during distraction osteogenesis in rabbits. *Bone*. 2000;27(3):453–459.
- Yonezawa H, Harada K, Ikebe T, Shinohara M, Enomoto S. Effect of recombinant human bone morphogenetic protein-2 (rhBMP-2) on bone consolidation on distraction osteogenesis: A preliminary study in rabbit mandibles. *J Craniomaxillofac Surg*. 2006;34(5):270–276.
- Tavakoli K, Yu Y, Shahidi S, Bonar F, Walsh WR, Poole MD. Expression of growth factors in the mandibular distraction zone: A sheep study. *Br J Plast Surg*. 1999;52(6):434–439.
- Bragdon B, Lybrand K, Gerstenfeld L. Overview of biological mechanisms and applications of three murine models of bone repair: Closed fracture with intramedullary fixation, distraction osteogenesis, and marrow ablation by reaming. *Curr Protoc Mouse Biol*. 2015;5(1):21–34.
- Morgan EF, Hussein AI, Al-Awadhi BA, et al. Vascular development during distraction osteogenesis proceeds by sequential intramuscular arteriogenesis followed by intraosteal angiogenesis. *Bone*. 2012;51(3):535–545.
- Matsubara H, Hogan DE, Morgan EF, Mortolock DP, Einhorn TA, Gerstenfeld LC. Vascular tissues are a primary source of BMP2 expression during bone formation induced by distraction osteogenesis. *Bone*. 2012;51(1):168–180.
- McCarthy JG, Schreiber J, Karp N, Thorne CH, Grayson BH. Lengthening the human mandible by gradual distraction. *Plast Reconstr Surg*. 1992;89(1):1–8;discussion 9–10.
- McCarthy JG. The role of distraction osteogenesis in the reconstruction of the mandible in unilateral craniofacial microsomia. *Clin Plast Surg*. 1994;21(4):625–631.
- Guerrero CA. Surgical jaw expansion [in Spanish]. *Rev Venez Ortod*. 1990;7(1/2):48–50.
- Molina F, Ortiz Monasterio F. Mandibular elongation and remodeling by distraction: A farewell to major osteotomies. *Plast Reconstr Surg*. 1995;96(4):825–840;discussion 841–842.
- McCarthy JG. The development of various distraction devices. In: *Abstract Book of the International Congress on Cranial and Facial Bone Distraction Processes*. Paris, France; 1997:019.
- Diner PA, Kollar EM, Viguier E, Maurin N, Vasquez MP. Intraoral submerged bidirectional device for mandibular distraction. In: *Abstract Book of the International Congress on Cranial and Facial Bone Distraction Processes*. Paris, France; 1997:017.
- Bell WH, Gonzalez M, Samchukov ML, Guerreo CA. Intraoral widening and lengthening of the mandible by distraction osteogenesis. *J Oral Maxillofac Surg*. 1999;57(5):548–562;discussion 563.
- Razdolsky Y, Pensler JM, Dessner S. Skeletal distraction for mandibular lengthening with a completely intraoral tooth-borne distractor: A preliminary report. In: McNamara JA Jr., Trotman CA, eds. *Distraction Osteogenesis and Tissue Engineering*. Ann Arbor, USA: Center for Human Growth and Development, University of Michigan; 1998:117–140.
- Razdolsky Y, Pensler JM. Skeletal distraction for mandibular lengthening with a completely intraoral tooth-borne distractor. In: *Abstract Book of the International Congress on Cranial and Facial Bone Distraction Processes*. Paris, France; 1997:050.
- Seldin EB, Troulis MJ, Kaban LB. Evaluation of a semiburied, fixed trajectory, curvilinear, distraction device in an animal model. *J Oral Maxillofac Surg*. 1999;57(12):1442–1446;discussion 1447–1448.
- Moss ML, Salentijn L. The unitary logarithmic curve descriptive of human mandibular growth. *Acta Anat (Basel)*. 1971;78(4):532–542.
- Ricketts RM. The biologic significance of the divine proportion and Fibonacci series. *Am J Orthod*. 1982;81(5):351–370.
- Smartt JM Jr, Low DW, Bartlett SP. The pediatric mandible: I. A primer on growth and development. *Plast Reconstr Surg*. 2005;116(1):14e–23e.
- Schendel SA. Treatment of maxillo-mandibular deformities with internal curvilinear distraction. *Ann Plast Surg*. 2011;67(6):S1–S9.
- Shetye PR, Davidson EH, Sorkin M, Grayson BH, McCarthy JG. Evaluation of three surgical techniques for advancement of the midface in growing children with syndromic craniosynostosis. *Plast Reconstr Surg*. 2010;126(3):982–994.
- Hopper RA, Sandercoe G, Woo A, et al. Computed tomographic analysis of temporal maxillary stability and pterygomaxillary generate formation following pediatric Le Fort III distraction advancement. *Plast Reconstr Surg*. 2010;126(5):1665–1674.
- Burstein F, Soldanska M, Granger M, Berhane C, Schoemann M. Initial experience with a new intraoral midface distraction device. *J Craniofac Surg*. 2015;26(4):1224–1228.
- Goldwasser BR, Papadaki ME, Kaban LB, Troulis MJ. Automated continuous mandibular distraction osteogenesis: Review of the literature. *J Oral Maxillofac Surg*. 2012;70(2):407–416.
- Hatefi S, Sh ME, Yihun Y, Mansouri R, Akhlaghi A. Continuous distraction osteogenesis device with MAAC controller for mandibular reconstruction applications. *Biomed Eng Online*. 2019;18(1):43.
- Tessier P. The definitive plastic surgical treatment of the severe facial deformities of craniofacial dysostosis. Crouzon's and Apert's diseases. *Plast Reconstr Surg*. 1971;48(5):419–442.
- Ortiz-Monasterio F, del Campo AF, Carrillo A. Advancement of the orbits and the midface in one piece, combined with frontal repositioning, for the correction of Crouzon's deformities. *Plast Reconstr Surg*. 1978;61(4):507–516.
- Wolfe SA, Morrison G, Page LK, Berkowitz S. The monobloc frontofacial advancement: Do the pluses outweigh the minuses? *Plast Reconstr Surg*. 1993;91(6):977–987;discussion 988–989.
- Bradley JP, Gabbay JS, Taub PJ, et al. Monobloc advancement by distraction osteogenesis decreases morbidity and relapse. *Plast Reconstr Surg*. 2006;118(7):1585–1597.
- Ahmad F, Cobb ARM, Mills C, Jones BM, Hayward RD, Dunaway DJ. Frontofacial monobloc distraction in the very young: A review of 12 consecutive cases. *Plast Reconstr Surg*. 2012;129(3):488e–497e.
- Polley JW, Figueroa AA, Charbel FT, Berkowitz R, Reisberg D, Cohen M. Monobloc craniomaxillofacial distraction osteogenesis in a newborn with severe craniofacial synostosis: A preliminary report. *J Craniofac Surg*. 1995;6(5):421–423.
- Refai H, Radwan D, Hassanien N. Radiodensitometric assessment of the effect of pulsed electromagnetic field stimulation versus low intensity laser irradiation on mandibular fracture repair: A preliminary clinical trial. *J Maxillofac Oral Surg*. 2014;13(4):451–457.
- Aronson J. Modulation of distraction osteogenesis in the aged rat by fibroblast growth factor. *Clin Orthop Relat Res*. 2004;(425):264–283.
- Tekin U, Tüz HH, Onder E, Ozkaynak O, Korkusuz P. Effects of alendronate on rate of distraction in rabbit mandibles. *J Oral Maxillofac Surg*. 2008;66(10):2042–2049.
- Pampu AA, Dolanmaz D, Tüz HH, Avunduk MC, Kişniçi RS. Histomorphometric evaluation of the effects of zoledronic acid on mandibular distraction osteogenesis in rabbits. *J Oral Maxillofac Surg*. 2008;66(5):905–910.

49. Buchignani VC, Germano EJ, Dos Santos LM, et al. Effect of low-level laser therapy and zoledronic acid on bone repair process. *Lasers Med Sci.* 2019;34(6):1081–1088.
50. Barushka O, Yaakobi T, Oron U. Effect of low energy laser (He-Ne) irradiation on the process of bone repair in the rat tibia. *Bone.* 1995;16(1):47–55.
51. Cerqueira A, Silveira RL, Oliveira MG, Sant'ana Filho M, Heitz C. Bone tissue microscopic findings related to the use of diode laser (830 nm) in ovine mandible submitted to distraction osteogenesis. *Acta Cir Bras.* 2007;22(2):92–97.
52. Blaya DS, Guimarães MB, Pozza DH, Blessmann Weber JB, de Oliveira MG. Histologic study of the effect of laser therapy on bone repair. *J Contemp Dent Pract.* 2008;9(6):41–48.
53. Lirani-Galvão AP, Jorgetti V, da Silva OL. Comparative study of how low-level laser therapy and low-intensity pulsed ultrasound affect bone repair in rats. *Photomed Laser Surg.* 2006;24(6):735–740.
54. Garavello-Freitas I, Baranauskas V, Joazeiro PP, Padovani CR, Dal Pai-Silva M, da Cruz-Höfling MA. Low-power laser irradiation improves histomorphometrical parameters and bone matrix organization during tibia wound healing in rats. *J Photochem Photobiol B.* 2003;70(2):81–89.
55. Pires Oliveira DAA, de Oliveira RF, Zangaro RA, Soares CP. Evaluation of low-level laser therapy of osteoblastic cells. *Photomed Laser Surg.* 2008;26(4):401–404.
56. Stein E, Koehn J, Sutter W, et al. Initial effects of low-level laser therapy on growth and differentiation of human osteoblast-like cells. *Wien Klin Wochenschr.* 2008;120(3–4):112–117.
57. Amid R, Kadkhodazadeh M, Ahsaie MG, Hakakzadeh A. Effect of low level laser therapy on proliferation and differentiation of the cells contributing in bone regeneration. *J Lasers Med Sci.* 2014;5(4):163–170.
58. de Freitas LF, Hamblin MR. Proposed mechanisms of photobiomodulation or low-level light therapy. *IEEE J Sel Top Quantum Electron.* 2016;22(3):7000417.
59. Huang YY, Chen ACH, Carroll JD, Hamblin MR. Biphasic dose response in low level light therapy. *Dose Response.* 2009;7(4):358–383.
60. Lou S, Lv H, Li Z, Tang P, Wang Y. Effect of low-intensity pulsed ultrasound on distraction osteogenesis: A systematic review and meta-analysis of randomized controlled trials. *J Orthop Surg Res.* 2018;13(1):205.
61. Fedotov SN, Minin EA, Borisov IN. Effect of local cooling and ultrasound on the reparative processes following mandibular fracture [in Russian]. *Stomatologiya (Mosk).* 1986;65(4):4–6.
62. Harris M. The conservative management of osteoradionecrosis of the mandible with ultrasound therapy. *Br J Oral Maxillofac Surg.* 1992;30(5):313–318.
63. Mayr E, Frankel V, Rüter A. Ultrasound – an alternative healing method for nonunions? *Arch Orthop Trauma Surg.* 2000;120(1–2):1–8.
64. Chang WHS, Sun JS, Chang SP, Lin JC. Study of thermal effects of ultrasound stimulation on fracture healing. *Bioelectromagnetics.* 2002;23(4):256–263.
65. Welgus HG, Jeffrey JJ, Eisen AZ, Roswit WT, Stricklin GP. Human skin fibroblast collagenase: Interaction with substrate and inhibitor. *Coll Relat Res.* 1985;5(2):167–179.
66. Fyfe MC, Chahl LA. The effect of ultrasound on experimental oedema in rats. *Ultrasound Med Biol.* 1980;6(2):107–111.
67. Harrison A, Lin S, Pounder N, Mikuni-Takagaki Y. Mode & mechanism of low intensity pulsed ultrasound (LIPUS) in fracture repair. *Ultrasonics.* 2016;70:45–52.
68. Doan N, Reher P, Meghji S, Harris M. In vitro effects of therapeutic ultrasound on cell proliferation, protein synthesis, and cytokine production by human fibroblasts, osteoblasts, and monocytes. *J Oral Maxillofac Surg.* 1999;57(4):409–419;discussion 420.
69. Vavva MG, Grivas KN, Carlier A, et al. Effect of ultrasound on bone fracture healing: A computational bioregulatory model. *Comput Biol Med.* 2018;100:74–85.
70. Baron C, Guivier-Curien C, Nguyen VH, Naili S. Bone repair and ultrasound stimulation: An insight into the interaction of LIPUS with the bone callus through a multiscale computational study. *J Acoust Soc Am.* 2017;142(4):2600.
71. Ding Y, Li G, Zhang X, et al. Effect of low intensity pulsed ultrasound on bone formation during mandible distraction osteogenesis in a canine model – a preliminary study. *J Oral Maxillofac Surg.* 2009;67(11):2431–2439.
72. Kocyigit ID, Coskunses FM, Pala E, Tugcu F, Onder E, Mocan A. A comparison of the low-level laser versus low intensity pulsed ultrasound on new bone formed through distraction osteogenesis. *Photomed Laser Surg.* 2012;30(8):438–443.
73. Alkaisi A, Ismail AR, Mutum SS, Rifin Ahmad ZA, Masudi S, Abd Razak NH. Transplantation of human dental pulp stem cells: Enhance bone consolidation in mandibular distraction osteogenesis. *J Oral Maxillofac Surg.* 2013;71(10):1758.e1–e13.
74. Plachokova AS, Nikolidakis D, Mulder J, Jansen JA, Creugers NHJ. Effect of platelet-rich plasma on bone regeneration in dentistry: A systematic review. *Clin Oral Implants Res.* 2008;19(6):539–545.
75. Mihmanli A, Dolanmaz D, Avunduk MC, Erdemli E. Effects of recombinant human erythropoietin on mandibular distraction osteogenesis. *J Oral Maxillofac Surg.* 2009;67(11):2337–2343.
76. McCarthy JG, Grayson B, Williams JK, Turk A. Distraction of the mandible: The New York University experience. In: McCarthy JG, ed. *Distraction of the Craniofacial Skeleton.* New York, USA: Springer; 1999:80–203.
77. Hassfeld S, Mühling J. Computer assisted oral and maxillofacial surgery – a review and an assessment of technology. *Int J Oral Maxillofac Surg.* 2001;30(1):2–13.
78. Tan A, Chai Y, Mooi W, et al. Computer-assisted surgery in therapeutic strategy distraction osteogenesis of hemifacial microsomia: Accuracy and predictability. *J Craniomaxillofac Surg.* 2019;47(2):204–218.
79. Paeng JY, Lee JH, Lee JH, Kim MJ. Condyle as the point of rotation for 3-D planning of distraction osteogenesis for hemifacial microsomia. *J Craniomaxillofac Surg.* 2007;35(2):91–102.
80. Scolozzi P, Herzog G. Computer-assisted virtual planning for surgical guide manufacturing and internal distractor adaptation in the management of midface hypoplasia in cleft patients. *Cleft Palate Craniofac J.* 2017;54(4):457–464.
81. Badiali G, Cutolo F, Roncari A, Marchetti C, Bianchi A. Simulation-guided navigation for vector control in pediatric mandibular distraction osteogenesis. *J Craniomaxillofac Surg.* 2017;45(6):969–980.
82. Grayson BH, Santiago PE. Treatment planning and biomechanics of distraction osteogenesis from an orthodontic perspective. *Semin Orthod.* 1999;5(1):9–24.
83. Pucci R, Priore P, Manganiello L, Cassoni A, Valentini V. Accuracy evaluation of virtual surgical planning (VSP) in orthognathic surgery: Comparison between CAD/CAM fabricated surgical splint and CAD/CAM cutting guides with PSI. *J Oral Maxillofac Surg.* 2019;77(9):E4–E5.
84. Kim MJ, Seo J, Kim DK, Baek SH. Three-dimensional virtual-surgery simulation-assisted asymmetric bilateral mandibular distraction osteogenesis for a patient with bilateral condylar fractures. *Am J Orthod Dentofacial Orthop.* 2017;151(1):186–200.

Acrylic resins in the CAD/CAM technology: A systematic literature review

Zbigniew Raszewski^{A,B,D–F}

SpofaDental a.s., Jicin, Czech Republic

A – research concept and design; B – collection and/or assembly of data; C – data analysis and interpretation;
D – writing the article; E – critical revision of the article; F – final approval of the article

Dental and Medical Problems, ISSN 1644-387X (print), ISSN 2300-9020 (online)

Dent Med Probl. 2020;57(4):449–454

Address for correspondence

Zbigniew Raszewski
E-mail: Zbigniew.Raszewski@kavokerr.com

Funding sources

None declared

Conflict of interest

None declared

Received on April 28, 2020

Reviewed on June 1, 2020

Accepted on June 25, 2020

Published online on December 31, 2020

Abstract

At present, new acrylic plastic technologies are being developed in dentistry. Although this kind of material has been used for dental prostheses for over 80 years, it has been produced in the form of disks with the computer-aided design/computer-aided manufacturing (CAD/CAM) technology for over 15 years.

The purpose of the article was to collect information from the literature on acrylic materials processed through the milling technology (CAD/CAM). The publicly available databases PubMed, Google Scholar and Scopus were searched using the key word “acrylic resins, CAD/CAM”. All articles describing the application and testing of CAD/CAM disks were selected. Duplicate articles were removed. More than 100 articles that described the use of materials machined using the milling equipment were found. These included works comparing the mechanical properties, biocompatibility and clinical use of the materials. After the initial selection, 36 papers on this subject were included in this review.

The number of studies on the processing of acrylic materials with the use of the CAD/CAM technology has been increasing worldwide. Since such materials have better mechanical properties, no polymerization shrinkage occurs during processing, the amount of residual monomer material is very low and they have better color stability than self-curing materials.

Key words: acrylic resin, surface, flexural strength, residual monomer, CAD/CAM

Cite as

Raszewski Z. Acrylic resins in the CAD/CAM technology: A systematic literature review. *Dent Med Probl.* 2020;57(4):449–454. doi:10.17219/dmp/124697

DOI

10.17219/dmp/124697

Copyright

© 2020 by Wrocław Medical University

This is an article distributed under the terms of the Creative Commons Attribution 3.0 Unported License (CC BY 3.0) (<https://creativecommons.org/licenses/by/3.0/>).

Introduction

Traditional acrylic materials consist of a powder and a monomer mixed together to form dough. In the case of thermally polymerized materials, it is necessary to supply heat energy to start the reaction. Self-curing materials polymerize at room temperature or in warm water of a temperature below 65°C. So far, the polymerization process have been carried out in a dental technician's workshop, or in special cases – in a dentist's office.^{1–5}

This type of process leads to the contraction of the material, and in some cases, it can lead to the formation of porous structures inside the material after polymerization.⁶ In the computer-aided design/computer-aided manufacturing (CAD/CAM) technology using acrylic disks, the curing process is carried out directly at the manufacturer's. Although the details of the production process are a trade secret, some stages remain unchanged. These include mixing the powder and the liquid in appropriate proportions, and storing the dough at a low temperature (–18°C) for about 24 h. In the next step, the dough is placed into molds, pressed, and gradually polymerized at gradually increasing temperatures. The whole task is to increase the degree of polymerization without creating voids (pores inside the material). The result is a product with very long polymer chains, low residual monomer content and high hardness.^{7,8}

Currently, disks in tooth colors A1–C4 in the Vita® classical system are monochromatic or in 3–5 layers (from the lightest – A1 to A4). Thus, from one block it is possible to make crowns and bridges smaller in the cervical layer and lighter on the incisal edge.^{9,10}

Apart from that, there are acrylic blocks in pink for making denture bases and transparent ones for making surgical guides in implantology.¹⁰

There are also hybrid materials on the market, which are a combination of ceramic and acrylic disks, so-called polymer-infiltrated ceramic (Vita Enamic®; Vita Zahnfabrik, Bad Säckingen, Germany). According to Patel, this kind of material has a very high fracture strength of about 180 MPa.⁹

In some systems for making dentures, the denture plate itself is milled and the teeth, produced with the traditional technology, are glued into the prepared holes with a self-curing material and a bonding agent (e.g., from Ivoclar Vivadent, Schaan, Liechtenstein). Other manufacturers recommend cutting teeth from one block and denture plates from another (AvaDent, Omaha, USA).¹⁰

A comparison of commercially available systems for the production of dentures based on the CAD/CAM system is comprehensively presented in an article by Baba (Ceramill® Full Denture System; Amann Girrbach, Pforzheim, Germany; Dentca™; Dentca Inc., Torrance USA; Avadent™; Global Dental Science, Scottsdale, USA; Wieland®; Wieland Dental + Technik, Pforzheim, Germany) and by other researchers.^{1,10}

Material and methods

The publicly available PubMed, Google Scholar and Scopus databases were searched with the key word “acrylic resins, CAD/CAM” for articles from 2010 through 2020. The 1st screening of the literature databases returned 106 articles. The availability of articles in English or Polish (with an English abstract) was used as the 1st criterion. The selection was then checked and duplicate articles were rejected. Articles describing the application and testing of CAD/CAM acrylic disks were used. The total number of studies and the methods applied for screening for the review as well as the summary of the screening results are presented in Fig. 1. All the excluded articles together with the reasons for exclusion are shown in Table 1.

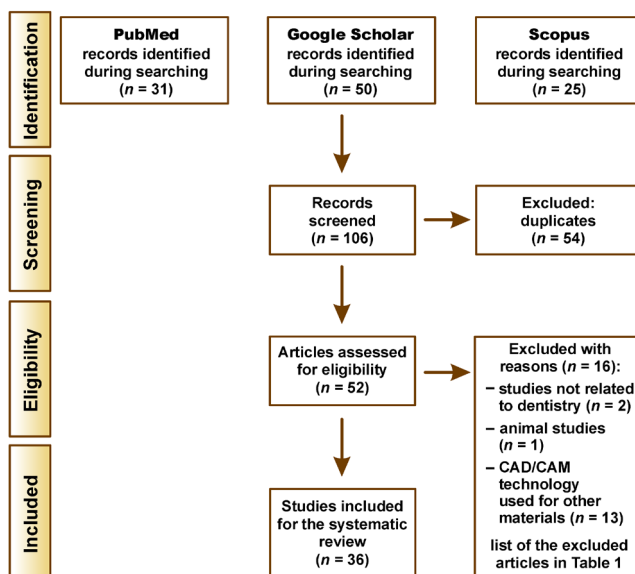


Fig. 1. Flow chart of the criteria for selecting articles
CAD/CAM – computer-aided design/computer-aided manufacturing.

Results

After the exclusion criteria were applied, 36 source articles were identified. Four of them appeared in more than 1 database, so they were used only once. The remaining articles were divided into 3 groups depending on what they referred to: mechanical properties; biocompatibility; and clinical use.

Mechanical properties

Andreescu et al. compared the mechanical properties of various acrylic materials available in the form of disks and intended for making denture plates.¹⁰ The following were used in the research: Avadent, Baltic Denture System™ (Merz Dental, Lütjenburg, Germany), Ceramill Full Denture System, Dentca/Whole You™ (Dentca Inc.), and Wieland Digital Denture™ (Wieland Dental + Technik).¹⁰ The flexural strength of the prefabricated materials is up to 146 MPa. The residual monomer content is also very low (less than 1%).

Table 1. Selection of publications

No.	Publication	Reason for exclusion
1	Wimmer T, Huffmann AMS, Eichberger M, Schmidlin PR, Stawarczyk B. Two-body wear rate of PEEK, CAD/CAM resin composite and PMMA: Effect of specimen geometries, antagonist materials and test set-up configuration. <i>Dent Mater.</i> 2016;32(6):e127–e136.	PMMA used for testing; it is not a CAD/CAM sample
2	Papaspyridakos P, Lal K. Immediate loading of the maxilla with prefabricated interim prosthesis using interactive planning software, and CAD/CAM rehabilitation with definitive zirconia prosthesis: 2-year clinical follow-up. <i>J Esthet Restor Dent.</i> 2010;22(4):223–234.	zirconium dioxide used as the main construction component, not an acrylic resin
3	Drago C, Saldarriaga RL, Domagala D, Almasri R. Volumetric determination of the amount of misfit in CAD/CAM and cast implant frameworks: A multicenter laboratory study. <i>Int J Oral Maxillofac Implants.</i> 2010;25(5):920–929.	the implant made with the use of the CAD/CAM and lost-wax technologies, the prosthesis made from a heat-curing resin, not CAD/CAM
4	Proussaefs P. Immediate provisionalization with a CAD/CAM interim abutment and crown: A guided soft tissue healing technique. <i>J Prosthet Dent.</i> 2015;113(2):91–95.	the final crown made from a ceramic material
5	Albero A, Pascual A, Camps I, Grau-Benitez M. Comparative characterization of a novel cad-cam polymer-infiltrated-ceramic-network. <i>J Clin Exp Dent.</i> 2015;7(4):e495–e500.	ceramic CAD/CAM materials tested
6	Cho Y, Raigrodski AJ. The rehabilitation of an edentulous mandible with a CAD/CAM zirconia framework and heat-pressed lithium disilicate ceramic crowns: A clinical report. <i>J Prosthet Dent.</i> 2014;111(6):443–447.	a ceramic CAD/CAM material used for rehabilitation
7	Bonfante EA, Suzuki M, Lorenzoni FC, et al. Probability of survival of implant-supported metal ceramic and CAD/CAM resin nanoceramic crowns. <i>Dent Mater.</i> 2015;31(8):e168–e177.	a ceramic CAD/CAM material tested
8	Dehurtevent M, Robberecht L, Béhin P. Influence of dentist experience with scan spray systems used in direct CAD/CAM impressions. <i>J Prosthet Dent.</i> 2015;113(1):17–21.	a heat-curing acrylic resin used for testing
9	Başaran EG, Ayna E, Vallittu PK, Lassila LVJ. Load bearing capacity of fiber-reinforced and unreinforced composite resin CAD/CAM-fabricated fixed dental prostheses. <i>J Prosthet Dent.</i> 2013;109(2):88–94.	a composite resin used for testing
10	Ji MK, Park JH, Park SW, Yun KD, Oh GJ, Lim HP. Evaluation of marginal fit of 2 CAD-CAM anatomic contour zirconia crown systems and lithium disilicate glass-ceramic crown. <i>J Adv Prosthodont.</i> 2015;7(4):271–277.	a ceramic CAD/CAM material tested
11	Lin WS, Metz MJ, Pollini A, Ntounis A, Morton D. Digital data acquisition for a CAD/CAM-fabricated titanium framework and zirconium oxide restorations for an implant-supported fixed complete dental prosthesis. <i>J Prosthet Dent.</i> 2014;112(6):1324–1329.	a ceramic CAD/CAM material tested
12	Tsitrou EA, Helvatjoglu-Antoniades M, van Noort R. A preliminary evaluation of the structural integrity and fracture mode of minimally prepared resin bonded CAD/CAM crowns. <i>J Dent.</i> 2010;38(1):16–22.	composite and ceramic materials used for testing
13	Spyropoulou PE, Razzoog ME, Duff RE, Chronaios D, Saglik B, Tarazzi DE. Maxillary implant-supported bar overdenture and mandibular implant-retained fixed denture using CAD/CAM technology and 3-D design software: A clinical report. <i>J Prosthet Dent.</i> 2011;105(6):356–362.	titanium used in the CAD/CAM technology
14	Bentz RM, Balshi SF. Complete oral rehabilitation with implants using CAD/CAM technology, stereolithography, and conosopic holography. <i>Implant Dent.</i> 2012;21(1):8–12.	a composite material used for CAD/CAM
15	Maunula H, Hjerpe J, Lassila LLV, Närhi TO. Optical properties and failure load of thin CAD/CAM ceramic veneers. <i>Eur J Prosthodont Restor Dent.</i> 2017;25(2):86–92.	a ceramic material used for testing
16	Ciocca L, Mingucci R, Gassino G, Scotti R. CAD/CAM ear model and virtual construction of the mold. <i>J Prosthet Dent.</i> 2007;98(5):339–343.	non-dental use (ear making)

PMMA – polymethyl methacrylate.

Similar work was performed by Saad et al., who tested flexural strength, impact resistance, surface roughness, and residual monomer concentration.¹¹ Comparison tests were conducted for the heat-curing materials Acrostone® (Acrostone, Cairo, Egypt) and Momentive Performance Materials (MP-M) (Merz Dental). Acrylic resins were polymerized in long cycles – for 7 h at 70°C and for 30 min at 100°C. The results from this study show that the MP-M samples have better mechanical properties than the conventional acrylic resin. For example, the flexural strength for the CAD/CAM samples was 116.79 ±24.95 MPa, and for the heat-curing resin it was 94.58 ±5.75 MPa.¹¹

The higher resistance to swapping and greater flexibility module of acrylic disks have also been confirmed by other authors (Yilmaz et al.¹² and Neves Pascutti et al.¹³). They tested 8 different brands of acrylic CAD/CAM disks and compared them with the values provided by

the producers. In some cases, the fracture toughness value was up to 10–15% lower. Buduru et al. stated that some disk had 0.16% unpolymerized methyl methacrylate (MMA) inside the material.¹⁴

Steinmassl et al. performed an investigation of the residual monomer releasing from a conventional denture made with the CAD/CAM technology after 7-day storage in water.¹⁵ Four systems were investigated: Baltic Denture System, Vita VIONIC® (Vita Zahnfabrik), Wieland Digital Denture, and Whole You Nexteeth™ (Whole You Inc., San Jose, USA). In addition, the authors examined the density of the milled dentures and their surface area. Baltic Denture System and Whole You Nexteeth had a significantly higher density as compared to the conventional acrylic resin; Baltic Denture System had a significantly smaller surface area. The concentration of residual monomer varied from 0.6 to 6 ppm, depending on the manufacturer.¹⁵

One of the important mechanical parameters, even one that is required by the standard ISO 20795-1:2013,¹⁶ is the stability of the bars of the material from which the medical device is made. This topic was raised in a study by Dayan et al., who compared the color change of self-curing (Weropress®; Merz Dental), heat-curing (Paladent®; Heraeus Kulzer, Hanau, Germany), light-curing (Eclipse®; Dentsply Sirona, York, USA) resins, and samples milled from CAD/CAM disks (M-PM).¹⁷ Standard solutions were used for the tests – coffee, cola, red wine, and distilled water (control group). The results were measured with a spectrophotometer before and after storage (after 7 and 30 days), and any color changes (ΔE) were calculated. The smallest color changes were recorded for the samples made from a CAD/CAM disk. The greatest color changes were seen in the case of the materials which were treated with red wine.¹⁷ Similar observations about color changing were reported by Al-Qarni et al.¹⁸

Rayyan et al. tested differences in color, water sorption and solubility, and dye penetration between various materials for interim restorations, which are used to protect the pulp against thermal, mechanical, physical, and bacterial contamination.¹⁹ One representative was chosen for each group: CAD/CAM (Cercon® PMMA; DeguDent, Rosbach vor der Höhe, Germany), self-curing powder/liquid (Alike™; GC Corporation, Tokyo, Japan), bis-acrylic (Acrytemp™, Zhermack, Badia Polesine, Italy), and DuraCetal® (Myerson, Chicago, USA). Under a microscopic examination, the samples prepared from the polymethyl methacrylate (PMMA) block showed no dye penetration through zinc oxide-based interim cement (RelyX Temp NE®; 3M ESPE, Seefeld, Germany) when placed in a polyester mold. A comparison between the sorption of individual materials interestingly showed that in the case of the samples milled from PMMA, it was $8.7 \pm 0.7 \mu\text{g}/\text{mm}^3$, while for the traditional acrylic resin it was $28.5 \pm 2.0 \mu\text{g}/\text{mm}^3$. Similar observations were presented for abrasion – the samples made from a CAD/CAM disk had values which were half that of the other materials.¹⁹

Materials used for dentures have to demonstrate proper light translucency and fluorescence to imitate soft tissues and the teeth in the patient's mouth. This issue has been presented by Güth et al. for 5 manual and 11 CAD/CAM polymer materials, using a spectrophotometer.²⁰

Marginal adaptation, wear resistance and fracture resistance were compared between heat-curing and CAD/CAM acrylic resins by Elagra et al.²¹ Marginal adaptation was tested using a stereomicroscope; afterward, the images were analyzed by means of software to measure the marginal gap between the model and the crown. CAD-Temp® (Vita Zahnfabrik) had an average space of $15.026 \pm 4.340 \mu\text{m}$, while the value for the self-curing resin TempSpan® (Kerr Corporation, Orange, USA) was ten-fold higher: $145.418 \pm 25.365 \mu\text{m}$.²¹

Modern prosthetics very often requires very different materials to be joined together – acrylic, composite,

metal, and others. It can be particularly difficult in the case of the acrylic ones made with the CAD/CAM technology, where the material is polymerized under high pressure and at temperatures exceeding 100°C. This issue was discussed in more detail by Stawarczyk et al., who tested the connection between the Gradia® composite (GC Corporation) and 3 different PMMA blocks – CAD-Temp, artBloc® Temp (Merz Dental) and Telio CAD® (Ivoclar Vivadent) – after 7-days storage in distilled water.²² Such joints are crucial, for example, when it is necessary to customize teeth milled from a PMMA block by using composite dyes, which are available in a larger range of colors. The authors prepared the acrylic surface in the following ways: no treatment; air abrasion ($50 \mu\text{m Al}_2\text{O}_3$); air abrasion with a silanating agent ($50 \mu\text{m Al}_2\text{O}_3 + 3\text{-methacryloxypropyltrimethoxysilane (MPS) (Monobond S®; Ivoclar Vivadent))$ and an adhesive resin (StickRESIN®; Everstick, Turku, Finland) for Gradia/MMA application; and silica coating and silanization (CoJet-System™; 3M ESPE). The conclusion reported in this study was that CAD/CAM polymers could be veneered only with a PMMA-based veneer, with and without air abrasion. Adhesion between the acrylic block and the composite after water storage was very weak; mainly cohesive delamination was observed.²²

During use, dentures should be cleaned to maintain hygiene; some patients use toothbrushes and pastes for this purpose. The resulting increase in surface roughness and weight loss has been tested by Shinawi.²³ For this purpose, Polident disks (Polident, Volčja Draga, Slovenia) were used, being subjected to abrasion tests with 40,000 and 60,000 brush strokes, which corresponds to approx. 3 years of brushing. Increased surface roughness leads to faster biofilm accumulation and colonization of various microorganisms, which can lead to mucosal inflammation and halitosis. As a result, surface roughness increased by 0.06 and 0.08 μm , and the simultaneous weight loss was 0.22 and 0.4 mg after 40,000 and 60,000 brushing cycles, respectively.²³

Studies on the smoothness of the surface of acrylic plastics in the form of CAD/CAM disks were presented by Alammari.²⁴ The samples were polished by mechanical (pumice slurry and a polishing paste with Al_2O_3 (Universal Polishing Paste®; Ivoclar Vivadent)) and chemical means, and their surface roughness was measured. Chemical polishing was performed in a preheated jar containing MMA monomer at $75 \pm 1^\circ\text{C}$ for 10 s. The author considered mechanical polishing as the most effective polishing technique and concluded that a better surface was obtained for the samples of CAD/CAM resins as compared to the heat-curing material.²⁴

Biological compatibility

One of the first screening tests to determine whether a material is biocompatible is cytotoxicity testing on different cell cultures. In the data provided by manufacturers,

it is sometimes possible to find such information. For example, inno/Blanc CORiTEC® (imes-icore, Eiterfeld, Germany) has a cell survival rate of 96–98% under 24-hour exposure.¹⁴

The adhesion of *Candida albicans* to the surfaces of denture plates made with the CAD/CAM technology was tested in relation to the traditional resins by Al-Fouzan et al.²⁵ After a 24-hour incubation period, the number of colonies present on the surface of the acrylic sample was calculated. In the case of CAD/CAM disks, this value was 1.1×10^3 , while for the traditional heat-polymerized resin it was 2.3×10^3 .²⁵

Souza et al. tested a very important property of acrylic materials, i.e., cytotoxicity.²⁶ The samples of materials for manufacturing crowns and bridges were in contact with a cell culture for 24 h. One of the tested materials was VIPI BLOCK TRILUX® (VIPI, Pirassununga, Brasil) – an acrylic resin material used in the CAD/CAM technology, which was analyzed for the viability of oral keratinocytes (NOK-SI (RRID:CVCL-BW57)) from human oral mucosa. Alamar blue was used for detection. Cell survival for this material was not disturbed, in contrast to the self-curing type of acrylic materials. In addition, the authors compared surface smoothness and the adhesion of cells to the selected materials. The lowest roughness value was reported for the material in the form of milling disks.²⁶

Clinical use

Buduru et al. made a comparison of 2 new methods used to make splints with the CAD/CAM and three-dimensional (3D) printing technologies.¹⁴ Such devices allow the etiology of pain to be diagnosed, muscle or temporomandibular joint pain to be treated, or new occlusal positions to be tested. In both methods, instead of the traditional impression, an intraoral scanner (3Shape Trios®; 3Shape, Copenhagen, Denmark) was used. During the next step, a digital splint, 3-millimeter-thick, was made using the 3Shape Appliance Designer™ (3Shape). The 1st splint was fabricated from a disk (imes-icore), using the Zenotec Select™ milling machine (Wieland Dental + Technik). The 2nd device was prepared with Dental LT Clear Resin® (Formlabs Inc., Somerville, USA) and the printer used was Form 2 (Formlabs Inc.) with the stereolithography technique. The benefits of digital splints were appreciated in terms of working time, because the traditional technique required more than 5 h in the dental laboratory. Computer processing takes 1 h, a CAD/CAM device can be milled in 75 min and using the 3D printing technology takes 90 min. The 2nd parameter – the fit of the digital splint (both milled and printed) – was significantly better than that of the conventional splint. The best occlusion was obtained from the printed splint, and with the same benefits for the cost, since the cost of printing

an occlusal splint is lower than the cost of milling one. In addition, there is not as much material waste as in the case of CAD/CAM.¹⁴

Infante et al. gave a detailed description on using the AvaDent system to produce removable dentures.²⁷ Firstly, impressions are taken using individual trays with silicones; then, the contacts between the jaw and the mandible are established using special maxillary and mandibular anatomic measuring devices (AMDs). After all of the impressions are sent back to AvaDent, the company prepares the denture with the CAD/CAM technology. The teeth are fixed into the denture base with a self-curing material. There is also an option of milling a model of the denture in wax with embedded teeth, which goes to the dentist to test the position and color of the teeth.²⁷ Other systems for milling CAD/CAM dentures used in clinical practice were described in a study by Han et al.²⁸

Clinicians will be very interested in the accuracy and matching of prostheses made from an injection-molded material under pressure (Ivocap®; Ivoclar Vivadent) and restorations milled from acrylic disks (VIPI BLOCK TRILUX; VIPI). According to Lee et al., the accuracy measured in 2 points of the mid-palatal suture was significantly lower for than for the other method; however, the degree of fine reproducibility was higher in the case of the injection-molding technique.²⁹

A clinical examination was carried out by Ali and Al-Harbi on 2 upper dentures for 1 patient, one made from the traditional heat-polymerized acrylic resin and the other milled from an acrylic block.³⁰ Then, they tested the force required to dislodge the maxillary prosthesis. Their results indicated that a force of over 2,000 gf was needed to remove the restoration from the oral cavity, whereas the traditional one had a lower adhesion of about 1,400 gf.³⁰

Other authors compared the accuracy of dentures produced with the CAD/CAM technology to traditional supplements.^{31–35} Everyone is of the opinion that milled dentures have a slightly better fit in comparison with traditional dentures. This is due to the shrinkage of the material during polymerization, the lower surface roughness coefficient and the more homogeneous surface of the polymerized material in industrial conditions, among other things.


Conclusions

The literature review clearly indicates that acrylic materials used in the CAD/CAM technology have better mechanical and biological properties than traditional acrylic materials. The only disadvantage of these materials is the waste of the remaining material after milling the restoration, which can no longer be used. At present, a new 3D printing technology is becoming more and more important. However, it still has some limitations, e.g., the inability to print multicolor teeth with an appropriate degree of translucency.^{12,13,15,28,35,36}

Yet, CAD/CAM materials have a lower adhesion between the acrylic teeth and the denture plate. This is due to the fact that in the case of heat-curing materials, the teeth are polymerized along with the denture plate. In most CAD/CAM systems, however, the teeth are glued using a self-curing resin. In addition, CAD/CAM blocks are harder and more cross-linked. There are fewer double bonds to which the self-curing resin can be attached. Some authors have concluded that polymer beads may not dissolve completely into monomer prior to polymerization, and the fast drying of bonding agents after contact with CAD/CAM blocks and acrylic teeth gives poor mechanical retention.^{35,36}

Prosthetic processes in the CAD/CAM technology should be used when higher mechanical resistance, better surface smoothness and better color stability are required as well as when semi-permanent crowns and bridges and removable dentures are needed.

ORCID iDs

Zbigniew Raszewski  <https://orcid.org/0000-0002-1735-3879>

References

- Baba NZ. Materials and processes for CAD/CAM complete denture fabrication. *Curr Oral Health Rep.* 2016;3(3):203–208.
- Alghazaawi TF. Advancements in CAD/CAM technology: Options for practical implementation. *J Prosthodont Res.* 2016;60(2):72–84.
- Hamm J, Berndt EU, Beuer F, Zachriat C. Evaluation of model materials for CAD/CAM in vitro studies. *Int J Comput Dent.* 2020;23(1):49–56.
- Borowicz J, Tymczyna-Borowicz BW. Methods of obtaining metal structures used in dental prosthetics. *Prosthodontics.* 2019;69(2):129–190.
- Marcinowski M. *The Use of Interactive 3D Tooth Atlas Program in the Teaching of Dental Students* [doctoral thesis]. Poznań, Poland: Poznan University of Medical Sciences; 2012.
- Kasina SP, Ajaz T, Attili S, Surapaneni H, Cherukuri M, Srinath HP. To evaluate and compare the porosities in the acrylic mandibular denture bases processed by two different polymerization techniques, using two different brands of commercially available denture base resins – an in vitro study. *J Int Oral Health.* 2014;6(1):72–77.
- Reynaud PL, Chu MQ, Gonzalez M, Rajon C. Cad/cam-machinable disc for the manufacture of fiber inlay-cores. European Patent, 2017; WO2017098096A1. <https://patents.google.com/patent/WO2017098096A1/en>. Accessed on April 20, 2020.
- Sun BJ, Ammon D. Multiple layered denture block and/or disk. European Patent, 2018; WO2018009518A1. <https://patents.google.com/patent/WO2018009518A1/en>. Accessed on April 20, 2020.
- Patel A. Comparing flexural strength of acrylic processed by three different techniques. 2014; Graduate Theses, Dissertations, and Problem Reports. 517. <https://researchrepository.wvu.edu/etd/517>. Accessed on April 20, 2020.
- Andrescu CF, Ghergic DL, Botoaca O, Hancu V, Banateanu AM, Patroi DN. Evaluation of different materials used for fabrication of complete digital denture. *Mater Plast.* 2018;55(1):124–128.
- Saad YM, Abdelhamid AM, ElShabrawy SM. Laboratory evaluation of pre-polymerized denture base material used for CAD/CAM complete denture manufacturing. *Alex Dent J.* 2018;43(3):94–101.
- Yilmaz B, Alp G, Seidt J, Johnston WM, Vitter R, McGlumphy EA. Fracture analysis of CAD-CAM high-density polymers used for interim implant-supported fixed, cantilevered prostheses. *J Prosthet Dent.* 2018;120(1):79–84.
- Neves Pascutti FP, Kreve S, de Carvalho GAP, Grecco P, Gonçalves Franco AB, Dias SC. Evaluation in vitro of flexural strength of three resins for provisional crowns in CAD/CAM System. *Res Rev J Dent Sci.* 2017;5(2):75–82.
- Buduru S, Talmaceanu D, Baru O, Buduru R, Suzhanek C, Mesaros A. CAD-CAM occlusal splints: Milling and printing methods. *Rev Chim.* 2018;69(12):3461–3463.
- Steinmassl PA, Wiedemair V, Huck C, et al. Do CAD/CAM dentures really release less monomer than conventional dentures? *Clin Oral Investig.* 2017;21:1697–1705.
- ISO 20795-1:2013 – Dentistry – Base polymers – Part 1, 2013. <https://www.iso.org/standard/62277.html>. Accessed on April 20, 2020.
- Dayan C, Guven MC, Gencil B, Bural C. A comparison of the color stability of conventional and CAD/CAM polymethyl methacrylate denture base materials. *Acta Stomatol Croat.* 2019;53(2):158–167.
- Al-Qarni FD, Goodacre CJ, Kattadiyil MT, Baba NZ, Paravina RD. Stainability of acrylic resin materials used in CAD-CAM and conventional complete dentures. *J Prosthet Dent.* 2020;123(6):880–887.
- Rayyan MM, Aboushelib M, Sayed NM, Ibrahim A, Jimbo R. Comparison of interim restorations fabricated by CAD/CAM with those fabricated manually. *J Prosthet Dent.* 2015;114(3):414–419.
- Güth JF, Zuch T, Zwinge S, Engels J, Stimmelmayer JM, Edelhoff D. Optical properties of manually and CAD/CAM-fabricated polymers. *Dent Mater J.* 2013;32(6):865–871.
- Elagra MEI, Shalaby Y, Khalil MF, Elfawal N. Comparative study of marginal adaptation and mechanical properties of CAD/CAM versus dual polymerized interim fixed dental prosthesis. *Saudi J Oral Sci.* 2014;1(2):71–79.
- Stawarczyk B, Trottmann A, Hämmerle CHF, Özcan M. Adhesion of veneering resins to polymethylmethacrylate-based CAD/CAM polymers after various surface conditioning methods. *Acta Odontol Scand.* 2013;71(5):1142–1148.
- Shinawi LA. Effect of denture cleaning on abrasion resistance and surface topography of polymerized CAD CAM acrylic resin denture base. *Electron Physician.* 2017;9(5):4281–4288.
- Alammari MR. The influence of polishing techniques on pre-polymerized CAD/CAM acrylic resin denture bases. *Electron Physician.* 2017;9(10):5452–5458.
- Al-Fouzan AF, Al-Mejrad LA, Albarrag AM. Adherence of *Candida* to complete denture surfaces in vitro: A comparison of conventional and CAD/CAM complete dentures. *J Adv Prosthodont.* 2017;9(5):402–408.
- Souza IR, Pansani TN, Basso FG, Hebling J, de Souza Costa CA. Cytotoxicity of acrylic resin-based materials used to fabricate interim crowns. *J Prosthet Dent.* 2020;124(1):122.e1–122.e9.
- Infante L, Yilmaz B, McGlumphy E, Finger I. Fabricating complete dentures with CAD/CAM technology. *J Prosthet Dent.* 2014;111(5):351–355.
- Han W, Li Y, Zhang Y, et al. Design and fabrication of complete dentures using CAD/CAM technology. *Medicine (Baltimore).* 2017;96(1):e5435.
- Lee S, Hong SJ, Paek J, Pae A, Kwon KR, Noh K. Comparing accuracy of denture bases fabricated by injection molding, CAD/CAM milling, and rapid prototyping method. *J Adv Prosthodont.* 2019;11(1):55–64.
- Ali MSA, Al-Harbi FA. Posterior palatal seal area established in conventional and CAD/CAM fabricated complete denture techniques: Clinical case study. *J Dent Craniofac Res.* 2016;1(3):1–6.
- Sierra JA. *Comparison of Anterior Denture Teeth Arrangements Made with the Tooth Mold Template and Definitive Computer-Aided Design & Computer-Aided Manufacturing Complete Removable Dental Prostheses* [master's thesis]. Milwaukee, USA: Marquette University; 2017.
- de Oliveira Lopes AC, Machado CM, Bonjardim LR, et al. The effect of CAD/CAM crown material and cement type on retention to implant abutments. *J Prosthodont.* 2019;28(2):e552–e556.
- Kanazawa M, Inokoshi M, Minakuchi S, Ohbayashn N. Trial of a CAD/CAM system for fabricating complete dentures. *Dent Mater J.* 2011;30(1):93–96.
- Aguirre BC, Chen JH, Kontogiorgos ED, Murchison DF, Nagy WW. Flexural strength of denture base acrylic resins processed by conventional and CAD/CAM methods. *J Prosthet Dent.* 2020;123(4):641–646.
- Eun Choi JJ, Uy CE, Plaksina P, Ramani RS, Ganjigati R, Waddell JN. Bond strength of denture teeth to heat-cured, CAD-CAM and 3D printed denture acrylics. *J Prosthodont.* 2020;29(5):415–421.
- Joshi N. *Physical and Optical Properties of Provisional Crown and Bridge Materials Fabricated Using CAD/CAM Milling or 3D Printing Technology* [master's thesis]. Fort Lauderdale, USA: College of Dental Medicine, Nova Southeastern University; 2019.

Scarlet fever – a diagnostic challenge for dentists and physicians: A report of 2 cases with diverse symptoms

Zuzanna Ślebioda^{A–D,F}, Agnieszka Mania-Końsko^{A–D,F}, Barbara Dorocka-Bobkowska^{A,E,F}

Department of Gerodontology and Oral Pathology, Faculty of Medicine, Poznan University of Medical Sciences, Poland

A – research concept and design; B – collection and/or assembly of data; C – data analysis and interpretation;
D – writing the article; E – critical revision of the article; F – final approval of the article

Dental and Medical Problems, ISSN 1644-387X (print), ISSN 2300-9020 (online)

Dent Med Probl. 2020;57(4):455–459

Address for correspondence

Zuzanna Ślebioda

E-mail: zuzia_slebioda@o2.pl

Funding sources

None declared

Conflict of interest

None declared

Received on May 9, 2020

Reviewed on June 6, 2020

Accepted on July 20, 2020

Published online on December 31, 2020

Abstract

Scarlet fever is an infectious disease caused by group A streptococcal bacteria, transmitted mainly through direct contact with the saliva and nasal fluids of infected people. It may also arise from streptococcal wound infections or burns. The disease most commonly affects children aged 5–15 years and manifests as a sore throat, fever and a sandpaper-like, papular skin rash. Due to the evident involvement of the oral structures, the awareness of the symptoms of scarlet fever is essential for dentists in order to avoid the spread of this highly contagious disease in crowded places, such as kindergartens and schools. As no vaccine is available to prevent scarlet fever, the early diagnosis and treatment of this condition are important in reducing the risk of developing local and systemic complications, which include acute rheumatic fever, glomerulonephritis, bacteremia, pneumonia, endocarditis, and meningitis.

In this report, 2 cases of scarlet fever are described in unrelated children with diverse symptoms, and diagnostic and therapeutic strategies are discussed.

Key words: oral pathology, oral mucosa, scarlet fever

Cite as

Ślebioda Z, Mania-Końsko A, Dorocka-Bobkowska B. Scarlet fever – a diagnostic challenge for dentists and physicians: A report of 2 cases with diverse symptoms. *Dent Med Probl.* 2020;57(4):455–459. doi:10.17219/dmp/125574

DOI

10.17219/dmp/125574

Copyright

© 2020 by Wrocław Medical University

This is an article distributed under the terms of the

Creative Commons Attribution 3.0 Unported License (CC BY 3.0)

(<https://creativecommons.org/licenses/by/3.0/>).

Introduction

Scarlet fever is a disease caused by infective group A streptococcal bacteria.^{1–3} The route of transmission is mainly through direct contact with the saliva and nasal fluids of infected people. Scarlet fever may also arise from streptococcal wound infections or burns. Food-borne outbreaks have also been reported.^{1,2} A recent report indicates a potential relationship between opportunistic *Streptococcus sanguis* (*S. sanguis*) and scarlet fever.⁴ The disease most commonly affects children 5–15 years of age, in winter and spring, and manifests as a sore throat, fever and a sandpaper-like, papular, general skin rash. Rare cases of scarlet fever in elderly patients have also been reported.⁵ The characteristic appearance of the tongue, described as ‘strawberry tongue’ or ‘raspberry tongue’, is a common symptom.^{4–8} Although the incidence of scarlet fever declined in the past few decades, an increase in the number of cases worldwide has been observed recently. A newer virulent streptococcal bacterium is one of the potential causes of this reemergence of the disease. Major outbreaks have been reported in Asia, particularly in Vietnam and mainland China; smaller outbreaks have also occurred in the USA and Canada. The largest outbreak in the UK since 1969 was reported in 2015.^{1,2,9–13} Meanwhile, no serious exacerbations of scarlet fever have been observed in New Zealand, which may be partially explained by the 2012 introduction of a nationwide program for reducing acute rheumatic fever by treating *Streptococcus pyogenes* (*S. pyogenes*) pharyngitis in children at high risk.¹⁴ A significantly higher incidence of scarlet fever in urban areas with denser populations and more developed transport infrastructure as compared to rural regions has been recently observed, which suggests that prevention and control measures for this disease should be focused more on metropolitan areas.¹

The early diagnosis and treatment of scarlet fever are important in order to avoid the development of complications, both local and systemic. Local complications



Fig. 1. Erythema of the face in a 7-year-old patient

present as peritonsillar and retropharyngeal abscesses. Systemic complications include acute rheumatic fever, glomerulonephritis, bacteremia, pneumonia, endocarditis, and meningitis. In rare cases, hepatitis, gallbladder hydrops or splenomegaly may develop as a consequence of scarlet fever.^{9,10} Due to the characteristic oral presentation of this disease, it is very important for dentists to be able to recognize and correctly diagnose patients with scarlet fever, which will facilitate proper treatment.

Case reports

Case 1

A 7-year-old schoolboy suddenly developed facial erythema – initially appearing unilaterally, and later bilaterally – in the buccal regions, excluding the mouth (Fig. 1). This was followed by a diffuse, pink, papular rash affecting the limbs, the groin, the armpits, the trunk, and the buttocks (Fig. 2). Subjective complaints included only a moderate soreness of the throat and fatigue. The body temperature was elevated during the first 2 days of the infection, but did not exceed 38°C. There was no evidence of lymphadenopathy.



Fig. 2. Papular rash in the flexor area in a male patient

An intraoral examination revealed the erythema of the posterior wall of the pharynx and redness of the tongue with the absence of coating.

Apart from the ongoing infection, the boy was generally healthy. However, he required regular neurological follow-ups due to childhood epilepsy without seizures, which had been diagnosed 1.5 years earlier; he had suffered pharyngitis approx. 1 month prior. Also, his father and younger sister were infected at the time, presenting with flu-like symptoms, including fever, malaise and a cough.

Scarlet fever was diagnosed by a pediatrician on the 3rd day of the onset of the symptoms based on the characteristic mucocutaneous findings, without any accessory tests. Treatment for 10 days with amoxicillin with clavulanic acid in suspension – (400 mg + 57 mg)/5 mL – adjusted to the child's body weight, was begun on the 3rd day of the onset of the symptoms. The skin lesions faded fully in approx. 1 week, and no desquamation of the skin was observed afterward.

Case 2

A 4-year-old, generally healthy girl reported fatigue, nausea and abdominal pain followed by vomiting. At night, her body temperature was slightly elevated, reaching 37.7°C. The next day she developed a pink, papular skin rash, which started on the neck, the chest and the armpits, and rapidly spread to her trunk, limbs, groin, and



Fig. 3. Sandpaper-like skin rash in a 4-year-old female patient

face (Fig. 3). The patient did not report itching. Simultaneously, redness of the palatal tonsils and erythematous macules on the soft palate were detected. Severe coating on the tongue was observed, which disappeared in 2 days, showing a reddened tongue surface with enlarged filiform papillae (Fig. 4). However, the girl did not complain of a sore throat. The submandibular, cervical, axillary, and inguinal lymph nodes were tender and enlarged.

Scarlet fever was diagnosed by a pediatrician, who recommended phenoxymethylpenicillin at a dose of 750 mg/5 mL thrice daily for 10 days. Shortly afterward, the rash and other symptoms resolved. However, soon after the termination of the antibiotic treatment, the girl again developed a pink skin rash located on the neck and the back, spreading to the buttocks and the legs, but not accompanied by any other evident systemic signs. She complained of a sore throat. An intraoral examination revealed reddened palatopharyngeal arches. The tongue was not coated at the front, but elongated papillae were evident in the posterior part. A bacteriological culture from the oropharyngeal area revealed a moderately high growth of *S. pyogenes*, which was sensitive to penicillin, erythromycin and clindamycin. Due to the spontaneous remission of the symptoms, by the time the result of the culture was received, no additional treatment with an antibiotic



Fig. 4. Strawberry tongue in a 4-year-old girl with scarlet fever

was advised by the doctor. Considering the type and location of the skin lesions as well as the positive family history, this time, the condition was diagnosed as atopic dermatitis. Treatment with a cream containing fusidic acid and betamethasone valerate, applied twice daily for 5 days, was prescribed. The skin lesions slowly resolved, but a further application of emollients was advised.

As mentioned before, the girl was generally healthy, but 2 weeks prior to the initial infection, she had developed paronychia of the right thumb. The nail wall was red, swollen and warm, but no pathological exudate was evacuated from the area (Fig. 5). It was first treated with medicinal soft soap (soaking the thumb in a soapy solution a few times daily), and then with a topical neomycin spray twice daily for 5 days, with no improvement observed. It healed shortly after a systemic antibiotic for scarlet fever was administered. In this case, the typical skin desquamation of the hands was observed 2 weeks after the termination of the antibiotic therapy.

Meanwhile, the child developed signs of acute genital candidiasis with massive, white, removable coating on erythematous genital mucosa, combined with itching. This was treated with topical nystatin at a dosage adjusted to the child's body weight, which quickly resolved the symptoms.



Fig. 5. Paronychia in a female patient with scarlet fever

Interestingly, the 2 children were in direct contact 8 days before the symptoms occurred in the boy. The girl was infected approx. 1 month later.

Discussion

Numerous options of a differential diagnosis in children with maculopapular dermatitis and fever must be considered. They include rubella, measles, Kawasaki syndrome, infectious mononucleosis, hand-foot-and-mouth disease, and the exanthematous drug reaction. A thorough history of all the clinical symptoms preceding dermatitis, a positive family history, the location of the lesions and their evolution as well as a history of medical treatment and recent travel history of the child and their caregivers are all essential for making a prompt diagnosis.^{8,15-17} Although the clinical appearance of scarlet fever is well established and well documented, we believe it is still important to describe the crucial signs of the disease and to emphasize the oral involvement, showing the potential role of a dentist in recognizing the disease. Considering the risk of complications in diseases with maculopapular dermatitis, an early diagnosis and the implementation of proper treatment are very important. For example, the clinical presentation of Kawasaki syndrome, which is defined as acute, generalized systemic vasculitis of an unknown etiology, may mimic scarlet fever, and there is a risk of acquired cardiac sequelae associated with both. However, treatment is different in each of those diseases.¹⁶

The gold standard for treating scarlet fever are antibiotics. Such a therapy decreases the duration of the illness and helps to prevent developing complications.^{10,15} It also stops the transmission of the disease between children, as a person is no longer contagious after 24 h of the treatment. The antibiotic of choice is penicillin V or amoxicillin for 10 days in a form and at a dosage adjusted to the child's body weight. If the patient is allergic to these drugs, first-generation cephalosporin, clindamycin or erythromycin can be used. The effectiveness of tonsillectomy did not appear to be high in the treatment of recurrent streptococcal pharyngitis, as the carrier state of group A streptococci is also common in patients who have had their tonsils removed.^{10,15,16}

In both of the cases presented herein, the patients were small children and the crucial symptom was a diffuse, sandpaper-like skin rash. The potential route of transmission in the 1st case was via the infected exudates of the family members. In the 2nd case, either direct contact with an infected person from a nursery school or the infection of a nail wall (paronychia) could be considered as the main route. It is worth noting that the oral symptoms were not so evident in the case of the boy, where the lymphadenopathy of the neck area was barely evident. Also, the phase of strawberry tongue with massive coating was not reported by the child's parents. No complications were observed as a consequence of this infection.


Contrary to those observations, in the 2nd case, all typical oropharyngeal signs of scarlet fever, including strawberry tongue and raspberry tongue with simultaneous pharyngitis and local lymphadenopathy, were preceded by abdominal pain and nausea, another common initial sign of this disease. Atopic dermatitis, which appeared in the girl shortly after the infection ended, could have been initiated by the presence of pathological streptococci or by the general dysregulation of the immune system due to infection. On the other hand, another complication which developed in this patient, i.e., acute pseudomembranous candidiasis, could have been a consequence of the antibiotic and steroid treatment, and again a sign of a temporarily reduced immune response. Although the 2 children were in contact with each other shortly before the boy developed the first signs of scarlet fever, it is not very likely that they infected each other, as the girl became ill approx. 10 weeks later than the boy. Considering the incubation period of scarlet fever, which is estimated to be 2–5 days, another route of transmission must be considered.


A diagnosis of scarlet fever is most commonly based on a detailed history and a characteristic clinical presentation. The recommended confirmation of the diagnosis is the culturing of a throat swab.^{10,15} Serological testing, where the antibodies against a streptococcal infection (antistreptolysin O and anti-deoxyribonuclease B) are detected, can be performed when assessing a person who may have one of the complications from a previous streptococcal infection, as it takes the body 2–3 weeks to produce these antibodies. Therefore, this type of testing cannot be used in diagnosing a current infection.¹²

As presented in these 2 case reports, the route of transmission and clinical appearance of scarlet fever may vary. Due to the evident involvement of the oral structures, the awareness of the symptoms of scarlet fever is essential for dentists in order to prevent the spread of this highly contagious disease in crowded places, such as kindergartens and schools. Currently, no vaccine is available to prevent scarlet fever, although the antibiotic treatment allows the complete resolution of the disease and prevents the development of complications. That is why a prompt diagnosis is so important.

ORCID iDs

Zuzanna Ślebioda  <https://orcid.org/0000-0002-5482-3964>

Agnieszka Mania-Końsko  <https://orcid.org/0000-0002-7345-2601>

Barbara Dorocka-Bobkowska  <https://orcid.org/0000-0003-3659-7761>

References

- Chen H, Chen Y, Sun B, Wen L, An X. Epidemiological study of scarlet fever in Shenyang, China. *BMC Infect Dis.* 2019;19(1):1074.
- Lu Q, Wu H, Ding Z, Wu C, Lin J. Analysis of epidemiological characteristics of scarlet fever in Zhejiang Province, China, 2004–2018. *Int J Environ Res Public Health.* 2019;16(18):3454.
- Lynskey NN, Jauneikaite E, Li HK, et al. Emergence of dominant toxigenic MIT1 *Streptococcus pyogenes* clone during increased scarlet fever activity in England: A population-based molecular epidemiological study. *Lancet Infect Dis.* 2019;19(11):1209–1218.
- Huang Y, Wen Y, Jia Q, et al. Genome analysis of a multidrug-resistant *Streptococcus sanguis* isolated from a throat swab of a child with scarlet fever. *J Glob Antimicrob Resist.* 2020;20:1–3.
- Mun SJ, Kim SH, Baek JY, et al. Staphylococcal scarlet fever associated with staphylococcal enterotoxin M in an elderly patient. *Int J Infect Dis.* 2019;85:7–9.
- Adya KA, Inamadar AC, Palit A. The strawberry tongue: What, how and where? *Indian J Dermatol Venereol Leprol.* 2018;84(4):500–505.
- Staszewska-Jakubik E, Czarkowski MP, Kondej B. Scarlet fever in Poland in 2014. *Przegl Epidemiol.* 2016;70(2):195–202.
- Muzumdar S, Rothe MJ, Grant-Kels JM. The rash with maculopapules and fever in children. *Clin Dermatol.* 2019;37(2):119–128.
- Mahajan VK, Sharma NL. Scarlet fever. *Indian Pediatr.* 2005;42(8):829–830.
- Basetti S, Hodgson J, Rawson TM, Majeed A. Scarlet fever: A guide for general practitioners. *London J Prim Care (Abingdon).* 2017;9(5):77–79.
- Brouwer S, Lacey JA, You Y, Davies MR, Walker MJ. Scarlet fever changes its spots. *Lancet Infect Dis.* 2019;19(11):1154–1155.
- Brockmann SO, Eichner L, Eichner M. Constantly high incidence of scarlet fever in Germany. *Lancet Infect Dis.* 2018;18(5):499–500.
- Sayers DR, Bova ML, Clark LL. Brief report: Diagnoses of scarlet fever in Military Health System (MHS) beneficiaries under 17 years of age across the MHS and in England, 2013–2018. *MSMR.* 2020;27(2):26–28.
- Moreland NJ, Webb RH. Against the trend: A decrease in scarlet fever in New Zealand. *Lancet Infect Dis.* 2019;19(12):1285–1286.
- Shulman ST, Bisno AL, Clegg HW, et al. Clinical practice guideline for the diagnosis and management of group A streptococcal pharyngitis: 2012 update by the Infectious Diseases Society of America. *Clin Infect Dis.* 2012;55(10):1279–1282.
- O’Connell J, Sloand E. Kawasaki syndrome and streptococcal scarlet fever: A clinical review. *J Nurse Pract.* 2019;9(5):259–264.
- Ribeiro de Castro MC, Ramos-E-Silva M. The rash with mucosal ulceration. *Clin Dermatol.* 2020;38(1):35–41.

Dental
and Medical Problems

